The Effect of HSV-2 infection on the expression of cellular Mitochondrial Aspartate Aminotransferase.

By

Terry Cordell Collins

A Thesis presented for the Degree of

Doctor of Philosophy

in

The Faculty of Science
University of Glasgow.

Division of Virology
Glasgow University
Church Street
Glasgow
G11 5JR

March 1998

ProQuest LLC.
789 East Eisenhower Parkway
P.O. Box 1346
Ann Arbor, MI 48106 – 1346

Abstract

Herpes simplex virus has long been implicated in the development of human genital cancers, especially carcinoma of the cervix. Recent epidemiological and biological studies suggest that a cooperative interaction between herpes simplex virus and human papillomavirus leads to an increased risk of developing cervical neoplasia.

A set of cell coded polypeptides has been detected in a transformed rat cell line (Bn5T) produced by transformation of rat embryo fibroblasts with a fragment of HSV-2. This group of polypeptides (200kDa, 90kDa (a doublet U90 and L90), 40kDa and 32kDa) were immunoprecipitated specifically from transformed cells by sera from tumour bearing rats, and from rats immunised with non-transformed HSV-2 infected cells. This suggested that HSV-2 might be inducing polypeptides with a function in transformed cells. This thesis describes studies on the 40kDa polypeptide from this group. The 40kDa polypeptide is specifically induced in transformed cells and is upregulated by HSV-2 infection.

The 40kDa polypeptide was purified from Bn5T cells by ammonium sulphate fractionation and fast protein liquid chromatography in an attempt to raise an antiserum to this protein. A poor immune response was observed in rabbits injected with this immunogen, an observation previously and independently reported in our laboratory. However, amino acid sequence data and subsequent immunological studies (Lucasson, 1992) demonstrated that the 40kDa polypeptide was related to mitochondrial aspartate aminotransferase (mAspAT).

The steady state level of mAspAT mRNA was examined to determine whether HSV-2 infection increased the amount of mRNA in transformed cells, as the protein level and enzyme activity had previously been shown to be increased. This study demonstrated an increase of approximately 80% in the level of mAspAT mRNA following HSV-2 infection of Bn5T cells. This conclusion was obtained from Northern blotting and reverse transcriptase PCR experiments.

During Western blotting experiments to confirm the increased mAspAT protein level following HSV-1/HSV-2 infection (previously observed by slot blot immunoblotting), a second polypeptide was identified specifically in the HSV infected samples. This polypeptide was found to have a slightly greater molecular

weight in cells infected with HSV-1 than in HSV-2 infected cells. This information was used to map the region of the HSV genome encoding this polypeptide, by analysis of the polypeptide produced following infection of cells with a panel of intertypic recombinant herpes simplex viruses. The polypeptide was identified as the HSV dUTPase enzyme, although no obvious reason for the cross-reactivity could be found.

A plasmid was constructed with the mAspAT cDNA under the control of the HCMV major immediate early promotor. This plasmid expressed the mAspAT polypeptide in transfected cells, as determined by immunofluorescence studies. Transfection of this plasmid into normal rat kidney cells led to an increase in the number of cells which formed colonies in soft agar medium, in comparison to cells transfected with the parental control plasmid. This experiment demonstrated a direct biological transforming effect of increased mAspAT expression in normal cells *in vitro*. Transformation assays *in vivo* using these cells injected into nude mice were inconclusive, as tumours also developed in animals injected with control cells.

During RT-PCR experiments to quantify the level of mAspAT mRNA following HSV infection, an additional PCR product was observed in HSV-2 infected Bn5T cell samples. This product was slightly smaller than the normal sized product, and might explain the appearance of a 40kDa mAspAT polypeptide (in addition to the consitutive cellular 44kDa enzyme) and the increased membrane mAspAT immunofluorescence observed in transformed cells (J.C.M. Macnab, unpublished results). The smaller PCR product was cloned into pGEM-T and partial DNA sequence was obtained. This demonstrated that the mitochondrial targetting pre-sequence was present in the smaller clones, and did not therefore explain the altered localisation of mAspAT to the cell surface observed in the transformed cell.

My results demonstrate an increase in the level of mAspAT mRNA in transformed cells following infection with HSV-2, and that increased expression of mAspAT can induce transformation in normal cells. The possible effects of increased mAspAT activity on tumour cell metabolism are discussed, along with the function of mAspAT as a plasma membrane long chain fatty acid binding protein (FABP(pm)) and a possible role for the dUTPase-mAspAT cross reactivity in promoting cervical neoplasia.

Acknowledgements

I would like to express my gratitude to Professor J.H. Subak-Sharpe for providing research facilities within the Institute of Virology, and to his successor Professor Duncan McGeoch for allowing continued access to the Institute during the writing of this thesis (and for his effective encouragement throughout that process).

I would like to thank my supervisor, Dr. Joan Macnab for her support and guidance during my time in the laboratory, and for her continued interest in and critical reading of this thesis. If awards for extreme patience were given, Joan would surely deserve one. Thanks.

To all those members of staff in the Institute who have helped me over the years, and to the members of the 'old Lab 301', my sincere thanks. Special mention is due to Dave McNab, who always had whatever I needed in the lab, for his technical guidance, and for inspiring me to get fit again by returning refreshed from his daily run. Thanks also to Dr. Paul Yeo for providing reliable computing facilities during the completion of this thesis.

I acknowledge the assistance of Dr. J.R. Mattingley in providing plasmids containing the mAspAT cDNA, and Professor B. Matz for providing the NRK 536 cells.

I should also like to thank those friends from within the Institute who encouraged me back into the hills, especially Gillian McVey, Richard Smith and others too numerous to name who were kind enough to pretend that they believed I knew what I was doing.

Finally, I would like to thank my parents for their continued financial support (a child is for life, not just for Christmas!), and Dr. Liz Homer, who has critically read this thesis throughout its' progress towards completion, and who has provided support and companionship during the last 18 months.

The author was in receipt of a Medical Research Council Studentship. Except where stated, the work presented in this thesis was carried out by the author.

Farewell to the Highlands

Farewell to the Highlands, farewell to the north,
The birth-place of Valor, the country of Worth;
Wherever I wander, wherever I rove
The hills of the Highlands for ever I love.

My heart's in the Highlands, my heart is not here,
My heart's in the Highlands, a-chasing the deer;
A-chasing the wild deer, and following the roe,
My heart's in the Highlands wherever I go.

Farewell to the mountains, high cover'd with snow,
Farewell to the straths and green vallies below;
Farewell to the forests and wild hanging woods,
Farewell to the torrents and loud pouring floods.

My heart's in the Highlands, my heart is not here,
My heart's in the Highlands, a-chasing the deer;
A-chasing the wild deer, and following the roe,
My heart's in the Highlands wherever I go

Robert Burns

"Facts are stubborn things; and whatever may be our wishes, our inclinations, or the dictates of our passions, they cannot alter the state of facts and evidence."

John Adams

Dedication.

This thesis is dedicated to the memory of my Grandfathers, who both died during the progress of this research, but who would have been proud to have seen it completed.

CONTENTS

ABSTRACT *i*
ACKNOWLEDGEMENTS *iii*
TABLE OF CONTENTS *iv*
LIST OF FIGURES *xiii*
LIST OF TABLES *xvi*
LIST OF ABBREVIATIONS *xvii*

1. INTRODUCTION. 1

1.1 HERPES SIMPLEX VIRUS. 1

1.1.1 Introduction. 1

1.1.2 Current classification of herpesviruses. 1

1.1.3 Aspects of herpes simplex virus disease. 2

1.1.3.1 Pathology and Pathogenesis of HSV infection. 2

1.1.3.2 Epidemiology. 3

1.1.3.2.1 Orolabial HSV infection. 3

1.1.3.2.2 Genital HSV infections. 4

1.1.3.3 Clinical manifestations of Disease. 5

1.1.3.3.1 Primary/recurrent Oropharyngeal disease. 5

1.1.3.3.2 Primary/recurrent Genital disease. 5

1.1.3.3.3 Neonatal HSV infection. 6

1.1.3.3.4 Other disease associated with herpes simplex virus infection. 6

1.1.3.4 Host immune response. 7

1.1.3.5 Latency. 8

1.1.4 The molecular biology of HSV-1. 8

1.1.4.1 Virion structure. 8

1.1.4.2 Viral genes. 10

1.1.4.3 Viral replication. 11

1.1.4.3.1 Initial stages of infection. 12

1.1.4.3.1.1 Attachment. 12

1.1.4.3.1.2 Penetration. 13

1.1.4.3.1.3 Release of viral DNA. 13

1.1.4.3.2 Synthesis and processing of viral proteins. 13

1.1.4.3.3 HSV DNA replication. 14

1.1.4.3.3.1 Proposed model of DNA replication. 14

1.1.4.3.3.2 HSV-1 origins of Replication. 14

1.1.4.3.3.3 HSV gene products essential for origin dependent replication. 15
1.1.4.3.3.3.1 Origin binding protein-UL9. 15
1.1.4.3.3.3.2 Single stranded DNA binding protein (SSB)- ICP8. 16
1.1.4.3.3.3.3 DNA Helicase-Primase. 16
1.1.4.3.3.3.4 DNA polymerase. 16
1.1.4.3.3.3.5 Protein-protein interactions. 17
1.1.4.3.3.3.6 Non-essential HSV-1 genes. 18
1.1.4.3.3.3.7 Cellular enzymes. 18
1.1.4.3.4 Capsid assembly and DNA packaging. 18
1.1.4.3.4.1 Structure of the HSV-1 Capsid. 18
1.1.4.3.4.2 DNA packaging. 20
1.1.4.3.4.3 Capsid envelopment and egress. 21
1.1.5 Regulation of viral gene expression. 23
1.1.5.1 Trans-activation of α genes by α-TIF. 23
1.1.5.2 Regulatory functions of the α gene products. 24
1.1.5.2.1 ICP0 (Vmw 110; [RL2]). 24
1.1.5.2.2 ICP4 (Vmw 175; [RS1]). 24
1.1.5.2.3 ICP27 (Vmw 63; [UL54]). 25
1.1.5.2.4 ICP22 (Vmw 68; [US1]) and ICP47 [US12]. 25
1.1.5.3 Regulation of α gene expression. 25
1.1.5.4 Regulation of β gene expression. 26
1.1.5.5 Regulation of γ gene expression. 26
1.1.5.6 Post-transcriptional regulation. 27
1.1.6 The fate of the infected cell. 27
1.1.6.1 Structural alterations. 27
1.1.6.2 Shut-off of host macromolecular synthesis. 27
1.1.7 Latency. 28
1.1.7.1 Viral gene expression in latently infected cells. 29
1.1.7.2 Copy number of viral DNA in latently infected neurons. 30
1.1.7.3 Maintenance of and reactivation from latency. 31
1.1.7.4 A model of latency. 31
1.1.8 Modulation of host defence mechanisms. 32

1.2 CELLULAR TRANSFORMATION BY VIRUSES. 33

1.2.1 Transformation by RNA tumour viruses. 34
1.2.1.1 The functions of some transduced retroviral oncogenes. 36
1.2.1.1.1 *Sis*: Growth factor. 36
1.2.1.1.2 *ErbB* and *fms*: Altered receptors and constitutive mitotic signals. 36
1.2.1.1.3 *Src* and *abl*: membrane bound non-receptor tyrosine kinases. 37
1.2.1.1.4 *Ras*: Growth regulatory GTPase. 37

1.2.1.1.5 *Mos* and *Raf*: Non- membrane associated serine/threonine kinases. 38
1.2.1.1.6 *Jun, Myc* and *erbA*: Transcription factors. 39
1.2.1.2 Cis-activation of oncogenes. 40
1.2.2 Transformation by DNA tumour viruses. **40**
1.2.2.1 Common cellular targets for DNA tumour virus oncoproteins. 41
1.2.2.1.1 Inactivation of p53 function. 42
1.2.2.1.2 Inactivation of the retinoblastoma protein function. 43
1.2.2.2 Other DNA tumour virus transforming activities. 44
1.2.2.2.1 Activation of cellular tyrosine kinase activity. 44
1.2.2.2.2 Inhibition of cellular apoptosis. 44
1.2.3 Other DNA viruses linked with human cancers. **44**
1.2.3.1 Hepatitis B virus and hepatocellular carcinoma. 44
1.2.3.2 Epstein-Barr virus related malignancies. 45
1.2.3.3 Human herpesvirus 8 and Kaposi's sarcoma. 46
1.2.4 The viral basis of cervical cancer. **47**
1.2.4.1 The incidence of cervical cancer. 47
1.2.4.2 Evidence for a role for HPV in the aetiology of cervical cancer. 48
1.2.4.2.1 Epidemiological evidence. 48
1.2.4.2.2 Biological Studies. 49
1.2.4.2.2.1 The role of HPV E7 in transformation. 50
1.2.4.2.2.2 The role of HPV E6 in transformation. 50
1.2.4.2.3 The co-operative effect of E6 and E7 on the cell cycle. 51
1.2.4.3 Herpes simplex virus as a co-factor in the induction of cervical neoplasia. 52
1.2.4.3.1 Epidemiological evidence. 52
1.2.4.3.2 Biological evidence relating HSV to cervical cancer. 53
1.2.4.3.3 Activation of cellular gene expression by HSV. 55

1.3 MITOCHONDRIAL ASPARTATE AMINOTRANSFERASE. **56**
1.3.1 Introduction. **56**
1.3.2 Protein folding and mitochondrial import of pre-mAspAT. **58**
1.3.3 Transamination by mAspAT. **60**
1.3.3.1 Reaction mechanism. 60
1.3.3.2 Structural studies of mAspAT enzyme mechanism. 61
1.3.4 The metabolic functions of aspartate aminotransferases. **63**
1.3.4.1 The malate-aspartate shuttle. 63

2. MATERIALS AND METHODS. **65**

2.1 MATERIALS. **65**
2.1.1 Chemicals and reagents. **65**

2.1.2 Restriction and DNA modifying enzymes. 67
2.1.3 Radiochemicals. 67
2.1.4 Other materials and apparatus. 67
2.1.5 Cells. 68
2.1.6 Virus strains. 68

2.2 METHODS. 69

2.2.1 General procedures. 69
2.2.1.1 pH measurement. 69
2.2.1.2 Autoclaving and Glassware sterilisation. 69
2.2.1.3 Filter sterilisation. 69
2.2.2 Tissue culture. 69
2.2.2.1 General Solutions. 69
2.2.2.2 Preparation of primary rat embryo cells 70
2.2.2.3 Maintenance of cell lines. 71
2.2.2.4 Cell harvesting. 71
2.2.2.5 Preparation and storage of cell stocks. 71
2.2.2.6 Mock infection and infection of cells with HSV. 72
2.2.2.7 Transfection with plasmid DNA. 72
2.2.2.7.1 Calcium Phosphate precipitation. 72
2.2.2.7.2 Lipofection with DOTAP. 72
2.2.3 Virus. 73
2.2.3.1 Virus stock production. 73
2.2.3.2 Titration of Virus stocks. 74
2.2.4 Antisera. 74
2.2.4.1 Production of tumour bearing serum (TBS). 74
2.2.4.2 Raising an antiserum against the 40 kDa polypeptide. 74
2.2.4.3 Raising antibody to mAspAT. 75
2.2.4.4 Antibody to HSV UL49. 75
2.2.4.5 Antibody to HSV dUTPase. 75
2.2.5 Protein purification and analysis. 75
2.2.5.1 Solutions. 75
2.2.5.2 Radiolabelling polypeptides with [α^{35}S] L-methionine. 75
2.2.5.3 Measurement of incorporation of radiolabel into polypeptides. 76
2.2.5.4 Immunoprecipitation. 76
2.2.5.5 Purification of the 40kDa polypeptide. 76
2.2.5.5.1 Cell lysis. 76
2.2.5.5.2 Ammonium sulphate fractionation. 76
2.2.5.5.3 Desalting. 77
2.2.5.5.4 Anion exchange chromatography. 77

2.1.4 Other materials and apparatus. 67
2.1.5 Cells. 68
2.1.6 Virus strains. 68

2.2 METHODS. 69

2.2.1 General procedures. 69
2.2.1.1 pH measurement. 69
2.2.1.2 Autoclaving and Glassware sterilisation. 69
2.2.1.3 Filter sterilisation. 69
2.2.2 Tissue culture. 69
2.2.2.1 General Solutions. 69
2.2.2.2 Preparation of primary rat embryo cells 70
2.2.2.3 Maintenance of cell lines. 71
2.2.2.4 Cell harvesting. 71
2.2.2.5 Preparation and storage of cell stocks. 71
2.2.2.6 Mock infection and infection of cells with HSV. 72
2.2.2.7 Transfection with plasmid DNA. 72
2.2.2.7.1 Calcium Phosphate precipitation. 72
2.2.2.7.2 Lipofection with DOTAP. 72
2.2.3 Virus. 73
2.2.3.1 Virus stock production. 73
2.2.3.2 Titration of Virus stocks. 74
2.2.4 Antisera. 74
2.2.4.1 Production of tumour bearing serum (TBS). 74
2.2.4.2 Raising an antiserum against the 40 kDa polypeptide. 74
2.2.4.3 Raising antibody to mAspAT. 75
2.2.4.4 Antibody to HSV UL49. 75
2.2.4.5 Antibody to HSV dUTPase. 75
2.2.5 Protein purification and analysis. 75
2.2.5.1 Solutions. 75
2.2.5.2 Radiolabelling polypeptides with [α^{35}S] L-methionine. 75
2.2.5.3 Measurement of incorporation of radiolabel into polypeptides. 76
2.2.5.4 Immunoprecipitation. 76
2.2.5.5 Purification of the 40kDa polypeptide. 76
2.2.5.5.1 Cell lysis. 76
2.2.5.5.2 Ammonium sulphate fractionation. 76
2.2.5.5.3 Desalting. 77
2.2.5.5.4 Anion exchange chromatography. 77
2.2.5.6 SDS-PAGE. 77
2.2.5.7 Western Blotting. 78
2.2.5.7.1 Solutions. 78

2.2.5.6 SDS-PAGE. 77
2.2.5.7 Western Blotting. 78
2.2.5.7.1 Solutions. 78
2.2.5.7.2 Protocol. 79
2.2.6 Indirect immunofluorescence (fitc). 79
2.2.6.1 General Solutions. 79
2.2.6.2 Antibodies. 80
2.2.6.3 Cells. 80
2.2.6.4 Immunofluorescence. 80
2.2.7 Ribonucleic acid extraction from eukaryotic cells. 81
2.2.7.1 Solutions and equipment for RNA work. 81
2.2.7.2 Single Step Extraction of total cellular RNA from tissue culture cells. 82
2.2.7.3 Isolation of poly(A)$^+$RNA. 83
2.2.7.3.1 Oligo(dT)$_{25}$-Dynabeads®. 83
2.2.7.4 Nucleic acid precipitation. 83
2.2.7.5 Quantification of DNA and RNA. 84
2.2.8 Electrophoresis of nucleic acid. 84
2.2.8.1 General Solutions. 84
2.2.8.2 Agarose gel electrophoresis. 85
2.2.8.2.1 Denaturing electrophoresis of RNA. 85
2.2.8.2.2 Electrophoresis of DNA. 86
2.2.8.2.3 Marker DNA and RNA. 86
2.2.8.3 Acrylamide Gels. 86
2.2.8.4 DNA Recovery from Gels. 87
2.2.8.4.1 Agarose Gels. 87
2.2.8.4.2 Acrylamide Gels. 87
2.2.9 Hybridisation. 88
2.2.9.1 General Solutions. 88
2.2.9.2 Radiolabelling of DNA probes. 88
2.2.9.2.1 Preparation of the DNA to be labelled. 88
2.2.9.2.2 Random priming of dsDNA. 89
2.2.9.2.3 Labelling of dsDNA by nick-translation. 89
2.2.9.2.4 End labelling. 89
2.2.9.2.5 Measurement of the incorporation of radionucleotides into DNA probes. 90
2.2.9.3 RNA Hybridisation. 90
2.2.9.3.1 Samples and gel electrophoresis. 90
2.2.9.3.2 RNA Transfer. 90
2.2.9.3.3 Hybridisation and washing. 91
2.2.9.3.4 Autoradiography. 91
2.2.9.3.5 Stripping filters of bound radioactive probe. 91

2.2.9.3.6 Staining of filter-bound RNA/DNA with methylene blue. 91
2.2.10 Bacteriology and manipulation of plasmid DNA. 92
2.2.10.1 The amplification and purification of plasmid DNA. 92
2.2.10.1.1 Media and supplements. 92
2.2.10.1.2 Solutions. 93
2.2.10.1.3 Bacterial strains and cloning vectors. 94
2.2.10.1.4 Preparation of competent bacterial cells. 95
2.2.10.1.4.1 Calcium Chloride method. 95
2.2.10.1.4.2 TSB Method. 95
2.2.10.2 Preparation of plasmid DNA. 96
2.2.10.2.1 Plasmid Isolation: 'Mini-Prep'. 96
2.2.10.2.2 Plasmid Isolation: QIAGEN Midi-Prep. 97
2.2.10.3 Restriction Enzyme Digestion of DNA. 98
2.2.10.4 Ligation. 98
2.2.11 Reverse transcriptase-PCR. 99
2.2.11.1 Buffers. 99
2.2.11.2 Protocol. 99
2.2.12 Dideoxy DNA sequencing. 100
2.2.12.1 Template preparation. 100
2.2.12.2 Annealing of template and primer. 100
2.2.12.3 Labelling and termination reactions. 101
2.2.12.4 Sequencing gel electrophoresis. 101
2.2.12.5 Sequence analysis. 101
2.2.13 Transformation assays. 101
2.2.13.1 Growth in soft agar. 101
2.2.13.1.1 Soft agar. 102
2.2.13.1.2 Protocol. 102
2.2.13.2 Loss of contact inhibition. 102
2.2.13.3 Tumourogenicity in nude mice. 102

RESULTS AND DISCUSSION.

3. PURIFICATION OF THE 40KDA POLYPEPTIDE AND PRODUCTION OF AN ANTISERUM. 103

3.1 INTRODUCTION 103
3.2 PURIFICATION OF THE 40KDA POLYPEPTIDE FROM Bn5T CELLS 104
3.3 IMMUNISATION OF A RABBIT WITH THE 40KDA POLYPEPTIDE AND TESTING OF ANTISERUM 106
3.4 DISCUSSION 107

4 THE EFFECT OF HSV-2 INFECTION ON THE STEADY-STATE LEVEL OF mAspAT mRNA IN A TRANSFORMED CELL LINE. 109

4.1 INTRODUCTION 109

4.2 SLOT-BLOT AND NORTHERN BLOT EXPERIMENTS TO ANALYSE THE EFFECT OF HSV-2 INFECTION ON THE STEADY STATE LEVEL OF mAspAT mRNA IN THE Bn5T TRANSFORMED CELL LINE. 110

4.2.1 Northern blotting 110

4.2.2 mAspAT cDNA probe labelling 110

4.2.3 Optimisation of washing protocol 111

4.2.4 Probing with a control probe 111

4.2.6 Representative calculation of altered mAspAT mRNA levels. 112

4.2.7 Increased mAspAT mRNA levels - cumulative results. 113

4.3 SEMI-QUANTITATIVE RT-PCR TO EXAMINE THE ALTERED LEVEL OF mAspAT RNA IN HSV-2 INFECTED Bn5T CELLS. 113

4.4 COMBINED RESULTS OF NORTHERN BLOTTING AND RT-PCR EXPERIMENTS ON THE EFFECT OF HSV-2 ON mAspAT mRNA LEVELS. 115

4.5 EXPERIMENTS TO CONFIRM THAT THE PHOSPHORIMAGER CAN RELIABLY DETECT A 2-FOLD INCREASE IN THE AMOUNT OF RADIOACTIVITY PRESENT IN DNA AND RNA SAMPLES. 115

4.5.1 Agarose gel electrophoresis of 5'[γ-^{32}P] labelled DNA molecular weight markers. 115

4.5.2 *In vitro* transcription analysis. 117

4.6 DISCUSSION. 117

4.7 CONCLUSIONS. 120

5. IDENTIFICATION OF A POLYPEPTIDE IN HSV INFECTED CELLS WHICH CROSS-REACTS WITH AN ANTISERUM RAISED AGAINST mAspAT. 121

5.1 INTRODUCTION 121

5.2 INITIAL INVESTIGATION 121

5.3 OPTIMISATION OF EXPERIMENTAL CONDITIONS 122

5.3.1 Gel electrophoresis conditions 122

5.3.2 Cell lysis conditions 122

5.3.3 Western blotting 122

5.4 THE EFFECT OF HSV INFECTION ON mAspAT LEVELS IN BHK C13 CELLS 123

5.5 ARE THE LOWER MOLECULAR WEIGHT POLYPEPTIDES CELL ASSOCIATED? 124

5.6 THE LOWER MOLECULAR WEIGHT POLYPEPTIDES ARE NOT DEGRADATION PRODUCTS 125

5.7 TIMECOURSE OF INDUCTION OF THE LOWER MOLECULAR WEIGHT POLYPEPTIDES 126

5.8 EXPERIMENTS TO IDENTIFY THE HSV INDUCED POLYPEPTIDES. 127

5.8.1 Infection of cells with HSV-1/HSV-2 intertypic recombinant viruses. 127

5.8.2 The UL49 gene product (p43) is not the induced polypeptide. 128

5.8.3 HSV mutants in the dUTPase gene fail to induce the lower molecular weight polypeptides in infected cells. 129

5.8.4 Western blotting with a dUTPase antiserum. 130

5.9 DISCUSSION. 130

5.9.1 Summary of Results. 130

5.9.2 Mapping of the HSV induced lower molecular weight polypeptides using HSV-1/HSV-2 intertypic recombinants. 133

5.9.3 Discussion of the cross reactivity between HSV dUTPase and mAspAT. 134

5.9.3.1 Sequence comparison 134

5.9.3.2 Comparison of the structure and function of dUTPase and mAspAT 135

5.9.4 Possible contamination of the immunogen. 137

5.10 CONCLUSIONS. 138

6. CLONING OF THE mAspAT cDNA INTO A EUKARYOTIC EXPRESSION VECTOR AND CELLULAR TRANSFORMATION ASSAYS 139

6.1 INTRODUCTION 139

6.1.1 Cells. 139

6.1.2 Plasmids. 140

6.2 CLONING OF mAspAT cDNA INTO A EUKARYOTIC EXPRESSION VECTOR 140

6.2.1 Directional cloning into pCMV10 140

6.2.2 Cloning non-directionally into pCMV10 141

6.2.2.1 Introduction 141

6.2.2.2 Ligation and bacterial transformation 142

6.2.2.3 Restriction digest analysis of ligated plasmids 143

6.3 CONFIRMATION OF mAspAT EXPRESSION FROM pCMV-mAspAT1. 144

6.3.1 Large scale preparation of pCMV-AspAT1 144

6.3.2 Immunofluorescence experiments to confirm expression of mAspAT in transfected cells. 144

6.4 LIPOFECTION OF CELLS WITH pCMV-AspAT1 AND TRANSFORMATION ASSAYS. 145

6.4.1 Lipofection. 145

6.4.2 Colony formation in soft agar 145

6.5 TUMOUROGENICITY IN NUDE MICE 147

6.6 DISCUSSION 148

7. AMPLIFICATION, CLONING AND DNA SEQUENCING OF A SMALLER mAspAT CDNA FROM HSV-2 INFECTED Bn5T CELLS. 151

7.1 INTRODUCTION 151

7.2 RT-PCR AMPLIFICATION USING PCR PRIMERS 9301 AND 9302 AND CLONING OF THE MINOR mAspAT TRANSCRIPT INTO M13 152

7.3 RT-PCR AMPLIFICATION USING PRIMERS 9301ECORI AND 9302XBAI, AND CLONING INTO pGEM-T. 152

7.4 DISCUSSION. 154

8. SUMMARY OF RESULTS AND GENERAL DISCUSSION. 156

8.1 SUMMARY OF RESULTS. 156

8.2 GENERAL DISCUSSION. 158

8.2.1 Plasma membrane fatty acid binding protein (FABP(pm)). 157

8.2.2 Hormonal regulation of mAspAT and citrate synthesis. 158

8.2.3 Increased flux through the malate-aspartate shuttle 159

8.2.4 Enhanced glutamine oxidation in tumour cells. 161

8.3 CONCLUSIONS. 162

REFERENCES I-XXVIII

APPENDICES XXIX

Appendix 1: Homology within the Aspartate Aminotransferase family.

Appendix 2A: FASTA comparison of the derived peptide sequences of rat mAspAT and HSV-1 dUTPase.

Appendix 2B: Gap alignment of HSV-1 UL50 ORF DNA sequence and rat mAspAT cDNA sequence.

Appendix 2C: Common motifs within the HSV-1 UL50 ORF DNA sequence and the cDNA sequence of rat mitochondrial aspartate aminotransferase.

List of Figures

Figure	
1.1	The structure of the HSV-1 genome.
1.2	The structure of the HSV-1 *a* sequence.
1.3	Proposed model of HSV-1 capsid assembly.
1.4	Packaging signals within the HSV-1 *a* sequence.
1.5	A generalised multi-step signal transduction pathway.
1.6	The roles of the tumour suppressor genes p53 and $p105^{Rb}$ in regulating cell growth.
1.7	Cervical intraepithelial neoplasia and carcinoma.
1.8	The effect of HSV-2 infection on the cyclin dependent kinases active at different stages of the cell cycle.
1.9	Proposed transamination reaction mechanism of mAspAT.
1.10A	The arrangement of active site residues of aspartate aminotransferase stabilises the substrate-pyridoxal phosphate co-enzyme complex in an orientation favouring transamination.
1.10B	Molecular model of aspartate aminotransferase with bound pyridoxamine phosphate co-enzyme.
1.11	Substrate induced domain closure in mAspAT.
1.12	Aspartate aminotransferase is involved in amino acid metabolism, and in the link between the tricarboxylic and Urea cycles.
1.13	The malate-aspartate shuttle.
3.1	Immunoprecipitation of a 40kDa polypeptide from infected control and transformed cells.
3.2	FPLC trace from MonoQ anion exchange column: 0-2.0M NaCl gradient.
3.3	Preparative SDS-PAGE gel for purification of the 40kDa polypeptide.
3.4	Immunprecipitations to test the rabbit antiserum 92A raised against purified 40kDa polypeptide.
3.5	FPLC trace from Heparin affinity chromatography column.

4.1 Comparison of steady-state level of mAspAT mRNA in Bn5T cells before and after infection with HSV-2. Analysis of data from Northern blot illustrated in Figure 4.2A.

4.2 Northern blot and slot blot experiments with HSV-2 infected Bn5T cell RNA reprobed with a γ-Actin cDNA probe after hybridisation with a mAspAT probe.

4.3 Northern blot to show increase in the level of mAspAT mRNA (relative to 28S rRNA) following infection of Bn5T cells with HSV-2.

4.4 Oligonucleotide primers used in semi-quantitative RT-PCR experiments to determine the relative level of mAspAT mRNA in Bn5T cell samples.

4.5 Phosphorimager image of a 1.5% agarose gel of 5'[γ-^{32}P] labelled λ *HindIII* molecular weight markers.

4.6 Linearity of Phosphorimager detection of radiolabelled nucleic acid.

5.1 Optimised Western blot to show detection of an additional polypeptide in Bn5T and RE cells after infection with HSV-2.

5.2 Induction of HSV type specific additional polypeptides following infection of BHK C13 cells with HSV-1 and HSV-2.

5.3 Experiment to determine whether the HSV induced polypeptides are cell associated, secreted or serum contaminants.

5.4 Western blot to demonstrate that the additional polypeptide detected by anti-mAspAT antiserum is not due to non-specific proteolytic degradation.

5.5A Timecourse of induction of HSV-1 specific band detected by an antiserum to mAspAT.

5.5B Timecourse of induction of the HSV specific polypeptide detected by an antiserum to mAspAT in infected cell extracts (large gel).

5.6 Genome maps of the intertypic HSV recombinants Fx9, R12-5 and Bx1.

5.7 Intertypic recombinant HSV viruses induce different molecular weight polypeptides in infected cells. Mapping of the genome region responsible and identification of the polypeptide as the HSV dUTPase.

5.8 Layout of the genes in the region 0.6-0.83 m.u. of the genome of HSV-1.

5.9 The additional polypeptides recognised by the mAspAT antiserum are not the product of the HSV UL49 genes.

5.10 Infection of Bn5T cells with dUTPase deficient mutants of herpes simplex virus.

5.11 A dUTPase antiserum recognises different molecular weight polypeptide bands in HSV-1 and HSV-2 infected BHK C13 cells.

5.12 Comparison of the nucleotide and amino acid sequences of rat mitochondrial aspartate aminotransferase and HSV-1 deoxyuridine triphosphatase.

6.1 Plasmids used in the construction of a eukaryotic vector expressing mAspAT.

6.2 Agarose gel analysis of ligation precursors and products for cloning mAspAT cDNA into pCMV10 expression vector.

6.3 Restriction digest analysis of pCMV-mAspAT plasmid clones.

6.4 Restriction digest analysis of pCMV-mAspAT plasmid.

6.5 Immunofluorescence in NRK 536 cells transfected with a mAspAT expressing plasmid.

6.6 Colony formation in soft agar following transfection of NRK 536 cells with a plasmid expressing mAspAT.

7.1 Different sized mAspAT PCR products from HSV-2 and mock infected Bn5T RNA.

7.2 PCR primers containing restriction enzyme sites.

7.3 Restriction analysis of pGEM-T recovered clones from RT-PCR of HSV-2 infected Bn5T cell RNA.

7.4 DNA sequence of pGEM-T clones of the smaller RT-PCR products from HSV-2 infected Bn5T cells.

8.1 Altered metabolic pathways operate in glycolytic tumour cells.

List of Tables

Table	
1.1	The Human Herpesviruses.
1.2	The localisation and function of HSV-1 virion proteins.
1.3	The functions of the HSV genes presently identified.
1.4	Tumour viruses and their associated cancers.
1.5	Three classes of transforming retroviruses.
1.6	Retroviral oncogenes and their cellular homologues.
1.7	Cellular targets of DNA tumour virus oncoproteins.
1.8	Three levels of EBV latency.
1.9	The incidence and mortality rates for cervical cancer in the United States and the United kingdom.
1.10	Association of cervical disease with HPV type.
4.1	The effect of HSV-2 infection on the relative level of mAspAT mRNA in Bn5T cells. Cumulative results from eight experiments.
4.2	RT-PCR analysis of mAspAT mRNA levels.
4.3	Volume of 5'[γ-^{32}P] labelled DNA molecular weight markers loaded onto an agarose gel to test the sensitivity of Phosphorimager analysis.
4.4	Confirmation of linearity in Phosphorimager detection of 5'[γ-^{32}P] radiolabelled nucleic acid.
5.1	Function of genes mapping within the 0.6-0.83 m.u. region of the HSV-1 genome.
6.1A	Colony formation in soft agar. Transformation assay following lipofection of NRK 536 cells with a mAspAT expressing plasmid.
6.1B	Total number of colonies obtained by transfection of various amounts of mAspAT expressing plasmid.
6.2	Percentage transformation efficiency for colonies obtained by lipofection of various amounts of mAspAT expressing plasmid into NRK 536 cells compared to control lipofections.
6.3	Tumour formation in nude mice following sub-cutaneous injection of cells lipofected with a mAspAT expressing plasmid.
7.1	Summary of sequence obtained from RT-PCR clones from HSV-2 infected Bn5T cells.

List of Abbreviations

α-TIF	alpha trans-inducing factor (Vmw 175)
Acetyl CoA	acetyl coenzyme A
ADCC	antibody dependent cell mediated cytotoxicity
ADP	adenosine diphosphate
AEV	avian erythroblastosis virus
AIDS	acquired immuno-deficiency syndrome
ALV	avian myelocytoma virus
amp	ampicillin
AMV	avian myeloblastosis virus
APS	ammonium persulphate
araC	cytosine arabinoside
ARE	androgen response element
ASV	avian sarcoma virus
ATP	adenosine triphosphate
bFGF-R	basic fibroblast growth factor receptor
BHK C13	baby hamster kidney cells clone 13
BHV-1	bovine herpesvirus type 1
(3x)BM	(3x concentration) SDS-PAGE sample loading buffer
βME	β-mercaptoethanol
BSA	bovine serum albumin
cMDH	cytoplasmic malate dehydrogenase
CA	cell associated
cAMP	cyclic adenosine monophosphate
CAPS	3-cyclohexylamino-1-propanesulphonic acid
cAspAT	cytoplasmic aspartate aminotransferase
CAT	chloramphenicol acetyl-transferase
CDK/CDC	cyclin dependent kinase
CGIN	cervical glandular intra-epithelial neoplasia
CIN	cervical intra-epithelial neoplasia
CIP	calf intestinal phosphatase
CIS	carcinoma *in situ*
CNS	central nervous system
CR1	complement receptor 1
CSF-1R	macrophage colony stimulating factor 1 receptor

CTL	cytotoxic T lymphocytes
DATD	N,N'-diallyltartramide
ddH_2O	double distilled water
DEPC	diethyl pyrocarbonate
DF	dye-ficoll (agarose gel loading buffer)
DHFR	dihydrofolate reductase
DMEM	Dulbecco's modified eagles medium
DMSO	dimethylsulphoxide
DNA/ cDNA	deoxyribonucleic acid/ complimentary DNA
DR1/DR2	direct repeat 1 or direct repeat 2
dut$^-$	dUTPase deficient mutant of HSV
dUTPase	deoxyuridine triphosphatase
E	early
EBNA	Epstein-Barr nuclear antigen
EBV	Epstein-Barr virus
ECL	enhanced chemiluminescence
EGF-R	epidermal growth factor receptor
EHV-1	equine herpesvirus type 1
ELISA	enzyme linked immunosorbant assay
EtBr	ethidium bromide
EtOH	ethanol
f.s.d.	full scale deflection
FAK	focal adhesion kinase
F_cR	receptor for the f_c portion of immunoglobulin
FeSV	McDonough feline sarcoma virus
FITC	fluorescein isothiocyanate conjugate
FIV	feline immunodeficiency virus
FPLC	fast protein liquid chromatography
GABA	γ-aminobutyrate
GAH	L-glutamic acid monohydroxamate
GAP	GTPase activating protein
GDH	glutamate dehydrogenase
GDP	guanosine diphosphate
GEF	guanine nucleotide exchange factor
GRE	glucocorticoid response element
GTP	guanosine triphosphate
HBV	hepatitis B virus
HCC	hepatocellular carcinoma

HCMV	human cytomegalovirus
HCMV mIEP	major immediate early promotor of HCMV
HeBS	hepes buffered saline
HFL	human foetal lung cells
HHV-(x)	human herpesvirus (x)
HPV	human papillomavirus
HRP	horse-radish peroxidase
HSV-1/HSV-2	herpes simplex virus type 1 or herpes simplex virus type 2
i.p.	immunoprecipitation
ICP	infected cell polypeptide
IE	immediate early
IL-1α	interleukin 1 alpha
IPTG	iso-propyl thiogalactoside
IR_L/IR_S	internal repeat (long) and internal repeat (short)
kb/kbp	kilobases/kilobase pairs
kDa	kilodaltons
KS	Kaposis' sarcoma
KSHV	Kaposis' sarcoma associated herpesvirus (HHV-8)
L	late
LAT(s)	latency associated transcript(s)
LB	L-broth
LD_{50}	lethal dose required to kill 50% of animals
LMP	latent membrane protein
LTR	long terminal repeat
mMDH	mitochondrial malate dehydrogenase
m.i.	mock infected
m.u.	map units
MAP kinase	mitogen activated protein kinase
mAspAT	mitochondrial aspartate aminotransferase
MC	carboxmethyl-cellulose
MeOH	methanol
mFABP/FABP(pm)	plasma membrane fatty acid binding protein
mGOT	mitochondrial glutamic-oxaloacetic transaminase
MHC	major histocompatability complex
MMTV	mouse mammary tumour virus
MoLTV	Moloney leukaemia virus
MOPS	3-[N-morpholino] propane sulphonic acid

MPF	maturation promotion factor
MSV	murine sarcoma virus
MTR	morphological transforming region (of HSV)
MuLV	murine leukaemia virus
MW	molecular weight
N-CAM	neuronal cell adhesion molecule
$NAD^+(P)$	nicotinamide adenine dinucleotide (phosphate)
ncr	non coding region
NCS/FCS	newborn calf serum/ foetal calf serum
NGF	nerve growth factor
NRK	normal rat kidney cells
O.D.	optical density
OAA	oxaloacetate
OAc	acetate
ORF	open reading frame
Ori_S/Ori_L	origin of replication within the U_S or U_L segment of the HSV genome
φ	phenol
PAA	phosphonoacetic acid
PAGE	polyacrylamide gel electrophoresis
PBS-A	phosphate buffered saline
PCR	polymerase chain reaction
PDGF	platelet derived growth factor
PEG	polyethylene glycol
pers. comm.	personal communication
pfu	plaque forming unit
PI	pre-immune
pI	iso-electric point
pK_a	$-\log_{10}$ [acid dissociation equilibrium constant (K)]
PLP	pyridoxal phosphate
PMP	pyridoxamine phosphate
PMSF	phenylmethylsulphonyl fluoride
PNK	polynucleotide kinase
pol	polymerase
PRV	pseudo-rabies virus
PVP	polyvinylpyrollidine
RAR	retinoic acid receptor
RAV	Rous associated virus
RE	rat embryo fibroblast cells

RIPA	radio-immunoprecipitation assay buffer
RNA/ mRNA	ribonucleic acid/ messenger RNA
RR (RR1/RR2)	ribonucleotide reductase (large/small subunit)
rRNA	ribosomal RNA
RSV	Rous sarcoma virus
RT	reverse transcriptase
RT-PCR	reverse transcriptase polymerase chain reaction
SDS	sodium dodecyl sulphate
SEM	standard error of the mean
SH	*src* homology domain
snRNPs	small nuclear ribonucleoprotein complexes
SSB	single stranded DNA binding protein
ssDNA/dsDNA	single stranded DNA/double stranded DNA
SSV	simian sarcoma virus
SV40	simian virus 40
TBP	TATA box binding protein (basal level transcription factor)
TBS	tumour bearing serum
TBS-T	tris buffered saline containing 0.5% Tween 20
TCA	trichloroacetic acid
TCA cycle	tricarboxylic acid cycle
TEMED	N,N,N',N'-tetramethylenediamine
TF	transcription factor
TGF-β	transforming growth factor β
THR	thyroid hormone receptor
TK	thymidine kinase
TNF- α	tumour necrosis factor alpha
TR_L/TR_S	terminal repeat (long) and terminal repeat (short)
ts	temperature sensitive
TSB	transformation and storage broth
U	enzyme units
U_L/U_S	unique long and unique short region of herpes simplex virus
UV	ultra-violet (light)
vhs	virion host shutoff
VP	virion protein
VZV	varicella-zoster virus
w/v	weight/volume
w/w	weight/weight
WHV	woodchuck hepatitis virus

1. INTRODUCTION.

1.1 HERPES SIMPLEX VIRUS.

1.1.1 INTRODUCTION.

Herpes simplex virus is one of approximately 100 viruses that belong to the family *Herpesviridae* (reviewed by Roizman, 1996). These viruses share similar general features. A linear double stranded DNA genome is packaged into an icosahedral capsid of approximately 125nm diameter, which is surrounded by an amorphous layer known as the tegument and enclosed in a lipoprotein envelope. The size of the herpesvirus virions ranges from 120nm to 300nm, determined largely by the shape of the envelope. A more detailed discussion of these common features is presented in Section 1.1.4.1 with respect to HSV-1, the most extensively studied herpesvirus.

Most animal species examined have yielded at least one herpesvirus. Eight human herpesviruses have so far been defined (see Table 1.1) and herpesviruses have been isolated from species ranging from non-human primates (e.g. B virus) to bony fish (e.g. Channel catfish herpesvirus).

In addition to their structural similarity, all herpesviruses can establish a latent infection in a specific subset of host cells. Herpes simplex virus latency is discussed in Section 1.1.8.

1.1.2 CURRENT CLASSIFICATION OF HERPESVIRUSES.

The family *Herpesviridae* is divided into three sub-families based upon their biological properties (Roizman *et al.*, 1992). These are the *alpha-, beta- and gamma-herpesvirinae.*

Alphaherpesvirinae. The members of this sub-family have a variable host range, short reproductive cycle, spread rapidly in tissue culture, destroy infected cells and establish latent infection mostly in sensory ganglia. This sub-family includes the *Simplexvirus* (e.g. HSV-1, HSV-2 and B-virus) and *Varicellovirus* (e.g. VZV, PRV and EHV-1) genera.

Betaherpesvirinae. This sub-family are characterised by a long reproductive cycle and an infection in tissue culture which progresses slowly. Infection often leads to

Table 1.1. The Human Herpesviruses.

Designation.	Common name	Sub-family	G+C content (%).	Size (kbp).	Site of Latency.	Disease Association.
Human Herpesvirus 1	Herpes simplex virus 1	α	68.3	152	Peripheral and central nervous system	Orolabial lesions ('cold sores')
Human Herpesvirus 2	Herpes simplex virus 2	α	70.4	155	Peripheral and central nervous system	Genital herpetic lesions
Human Herpesvirus 3	Varicella-zoster virus	α	46	125	Peripheral and central nervous system	Chickenpox (primary infection) and zoster ('shingles') (reactivation)
Human Herpesvirus 4	Epstein-Barr virus	γ	60	172	B lymphocytes	Infectious mononucleosis ('glandular fever') and associated with Burkitt's Lymphoma and naso-pharyngeal carcinoma
Human Herpesvirus 5	Cytomegalovirus	β	57	229	Lymphocytes and some other tissues	In the immunocompromised causes chronic respiratory disease resulting in viral pneumonia. Microcephaly in the newborn.
Human Herpesvirus 6		β	42	162	Peripheral blood mononuclear cells	Exanthem subitum in children, with possible neurological complications. Lymphadenopathy in adults. Transplant complications. Possible association with malignancies (e.g. non Hodgkin's Lymphoma).
Human Herpesvirus 7		β			CD4+ lymphocytes	No evidence of direct involvement in any human disease, but reactivates HHV-6 from latency.
Human Herpesvirus 8	Kaposi's sarcoma herpesvirus	α		230	Endothelial cells, and invading lymphocytes.	Kaposi's sarcoma in AIDS patients.

Data obtained from Block and Hill, 1997; Frenkel and Roffman, 1996; Pellet and Black, 1996; Roizman, 1996.

the formation of enlarged cells (cytomegalia) and latent virus is maintained in non-neuronal tissue. This sub-family contains the genera *Cytomegalovirus* (e.g. human cytomegalovirus (HCMV)).

Gammaherpesvirinae. Members of this sub-family have a narrow host range, restricted mainly to lymphoblastoid cells, establish latent infection in lymphoid tissue and can immortalise cells. The genera *Lymphocryptovirus* (e.g. EBV, associated with infectious mononucleosis, Burkitt's lymphoma and nasopharyngeal carcinoma (Sugden, 1992)) and *Rhadnovirus* (e.g. herpesvirus ateles) make up this sub-family.

There are problems with this classification scheme. For example, two distinct strains of HHV-6 have been identified, but these could be classified as separate viruses on the basis of their biological, DNA sequence and epidemiological characteristics (Schriemer *et al.*, 1991). Although the current classification system is based on biological characteristics, DNA sequence analysis of a number of herpesviruses has shown that most of the viruses would have been classified into the same sub-family using measures of evolutionary relatedness, such as the conservation of genes and gene clusters. Two exceptions are the Marek's disease herpesviruses which are members of the *gammaherpesvirinae* on the basis of biological classification, but are genetically more related to the *alphaherpesvirinae* (Buckmaster *et al.*, 1988), and HHV-6, biologically classified into the *gammaherpesvirinae* but more similar to the *betaherpesvirinae* in genome structure and sequence (Roizman, 1996).

1.1.3 ASPECTS OF HERPES SIMPLEX VIRUS DISEASE.

1.1.3.1 Pathology and Pathogenesis of HSV infection.

Primary and recurrent herpes simplex virus infection lead to characterisitc histopathological changes. Cells balloon, regions of condensed chromatin appear in the nucleus, and plasma membrane integrity is lost leading to the formation of multinucleated giant cells (Whitley, 1996). Upon cell lysis a clear vesicular fluid accumulates between the dermis and epidermal layers, and an intense immune response occurs. In skin lesions, as the lesion heals the vesicular fluid becomes pustular and scabs. In mucosal infection shallow ulcers rather than vesicular lesions are formed.

Human disease is acquired following intimate, personal contact with someone excreting HSV. Infection occurs by contact of the virus with abraded skin or mucosal surfaces. Viral replication at the site of infection is followed by retrograde axonal flow (Cook and Stevens, 1973) of the nucleocapsid to the dorsal root ganglia, where latency is established. Systemic infection (usually of neonates or the immunocompromised) and infection of the central nervous system (CNS) are rare, but serious events.

Infection with HSV-1 is generally limited to the oropharynx, and latent infection persists in the trigeminal ganglion. HSV-2 infection is usually the result of genital transmission, virus replicates in the genital, perigenital or anal skin and establishes latency in the sacral ganglion.

1.1.3.2 Epidemiology.

Herpes simplex viruses are distributed worldwide, including remote Brazilian tribes. The ability of HSV to establish latent infection and the fact that HSV infection is rarely fatal means that over one third of the world population probably has recurrent HSV infection. No animal vector has yet been described. Despite reports of clustered outbreaks of HSV infection, there is no evidence that the viruses cause epidemics (Whitley, 1996).

1.1.3.2.1 Orolabial HSV infection.

Primary infection usually occurs early in childhood, and is influenced by socio-economic class. Only five of 18 countries surveyed had HSV-1 antibody prevalence of less than 70%, with prevalence in excess of 95% observed in several countries, including Spain and Italy (Whitley and Gnann, 1993). Reactivation, assayed by the frequency of recurrent herpes labialis in 1800 graduate students in the U.S. occurred at a rate of 38% of cases. Interestingly, within a single community the rate of recurrence was greater in the more socially privileged (Ship *et al.* 1977).

Asymptomatic excretion of HSV-1 has been observed in approximately 1-5% of the normal adult population (Whitley, 1996).

1.1.3.2.2 Genital HSV infections.

HSV-2 infection is usually aquired by sexual contact and antibodies to HSV-2 are therefore rarely detected prior to the age of onset of sexual activity (Whitley, 1996). In the U.S. alone, 40-60 million people are estimated to be infected with HSV-2 (Magder *et al.*, 1989). The prevalence of antibodies to HSV-2 is greater in the lower socio-economic classes, and in patients routinely attending STD clinics (approximately 3-7%).

Asymptomatic shedding of HSV-2 is estimated to occur in 23% of women with non-primary HSV-2 infection (Koelle *et al.*, 1992). For women with established HSV-2 infection the rate of asymptomatic shedding was estimated to be 1% (Brock *et al.*, 1990). Seroprevalence rates in preganant women are estimated to be between 8% and 28%. Maternal genital infection carries a risk of foetal or neo-natal infection (discussed in Section 1.1.3.3.3), and occasionally a widely disseminated disease with high mortality in the mother. The major risk to the foetus or neo-nate is primary or initial genital infection of the mother, and infection before 20 weeks of gestation is associated with spontaneous abortion. Recurrent infection is the most common form of maternal disease, with transmission usually occurring at the time of delivery. Most infants who develop neonatal disease are born to mothers with asymptomatic HSV infection.

In the U.S. positive risk factors for acquisition of HSV-2 include the number of sexual partners, marital status, place of residence and race. Multiple sexual partners, irrespective of sexual preference correlates directly with acquisition of HSV-2 infection (Nahmias *et al.*, 1990).

Recurrent genital infection can be either symptomatic or asymptomatic, and usually has a shorter period of viral shedding than primary infection. Genital HSV-1 infection reoccurs less frequently than HSV-2 infection.

1.1.3.3 Clinical manifestations of Disease.

1.1.3.3.1 Primary/recurrent Oropharyngeal disease.

Primary infection with HSV-1 produces symptoms including fever, vesicular lesions, gingivostomatitis, anorexia and malaise. However, most primary infections are asymptomatic. Symptomatic disease is much more severe in children, and can last for 2-3 weeks.

Recurrent orolabial lesions appear approximately 24 hours after a period of itching or pain at the site of reactivation. Vesicles frequently appear at the vermillion border of the lip, and persist for about 48 hours prior to scabbing. Healing occurs in 8-10 days.

1.1.3.3.2 Primary/recurrent Genital disease.

Primary infection with HSV-2 results in the appearance of vesicles, pustules and ulcers which persist for about 3 weeks. Fever, dysuria and malaise are common in both men and women, although the severity of infection and rate of complications is higher in women than men. Systemic complications occur in almost 70% of cases, and include aseptic meningitis and extragenital lesions.

In women, lesions appear on the vulva and the cervix. The frequency of infection of the cervix without vulvar infection is unknown. In men, vesicular lesions are obvious on the penis, and extragenital lesions can occur. In both men and women, many primary infections are asymptomatic.

Non-primary infection of the genitals causes less severe disease and pre-existing antibodies to HSV-1 have been reported to have an ameliorative effect on disease severity (Whitley, 1996).

Recurrent HSV-2 disease is usually mild. The number of vesicles present and their duration is reduced, and virus is also shed for a shorter period of time. The frequency of recurrent infection (which varies from 2-3 per year to in excess of 8 recurrences per year) appears to correlate with the severity of the primary infection. Recurrent infection can be asymptomatic, resulting in unwitting transmission of the virus to sexual partners.

1.1.3.3.3 Neonatal HSV infection.

The rate of occurrence of neonatal HSV infection averages 1 in 3000 to 1 in 5000 births, and the likelihood of infection depends greatly upon the type of maternal genital infection at the time of birth. Primary or initial infection carries a ten-fold higher risk of transmission than recurrent infection. Infection occurs rarely *in utero* and postnatally (normally with HSV-1 when it does occur), but occurs commonly during birth.

Neonatal infection (reviewed by Whitley, 1996) is almost invariably symptomatic and often fatal, and disease generally falls into three categories. These are disease localised to the skin, eye or mouth; encephalitis or disseminated infection. Intrauterine infection results in serious disease, often involving encephalopathy. Disseminated disease, most frequently involving the liver and the adrenal glands has the worst prognosis for morbidity and mortality. Encephalitis occurs in approximately 60-75% of children with disseminated disease and in the absence of antiviral therapy 80% of babies will die and most survivors will be neurologically impaired.

Skin, mouth or eye infection is less severe, with limited mortality, but approximately 30% of these children develop neurological impairment.

1.1.3.3.4 Other disease associated with herpes simplex virus infection.

Several other diseases have been associated with HSV infection (reviewed by Whitley, 1996). Approximately 300,000 cases of HSV-1 infection of the eye are reported yearly in the U.S. with primary infection generally resulting in conjunctivitis. Healing can take up to 1 month, even with antiviral therapy and recurrent infections are common, resulting in the progressive opacification of the cornea and blindness.

Skin infections with HSV generally manifest as eczema herpeticum. In a Swedish study, approximately 2% of patients attending dermatology clinics had evidence of herpetic skin lesions. Infection of the fingers, known as herpetic whitlow is increasing in incidence amongst healthcare workers.

HSV encephalitis is the most common cause of sporadic, fatal encephalitis in the U.S. Mortality in untreated patients with HSV encephalitis exceeds 70% and few patients return to normal neurological function. The disease can be caused by either primary or recurrent HSV infection. Analysis of cerebrospinal fluid from patients with non-neonatal HSV encephalitis demonstrated that only approximately 2% (1/64) of cases were caused by HSV-2 infection (Dennett *et al.*, 1997), whilst in neonates HSV encephalitis was caused by HSV-2 in 62% of cases, and produced more severe disease (Corey *et al.*, 1988).

Patients who are immunocompromised suffer increased risk of severe HSV infection. Transplant patients are especially at risk of progressive disease, which may include infection of the gastro-intestinal tract. AIDS patients are at even greater risk of severe disease, and require aggressive antiviral therapy which can result in the emergence of resistant virus isolates.

1.1.3.4 Host immune response.

The natural history of HSV infections is influenced by specific and non-specific host responses (reviewed by Whitley, 1996). Host genetic background, macrophages, natural killer cells, specific T-cell populations, specific antibodies and lymphokine responses have all been implicated as important host defences against HSV infection. The typical response to HSV infection is a non-specific inflamation which co-incides with peak viral replication, followed by a cytotoxic T-cell response and the appearance of IgM and IgG specific antibodies. Antibody dependent cell mediated cytotoxicity (ADCC) correlates with improved clinical outcome.

The importance of the host immune response in disease progression is demonstrated by the following examples. Prior infection with HSV-1 appears to have a protective effect for HSV-2 infection, presumably due to antigenic cross-reactivity between the two viruses. In patients with recurrent infection it has been suggested that the cytotoxic T-cell response is decreased, while host immune responses in the newborn are delayed with respect to the adult population, which may explain the increased severity of disease in the neonate. Immunocompromised individuals also suffer more frequent and severe recurrent HSV infection.

1.1.3.5 Latency.

Latency provides a reservoir of virus which can be transmitted following reactivation for the lifetime of the carrier. Recurrences occur in the presence of cell mediated and humoral immunity, and are associated with physical or emotional stress, fever, UV-light, tissue damage and immune suppression (Whitley, 1996).

The molecular biology of HSV latency is discussed in Section 1.1.8.

1.1.4 THE MOLECULAR BIOLOGY OF HSV-1.

1.1.4.1 Virion structure.

The HSV-1 virion is complex, with at least 39 of the 84 HSV-1 protein coding genes encoding proteins which are components of the virion or are involved in virion assembly (Roizman, 1996).

The HSV-1 virion consists of four distinct components. The core contains the viral DNA and is enclosed within an icosahedral protein capsid. This is surrounded by an amorphous protein layer known as the tegument which is in turn surrounded by a trilamellar lipid envelope which is derived from the host cell and contains virus glycoproteins. The localisation or function of the HSV-1 proteins known to be associated with the HSV virion or involved in HSV virion assembly are shown in Table 1.2.

Table 1.2. The localisation and function of HSV-1 virion proteins.

Capsid	Minor Capsid	DNA packaging	Tegument		Envelope	
UL18	UL6	UL6	UL11	UL47	UL1	UL45
UL19	UL12.5	UL12	UL13	UL48	UL10	US4
UL26	UL15	UL15	UL21	UL49	UL20	US6
UL26.5	UL25	UL25	UL36	US9	UL22	US7
UL35		UL28	UL37	US11	UL27	US8
UL38		UL32	UL41	RL1	UL34	
		UL33	UL46	RS1	UL44	

Adapted from Homa and Brown, 1997.

Three of the proteins involved in DNA packaging are minor, non structural components of the capsid. The function and virion localisation of the other DNA packaging proteins is presently unknown.

Three capsid types have been defined depending on whether the capsids contained DNA or were enveloped. These were designated A-, B- and C-capsids, and are discussed in relation to capsid assembly in Section 1.1.5.1.

The tegument contains the remainder of the virion proteins, including the α-*trans*-inducing factor (α-TIF, VP16, Vmw65), the virion host shutoff protein (UL41) and a large protein (VP1-2) which binds to the terminal *a*-sequence of the viral genome, and may have a role in DNA packaging (Table 1.2).

The structure of the HSV-1 genome is shown diagramatically in Figure 1.1. The genome is approximately 152kbp linear double stranded DNA with a G+C content of 68% (HSV-1) or 70.4% (HSV-2). It contains two covalently linked unique sequences (U_L and U_S) bracketed by inverted repeats (a,b and c in Figure 1.1). The number of *a* sequence repeats is variable at the L/S junction and at the L terminus. The structure of the *a* sequence (Figure 1.2) is highly conserved, containing a 20bp direct repeat (DR1), a 65bp unique region (U_b), a 12bp direct repeat (DR2) present in 19-23 copies, a 37bp direct repeat (DR4) present in 2 or 3 copies, a unique region (U_c) and a final copy of DR1. The terminal DR1 repeats are truncated, with a single nucleotide overhang, and a complete DR1 repeat is formed upon genome circularisation.

The L and S components of the HSV genome can invert relative to each other by a process of intramolecular recombination involving the repeated sequences to yield four isomers (see Figure 1.1). The four isomers are present in equimolar amounts during natural infection. The internal repeat sequences are not essential for virus growth in cell culture, although these viruses are locked in one genome configuration.

Figure 1.1. The structure of the HSV-1 genome.

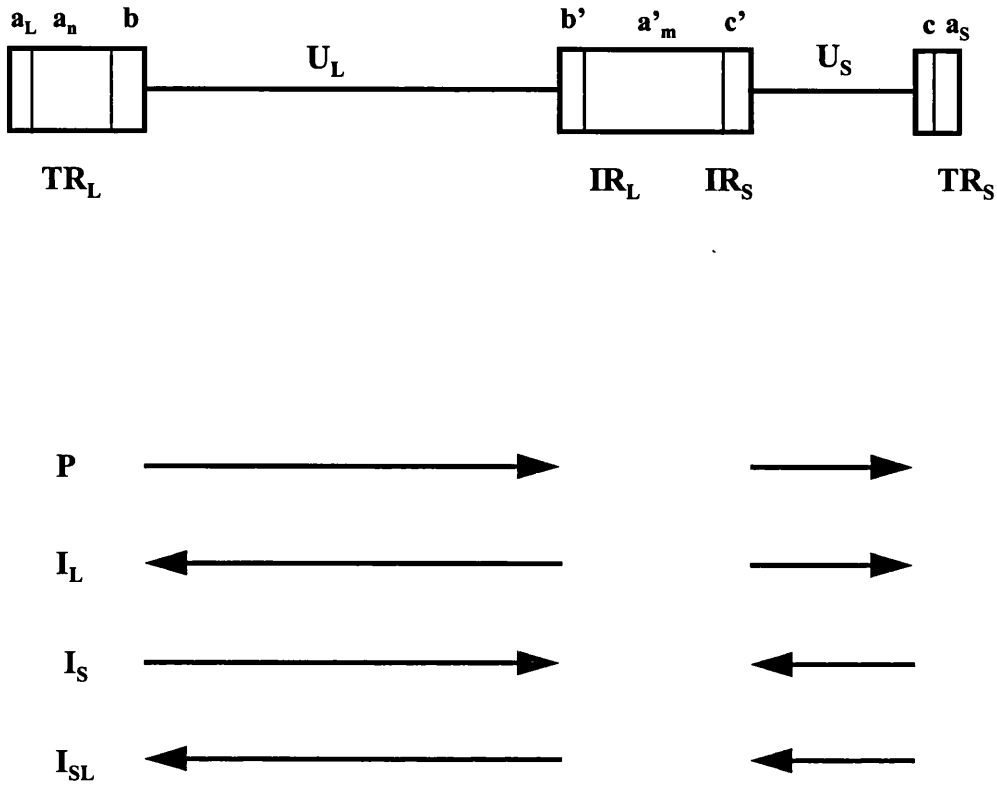

Legend. The HSV-1 genome is shown schematically, with unique sequences as solid lines (U_S and U_L). The repeats TR_L, IR_L, IR_S and TR_S are illustrated as boxes with their component parts a, b, c and a', b', c' labelled.
Below the genome diagram, the isomerisation of the HSV-1 genome is illustrated. The four isomers are: P (prototype); IL (L inverted with respect to P); IS (S inverted with respect to P) and ISL (both L and S inverted with respect to P)

Figure 1.2. The structure of the HSV-1 *a* sequence.

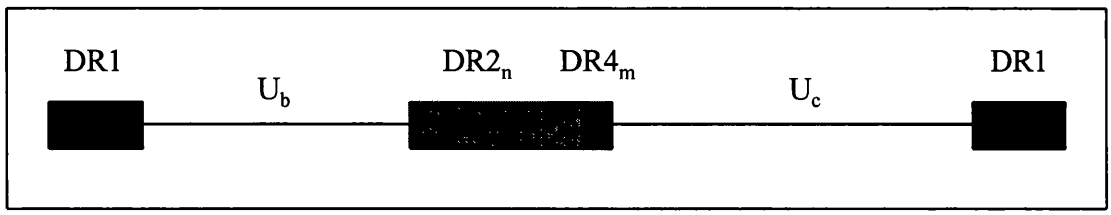

The HSV virion contains the polyamines spermidine and spermine at levels of 70,000 and 40,000 molecules per virion. These molecules are proposed to neutralise the charge due to DNA phosphate, a function which would normally be performed by histone proteins.

The lipid composition of the virion envelope is derived from the cell, and was initially thought to be derived from the nuclear membrane. Recent studies however, suggest that the composition is more similar to cytoplasmic membranes (vanGenderen *et al.*, 1994).

1.1.4.2 Viral genes.

The complete sequence of HSV-1 was published by McGeoch *et al.*, (1988) and 72 open reading frames were identified. Since then a further ten open reading frames have been identified (reviewed by Roizman and Sears, 1996), including those encoding the neurovirulence factor (ICP34.5) and the scaffold protein (UL26.5). The current knowledge concerning the protein products of the HSV-1 genes is presented in Table 1.3.

The HSV-1 genes are expressed in a sequentially ordered fashion divided into three main temporal classes. Where the information is available, the temporal class of the viral genes is shown in Table 1.3.

The α (immediate early; IE) genes are the first to be expressed, and are expressed in the absence of viral protein synthesis. All α genes contain at least a single copy of a consensus TAATGArATT sequence near the cap site, which is necessary for their transactivation by α-TIF (Mackem and Roizman, 1982). Trans-activation of HSV-1 α genes is discussed further in Section 1.1.6.1. The synthesis of α proteins peaks at 2-4 hours post infection, but continues until late in infection. All α proteins except

Table 1.3. The functions of the HSV genes presently identified.

Gene	Protein/Function	Dispensible in tissue culture	Temporal class
RL1	Neurovirulence factor (ICP34.5).	Y	γ_1
ORF P	248 amino acid polypeptide-antisense to ICP34.5.	Y	
ORF O	ORF partially antisense to ICP34.5.	Y	
RL2	IE protein- Vmw110 transcriptional regulator (ICP0).	Y	α
UL1	Glycoprotein L- role in virion entry.	N	γ
UL2	Uracil DNA glycosylase.	Y	β
UL3	Function unknown- nuclear phosphoprotein.	Y	
UL4	Function unknown- found in virions and light particles.	Y	γ_2
UL5	Component of DNA helicase-primase.	N	β
UL6	Virion protein- involved in cleavage/packaging nascent DNA.	N	
UL7	Function unknown.	N	
UL8	Component of DNA helicase-primase- necessary for DNA replication.	N	β
UL8.5	486 amino acid polypeptide (OBP-C)- possible role in HSV DNA replication.		
UL9	*Ori*-binding protein- essential for DNA replication.	N	γ?
UL10	Glycoprotein M.	Y	γ
UL11	Myristylated tegument protein- role in envelopment and egress of virions.	Y	γ?
UL12	Alkaline exonuclease- role in maturation/packaging of nascent DNA.	Y	β
UL13	Tegument protein- protein kinase.	Y	γ
UL14	Function unknown.	N	
UL15	Role in cleavage of concatameric DNA.	N	γ
UL16	Function unknown.	Y	
UL17	Function unknown.	N	γ
UL18	VP23- capsid protein triplex component.	N	γ
UL19	VP5- major capsid protein.	N	γ_1
UL20	Integral membrane protein- role in egress of virions	Y	γ
UL20.5	Function unknown.	Y	γ_2
UL21	Function unknown- nucleotidylyated phoshoprotein.	Y	
UL22	Glycoprotein H- role in entry, egress and cell-cell spread.	N	γ_2
UL23	Thymidine kinase (TK)- role in DNA replication.	Y	β
UL24	Function unknown- membrane associated?	Y	γ
UL25	Virion protein- role in capsid maturation and DNA packaging.	N	γ
UL26	Proteinase- N-terminal portion is capsid protein VP24; C-terminal is VP21 (capsid assembly).	N	γ
UL26.5	VP22a- scaffold protein for B capsids; processed by UL26 protease.	N	γ
UL27	Glycoprotein B- role in virion entry; forms a dimer.	N	γ_1
UL28	Role in capsid maturation/DNA packaging.	N	γ
UL29	ssDNA binding protein (ICP8)- essential for DNA replication.	N	β
UL30	Catalytic subunit of replicative DNA polymerase.	N	β
UL31	Nucleotidylyated phosphoprotein- nuclear matrix associated.	N	γ_2
UL32	Role in DNA packaging.	N	γ_2
UL33	Role in capsid maturation/DNA packaging.	N	
UL34	Membrane associated non-glycosylated phosphoprotein.	N	
UL35	VP26- capsid protein present on tips of hexons.	N	γ_2
UL36	VP1-2 (ICP1-2, Vmw273)- tegument phosphoprotein.	N	γ_2

Table 1.3 continued

Gene	Protein/Function	Dispensible in tissue culture	Temporal class
UL37	Tegument phosphoprotein- binds to ICP8, may have DNA binding function.	N	γ
UL38	VP19C- component of triplexes. DNA anchor?	N	γ_2
UL39	Ribonucleotide reductase large subunit (RR1).	Y	β
UL40	Ribonucleotide reductase small subunit (RR2).	Y	β
UL41	Virion Host Shutoff (*vhs*)- 55kDa polypeptide located in tegument.	Y	γ
UL42	Subunit of replicative DNA polymerase- increases processivity	N	β
UL43	Function unknown- probably membrane associated.	Y	
UL44	Glycoprotein C- role in virion attachment.	Y	γ_2
UL45	18kDa polypeptide- function unknown.	Y	γ_2
UL46	VP11/12- tegument phosphoprotein; modulates α-TIF.	Y	γ
UL47	VP13/14- nucleotidylyated tegument phosphoprotein; modulates α-TIF (VP16).	Y	γ_2
UL48	VP16 (Vmw65, αTIF)- major tegument protein; transactivator of IE(α) genes	N	γ
UL49	VP22- Nucleotidylyated tegument phosphoprotein.	N	γ
UL49.5	6.7kDa non-glycosylated membrane polypeptide-associated with tegument (disulphide bridge?).	N	γ_2
UL50	Deoxyuridine triphosphatase (dUTPase).	Y	β
UL51	Function unknown.	Y	γ
UL52	Component of DNA helicase-primase.	N	β
UL53	Glycoprotein K; role in cell fusion and viral exo-cytosis.	N	γ
UL54	ICP27 (Vmw63)- IE protein, positive regulator of late gene expression; negatively regulates early genes. SnRNP redistribution inhibits splicing.	N	α
UL55	Function unknown.	Y	
UL56	Function unknown.	Y	
RS1	ICP4 (Vmw175)- IE protein, positive transcriptional regulator of most β and γ genes.	N	α
US1	ICP22 (Vmw68)- IE protein, required for optimal expression of ICP 0 and subset of γ genes.	Y	α
US1.5	Function unknown- co-terminal with US1.	Y	α
US2	Function unknown.	Y	
US3	Protein kinase- main substrate is UL34.	Y	β
US4	Glycoprotein G; involved in entry, egress and cell-cell spread.	Y	γ
US5	Glycoprotein J (*predicted*).	Y	
US6	Glycoprotein D; role in virion entry post-attachment.	N	γ_1
US7	Glycoprotein I; complexed with gE has role in transport to plasma membrane. High affinity receptor for Fc of IgG.	Y	g
US8	Glycoprotein E; complexes with gI. Basolateral spread of virus in polarised cells.	Y	γ_2
US8.5	Function unknown.	Y	β or γ_1
US9	Tegument protein.	Y	
US10	Tegument protein.	Y	
US11	Tegument protein- ribosome associated in infected cells. Binds UL34 mRNA- possible attenuation factor.	Y	γ_2
US12	ICP47- IE protein, blocks presentation of viral polypeptides to MHC class I restricted cells.	Y	α
Ori_STU	RNA transcribed across Ori_S- probably not translated.	Y	γ_2
LAT	Family of transcripts expressed during latency, of unknown function and uncertain protein coding capacity	Y	

Adapted from Roizman and Sears, 1996; Homa and Brown, 1997; Boehmer and Lehman, 1997.

α47 (US12) have a regulatory function and are required for the synthesis of subsequent temporal classes of proteins.

The β (early; E) genes require functional α gene products for their expression. Peak rates of synthesis occur at 5-7 hours post infection. The β genes can be sub-divided into those that appear very early (e.g. UL39-RR1) and those that appear later (e.g. UL23-TK), but all require α4 (Vmw175) for their expression. The appearance of the β genes signals the onset of DNA synthesis.

The γ (late; L) genes are classified into two groups differing in the timing of their expression and dependence upon DNA synthesis. γ_1 genes, (e.g. gB) are expressed relatively early (overlapping with β gene expression) and are minimally affected by inhibitors of DNA synthesis, while γ_2 genes (e.g. gC) are expressed later and require DNA synthesis for their expression. These genes encode mostly structural proteins (see Table 1.3).

The α0 (Vmw110) and α4 genes are located within the inverted repeats of the L and S regions and are therefore diploid. The HSV-1 genome is organised such that the α genes form two clusters (α0, α4, α22 and α47, α4, α0) in the circularised genome, and each contains an origin of replication. The β and γ genes are scattered throughout the U_L and U_S regions, with the exception of γ34.5 and ORF P genes which are located in the repeat region of U_L. Two functional clusters have been noted, although the biological relevance of this is uncertain. The DNA polymerase and ssDNA binding protein (both β genes) flank Ori_L and the genes for glycoproteins D, E, G, I and J (all γ genes) map next to each other within U_S.

1.1.4.3 Viral replication.

The events involved in the replication of HSV have been reviewed recently by Roizman and Sears, 1996.

1.1.4.3.1 Initial stages of infection.

1.1.4.3.1.1 Attachment.

The study of HSV attachment to tissue culture cells is complicated by the un-natural distribution of potential cell surface receptors in non-polarised cells. For example, it has been shown that gC is necessary for attachment to an apical but not basal cell surface receptor (Sears *et al.*, 1991). The deletion, in turn, of individual HSV-1 glycoproteins failed to eliminate cell surface attachment, suggesting that HSV-1 can utilise several attachment pathways.

Cell surface heparan sulphate has been identified as the major factor in HSV attachment to the cell surface (Wudunn and Spear, 1989; Shieh *et al.*, 1992; Gruenheid *et al.*, 1993). Removal of heparan sulphate from the cell surface reduced attachment by 85%, but did not completely eliminate binding. This suggested that heparan sulphate is one of multiple receptors. gC is a heparin binding protein, and gC negative viruses have been shown to bind to cells with reduced efficiency (Fuller and Spear, 1985; Trybala *et al.*, 1994). In the absence of gC, gB is thought to bind weakly to heparan sulphate to facilitate adsorption, as double mutants in both gB and gC bind with lower efficiency than a gC mutant alone (Herold *et al.*, 1994). Following initial attachment (by either gB or gC), a stable interaction between gD (Johnson and Ligas, 1988; Johnson *et al.*, 1990) and a saturable cell surface receptor occurs. This receptor has recently been identified in some HSV-1 strains as a novel member of the NGF receptor family (Montgomery *et al.*, 1996; Whitbeck *et al.*, 1997). Other potential cellular receptors for HSV include the basic fibroblast growth factor receptor (bFGFR) (Kaner *et al.*, 1990) although this could not be confirmed by other workers, and the CR1 receptor, which is reported to be responsible for gC mediated attachment at the apical surface of polarised epithelial cells (Roizman and Sears, 1996).

Recently however, Griffiths *et al.* (1998), have reported that in certain strains of HSV-1, mutants in glycoproteins C, E, G, I and J are able to infect both apical and basal surfaces of cells with efficiencies comparable to wild type virus, suggesting that in certain virus strains gC has little or no role in adsorption. The mechanism of viral attachment therefore remains unclear at present.

1.1.4.3.1.2 Penetration.

The mechanism of penetration is poorly understood, but is known to be very rapid and to occur via membrane fusion mediated by virus envelope glycoproteins (Roizman and Sears, 1996). In non-polarised cells, viruses with mutations in the gB and gD genes attach to but do not penetrate the cell surface and cells expressing gD allow attachment but not membrane fusion. Penetration is thought to involve gB and the gH:gL heterodimer whilst the other glycoproteins are dispensible and the expression of gD, gB and gH:gL in transfected cells has recently been shown to be sufficient to allow cell-cell fusion (Turner *et al.*, 1998).

1.1.4.3.1.3 Release of viral DNA.

After entry into the cell the viral capsids are transported to the nuclear pores in a process probably mediated by the cytoskeleton (Kristensson *et al.*, 1986). Release of the DNA into the nucleus occurs by a process that requires a viral function. Empty capsids are readily observed at the nuclear pore of infected cells.

1.1.4.3.2 Synthesis and processing of viral proteins.

Viral polypeptides are synthesised on both free and bound host polyribosomes, and are extensively modified following synthesis. Processing includes cleavage, phosphorylation, glycosylation, sulphation, myristylation, ADP-ribosylation and nucleotidylylation (Roizman and Sears, 1996). Except for some of the glycoproteins, it is unclear whether much of the processing is essential for virus growth.

HSV encodes a protease (UL26) which catalyses self cleavage and the cleavage of the scaffold protein to facilitate DNA packaging into capsids (see Section 1.1.5). At least three protein kinases have been identified, although substrates have only been defined for the UL13 kinase (which include the UL26 protease and its pre-VP22a substrate). ICP4 has been reported to be ADP-ribosylated (Preston and Notarianni, 1983), and several viral polypeptides have been reported to be nucleotidylylated (including ICP4 and ICP0 (Blaho *et al.*, 1994)), although the importance of these modifications is unclear.

1.1.4.3.3 HSV DNA replication.

Herpes simplex virus DNA synthesis has been recently reviewed by Boehmer and Lehman (1997). The HSV genome contains three origins of replication and encodes seven proteins that are essential for DNA replication. These are encoded by herpes simplex virus genes of the β temporal class. A set of enzymes involved in nucleotide metabolism are also encoded by the HSV genome, but these are dispensable in tissue culture.

Viral DNA synthesis is detectable as early as 3 hours post-infection, and continues up to 15 hours post-infection, with most replication occurring later in this period (Igarashi *et al.*, 1993).

1.1.4.3.3.1 Proposed model of DNA replication.

Boehmer and Lehman (1997) suggest a model for replication of the HSV-1 genome, which is presented briefly below, before a more detailed discussion of the replication origins and the HSV proteins involved in DNA synthesis.

Early in infection the linear HSV genome circularises, and DNA replication initiates at an origin, proceeds initially via theta replication and then switches to rolling circle replication. Recombination events lead to the formation of extensively branched DNA intermediates, which are resolved to unit length genomes upon packaging into empty pre-formed capsids.

No direct evidence has been reported for the presence of the theta replication intermediate, but the presence of head to tail concatameric DNA molecules (Severini *et al.*, 1994) supports a rolling circle replicative mechanism. Furthermore, branched DNA intermediates indicative of rolling circle replication from several origins have been observed by electron microscopy and 2-D electrophoresis (Severini *et al.*, 1996).

1.1.4.3.3.2 HSV-1 origins of Replication.

The HSV-1 genome contains three origins of replication, one copy of Ori_L located between the UL29 and UL30 open reading frames in U_L, and two copies of ori_S

within the c sequence of the short repeats (Stow, 1982). Ori_S and Ori_L contain large palindromes of 45bp and 144bp centered respectively around an A+T region of 18bp and 20bp. Flanking the A+T region are inverted repeats that are binding sites for the origin binding protein (UL9). Ori_L contains two high affinity UL9 sites (Box 1), and ori_S one high affinity and one low affinity site (Box 2). The box1 sites in Ori_L are flanked by homolgous sequences with lower affinity for UL9 (Box 3), whilst Ori_S contains only a single Box 3 element. Efficient replication from Ori_S requires intact Box 1 and Box 2 elements. However neither copy of Ori_S is essential in tissue culture. These HSV-1 origins therefore appear to be redundant, and are conserved for an unknown reason.

1.1.4.3.3.3 HSV gene products essential for origin dependent replication.

1.1.4.3.3.3.1 Origin binding protein-UL9.

UL9 encodes an 851 amino acid polypeptide which binds to Boxes 1 and 2 of Ori_S, and contains ATP binding and helicase motifs that are essential for viral replication (Stow *et al.*, 1993). The UL9 protein binds as a homodimer formed through a leucine zipper motif within the N-terminal region (Deb and Deb, 1991), while the sequence specific DNA binding activity resides in the C-terminal portion of the protein (Arbuckle and Stow, 1993).

The region within Box 1 of Ori_S recognised by the UL9 protein has been mapped to a 10bp sequence (Hazuda *et al.*, 1992), homologues of which are contained in inverted orientation in Boxes 2 and 3. Box 1 and Box 2 are seperated by three turns of the DNA helix, suggesting that two UL9 dimers bind in inverted orientation on the same side of the DNA molecule. Co-operative binding of UL9 to the lower affinity boxes within Ori_S is suggested to be mediated by protein-protein interactions between the N-terminal regions of UL9 (Elias *et al.*, 1992).

UL9 also exhibits an ATP dependent helicase activity which proceeds in a 3'-5' direction and is dependent upon the length of the DNA substrate. The processivity of the helicase is greatly increased in the presence of ICP8, the HSV-1 single stranded DNA binding protein (Fierer and Challberg, 1992). A model of origin specific DNA unwinding has been proposed (Boehmer and Lehman, 1997). Binding of UL9 at the origin is proposed to induce bending and looping out of an A+T rich region within

the origin preventing processivity of the UL9 protein, and causing the DNA to be spooled through the protein complex as single stranded DNA. The unwound DNA is stabilised by SSB/UL9 which then recruits the primase complex to the origin.

1.1.4.3.3.3.2 Single stranded DNA binding protein (SSB)- ICP8.

The single stranded DNA binding protein (SSB), the 1196 amino acid protein product of the UL29 gene (Quinn and McGeoch, 1985) contains a consensus DNA-binding sequence and a zinc-finger motif (Berg, 1986). SSB binds co-operatively to single stranded DNA with a five-fold greater affinity than for double stranded DNA (Lee and Knipe, 1985), holding the DNA in an extended filamentous form (Machov *et al.*, 1996). SSB has an ATP and direction independent helix destabilising activity (Boehmer and Lehman, 1993) which may facilitate the unwinding reaction. SSB also plays a key role in the assembly of the DNA replication apparatus.

1.1.4.3.3.3.3 DNA Helicase-Primase.

The helicase-primase complex consists of the products of the UL52, UL5 and UL8 genes (Crute *et al.*, 1989), and unwinds DNA as it translocates along the lagging strand. The UL5 protein has ATP binding and DNA helicase motifs, while the UL52 component contains the primase active site (Klinedinst and Challberg, 1994). The UL5 and UL52 subunits represent the core enzyme (Calder and Stow, 1990), while the UL8 component stimulates the rate of primer synthesis (Tenney *et al.*, 1994), although there is no apparrent effect on the helicase activity.

1.1.4.3.3.3.4 DNA polymerase.

The HSV DNA polymerase is encoded by the UL30 gene, and exhibits high homology to other DNA polymerases. Formation of a heterodimer with the UL42 gene product which possesses double stranded DNA binding activity is essential for viral replication (Reddig *et al.*, 1994).

The UL30 subunit possesses a 3'-5' exonuclease activity (Hall *et al.*, 1996) which ensures high fidelity DNA replication ('proof-reading'), and an RnaseH activity which facilitates primer degradation (Crute and Lehman, 1989).

The UL42 subunit increases the processivity of the UL30 DNA polymerase. Unlike processivity factors from other organisms, UL42 exhibits an intrinsic DNA binding

activity. The UL42 protein binds at the primer-template junction and reduces the rate of dissociation of the UL30 subunit from the DNA substrate (Gottlieb and Challberg, 1994).

The site of interaction between the UL30 and UL42 proteins has been localised to amino acids 1209-1235 at the C-terminus of UL30 (Digard *et al.*, 1995) while the N-terminal 340 amino acids of UL42 are sufficient for binding UL30 and the activation of the polymerase activity (Tenney *et al.*, 1993).

1.1.4.3.3.3.5 Protein-protein interactions.

The interaction between the components of the replication complex (replisome) are important for the efficient replication of viral DNA. Boehmer and Lehman (1997) suggest a model in which assembly of this complex is initiated by UL9 binding to the high affinity site within the origin. UL9 recruits ICP8, the single stranded DNA binding protein (SSB) which facilitates unwinding of the template DNA. UL9 is thought to recruit the helicase-primase to the origin. Following processive DNA unwinding the UL9 dissociates and unwound regions of DNA are coated with ICP8. Additional replication enzymes are then recruited to the replication fork by ICP8. An interaction between the UL8 subunit of the helicase-primase and ICP8 (SSB) is proposed to ensure concomitant DNA unwinding and priming at the replication fork. The alkaline endo-exonuclease (UL12) which plays a role in the processing of branched DNA replication intermediates also interacts with ICP8.

Punctate pre-repliction sites within the infected cell nucleus have been identified by immunofluorescence studies. With the onset of DNA replication the distribution of the HSV-1 replication proteins changes to globular nuclear domains which may also contain cellular components Studies of the protein interactions suggest that interactions between UL9 bound with ICP8 at an origin of replication and the helicase-primase initiates unwinding and primer synthesis at the origin. The UL30/UL42 polymerase is then recruited.

1.1.4.3.3.3.6 Non-essential HSV-1 genes.

Several HSV-1 genes are dispensable for viral DNA repliction in tissue culture. These include the alkaline endo-exonuclease (UL12); uracil-N-glycosylase (UL2) responsible for removing uracil residues from DNA; dUTPase (UL50) which degrades dUTP to prevent its incorporation into DNA; thymidine kinase (UL23) which phosphorylates thymidine and deoxycytosine, and ribonucleotide reductase $(UL39/UL40)_2$ which reduces ribonucleotides to form DNA precursors.

1.1.4.3.3.3.7 Cellular enzymes.

HSV-1 does not encode a DNA ligase or DNA topoisomerase, and must therefore use the host enzymes. The cellular DNA polymerase α-primase may also be required for viral DNA replication.

1.1.4.3.4 Capsid assembly and DNA packaging.

1.1.4.3.4.1 Structure of the HSV-1 Capsid.

Recent studies of capsid assembly (reviewed by Rixon, 1993; Homa and Brown, 1997) have demonstrated that HSV-1 capsid assembly resembles capsid formation in double stranded DNA phage such as λ and T7.

Three distinct forms of HSV-1 capsid can be isolated from infected tissue culture cells. 'A' capsids are empty capsids which contain no DNA core and are thought to result from abortive packaging of the viral genome (Dilanni *et al.*, 1993). 'B' capsids contain VP22a (cleaved scaffold protein) in the core and were once thought to be precursors of DNA containing capsids, although they are now thought to dead end products. Large cored 'B' capsids, similar to those produced by the protease deficient temperature sensitive mutant ts1201 are now thought to be the precursors capable of DNA packaging. 'C' capsids contain a liquid crystalline DNA core (Booy *et al.*, 1991) and can mature into infectious virions (Perdue *et al.*, 1976).

Cryo-electron microscopy and image reconstruction (Booy *et al.*, 1991; Zhou *et al.*, 1995) have shown that the HSV-1 capsid is an icosahedral protein shell approximately 15nm thick and 125nm in diameter. The major structural components

are 162 capsomers; 150 hexamers make up the edges and faces of the capsid, and 12 pentamers are located at the vertices. The capsomers are made of VP5, the major capsid protein (Schrag *et al.*, 1989; Newcomb *et al.*, 1993) and are held in position by 320 triplexes, which contain two copies of VP23 and a single copy of VP19C (Newcomb *et al.*, 1993; Desai *et al.*, 1994). VP26 is thought to sit at the tip of the hexon, with one VP26 molecule bound to each VP5 subunit in the hexamer (Zhou *et al.*, 1995).

The 75kDa protein encoded by the UL6 ORF is associated with the capsid (Patel and Maclean, 1995). It is present in very low amounts, is maintained in the capsid after packaging of DNA, and possibly has a role in the packaging of viral DNA.

B-capsids contain a large amount of the scaffold protein, and smaller amounts of VP21 and VP24, the UL26 gene products, formed by self cleavage. The scaffold forms a core and interacts directly with the C-terminal portion of VP5 (Hong *et al.*, 1996) to facilitate capsid assembly, and is then lost prior to DNA packaging. The UL26 and UL26.5 open reading frames are co-incident, and as such the C-terminal cleavage site present in the protease (VP24) is also present in the scaffold protein (preVP22a). Cleavage at this site is thought to release the scaffold from the completed capsid, as the C-terminal VP5 binding domain releases the remainder of the polypeptide.

Recombinant baculovirus studies (Tatman *et al.*, 1994; Thomsen *et al.*, 1994) have shown that the minimum number of HSV-1 genes required to produce B capsids is four, the genes encoding the structural proteins (VP5, VP19C and VP23) and the UL26.5 gene (pre-VP22a scaffold). Mutant virus studies suggest that the UL26 product VP21 can substitute for the preVP22a scaffold but the virus yields were significantly reduced (Gao *et al.*, 1994). The presence of the VP24 protease function is essential for the transformation of large cored B capsids formed in insect cells infected with recombinant baculoviruses expressing the VP5, VP19C, VP23 and preVP22a and by infection of cells with the mutant HSV-1 virus *ts*1201, to small cored B capsids.

The transport of the capsid components to the nucleus has been studied (Rixon *et al.*, 1996). PreVP22a and VP19C localise to the nucleus on their own, while VP5, VP23

and VP26 require to interact with other proteins for transport to occur. VP5 can interact with either preVP22a or VP19C, while VP23 is brought to the nucleus by VP19C. The interaction of the proteins also prevents the formation of aberrant capsid structures in the cytoplasm.

Capsids have also been produced from cell free extracts of insect cells infected with the capsid protein expressing baculoviruses (Newcomb *et al.*, 1996). Their formation was dependent upon the presence of VP5, VP19, VP23, and preVP22a.

A recent study using a temperature sensitive mutant in the UL26 encoded maturational protease (*ts*Prot.A) allowed a synchronous wave of virus assembly to be followed (Church and Wilson, 1997). Blocking UL26 protease action resulted in the accumulation of large cored B capsids. Cleavage of preVP22a correlated with the formation of small cored B capsids that are able to package DNA and expel the protein scaffold. The mature C capsids bud into the inner nuclear membrane and become enveloped, although the precise mechanism of envelopment is unclear. Electron microscopy showed that clusters of large cored B capsids were present in cells at the non permissive temperature, and that these began to mature within 2 hours of release. Capsids were observed budding through the nuclear membrane, and enveloped and naked capsids were observed in the cytoplasm 2 hours post-release.

A model for the assembly of HSV-1 capsids is presented in Figure 1.3, based upon information obtained using the cell free assembly system (Thomsen *et al.*, 1994). Partial capsids consisting of a region of shell surrounding a region of scaffold core have been isolated. These form into closed procapsids, which are spherical, contain larger pores and are primarily held together by the triplexes. A conformational switch then occurs to change the procapsid to an icosahedral form. This is analagous to dsDNA bacteriophage capsid assembly (Prevelige and King, 1993).

1.1.4.3.4.2 DNA packaging.

HSV-1 DNA is packaged free of histones, and is highly condensed within the capsid. The DNA is considered to be mostly in a disordered state, similar to the liquid crystalline state of packaged bacteriophage DNA (Booy *et al.*, 1991). Cleavage of concatameric DNA and packaging into capsids is tightly coupled, and involves cis-acting elements within the *a* sequence, seven essential viral gene products, and the

Figure 1.3. Proposed model of HSV-1 Capsid assembly.

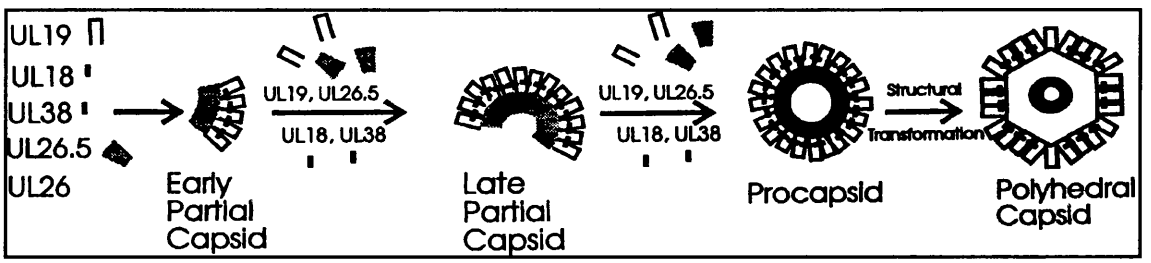

Legend. Partial capsids consisting of a region of shell surrounding a region of scaffold core have been observed. Early partial capsids continue to grow by addition of scaffold (UL26.5) and structural capsid components (UL19, UL18 and UL38: VP5, VP23 and VP19C respectively) to the early partial capsids. The late partial capsids formed in this manner close in on themselves to form closed procapsids, held together primarily by the triplexes (VP23 and VP19C). A conformational switch transforms these procapsids into a mature icosahedral form, with a small scaffold core.

From Homa and Brown, (1997).

UL12 encoded alkaline endo-exonuclease which may be involved in processing the branched DNA intermediates to facilitate packaging (Martinez *et al.*, 1996). The cleavage reaction occurs within the *a* sequence producing an L-terminus with 18bp of the DR1 repeat and a single 3'nucleotide extension, and an S terminus with 1bp of DR1 and a single 3' nucleotide extension. Circularisation reconstitutes the complete DR1 (Mocarski and Roizman, 1982). The sequences within the *a* sequence responsible for cleavage and packaging are designated pac1 and pac2 respectively (Figure 1.4; Deiss *et al.*, 1986). Concatameric DNA is proposed to be bound at the pac sites by a complex of proteins including a component of the capsid (Chou and Roizman, 1989). The DNA is inserted into the capsid until the next *a* sequence of like polarity is reached. Linear full length genomes are produced by a recombination event. Viral proteins essential for cleavage and packaging include the pac2 binding proteins (Chou and Roizman, 1989) and the virus induced DNA endonuclease, which cuts within the Uc region of the *a* sequence (Dutch *et al.*, 1994). Mutational studies implicate several non-structural proteins and capsid proteins in the cleavage-packaging process. The UL25 protein is thought have a role in retaining full length cleaved genomes within the capsid (McNab *et al.*, 1996).

Figure 1.4. Packaging signals within the HSV-1 *a* sequence.

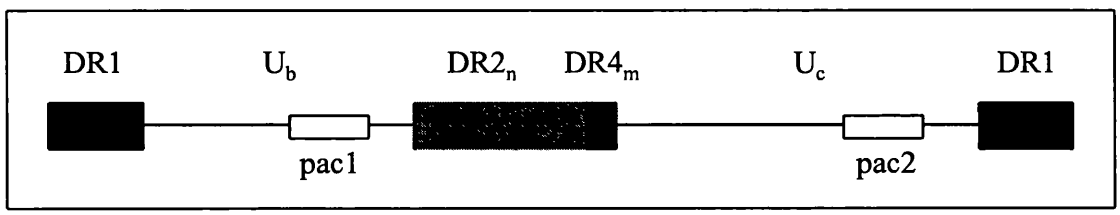

1.1.4.3.4.3 Capsid envelopment and egress.

Regions of modified reduplicated and convex/concave nuclear membrane are observed late in infection. Virus is enveloped at these sites (Roizman and Sears, 1996) which are expected to contain viral glycoproteins on the external surface, and anchorage and tegument proteins on the inner face. HSV glycoproteins are synthesised in essentially the same manner as cellular glycoproteins (Spear, 1985), and HSV glycoproteins containing high mannose N-linked, O-linked and complex

oligosacharide chains have been identified. N-linked glycosylation is required for infectivity, but the requirement for O-linked glycosylation is unknown.

HSV capsids containing DNA attach to these modified areas of the inner lamella of the nuclear membrane and become enveloped. Envelopment of capsids containing less than a full length genome occurs only rarely (Vlazny *et al.*, 1982). Although there is agreement that initial envelopment occurs within the nucleus, envelopment has been observed in the cytoplasm in thin section electron micrographs (Roizman and Sears, 1996), and the lipid content of the virion envelope is more similar to cytoplasmic than nuclear membrane (vanGenderen *et al.*, 1994). Stackpole (1969) proposed a model in which capsids enveloped in the nucleus are de-enveloped at the outer lamella, re-enveloped in the endoplasmic reticulum and released into the extracellular environment by either envelopment at the plasma membrane or fusion of vesicles carrying enveloped virus with the plasma membrane. However, the appearance of de-enveloped capsids in the cytoplasm could represent capsids arrested during transport, or virus reinfecting the cell from within the endoplasmic reticulum, which has become trapped in the cytoplasm rather than being transported to the nuclear pore (Roizman and Sears, 1996). Recent studies (Church and Wilson, 1997) following a synchronous wave of capsid assembly, suggested that pinching off of both nuclear membranes could result in the formation of an enveloped virion within an outer lipid vesicle which could deliver the virions to later stages of the secretory pathway. Alternatively, they suggest that the strain induced in the membrane by the curvature induced during budding could result in fusion of the nuclear membrane with the envelope and the release of naked viral capsids into the cytoplasm. The exact nature of viral envelopment therefore remains unclear.

Translocation across the cytoplasm to the extracellular space was proposed to occur through the Golgi apparatus in a manner similar to the secretion of soluble celluar proteins (Johnson and Spear, 1982). Several recent observations suggest that the process may be at least partially controlled by HSV. For example, in cells defective in processing glycoproteins to a mature form transport does not occur (Banfield and Tufaro, 1990), and gI and gE are essential for the basolateral spread of virus in polarised epithelial cells (Bloom *et al.*, 1997).

1.1.5 REGULATION OF VIRAL GENE EXPRESSION.

HSV genes contain signals that enable their transcription by cellular factors, and in addition contain response elements transactivated by other viral proteins. The HSV-1 genes and *cis*-acting sequences are discussed in the following section.

1.1.5.1 Trans-activation of α genes by α-TIF.

Mackem and Roizman (1982) reported a consensus sequence present in all α genes, and noted that some promoters also contained sites later identified as SP-1 sites. This α-TIF (VP16; Vmw65) consensus binding sequence was identified as 5'-GyATGnTAATGArATTCyTTGnGGG-3'. The α-TIF was localised to the UL48 gene by Campbell *et al.*, (1984). α-TIF forms complexes with DNA in the presence of the cellular protein Oct-1 (McKnight *et al.*, 1987). The functional domains of α-TIF have been mapped. Region 1 (residues 173-241) is basic and intertacts with DNA, while region II (residues 378-389) appears to be responsible for binding the Oct-1 POU domain (Stern and Herr, 1991). The activation domain has been mapped within the highly acidic C-terminal 80 amino acids (Sadowski *et al.*, 1988), and appeared to involve specific hydrophobic interactions as well as less specific charge effects (Cress and Triezenberg, 1991). The identity of the protein that transduces the α-TIF signal is unknown, but reports have suggested that TFIID (Stringer *et al.*, 1990), TFIIB (Lin and Green, 1991) or an unknown adaptor protein (Kelleher *et al.*, 1990) may be involved.

α-TIF is also a structural component of the capsid and although its precise role is unclear, it has been reported to bind to the *vhs* protein (Smibert *et al.*, 1994). This latter interaction would prevent the activation of α genes late in infection by the large levels of α-TIF present in cells at this stage.

The Oct-1 protein with which α-TIF forms a complex interacts with the 'octamer' motif of the cis-regulatory element in the promoters of ubiquitously expressed cellular sequences, such as small nuclear RNAs (LaBella *et al.*, 1988). Oct-1 is a member of a recently recognised homeobox protein family termed POU proteins. Each member contains a conserved POU domain approximately 150 amino acids long, which can be further subdivided into POU-homeo and POU-specific domains.

The POU-homeo domain is involved in DNA binding and in complex formation with α-TIF, while the POU-specific domain of Oct-1 may contribute to DNA binding. The POU domain has been suggested to be a bi-partite DNA binding domain (Sturm and Herr, 1988), which can accomodate the introduction of extra amino acid residues within the linker between the POU-homeo and POU-specific regions.

Stable formation of a complex between α-TIF and Oct-1 requires an additional factor, termed C1 which binds to α-TIF. Another factor, C2 has also been reported. Roizman and Sears (1996) suggest that the multiprotein complex responsible for induction of α genes is initiated by the binding of Oct-1 to the 'octamer' motif within the promoter. The α-TIF/C1 complex binds to the Oct-1/DNA complex and is stabilised by specific protein-protein and protein-DNA interactions. The C2 interaction is thought to involve only protein-protein interactions.

1.1.5.2 Regulatory functions of the α gene products.

1.1.5.2.1 ICP0 (Vmw 110; [RL2]).

ICP0 is a protein of approximate molecular weight 110kDa which is dispensable in tissue culture. ICP0 has been reported to promiscuously *trans*-activate target genes alone, or in conjunction with ICP4 (Vmw 175). Studies of mutants in α0 (Chen and Silverstein, 1992) led to the conclusion that α0 was not essential for viral replication in some cells, but that defects in this gene delay β and γ gene expression.

1.1.5.2.2 ICP4 (Vmw 175; [RS1]).

ICP4 is a phosphoprotein essential for virus gene expression and replication. The phosphate is thought to cycle on and off ICP4. Only phosphorylated ICP4 binds to β and γ promoters. Two molecules of ICP4 bind directly to DNA at consensus and non-consensus sequences (Michael and Roizman, 1990). Most of the key functions of ICP4 reside in the C-terminal half of the protein. Transactivation by ICP4 occurs by binding to constituents of the Pol II transcription machinery, for example TFIIB or the TATA binding protein (Smith *et al.*, 1993).

ICP4 positively regulates β and γ genes, but also negatively regulates specific α genes. ICP4 represses the expression of its own gene and that of α0 by binding to *cis*-acting DNA sequences at the transcription initiation site. Positive regulation of β

and γ genes requires cellular factors in addition to ICP4. It is likely that ICP4 acts by stabilising the assembly of TATA box dependent transcriptional factors, and possibly by localised effects on the DNA (e.g. ICP4 bends DNA) (Roizman and Sears, 1996). Interestingly, ICP4 has been reported to activate some cellular genes (e.g. β-globin) introduced into cells by transfection, probably by the stabilisation of transcription factor interactions.

1.1.5.2.3 ICP27 (Vmw 63; [UL54]).

ICP27 is an essential gene which exhibits both activator and repressor functions. In ICP27$^-$ mutant infections, α genes are over-expressed while β and γ genes are poorly expressed. This effect is mediated at the transcriptional level (McCarthy *et al.*, 1989). Other studies have defined a role for ICP27 in the selection of polyadenylation sites where more than one signal exists (McLauchlan *et al.*, 1989) and in the inhibition of splicing by sequestering snRNPs (Hardy *et al.*, 1992).

1.1.5.2.4 ICP22 (Vmw 68; [US1]) and ICP47 [US12].

As both of these proteins are dispensable in tissue culture neither has been studied in detail. In BHK cells ICP22 mutants exhibited delayed shut-off of β genes, and the expression of γ genes was reduced. The ICP47 gene product is dispensable, and has a role in modulating the host immune response (see Section 1.1.9).

A further regulatory protein is the product of the US11 gene which binds to the 60S ribosomal RNA component, and also to the UL34 mRNA where it may act as an anti-terminator protein upregulating the expression of the UL34 gene (Roizman and Sears, 1996).

1.1.5.3 Regulation of α gene expression.

The trans-activation of α genes by α-TIF has already been described (Section 1.1.6.1). However, studies have shown the activation of α genes in the absence of α-TIF (Post *et al.*, 1981), suggesting that the promoters contain *cis*-acting sites for other transcriptional activators.

The switch off of α proteins which occurs during the expression of the later temporal classes of genes in the presence of both Oct-1 and α-TIF may be explained by the interaction of α-TIF with the *vhs* protein, a γ protein.

Further modulation of the α proteins may occur at the post-transcriptional level, for example the accumulation of ICP0 in BHK cells is modulated by phosphorylation with the UL13 protein kinase.

1.1.5.4 Regulation of β gene expression.

β genes can be expressed readily in the context of the cellular genome, and have response elements for the cellular transcriptional apparatus (TFs, TATA box and a cap site). However, in the context of viral infection, α gene products (especially ICP4) are required for β gene expression. The role of ICP4 in this transactivation is currently unknown.

1.1.5.5 Regulation of γ gene expression.

The regulation of γ genes is affected by the surrounding environment of the gene. In transfection studies using reporter genes fused to a γ promoter, the reporter was expressed as a β protein (Dennis and Smiley, 1984). γ gene expression is dependent upon DNA synthesis. ICP8, the ssDNA binding protein has been proposed to repress γ gene expression. DNA replication may release this repression by seconding ICP8 into the DNA replication machinery. Roizman and Sears, (1996) conclude that DNA synthesis is necessary, but not sufficient for γ gene expression.

The roles of α gene products are as follows. ICP4 is required but is not sufficient for γ gene expression. ICP0 enhances the capacity of ICP4 to transactivate γ genes, while deletion of ICP27 reduced γ gene expression. The requirement for ICP22 is cell type dependent.

The structure of γ promoters remains unclear, with evidence that the presence of a cap site and a TATA box are sufficient for regulated expression of the US11 gene (Johnson and Everett, 1986), contradicted by evidence from studies of gC and gH promoters which suggested that regions within the 5' transcribed noncoding region (5' ncr) are involved (Homa *et al.*, 1986; Steffy and Weir, 1991). Roizman and Sears, (1996) report experiments which show that deletion of regions of the 5' ncr allow the expression of γ_2 genes as α genes, and that the γ_2 5' ncr could theoretically form stem-loop strucures which cannot be formed by the deletion mutant gene

expressed as an α gene. However, direct physical evidence for the presence of this structure is lacking.

1.1.5.6 Post-transcriptional regulation.

Post-transcriptional control of HSV gene expression is proposed to occur at the level of transport of mRNA from the nucleus to the cytoplasmic translation apparatus, and at the translational level (Roizman and Sears, 1996). Translational control is supported by the fact that the repression of host protein synthesis and of viral α genes later in infection occurs in cells lacking nuclei. α-TIF is reported to inhibit the production of host and HSV α genes at the translational level.

1.1.6 THE FATE OF THE INFECTED CELL.

1.1.6.1 Structural alterations.

Early in infection the nucleolus becomes enlarged and is displaced towards the nuclear membrane. At the same time host chromosomes become marginated, although this may not be linked with chromosome breakage (Roizman and Sears, 1996). Later in infection regions of duplicated membrane associated with viral material (possibly tegument proteins) are observed in the nucleus and endoplasmic reticulum and HSV glycoproteins become apparent in the cytoplasmic and plasma membranes.

Infection with wild-type virus causes cells to round up and stick together, while some viral mutants (syn^-) cause cells to fuse into polykaryotes.

1.1.6.2 Shut-off of host macromolecular synthesis.

HSV infection of cells results in the rapid shut-off of host macromolecular metabolism. Host DNA and protein synthesis are shut off, and glycosylation of host glycoproteins ceases. Two stages of shut-off have been identified. The first involves the virion host shutoff (*vhs*, product of UL41) function carried into the cell in the tegument, whilst the second stage requires *de-novo* protein synthesis, and coincides with the expression of β proteins (Roizman and Sears, 1996).

The *vhs* function is responsible for both the destabilisation and degradation of host mRNA, and has also been shown to be responsible for the nondiscriminatory

degradation of HSV α, β and γ mRNAs (Kwong *et al.*, 1988). In vhs⁻ mutants the expression of α and β proteins is extended.

The shutoff of host macromolecular synthesis has two advantages for virus replication. The removal of host mRNAs allows viral messages to be efficiently translated, while the destabilisation of all classes of HSV genes facilitates the rapid transition from one temporal class to the next.

1.1.7 LATENCY.

HSV has the ability to remain latent for the lifetime of the host, a unique phenomenon of herpesviruses (Stevens and Cook, 1971; Stevens 1994). Following replication at the site of primary infection, the virus enters sensory nerves within the mucosal membranes, and the capsid is transported to the neuronal cell body by retrograde axonal flow. The viral genome exists in a circular form in latently infected neurons (Mellerick and Fraser, 1987). No viral gene function is required for the establishment or maintenance of latency (Roizman and Sears, 1996). A fraction of neurons periodically reactivate virus, and infectious virus is transported back to the periphery near the initial site of infection by axonal transport (Cook *et al.*, 1973).

In-vivo experimental models of latency include the mouse eye, footpad or ear models for HSV-1 (Blyth *et al.*, 1976), and the guinea pig vaginal model for HSV-2 (Stanberry *et al.*, 1982). Reactivation from latency occurs at a very low level in the mouse model, but recurrent lesions are observed in the guinea pig. *In-vitro* models of latency involve neuronal tissue culture. However, neurons in culture become permissive for infection and require treatment with nerve growth factor (NGF) to maintain virus in the latent state. Reactivation is induced by the removal of NGF (Wilcox and Johnson, 1987). Only the latency-associated transcripts (LATs) are detected in this system (Doerig *et al.*, 1991).

Results obtained using these model systems led Roizman and Sears, (1996) to propose the division of latency into three stages. The first stage involves the establishment of latency. After infection with wild-type virus, replication occurs at the site of innoculation, and contact with the sensory nerve endings takes place. The severity of the initial infection has an effect on the frequency of reactivation, thought

to be a function of the number of neurons which become infected at this stage. The capsid is transported to the neuronal nucleus by retrograde axonal transport involving microtubules (Lycke *et al.*, 1984; Kristensson *et al.*, 1986). In animal models a short period of viral replication occurs in the ganglia, but this is thought to be an artifact of the animal system. For example, corneal scarification induces host and viral trans-activating factors in neurons containing latent virus which might induce viral replication (Valyi-Nagy *et al.*, 1991).

In the second stage, which begins at most 2-4 weeks after infection, the virus is maintained in a latent state, and no viral replication can be detected.

The final stage is reactivation. In response to certain stimuli (stress, tissue damage or UV light, for example) virus multiplication is stimulated, and viral progeny are translocated by axonal transport to a site near the site of initial infection. The virus multiplication that accompanies reactivation is thought to destroy the cell.

1.1.7.1 Viral gene expression in latently infected cells.

The only transcripts detected to date are the latency associated transcripts (LATs), which are abundant (40-80,000 copies per neuron; Wagner *et al.*, 1988), accumulate in the nuclei of infected neurons and are not polyadenylated (Devi-Rao *et al.*, 1991). However, as many as 80% of latently infected cells do not express detectable concentrations of LAT (Maggioncalda *et al.*, 1996). The major LAT expressed during productive infection is a stable intron approximately 2kb long (Farrell *et al.*, 1991) spliced from a primary 8.3kb transcript (Mitchell *et al.*, 1990), while during latent infection the 2kb LAT and a further splice product of 1.45-1.5kb are present. The 1.45 and 2kb LATs exist in a stable non-linear form (Wu *et al.*, 1996; Rodahl and Haar, 1997). This was shown to be a lariat structure with an unusual branch point which is proposed to increase the stability of the LAT structure (reviewed by Block and Hill, 1997).

The function of the LAT remains unclear, especially as much data demonstrates that LAT is not essential for establishment (Ho and Mocarsky, 1989) or reactivation (Hill *et al.*, 1990), while other studies demonstrate that viruses with mutations in the LAT promoter region reactivate much less efficiently than wild type virus (Fraser *et al.*, 1992). The LAT has not been demonstrated to encode a protein expressed during

latency *in vivo*. It has been suggested that as the LAT is colinear with part of the α0 gene, it may prevent expression of α0 in latently infected cells by an antisense interaction (Stevens *et al.*, 1987). However, a recent *in-vivo* study demonstrated that a normal reactivation phenotype could be restored to a LAT null virus by insertion of the region of LAT lacking this antisense sequence (Perng *et al.*, 1996), and enthusiasm for the antisense model has therefore been reduced (Block and Hill, 1997). ORF P, which is contained within the 8.3kb LAT region has the potential to express a transcript which runs antisense to the neurovirulence factor, γ34.5 (Lagunoff and Roizman, 1994) but so far neither the transcript or the protein have been detected in latently infected neurons. The role of γ34.5 in preventing apoptosis is discussed in Section 1.1.9.

Block and Hill (1997) have suggested possible functions for the LATs based upon recent advances in the study of the function of stable nuclear RNAs. They propose that LAT could: 1) act as a 'sink' for host RNA binding proteins; 2) induce nicks in regions of homologous DNA, or 3) induce the methylation of cytosine residues which has been shown to repress gene transcription.

HSV α gene expression in latently infected neurons is repressed. The lack of α gene products is most likely due to a host cell repressor protein, as both α-TIF and Oct-1 have been demonstrated in latent neurons, and α gene expression would therefore be expected to be stimulated.

1.1.7.2 Copy number of viral DNA in latently infected neurons.

Viral DNA is present in latently infected trigeminal ganglia at levels of approximately 0.1-1 viral genome per cell (Rock and Fraser, 1985). As only about 10% of cells in the ganglia are neurons, each neuron must contain more than one copy of the viral genome (Roizman and Sears, 1987). Either more than one viral genome can enter the neuron at the establishment of latency, or the viral genome is replicated by the cellular machinery during latency, a proposal supported by the identification of a host dependent origin in the viral genome (Sears and Roizman, 1990).

1.1.7.3 Maintenance of and reactivation from latency.

No gene has yet been identified as being essential for the maintenance of latency.

In humans latent virus is reactivated following local stimuli such as injury to tissues harbouring latently infected neurons, or by systemic stimuli such as stress. The molecular basis and order of viral gene expression is unknown, and conflicting evidence exists about the possible role of the LATs and ICP0 in reactivation. Block and Hill (1997) have reviewed studies using viral mutants within the LAT region, and identified specific regions that are essential for maximal adrenergic reactivation which may be different from the regions required for spontaneous reactivation. Deletions within the cAMP response element within the LAT promoter abolish the adrenergic reactivation response (Bloom *et al.*, 1997), and further regions within the LAT promoter have been identified as being essential for *in-vivo* reactivation in the rabbit eye model (Hill *et al.*, 1997).

1.1.7.4 A model of latency.

Roizamn and Sears (1996) proposed the following model of the latent state.

A lack of α gene expression is observed in latently infected neurons, and this may be due to the lack of host factors other than Oct-1, or the presence of a repressor protein. Repression could also be an effect of DNA secondary structure. Either mechanism of repression could be released by DNA replication.

Activation of virus multiplication is the consequence of the cumulative effect of stimuli on each virus containing cell, resulting in the replication of the viral genome by the cellular machinery. Increase in the copy number of the viral genome dilutes the repression effect on α gene expression, probably in the presence of an activation factor such as the induction of a host transcription factor.

1.1.8 MODULATION OF HOST DEFENCE MECHANISMS.

HSV has evolved a variety of mechanisms to avoid the host defence mechanisms. These are discussed briefly below.

The γ34.5 gene product has been shown to affect the ability of HSV to replicate in the CNS (Whitley *et al.*, 1993), as determined by the high LD_{50} for intracerebral innoculation of a γ34.5 mutant virus (>10^7pfu). Study of mutants in this gene indicated that they trigger a premature total shut-off of protein synthesis, killing the cell but reducing viral replication dramatically in the process (Chou and Roizman, 1992). This response is linked to viral DNA synthesis. The γ34.5 protein has homology to cellular proteins (MyD116 and GADD34) induced by differentiation, growth arrest or DNA damage respectively. The carboxyl terminus of γ34.5 which is homologous to the cellular proteins is essential to prevent this cellular shut down (Chou and Roizman, 1994). From the point of view of the virus, the γ34.5 protein prevents early cell death which would prevent virus replication and spread throughout the body.

In addition HSV induces two types of Fc receptor (FcR) on the cell surface. One, a complex of gE and gI binds monomeric IgG (Johnson *et al.*, 1988), whilst gE alone binds polymeric IgG (Dubin *et al.*, 1991). Both FcRs appear to play a role in protection against antibody dependent cell cytotoxicity (Dubin *et al.*, 1991).

A further interaction with the immune system is the interaction of complement component C3b with HSV gC1 and gC2 (Siedel-Dugan *et al.*, 1988), via interactions which include, among others, a CR1 homologous domain within gC (Hung *et al.*, 1992). The functional significance of this interaction with respect to viral protection from complement has yet to be elucidated. Studies of this interaction and those of the HSV FcRs are hindered by the multifunctionality of the HSV proteins.

A final defence mechanism involves the modulation of the $CD8^+$ cytotoxic T-cell response ($CD8^+$ CTL). The α47 gene product was shown to cause the retention of MHC class 1 molecules within the cytoplasm, preventing peptide presentation at the

cell surface (York *et al.*, 1994) by direct interaction with the transporter involved in antigen presentation (TAP) (Hill *et al.*, 1995). A further, as yet undefined viral function also appears to have a role in inactivation $CD8^+$ CTLs (York and Johnson, 1993).

1.2 CELLULAR TRANSFORMATION BY VIRUSES.

Cellular transformation can be induced by both RNA and DNA tumour viruses, although each group utilises distinct mechanisms (recently reviewed by Nevins and Vogt, 1996). Table 1.4 summarises some of the viral groups involved in transformation and the type of tumour they induce. Tumour formation is not an inevitable consequence of viral infection, suggesting that oncogenesis is a multi-step process in which each step constitutes an independent and irreversible genetic change that contributes to the deregulation of cell growth. Viral infection is only one of these steps, and transformation only occurs if other changes also occur in the same cell.

All mechanisms of virus induced oncogenic transformation share important characteristics.

1) A single infectious virus particle is sufficient for transformation- a single hit process.

2) All or part of the viral genome persists in the transformed cell, but often no virus progeny are produced.

3) In almost all cases of viral transformation at least part of the viral genome is expressed.

4) Transformation results from the corruption of cellular growth signals.

5) Reversion of the transformed phenotype can be achieved by specific interference with the viral effector molecule.

Transformation induces changes in both cell growth (formation of foci, reduced growth factor requirement and loss of anchorage independence) and morphology (loss of actin stress fibers, redistribution of microfilaments).

Table 1.4. Tumour viruses and their associated cancers.

Virus Group	Examples	Tumour types
Retroviridae		
Mammalian B type.	Mouse mammary tumour virus	Mammary carcinoma
		T-cell lymphoma
Mammalian C type.	Murine leukaemia virus	Leukaemia, lymphoma,
	Kirsten sarcoma virus	sarcoma and other
	Feline leukaemia viruses	malignancies.
Avian C type.	Avian leukosis and sarcoma viruses	Sarcoma, B-cell lymphoma,
	Rous sarcoma virus	leukaemia, various
		carcinomas.
HTLV-BLV.	**Human T-lymphotrophic virus**	**T cell leukaemia**
	Bovine leukaemia virus	B-cell lymphoma
DNA viruses		
Adenoviridae	**All types**	**Various solid tumours**
Hepadnaviridae	**Hepatitis B virus**	**Hepatocellular carcinoma**
Herpesviridae	**EBV**	**Burkitt's lymphoma,**
		nasopharyngeal carcinoma
	HHV-8	**Kaposi's sarcoma**
Papovaviridae	SV40, polyoma virus	Various solid tumours
	HPV, Shope papillomavirus	**Carcinomas**, Papillomas
Poxviridae	Shope fibroma virus	Myxomas, fibromas

Data from Nevins and Vogt (1996).

Viruses and cancers highlighted in **bold** are human pathogens or diseases.

Virus induced transformation has provided insights into intracellular signalling (RNA tumour viruses) and cell cycle regulation (DNA tumour viruses), and each of these transforming viral groups will be discussed in the following sections.

1.2.1 TRANSFORMATION BY RNA TUMOUR VIRUSES.

RNA tumour viruses have been shown to encode proteins involved in almost every stage of the signal transduction pathway (Figure1.5 and Table 1.6).

RNA tumour viruses (retroviruses) have a single stranded RNA genome bounded by long terminal repeats which contain promoter elements. This is reverse transcribed into double stranded DNA, and becomes integrated into the host cell genome, where expression of the provirus occurs from the viral transcriptional regulatory sequences. Integration of the virus into the genome is the basis for the acquisition of cellular DNA sequences (transduction) and insertional activation (or inactivation) of cellular genes.

Retroviruses can transform cells by three distinct mechanisms (reviewed by Nevins and Vogt, 1996; see Table 1.5).

Table 1.5. Three classes of transforming retroviruses.

Virus category	Tumour latency period	Efficiency of tumour formation	Oncogenic effector	State of viral genome	Transforms cultured cells?
Transducing retroviruses	Short-days	High (~100%)	Cellular oncogene carried in viral genome (v-onc)	Integrated. Replication defective	Yes
cis-activating retroviruses	Mid-weeks/months	High/mid	Cellular oncogene activated in situ	Intact. Replication competent	No
trans-activating retroviruses	Long-months/years	Low (5%)	Virus coded transcription regulator	Intact. Replication competent	No

Data from Nevins and Vogt, 1996.

Two of these mechanisms involve the action of oncogenes. The 'transducing retroviruses' have picked up cellular oncogenes which have often then acquired

Figure 1.5. A generalised multi-step signal transduction pathway.

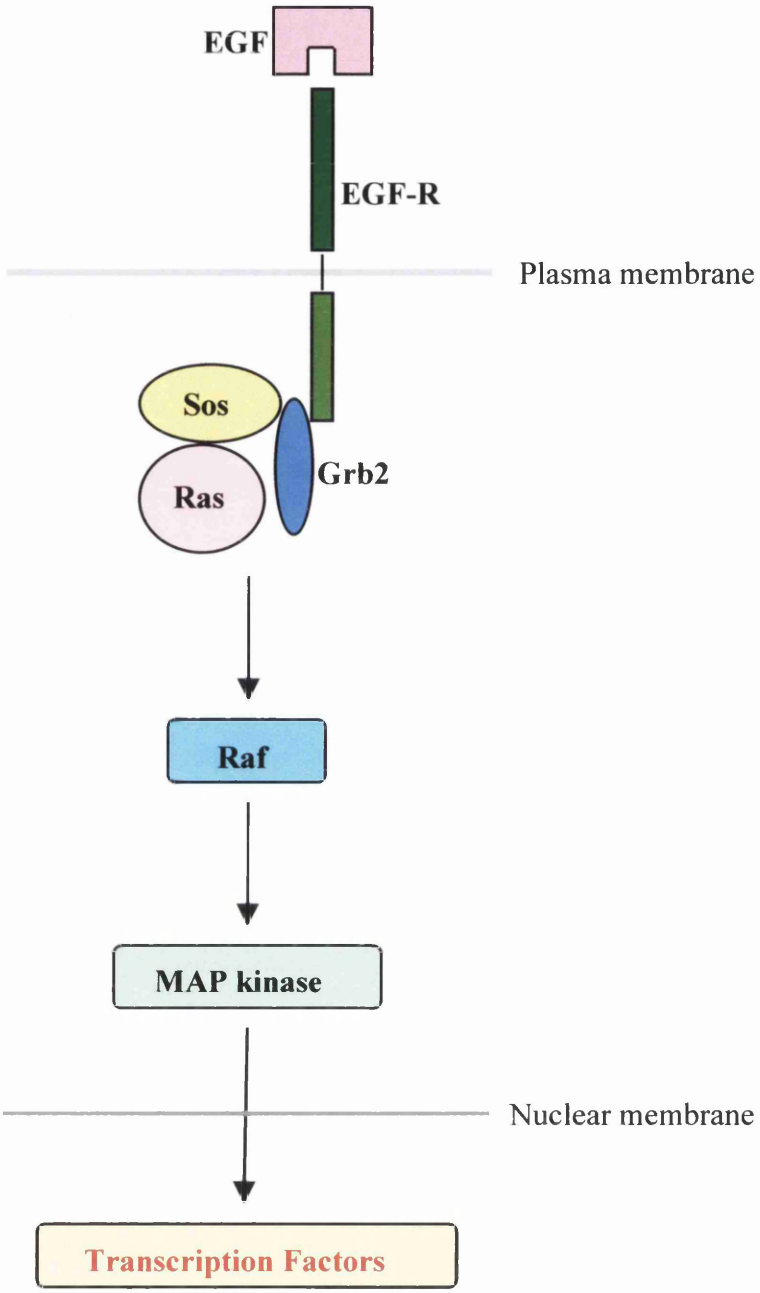

Epidermal growth factor (EGF) binds to the EGF receptor inducing dimerisation. The tyrosine kinase activity of the receptor is increased, and regulatory autophosphorylation of the cytoplasmic tail occurs. The adaptor protein Grb2 (which contains *src* homology (SH) regions) binds to phosphotyrosines in the receptor. The SH3 domains of Grb2 are recognised by the Sos protein, and this complex binds to Ras. The Sos is a nucleotide exchange factor which moves *Ras* into the active GTP bound state. GTP-*Ras* binds to the cytoplasmic serine/threonine kinase Raf, increasing its activity and initiating a kinase cascade which includes MAP kinase and results in signal transduction to transcription factors in the nucleus (by an as yet unknown mechanism). Derived from Nevins and Vogt, 1996.

Table 1.6. Retroviral oncogenes and their cellular homologues.

Oncogene	Retrovirus	Function of cellular homologue
Growth Factors		
sis	Simian sarcoma virus (SSV)	PDGF
Tyrosine kinase growth factor receptors		
erbB	Avian erythroblastosis virus (AEV)	EGF receptor
fms	McDonough feline sarcoma virus (FeSV)	CSF-1 receptor
Hormone receptors		
erbA	AEV	Thyroid hormone receptor
G proteins		
H-ras	Harvey murine sarcoma virus (MSV)	GTPase
K-ras	Kirsten MSV	GTPase
Adaptor protein		
crk	Avian sarcoma virus (ASV)	Signal transduction
Non-receptor tyrosine kinases		
src	Rous sarcoma virus (RSV)	Signal transduction
abl	Abelson murine leukaemia virus (MuLV)	Signal transduction
Serine-threonine kinases		
mos	Moloney MSV	Germ cell maturation
raf	MSV	Signal transduction
Nuclear proteins		
jun	ASV	AP-1 transcription factor
fos	MSV	AP-1 transcription factor
myc	Avian myelocytoma virus; ALV	Transcription factor
myb	Avian myeloblastosis virus (AMV)	Transcription factor

Data from Hesketh, (1995) and Nevins and Vogt, (1996).

mutations. These viruses have almost always lost sequences necessary for replication and therefore require helper virus to produce infectious progeny. The transducing retroviruses induce tumours and transform cells very rapidly. The *cis*-acting retroviruses act by integrating into the cellular genome in the vicinity of a cellular oncogene. These viruses are replication competent, produce tumours more slowly, and fail to induce oncogenic transformation in tissue culture cells. The third (currently hypothetical) group of viruses code for a viral transactivating protein which may interfere with host gene expression.

The cellular oncogenes acquired by the transducing retroviruses are involved in the control of cell growth. Table 1.6 presents examples of viral oncogenes from each class of protein involved in a generalised signal transduction pathway (illustrated in Figure 1.5). Cellular oncogenes expressed under normal conditions are not oncogenic. Unregulated expression of the cellular oncogene, or alterations in the structure of the oncoprotein are required for transformation.

All of the transduced retroviral oncogenes are non-essential for viral replication. In addition to carrying the oncogene into the cell, the virus also exercises transcriptional control over the oncogene. Thus point mutation, gene amplification or transcriptional upregulation can activate the intrinsic malignant potential of cellular oncogenes. Temperature sensitive and non-conditional mutants in transduced oncogenes have shown that the oncogene is required for both the initiation and maintenance of the transformed phenotype (Kawai and Hanafusa, 1971: Shih *et al.*, 1979). Furthermore, transduced oncogenes have been excised from their parental virus and expressed at high levels from expression vectors where they confer oncogenicity on the new vector (Hughes *et al.*, 1987). Cellular transformation is an inevitable consequence of infection with a transducing retrovirus, and as this transformation is a single hit process, the tumours are normally polyclonal. Some retroviruses contain two co-operating oncogenes. For example, avian erythroblastosis virus R carries the transforming *erbB* oncogene and the *erbA* oncogene which enhances the transformation efficiency of *erbB* (Bister, 1986).

1.2.1.1 The functions of some transduced retroviral oncogenes.

A brief description of the function of some of the known retroviral oncogenes from each of the groups identified in Table 1.6 will now be presented. The structure and function of these oncogenes is reviewed by Hesketh (1995) and Nevins and Vogt (1996).

1.2.1.1.1 *Sis*: Growth factor.

Sis is the oncogene of simian sarcoma virus, and displays 88% homology to the B chain of human platelet derived growth factor (PDGF). *V-sis* is expressed as a fusion with the viral envelope protein which facilitates the targetting of protein into the endoplasmic reticulum. Processing of the *v-sis* product produces a p24 homodimer similar in structure to PDGF, which binds to the PDGF-receptor and induces receptor internalisation, phosphorylation, and stimulates the mitogenic response of the cell. Nevins and Vogt (1996) suggest that transformation results from an autocrine stimulation of cell growth (due to expression of *v-sis* from the integrated provirus), and this is supported by evidence that cellular PDGF is transforming if expressed at high levels.

1.2.1.1.2 *ErbB* and *fms*: Altered receptors and constitutive mitotic signals.

Hesketh (1995) reports that *v-erbB* has close homology to the EGF receptor. EGFR has four functional domains- an amino terminal extracellular ligand binding domain, a transmembrane domain, a kinase domain and a carboxyl terminal regulatory domain containing phosphorylation sites. *v-erbB* lacks the negative regulatory phosphorylation site and extracellular ligand binding domain, and acts as a constitutively active EGF receptor, stimulating the activation of *Ras* and subsequently of cellular transcription factors.

V-fms is derived from the gene for the macrophage colony stimulating factor receptor (CSF-1R), which has a role in haemopoiesis and possibly during embryogenesis (Hesketh, 1995). The receptor has five external immunoglobulin repeats which are involved in ligand binding and receptor dimerisation. Point mutations within this dimerisation domain are essential for the oncogenic potential of *v-fms*. The absence of phosphorylation sites within the C-terminal regulatory domain prevents negative

regulation of the intrinsic tyrosine kinase domain, resulting in a constitutively active receptor. This activates *Src* family kinases and the Ras-GTP pathway (illustrated in Figure 1.5).

1.2.1.1.3 *Src* and *abl*: membrane bound non-receptor tyrosine kinases.

Src encodes a 60kDa tyrosine kinase that is associated with the plasma membrane. *C-src* contains an amino terminal myristylation domain, two *src* homology domains (SH2 and SH3), a kinase domain and a C-terminal regulatory domain. The *v-src* protein has lost part of the regulatory domain including the site of negative regulatory phosphorylation (residue Y527), which causes the *c-src* protein to fold into an inactive conformation. Downstream targets of *src* include SHC, an adapter protein which associates with Grb2 and Sos to activate *ras* (see Figure 1.5), and focal adhesion kinase (FAK) which is maintained in an active state and causes the over-phosphorylation of cytoskeletal proteins which is involved in anchorage independent growth.

The *abl* oncogene (derived from Abelson murine leukaemia virus (A-MuLV)) is also plasma membrane associated and has a weak intrinsic tyrosine kinase activity. The viral protein is expressed as a gag-*abl* fusion and interacts with the membrane via viral gag sequences. The gag domain also increases the half life of the fusion protein. *V-abl* contains SH2 and SH3 domains which interact with the signal transduction proteins, and a catalytic domain. The *c-abl* protein appears to be a negative regulator of cell growth, with the SH3 domain being a target of negative regulation. Deletion of this domain activates the oncogenic potential of *abl*. An activated *abl* gene is also found in human chronic myeloid leukaemia, where the c-onc is translocated to the *bcr* region, resulting in a single fused transcript in leukaemic cells.

1.2.1.1.4 *Ras*: Growth regulatory GTPase.

Three closely related *ras* genes have been identified in human cells, of which only *N-ras* encodes a functional 21kDa GTPase protein. Two of the human genes (*H-ras* and *K-ras*) have been found in a number of 'transducing retroviruses', including Harvey and Kirsten murine sarcoma viruses.

Ras proteins are nodal points in the signal transduction pathway, and can be considered as membrane bound binary switches. When bound to GTP the *ras* protein is in an active state: hydrolysis of the GTP to GDP transforms the protein to an inactive form. At least three classes of protein regulate *ras*. Guanine nucleotide exchange factors (GEF) have an activating effect by stimulating exchange of GDP for GTP. GTPase activating proteins (GAP) attenuate *ras* by stimulating the conversion of GTP-*ras* to GDP-*ras*. Guanine nucleotide dissociation inhibitors are less well understood, but bind to GDP-*ras* and may interfere with both GEF and GAP functions.

Ras oncogenicity is greatly increased by point mutations which map to the region involved in interactions with GAP proteins and maintain *ras* in a GTP bound active state. Mutated ras genes have been found in human cancers, especially bladder, lung and colon cancers. Oncogenic *ras* activates protein kinase C and has been reported to activate transcription of other cellular oncogenes, including *fos*, *jun* and *myc*, and to repress the transcription of genes involved in differentiation (e.g. *myoD*).

1.2.1.1.5 *Mos* and *Raf*: Non- membrane associated serine/threonine kinases.

The *mos* oncogene was found in Moloney sarcoma virus, and can transform murine fibroblasts in culture. *V-mos* is expressed as an Env/*mos* fusion of 37kDa mostly in the nucleus, although *c-mos* is mainly cytoplasmic. *C-mos* can transform cells if overexpressed in culture, and has homology to *Src* and cAMP dependent protein kinases. The cellular protein is expressed at a very low level, except in germ cells. *C-mos* is required for meiosis and is a component of cytostatic factor (CSF), and also stabilises $p34^{cdc2}$ during meiosis. *C-mos* also associates with and phosphorylates tubulin and may therefore have a role in meiotic spindle formation, activates MAP kinase, and has been proposed to transform cells by pushing interphase cells into mitosis.

Raf is a cytoplasmic serine/threonine kinase, thought to be a second nodal point in the signal transduction pathway alongside *ras*. *Raf* is activated by a number of receptors with intrinsic tyrosine kinase activity, and can transduce this signal via activation of MAP kinase kinase independently of *ras*.

1.2.1.1.6 *Jun, Myc* and *erbA*: Transcription factors.

C-jun is a component of the AP-1 transcription factor, usually found in a heterodimer with *fos*, but also present as a *jun-jun* homodimer. The *jun* protein contains a leucine zipper dimerisation domain, a basic region that binds DNA and a transactivation domain (reviewed by Curran and Vogt, 1991). Dimerisation is essential for DNA binding, transactivation and transformation. The *v-jun* protein (from ASV) contains two point mutations affecting negative regulatory phosphorylation sites (S243) and a 27bp deletion in the 3' untranslated region which seems to stabilise the mRNA. The precise mechanism of transformation is unclear, but may be a function of altered DNA sequence preference and hence altered target gene activation, or to constitutive activation of target genes.

Myc is a helix-loop-helix/leucine zipper sequence specific DNA binding protein expressed in most cells during proliferation. Abberant expression of *myc* is involved in several human tumours. Many, but not all Burkitt's lymphomas contain the *myc* gene translocated to the Ig locus, resulting in the constitutive activation of *myc*. *Myc* forms a heterodimer with *Max* via a leucine zipper motif, and this interaction is essential for DNA binding, transformation and *myc*-induced apoptosis of haemopoietic cells. The expression of *myc* is growth factor dependent and is essential for cell-cycle progression, perhaps due to its activation of the cyclin A and E genes. High levels of *myc* expression accelerate growth, whilst reduced levels correlate with the onset of cellular differentiation. In addition, high levels of *myc* expression represses the activation of MHC-1 and N-CAM genes and correlates with increased metastatic potential.

A different class of transcriptional regulator is encoded by *v-erbA*. *V-erbA* is a homologue of the thyroid hormone receptor (THR), and has a ligand binding domain, a transactivation domain and a two zinc-finger DNA binding motif. Although *v-erbA* can act as a repressor of thyroid hormone dependent transcription, its oncogenic potential is primarily due to an inhibitory effect on the retinoic acid receptor (RAR). The *v-erbA* protein acts as a constitutive repressor of THR and RAR and thus prevents the apoptosis of early erythroblasts that normally occurs in the absence of differentiation signals.

1.2.1.2 Cis-activation of oncogenes.

Many retroviruses do not carry an oncogene, but cause transformation by insertion into the host genome (reviewed by Nevins and Vogt, 1996). These viruses induce monoclonal tumours with a long latent period, but cannot transform cells in culture. Viral coding sequences are not required for maintenance of the transformed state. Two mechanisms of insertional activation have been identified. The first is 'promoter insertion', in which a read through product from the viral (usually 3') LTR is expressed. This fusion often has regions of sequence deleted from the cellular homologue, and as these are often negative regulatory domains this contributes to the oncogenicity of the protein. 'Enhancer insertion' requires only that the virus integrates in the vicinity of the cellular oncogene, and the orientation/position is not important for activation.

Examples of insertional activation include Rous associated virus (RAV) induced tumours which show elevated *myc* transcription as a result of insertion of the viral promoter upstream of exon 2 of *c-myc*. In some RAV associated tumours integration downstream of the *myc* gene has been observed, an example of activation by enhancer insertion. Other insertional activation events include the 'promoter insertion' activation of *erbA* producing a truncated, constitutively active EGF receptor, and MMTV which integrates at several preferred sites which are close to three cellular genes designated int1, int2 and int3, known to be involved in development in Drosophila.

1.2.2 TRANSFORMATION BY DNA TUMOUR VIRUSES.

While retroviral oncogenes appear to have been transduced from the cell and have little or no role to play in the normal viral life-cycle, the DNA tumour virus oncogenes are essential viral gene products that bear no relation to cellular counterparts. The efficiency of DNA tumour virus transformation is low (Nevins and Vogt, 1996), due to inefficient integration of the virus into the host genome, and to the fact that viral infection of permissive cells leads to their destruction. Only in non-permissive cells can an oncogenic event be observed. The function of the DNA tumour virus oncogenes seems to be to induce quiescent or terminally differentiated

cells to enter the cell cycle to provide an environment suitable for viral replication. However in non-permissive cells, or in the presence of viral mutations which prevent replication, this stimulation to enter S-phase can lead to cellular transformation.

The genes encoding the transforming activities of adenovirus, polyomavirus/SV40 and papillomavirus have been identified, and share common mechanisms of transformation (reviewed by Nevins and Vogt, 1996). The adenovirus oncogenes were identified as the product of the E1A gene, and the 55kDa product of the E1B gene. A 19kDa polypeptide also expressed from the E1B gene is involved in preventing apoptosis (see Section 1.2.2.2.2). These proteins have been shown to interact with the cellular proteins $p105^{Rb}$ and p53 respectively. The functional significance of these interactions (and those of the viral oncoproteins described below) with respect to cellular transformation is discussed in Section 1.2.2.1.

In Polyoma virus and SV40 the transforming proteins are the T-antigens. Large T of SV40 binds to p53 and $p105^{Rb}$, whilst polyoma virus large T binds only to $p105^{Rb}$. The small t-antigen of both viruses has been reported to activate RNA Pol II and RNA Pol III dependent transcription, and to modulate the action of a cellular phosphatase. Thus small t-antigen has an enhancing effect on the efficiency of transformation. In addition to the T and t-antigens, polyoma virus encodes a middle T-antigen, which is a plasma membrane protein that binds to and activates *src* and PI-3 kinases.

The transforming functions of human papillomavirus (HPV) are provided by the E6 and E7 open reading frames. Integrated HPV DNA isolated from tumours is usually integrated via a disruption in the E2 ORF, which normally functions to regulate the expression of the E6 and E7 open reading frames. HPV E6 protein binds to p53 and the E7 protein binds to cellular $p105^{Rb}$. The relationship between HPV and cervical carcinoma is discussed in Section 1.2.4.2.

1.2.2.1 Common cellular targets for DNA tumour virus oncoproteins.

All of the small DNA tumour viruses encode oncoproteins that bind to either p53 or $p105^{Rb}$ (summarised in Table 1.7).

Table 1.7. Cellular targets of DNA tumour virus oncoproteins.

Virus	Gene product	Cellular target
Adenovirus	E1A	$p105^{Rb}$
	E1B	p53
SV40	T antigen	p53, $p105^{Rb}$
Polyoma	T antigen	$p105^{Rb}$
Papillomavirus	E6	p53
	E7	$p105^{Rb}$

The regions of the viral oncoproteins involved in binding to these cellular targets were shown to be important for the transforming ability of the viruses, suggesting a role for these cellular targets in the suppression of transformation. This is further supported by the status of the p53 and $p105^{Rb}$ genes within cervical cancer cell lines. Mutant p53 and $p105^{Rb}$ genes were observed in HPV negative cell lines, while p53/$p105^{Rb}$ are wild type in HPV positive cell lines (Crook *et al.*, 1992) and are inactivated by interaction with the products of the HPV E6/E7 open reading frames.

1.2.2.1.1 Inactivation of p53 function.

The identification of p53 as a tumour supressor gene (reviewed by Lane, 1992) and its interaction with viral oncoproteins led to the proposal that these interactions may play a role in cellular transformation. Although each of the viral oncoproteins binds to different regions of the p53 protein via different mechanisms, the effect of these interactions is the same- inactivation of p53 function (reviewed by Hesketh, 1995). The HPV E6 protein triggers the ubiquitin mediated degradation of p53 via a cellular protein termed E6-AP (Hurbregste *et al.*, 1992), whilst large T antigen appears to stabilise p53 in an inactive state. p53 oligomers act as a sequence specific transcription factor (Funk *et al.*, 1992), and cellular targets have recently been identified. The gene termed WAF1 is one such target (ElDiery *et al.*, 1993), the product of which ($p21^{waf1}$) has previously been identified as an inhibitor of the G1 cyclin/kinase activity (Xiong *et al.*, 1993). By inhibiting the function of the G1 cyclin dependent kinases, $p21^{waf1}$ induction by p53 may be one mechanism by which

p53 suppresses cell growth. Degradation of p53 could therefore lead to constitutive activation of G1 cyclin/kinase activity, and promote passage through the cell cycle (see Figure 1.6A). Furthermore, the product of a cellular gene termed *mdm2* interacts with p53 in a manner similar to the adenovirus E1B protein, and has been proposed to block p53 growth suppression in normal cells. Amplification of the *mdm2* gene has been implicated in oncogenesis (Fakharzadeh *et al.*, 1991). In addition, p53 represses the expression of cellular genes including *bcl2*, *fos*, *jun*, *myb* and $p105^{Rb}$ (Hesketh, 1995). Interfering with this inhibitory action of p53 would allow the over-expression of the cellular oncogenes which may then contribute to cellular transformation. Wild type p53 also functions to prevent mitosis occurring if DNA damage is detected in the cell. In the presence of mutated or inactivated p53 mitosis can occur in the cell before DNA damage is repaired, and this may lead to the production of malignant clones. This is illustrated in Figure 1.6A.

1.2.2.1.2 Inactivation of the retinoblastoma protein function.

The $p105^{Rb}$ protein has been identified as a component of a cellular transcription factor complex, E2F (Bandara and LaThangue, 1991). In this complex $p105^{Rb}$ acts to repress the binding of E2F to specific DNA targets, including cellular genes involved in DNA synthesis or nucleotide biosynthesis and the adenovirus E2 open reading frame (Qin *et al.*, 1992). The interaction between E2F and $p105^{Rb}$ is dependent upon a conserved sequence in the retinoblastoma family proteins known as the 'Rb pocket'. The viral oncoproteins of SV40/polyoma, adenovirus and papilloma viruses (T-antigen, E1A and E7 respectively) bind to this pocket, and can disrupt the $p105^{Rb}$-E2F complex, facilitating activation of the E2F target genes. $p105^{Rb}$ elicits a block at G1 of the cell cycle, which is released by the disruption of the $p105^{Rb}$-E2F complex. This model is presented diagramatically in Figure 1.6B. Other cellular targets have been proposed for the $p105^{Rb}$ family of proteins, including the transcription factors *c-myc* and *myoD* (Rugsti *et al.*, 1991; Gu *et al.*, 1993).

Figure 1.6A. The role of p53 in cell cycle regulation.

Legend. p53 is a sequence specific transcription factor, with several targets that have a role in control of the cell cycle. One of these targets is *WAF1*, which is an inhibitor of G1 cyclin dependent kinases (CDC2/cyclin E in this instance), and acts to prevent entry into S-phase in response to elevated levels of p53. Inactivation of p53 therefore allows passage through the cell cycle without the normal check point controlled by $p21^{WAF1}$. This could allow replication of the damaged DNA before repair was completed. The inactive cyclin dependent kinase complexes are shaded red, and the active forms in green.
p53 induced apoptosis is the normal cellular response to DNA damage that cannot be repaired. Inactivation or mutation of p53 prevents the apoptotic response to DNA damage, and mitosis can proceed with mutations present in the genome, potentially leading to transformed clones of cells.

Figure 1.6B. The role of $p105^{Rb}$ in cell cycle regulation.

Legend. $p105^{Rb}$ is a component of the transcription factor complex E2F, where it acts to repress the activation of E2F bound to the target DNA sequences. $p105^{Rb}$ elicits a block in G1 of the cell cycle, by preventing the activation of E2F responsive genes.
The affinity of $p105^{Rb}$ for the E2F component of the complex is modulated by phosphorylation. The phosphorylated form of $p105^{Rb}$ is unable to bind to E2F, and the target genes are therefore able to be activated, stimulating progression to S-phase (scheme **A**).
The hypo-phosphorylated form of $p105^{Rb}$ can bind to E2F bound to its' target sequence, and prevents transcription of the target genes, thereby maintaining the cell in G1 (scheme **B**).
The viral oncoproteins of human papillomavirus, adenovirus and SV40 (E7, E1A and T-antigen respectively) can mimic the effect of phosphorylation of $p105^{Rb}$ by binding to the protein and preventing it's association with E2F. This allows expression of the target genes and passage into S-phase (scheme **C**).
In this figure, active proteins (and genes) are shaded green, and inactive forms are shaded red. For example, in scheme **C**, $p105^{Rb}$ (red) is inactivated by the viral oncoproteins, leaving E2F in an active form to stimulate transcription of the target gene (both green).

Figure 1.6. The role of the tumour supressor genes p53 (**A**) and $p105^{Rb}$ (**B**) in regulating cell growth.

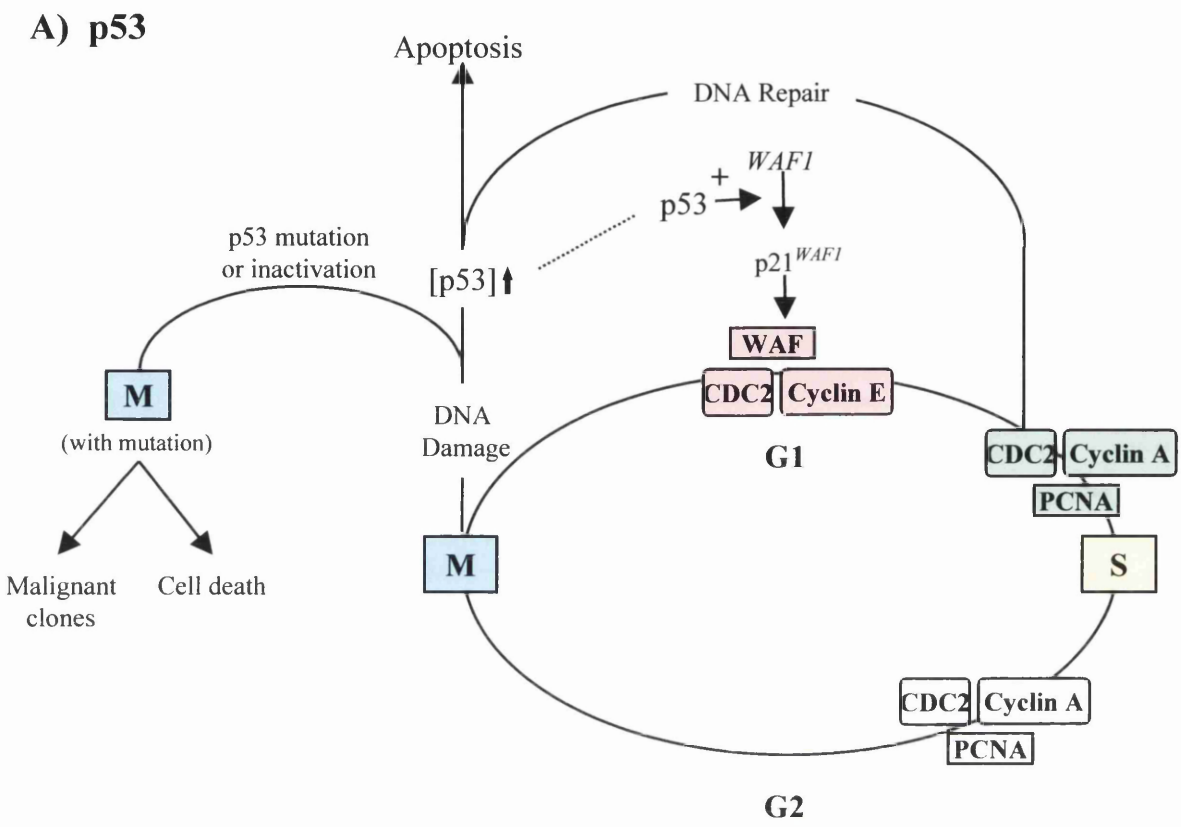

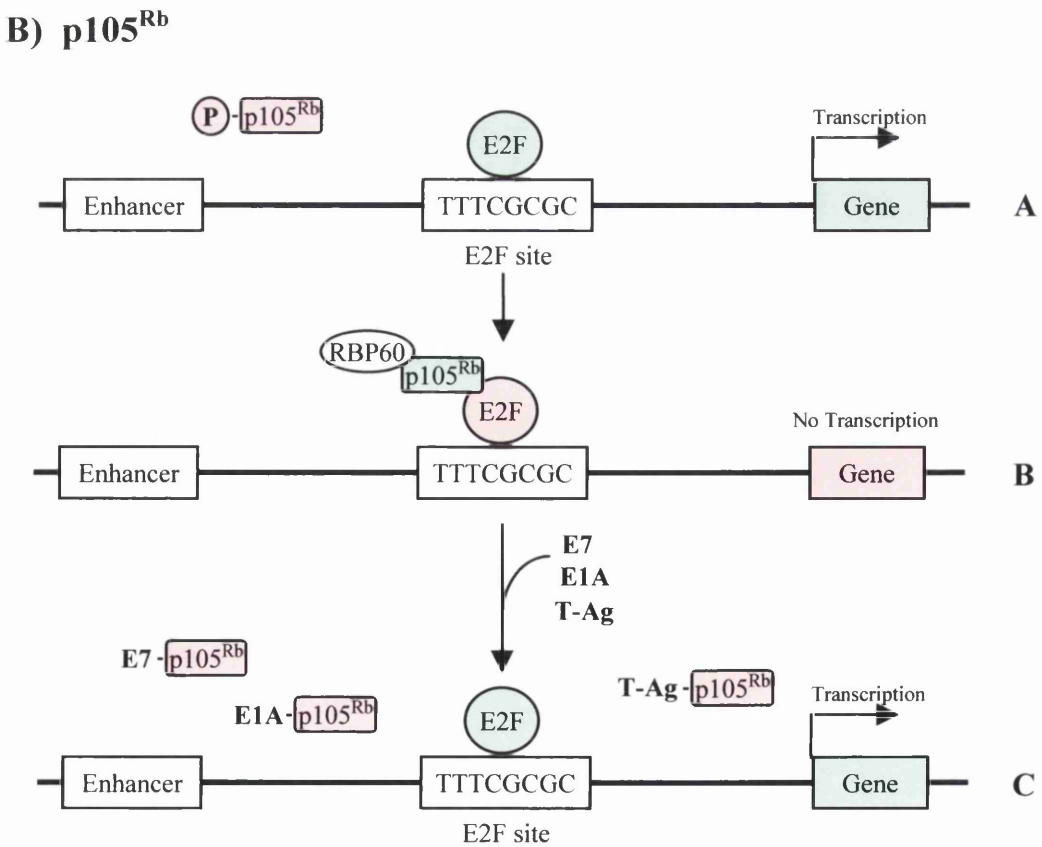

1.2.2.2 Other DNA tumour virus transforming activities.

1.2.2.2.1 Activation of cellular tyrosine kinase activity.

Polyoma virus middle T antigen has been shown to interact with the *c-src* proto-oncogene product at a region involved in the negative regulation of the kinase activity of *c-src*, resulting in the constitutive activation of the *c-src* kinase (Courtneidge, 1985). As previously described for retroviral activation of *src* kinases (Section 1.2.1.1.3) the activation of the *src* kinase leads to downstream activation of cellular targets (e.g. FAK) and is transforming in polyoma virus infected cells. Furthermore, the *c-src*/middle T complex recruits the phosphatidyl inositol-3 kinase (PI-3), and middle T can bind to and activate other cellular tyrosine kinases such as *c-yes* and *c-fyn*. The association between the *c-src* kinase and middle T antigen is not absolutely critical for transformation, but is sufficient to transform cells. However the co-operation of middle T with large T inactivation of $p105^{Rb}$ may be important for increased transformation efficiency in certain circumstances (Nevins and Vogt, 1996).

1.2.2.2.2 Inhibition of cellular apoptosis.

Expression of adenovirus E1A alone in cells leads not to transformation, but to induced cell death (apoptosis). Co-expression of E1B suppresses this apoptotic effect and allows the cells to become stably transformed. The induction of apoptosis is also dependent on the induction of the p53 protein. The mechanism of apoptotic induction by E1A is unknown, but is prevented by both of the protein products of the E1B open reading frame. The 55kDa polypeptide blocks p53 function directly, while the 19kDa polypeptide seems to prevent a p53 dependent downstream event that triggers apoptosis, mimicking the action of the cellular oncogene *bcl-2* (Nevins and Vogt, 1996).

1.2.3 OTHER DNA VIRUSES LINKED WITH HUMAN CANCERS.

1.2.3.1 Hepatitis B virus and hepatocellular carcinoma.

HBV DNA is frequently found integrated in human hepatocellular carcinoma (HCC) and in the woodchuck model, woodchuck hepatitis virus (WHV) integration has been shown to *cis*-activate *c-myc* and *N-myc*, although there is no evidence for a similar

effect in humans (reviewed by Slagle *et al.*, 1994; Hildt *et al.*, 1996). In human HCC, cellular genes are thought to be activated *in trans* by the HBV transactivator proteins, X and PreS2, while the X protein has also been shown to interact with p53 (Truant *et al.*, 1995), although the role of this p53 interaction is unclear. The viral transactivators have also been shown to trigger protein kinase C/*Raf* signalling pathways, leading to the activation of transcription factors (AP-1 and NF-κB) and their target genes, some of which are important in inducing cellular proliferation (reviewed by Hildt *et al.*, 1996). The immune response to chronic HBV infection is also thought to play a role in the development of HCC.

1.2.3.2 Epstein-Barr virus related malignancies.

Epstein-Barr virus (EBV) is associated with lymphoma in the immunosuppressed, with Burkitt's lymphoma in children (predominantly in equatorial Africa), and with naso-pharyngeal carcinoma in Southern China in particular (reviewed by Raab-Traub, 1996). EBV can establish latent infection in lymphoid cells, and induces proliferation. The virus enters the cell and circularises to form an episome that is then replicated to high copy number and segregates equally to daughter cells during mitosis. Integration into the host genome is infrequent, and is not thought to be important in the transformation process. In EBV transformed cells, a subset of viral genes are expressed. These include two integral membrane proteins (LMP1 and LMP2), and six nuclear antigens (EBNA1-6) and some small non-coding nuclear transcripts (reviewed by Kieff, 1996). The function of some of these proteins is discussed below.

The EBNA1 protein allows the viral genome to be replicated by the host cell DNA polymerase by binding to the episomal viral origin of replication, and EBNA1 transgenic mice have been shown to have an increased incidence of lymphoma (Wilson *et al.*, 1996). EBNA2 is essential for the transformation of lymphocytes, and is a transcriptional activator, acting on the viral LMP promoters and some B-cell activation markers (Kieff, 1996). LMP1 is essential for EBV induced transformation *in vitro*, and is directly transforming when expressed in rodent cells. In lymphocytes LMP1 activates the expression of genes including the anti-apoptotic genes *Bcl-2* and A20 (A20 blocks both tumour necrosis factor and p53 mediated apoptosis; Fries *et*

al., 1996). The LMP2 protein is expressed from a highly spliced mRNA which is complete only in the episomal form of the genome. It has been shown to inhibit the activation of B-cell replication by interfering with the mitogenic signal transduction pathway, and thus prevents activation of the viral replicative cycle. The most abundant mRNA in EBV infected cells are the non-coding transcripts, termed EBER, which are not essential for transformation but may be involved in the maintenance of EBV latency *in vivo*. Three levels of EBV latency have been defined, and appear to be associated with particular mailgnancies (Rickinson and Kieff, 1996). Table 1.8 summarises this information.

Table 1.8. Three levels of EBV latency.

	Genes expressed	Cancer association.
Latency 1	EBNA1 and EBERs	Burkitt's lymphoma
Latency 2	EBNA1, LMP1, LMP2, EBERs and BamHI A	Naso-pharyngeal carcinoma, Hodgkin's disease and post-transplant lymphoma
Latency 3	EBNAs 1-6, LMP1 and LMP2 and EBERs.	*In vitro* transformed B-cell lines

1.2.3.3 Human herpesvirus 8 and Kaposi's sarcoma.

Since the emergence of human immunodeficiency virus (HIV), Kaposi's sarcoma (KS) is no longer just a rare tumour of Mediterranean men, but is now the leading neoplasm of AIDS patients (reviewed by Ganem, 1996). Epidemiological evidence demonstrates that infection with human herpesvirus 8 (HHV-8 or KSHV) is tightly linked to KS risk (>95% of AIDS related KS cases harboured the HHV-8 genome). HHV-8 is also associated with rare 'body cavity based lymphomas' and Castlemans disease (a complex lymphoproliferative disorder) in AIDS patients. Two highly expressed transcripts of HHV-8 have been identified from KS tumours, termed 'nut1' and 'kaposin', although no function has yet been assigned to either transcript (Ganem, 1996).

1.2.4 THE VIRAL BASIS OF CERVICAL CANCER.

1.2.4.1 The incidence of cervical cancer.

Cervical cancer is the most common cancer in women in developing countries, and the second most common worldwide. Over 500,000 new cases and 300,000 deaths are reported globally each year, with three-quarters of these occurring in the developing world (WHO Press Release, 3/07/96; http//www.who.ch/). However, the disease is still a significant health problem in the developed world, as demonstrated by the data presented in Table 1.9.

Table 1.9. The incidence and mortality rates for cervical cancer in the United States and the United Kingdom.

	United States				United Kingdom			
	Mortality		Incidence		Mortality		Incidence	
Year	Deaths	**ASR(w)*	Cases	**ASR(w)*	Deaths	**ASR(w)*	Cases	**ASR(w)*
1985	4508	2.7	14455	9.9	2198	4.9	4554	12.2
1990	4627	2.7	13714	9.2	1981	4.3	4827	12.1
1994	**n/a*	**n/a*	**n/a*	**n/a*	1561	3.1	**n/a*	**n/a*

**ASR(w): Age Standardised Rate (World Population) per 100,000. *n/a: data not available.*

Data obtained from WHO Databank and 'Globocan' accessible from 'http://www.who.ch/'.

The squamous ('tile-like') epithelium of the transformation zone of the cervix undergoes frequent regeneration and beneath the differentiated outer epithelial cells consists of 3-4 layers of parabasal cells overlying a single layer of basal cells and the basement membrane. The pathology of cervical neoplasia is clinically graded (in order of increasing severity) into cervical intraepithelial neoplasia (CIN) grades 1 to 3, carcinoma *in situ* (CIS) and then invasive cervical carcinoma. With increasing CIN grade, more layers of parabasal cells show dysplasia, with CIS involving all of the epithelial cells including the basal cells. Following breakdown of the basement membrane, the disease is classified as invasive cervical carcinoma. Figure 1.7 illustrates the histology of these disease states, and of cervical adenocarcinoma (a glandular tumour).

Figure 1.7. Cervical intraepithelial neoplasia and carcinoma.

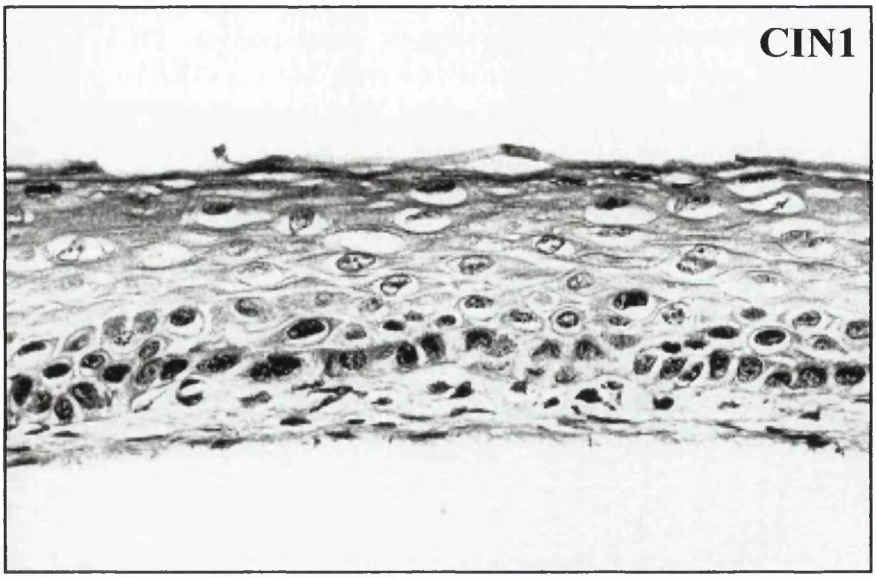

Cervical intraepithelial neoplasia Grade 1. Nuclear hyperchromasia and pleiomorphism is present in the basal third of the epithelium: the nuclear atypia persists to the surface of the epithelium, but cytoplasmic maturation occurs in the outer two thirds.

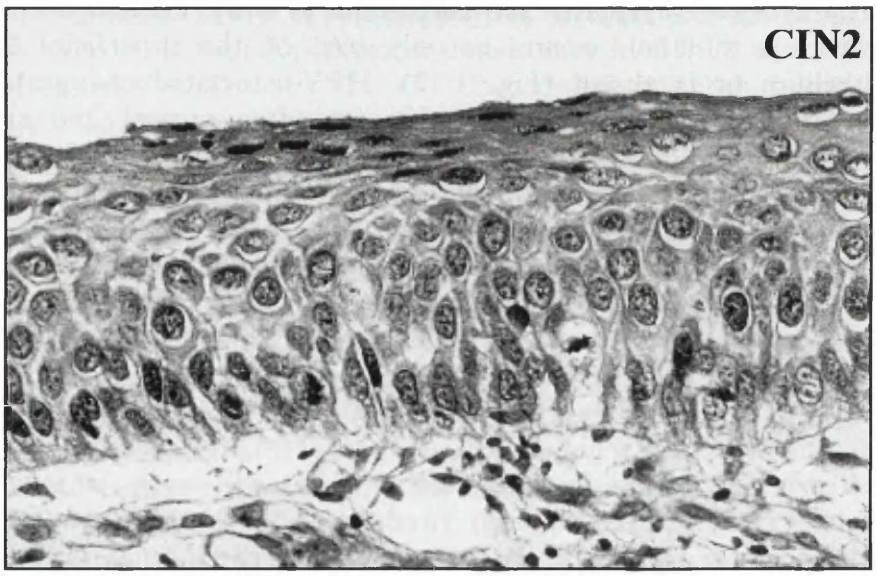

Cervical intraepithelial neoplasia Grade 2. Nuclear enlargement and mild pleiomorphism is present at all levels in the epithelium, and cytoplasmic maturation occurs only in the outer half.

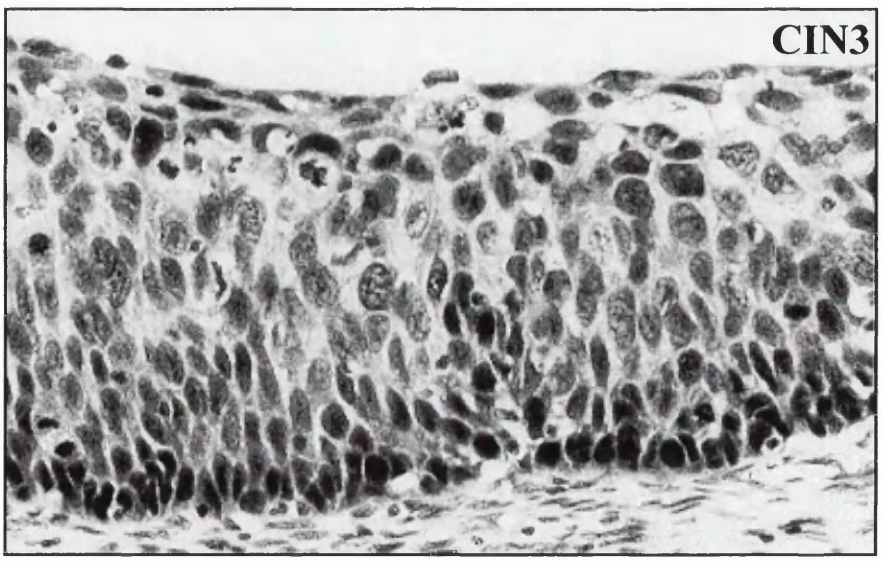

Cervical intraepithelial neoplasia Grade 3.

A population of cells with large, rather pleiomorphic nuclei and very little cytoplasm occupies the full thickness of the epithelium.

Figure 1.7. continued.

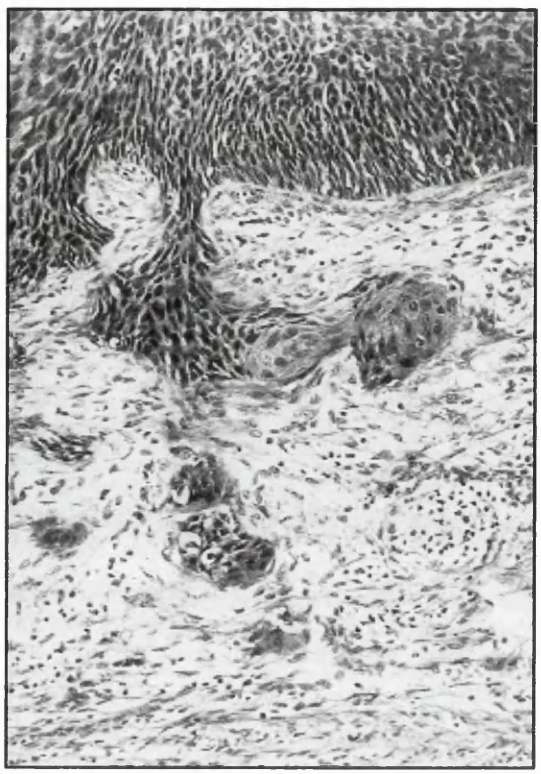

Micro-invasive carcinoma of the cervix. Early stromal invasion- an epithelium with the features of CIN3 lies at the top of the image, with tongues of invading tumour cells arising from the base (these have a larger amount of pale cytoplasm than the CIN cells from which they derive).

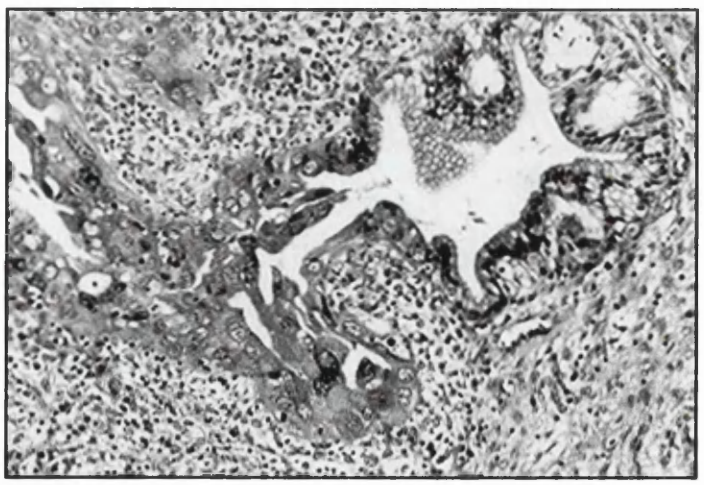

Micro-invasive adenocarcinoma of the cervix. The crypt (to the top right) is lined in its' lower part by an epithelium with features of CGIN and from it (at the lower left) there arises a focus of superficially invasive adenocarcinoma.

Images derived from Buckley, 1994.

1.2.4.2 Evidence for a role for HPV in the aetiology of cervical cancer.

1.2.4.2.1 Epidemiological evidence.

The epidemiological evidence linking infection with HPV and the risk of cervical neoplasia is compelling (reviewed by Woodman, 1994), such that HPV 16 and 18 have been officially classified as 'oncogenic' and HPV 31 and 33 as 'probably oncogenic'. Over 90% of all cervical cancers have been reported to contain HPV DNA (zurHausen, 1991a) whilst a study of HPV infection rates in 2627 women in the U.S. (Lorincz *et al.*, 1992) determined that cervical samples from 79.3% of women with definite cervical disease contained HPV DNA (n=791) detected by low stringency Southern blotting, whilst only 23.7% (n=270) of patients with 'borderline atypia' and 6.4% (n=1566) of normal controls were HPV positive. By re-probing at higher stringency to determine HPV type, these workers were able to define four risk groups of HPV (summarised in Table 1.10 below), although other workers have noted slightly different disease associations (e.g. Hagmar *et al.*, 1995).

Table 1.10. Association of cervical disease with HPV type.

Risk Group	HPV Types	Disease association.
Low	6/11, 42, 43, 44	20.2% of low grade lesions; absent from all cancers.
Intermediate	31, 33, 35, 51, 52, 55, 58	23.8% of high grade lesions and 10.5% of cancers.
High (HPV 16)	16	47.1% of high grade lesions and cancers.
High (HPV 18)	18, 45, 56	26.8% of invasive cancers but only 6.5% of high grade lesions.

Data from Lorincz *et al.*, 1992.

Interestingly, Iwasawa *et al.*, (1996) have reported a difference in the HPV type associated with squamous cell carcinoma (HPV 16 =78%; HPV 18 =17%) and adenocarcinoma of the cervix (HPV 16 =16%; HPV 18 =56%), which correlates with the relationship of HPV 18 and invasive carcinoma reported in Table 1.10 (adenocarcinoma tends to be more invasive). Non-prototype variants of HPV 16 have recently been demonstrated to confer a six-fold greater risk of developing CIN 2

or 3 than infection with prototype-like variants (Xi *et al.*, 1997), suggesting that some of the HPV 16 variants are more oncogenic than others, possibly due to differences in the E6 and/or E7 oncoproteins. Low risk and high risk HPV E6 and E7 proteins have been shown to have different affinites for p53 and $p105^{Rb}$ which correlates with their transformation ability (see Section 1.2.2.1 for the functions of p53 and $p105^{Rb}$).

Although the situation is complicated by the various types of epidemiological study which have been performed, and because different HPV detection methods (e.g. *in-situ* hybridisation/ PCR) produce different odds ratios relating HPV infection to cervical neoplasia within the same sample group, the overall trend suggests a causal link between HPV infection and cervical neoplasia (e.g. Munoz *et al.*, 1992). This is not to say that HPV causes cervical cancer, but that infection with a high risk HPV type is a major event in a multistage process of oncogenesis (zurHausen, 1991b). In addition to risk factors associated with the transmission of sexually transmissible agents (number of sexual partners, age at first intercourse etc.), other studies have reported that risk is increased in smokers (increased levels of cotinine and nicotine in the cervical mucous; Hellberg *et al.*, 1988) and is affected by diet (Vitamins C and E were reported to have a protective effect; Verreault *et al.*, 1989). The involvement of HSV in the progression of cervical neoplasia is discussed in Section 1.2.4.3.

1.2.4.2.2 Biological Studies.

The role of the E6 and E7 oncoproteins in the de-regulation of cell growth by interacting with p53 and $p105^{Rb}$ (respectively) was discussed briefly in Section 1.2.2.1. The importance of these and other interactions of E6 and E7 in cervical neoplasia (reviewed by Vousden, 1994a, 1994b; Kubbutat and Vousden, 1996) will be discussed briefly in Sections 1.2.4.2.2.1-2 respectively.

In contrast to benign lesions, in the majority of HPV associated cancers the viral DNA is integrated into the host cell genome, often by a break within the E2 open reading frame (a transcriptional regulator), which, in combination with increased stability of the E6-E7 mRNA (Jeon and Lambert, 1995) leads to the deregulated expression of the E6 and E7 oncoproteins. Transfection of the E6 and E7 open reading frames from high risk (but not low risk) HPVs into human foreskin keratinocytes is necessary and sufficient for the immortalisation of these cells

(Hawley-Nelson *et al.*, 1989), but these cells did not display the characteristics of fully transformed cells (e.g. anchorage independent growth). As HPV infects epithelial cells which are destined to cease proliferation and terminally differentiate, it is necessary for the virus to stimulate proliferation in infected cells in order to replicate. Transformation following integration is an undesirable side effect of this need to stimulate proliferation, both for the virus and the host, as the integrated DNA in the transformed cell is incapable of producing progeny virus.

1.2.4.2.2.1 The role of HPV E7 in transformation.

HPV E7 from oncogenic HPVs can transform established rodent cells alone, but also requires E6 to transform primary rodent cells or to immortalise human keratinocytes. The E7 protein contains two conserved domains at the N-terminus (CR1 and CR2) which have homology to adenovirus E1A and SV40 T antigen, and include the 'LXCXE' $p105^{Rb}$ binding motif, and two casein kinase II sites which are essential for transformation (but not $p105^{Rb}$ binding) and a C-terminal dimerisation domain. In addition to its role in binding $p105^{Rb}$ (Figure 1.6B), the E7 oncoprotein has recently been demonstrated to interact with components of the AP-1 transcription factor family (e.g. c-jun; c-fos) to cause up-regulation of AP-1 responsive genes (Antinore *et al.*, 1996), and to interact with TBP, the basal transcription factor (Massimi *et al.*, 1996).

1.2.4.2.2.2 The role of HPV E6 in transformation.

The E6 oncoprotein displays no homology to other cellular or viral proteins, but shares the ability to bind the tumour suppressor protein p53 with adenovirus E1B and SV40 large T (p53 was first identified by its ability to interact with SV40 T in SV40 transformed cells (Lane and Crawford, 1979)). In contrast to the other viral proteins however, E6 targets p53 for ubiquitin mediated degradation (Scheffner *et al.*, 1990). E6 associates with E6-AP (Huibregste *et al.*, 1992), a cellular protein which becomes loaded with activated ubiquitin via a complex pathway to form a ubiquitin ligase that can bind to p53, transfer the activated ubiquitin moiety and target p53 for destruction by the 26S proteasome (reviewed by Ciechanover, 1994).

E6 from HPV 16 has recently been shown (Klingelhutz *et al.*, 1996) to activate telomerase in human foreskin keratinocytes and mammary epithelial cells, but not in

cells which cannot be immortalised by E6 (e.g. primary rodent cells). Telomerase is a ribonucleoprotein complex that synthesises telomere repeat sequences, and has been implicated in immortalisation and cancer (Kim *et al.*, 1994), as shortening of the telomeres normally occurs during the process of cellular aging.

1.2.4.2.3 The co-operative effect of E6 and E7 on the cell cycle.

The basic functions of p53 and $p105^{Rb}$ have been outlined in Section 1.2.2.1. Recent work is beginning to show that p53 induced apoptosis is important in tumour suppression (reviewed by Wiman, 1997). One of the targets of p53 transcriptional activation (BAX) is implicated in priming cells for apoptosis via a direct physical interaction with the anti-apoptotic *Bcl-2* protein (Miyashita and Reed, 1995), although *bax* independent apoptosis also occurs. The abrogation of the anti-apoptotic effect of p53 by E6, combined with the induction of S-phase by E7 inactivation of $p105^{Rb}$ allows the cell to overcome the normal growth control mechanisms, leading to immortalisation. This model is supported by the work of Pan and Griep (1994), who demonstrated altered cell cycle control in the lens of HPV 16 E6 or E7 transgenic mice. Expression of E6 alone reduced the rate of apoptosis occurring during normal lens development, whilst E7 expression alone led to inappropriate proliferation and increased apoptosis. In E6/E7 double transgenic mice, the increased apoptosis observed with E7 alone was abolished, and there was a greater incidence of tumours during development.

The accumulated evidence suggests that infection with high risk HPV types may represent the first step towards malignant progression. As such, vaccination against HPV to prevent infection should reduce the risk of developing cancer, and much work is ongoing in this field (reviewed by Campo, 1994; Altman *et al.*, 1994). In addition, direct treatment of HPV positive tumours induced in nude mice with several E6-E7 antisense oligonucleotides reduced the tumour weight significantly compared to control random oligonucleotides (Tan and Ting, 1995). This may provide a method of directly targetting HPV positive cervical tumours in the future.

1.2.4.3 Herpes simplex virus as a co-factor in the induction of cervical neoplasia.

1.2.4.3.1 Epidemiological evidence.

The epidemiological evidence that links infection with a high risk human papillomavirus and the development of cervical intraepithelial neoplasia or cervical carcinoma (discussed in Section 1.2.4.2.1) also demonstrates that not all women who are infected with high risk HPVs will progress to serious disease. Various studies have shown that between 11.5% (n=1000; Kjaer *et al.*, 1997) and 23% (n=143; Gradilone *et al.*, 1996) of women with normal cervical cytology were infected with HPV 16, while Macnab *et al.*, (1986) reported that in women with genital cancer 73% (n=25) of internally paired normal tissue samples taken from within 3-5cm of the tumour contained HPV 16 DNA. These results, taken together, suggest that factors other than HPV infection are involved in disease progression.

Several epidemiological studies link HSV infection to increased risk of developing cervical disease. Kjaer *et al.*, (1988) studied the incidence rates of HPV (by *in situ* hybridisation) and HSV-2 (sero-positivity) in a randomly selected group of women aged 20-39 years in Greenland (n=586) and Denmark (n=661). They noted that the age corrected incidence of HPV 16/18 infection in Greenland was only 67% of the level observed in Denmark, despite the level of cervical cancer being 5.7-fold greater in Greenland. However, the observed incidence of HSV-2 was 2.2-fold higher in Greenland. More recently, Hildesheim *et al.*, (1991) studied 766 confirmed cases of invasive cervical cancer and 1,532 controls in South America, and noted that a) women sero-positive for HSV-2 had a 60% increased risk of cervical cancer compared to sero-negative women; b) women sero-positive for both HSV-2 and HPV 16/18 had a 2-fold increased risk of developing cervical cancer compared to women infected with HPV 16/18 alone. However, in Panamanian women with invasive cervical cancer HSV-2 sero-positivity was not significantly associated with prognosis (DeBritton *et al.*, 1993). Interestingly, recent studies have suggested a link between HSV-2 infection and other genitourinary malignancies. Hildesheim *et al.*, (1997a) reported a 2.1 fold increased risk of developing vaginal carcinoma (a rare disease) in women infected with HSV-2 after adjustment for infection with HPV and

C. Trachomatis, and HSV-2 seropositivity remained an independent risk factor for vulvar neoplasia after correction for HPV infection (Hildesheim *et al.*, 1997b). Jones (1995) has reviewed the available evidence regarding a role for HSV-2 as a co-factor in the development of cervical neoplasia, and concluded that HSV-2 might be a co-factor in some but not all cases of cervical cancer, hypothesising that persistent or abortive HSV infection might induce permanent genetic alterations that interfere with the differentiation of cervical epithelium and subsequently induce abnormal proliferation.

1.2.4.3.2 Biological evidence relating HSV to cervical cancer.

At the biological level, HSV-2 has been shown to directly influence both the state of the HPV genome, and the amplification of both integrated and episomal HPV DNA (Hara *et al.*, 1997). HeLa cells (a cervical cancer derived cell line containing integrated concatameric HPV 18 DNA) and an HPV negative cell line (A431) transiently transfected with a plasmid containing the EcoRI fragment of HPV 18 DNA were infected with HSV-1 or HSV-2. The integrated DNA in HeLa cells was amplified almost threefold following infection with either HSV-1 or HSV-2, and the episomal DNA in the A431 cells was shown to be replicated following HSV infection. Hara *et al.* (1997) proposed that concatameric HPV DNA is formed by replication with HSV factors and that this cannot be packaged and is either degraded or becomes integrated into the host cell genome, suggesting a role for HSV in promoting the development of cervical neoplasia. These results were however obtained at a very low level of DNA amplification/ replication. Earlier work by Gius and Laimins (1993) used a plasmid based system to demonstrate enhanced expression of a CAT reporter gene placed downstream of the HPV 18 constitutive enhancer after co-transfection with plasmids containing either the HSV-1 α-TIF or ICP0 genes into HeLa and to a lesser extent other cervical cancer cell lines. The activation of plasmid borne SV40 origins of replication in non-permissive cells (Danovich and Frenkel, 1988) and the amplification of resident SV40 sequences in SV40 transformed hamster cells (Schlelofer *et al.*, 1983) by infection with HSV has also been reported. More recently, Kulomaa *et al.* (1992) showed by flow cytometric analysis of bromodeoxyuridine incorporation, that infection of cervical cancer cell lines with HSV-2 resulted in either a rapid increase in the proportion of cells

undergoing DNA synthesis (HeLa cells) or an increase that occurred late in infection (C33-A, SiHa cells). Hossain *et al.*, (1997) examined the effect of HSV-2 infection on cyclin dependent kinases in CV-1 cells. They reported that both CDK2 and cyclin A were elevated following HSV-2 infection while CDK4, CDC2 and cyclin B were not activated. CDK2 forms a complex with cyclin A and is associated with replicating DNA and progression through S-phase (see Figure 1.8). The CDK2/cyclin A complex induced by HSV-2 was also proposed to play a role in the phosphorylation of $p105^{Rb}$, with the subsequent release of active E2F transcription factor (as previously discussed in Section 1.2.2.1.2), while the induction of unscheduled DNA synthesis could represent a single step in a multi-step mechanism of transformation. A further demonstration of the multi-step nature of carcinogenesis is provided by an experiment in which the transfection of HPV immortalised (but non-tumourogenic) cells with a sub-fragment of HSV resulted in the production of a locally invasive carcinoma when the cells were injected sub-cutaneously into nude mice (reviewed in DiPaolo *et al.*, 1993). Direct evidence of HSV induced cervical carcinoma was obtained in a mouse model system by the innoculation of the cervix with HSV-1 or HSV-2 (Wentz *et al.*, 1981; Anthony *et al.*, 1989), and disease induction could be prevented by vaccination with HSV-1 prior to challenge.

Macnab (1987) reviewed the potential role of HSV and HCMV in cellular transformation, and proposed mechanisms by which HSV could contribute to the transformation process. HSV-1 contains a single region (mapping in *XbaI*f and *BglII*i; Camacho and Spear, 1978) involved in the morphological transformation of cultured cells (designated MTRI) which is capable of transiently expressing gB, while HSV-2 contains two regions defined as MTRII and MTRIII which map to the BglIIn and BglIIc fragments of the genome respectively (Macnab and McDougall, 1980; Jariwalla *et al.*, 1983). Because HSV-2 DNA was often not retained in transformed cells, a 'hit and run' mechanism of transformation has been proposed (Skinner, 1976), and no evidence for an HSV coded transforming protein could be found (Cameron *et al.*, 1985). Several mechanisms for HSV transformation were proposed (Macnab, 1987), including the presence of a small stem-loop structure in BglIIn of HSV-2 (Galloway *et al.*, 1984), a possible effect of ribonucleotide reductase on cellular nucleotide pools, increased mutagenesis of cellular genes (Pilon

Figure 1.8. The effect of HSV-2 infection on the cyclin dependent kinases active at different stages of the cell cycle.

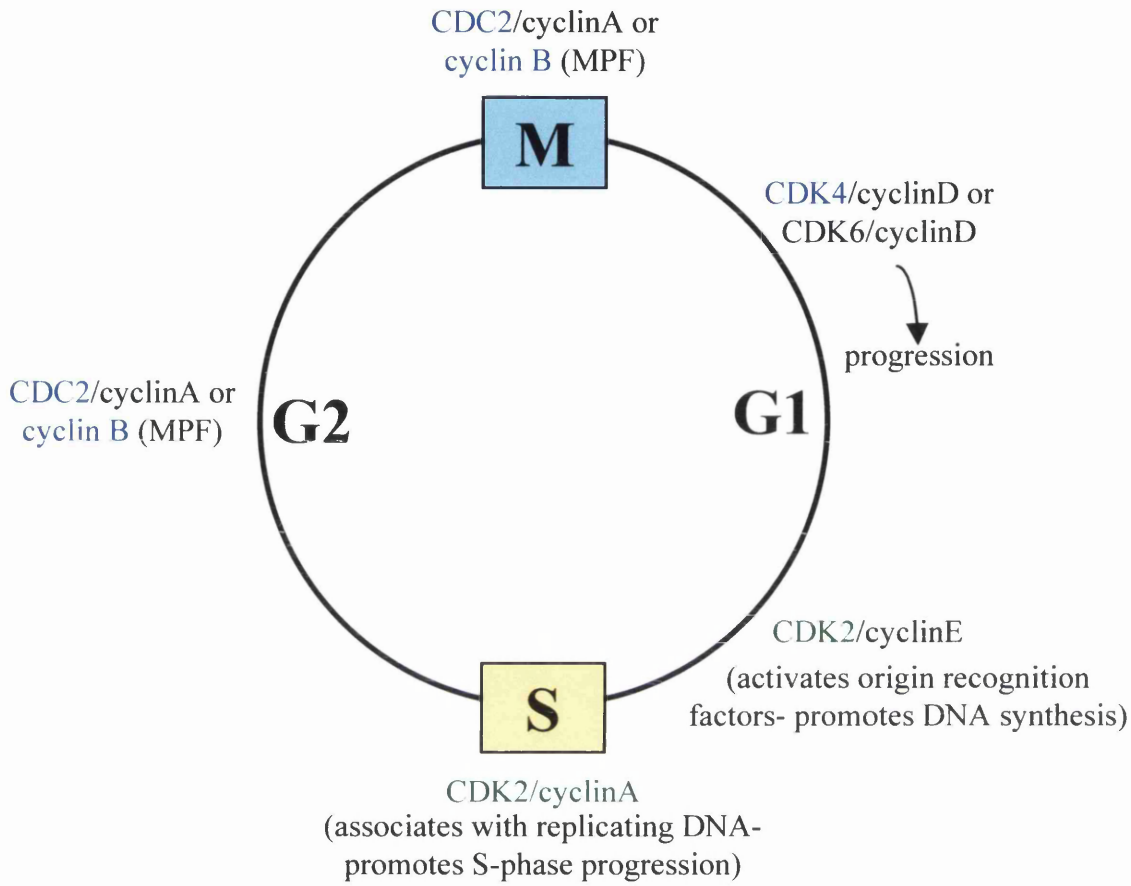

Legend. The cyclin dependent kinases active at various times during the cell cycle are shown diagramatically (from information in the text of Hossain *et al.*, (1997)- see Section 1.2.4.3.2). CDK2 forms a complex with cyclin A that was found to be associated with replicating DNA, and progression through S-phase. The effect of infection with HSV-2 on the levels of the cyclin dependent kinases was examined in CV-1 cells. Both CDK2 and cyclin A were elevated by HSV-2 infection while CDK4, CDC2 and cyclin B were not affected. No data was available regarding the other factors described. It is proposed that the elevation of the components of the S-phase associated kinase (CDK2/cyclinA) by HSV-2 could promote de-regulated DNA synthesis. In addition, this complex may play a role in the phosphorylation of $p105^{Rb}$ (see main text for details).

Key: MPF- maturation promotion factor. Green text- levels elevated by HSV-2 infection. Blue text- levels unaltered.

et al., 1985; Clarke and Clements, 1991) or amplification of cellular sequences (Heilbronn *et al.*, 1990). In addition, the activation of certain cellular genes following HSV infection has been reported (see Section 1.2.4.3.3).

1.2.4.3.3 Activation of cellular gene expression by HSV.

HSV has been demonstrated to activate the expression of cellular genes, by mechanisms that need not involve virus entry into the cell. A 56kDa cellular polypeptide was induced in human fibroblast cells by the specific interaction of HSV-1 ts1204 (a mutant which fails to penetrate the cell at the non permissive temperature; Addison *et al.*, 1984) with the cell surface (Preston, 1990). Viral protein synthesis is not required for the induction of some cellular genes by HSV infection (Kemp *et al.*, 1986), although in the case of a 40kDa polypeptide overexpressed in cervical cancer cells accumulation is dependent upon HSV-1 ICP27 (Estridge *et al.*, 1989) and HSV-1 ICP4 is essential for the increased transcription of the human Ubiquitin B gene (Kemp and Latchman, 1988). Cellular transcription factors (c-jun, c-fos and oct-1) have been induced by HSV-1 infection of the cornea (Valyi-Nagy *et al.*, 1991), and by infection of tissue culture cells (BHK C13) with HSV-1 (AP-1 induction, dependent on ICP0; Jang *et al.*, 1991). In a breast cancer cell line (MCF-7) infected with HSV, the 2-3 fold increase in the level of oestrogen receptor mRNA observed was dependent upon the virion α-TIF protein (Vmw 65) (Offord *et al.*, 1989).

A group of cell coded polypeptides were detected in HSV transformed rat embryo fibroblast cells by immunoprecipitation with a monoclonal antibody (TG7A- see below), a polyclonal antiserum raised against HSV-2 infected rat embryo fibroblasts (Macnab *et al.*, 1985), or by the sera of tumour bearing rats (TBS). TG7A was a monoclonal antibody raised against the DNA binding proteins of HSV-2 infected BHK C13 cells (Macnab *et al.*, 1985; LaThangue and Latchman, 1988). These polypeptides had molecular weights of 200kDa, 90kDa (actually a doublet termed U90 and L90), 40kDa and 32kDa, and could not be immunoprecipitated from primary, secondary or quaternary rat embryo cells, but could be immunoprecipitated from adenovirus 12 and Rous sarcoma virus transformed rat/mouse cells (Macnab *et*

al., 1985). This suggested that these polypeptides were not specific just to HSV transformation, but might be a general feature of virus transformed cells.

The U90 polypeptide from this group has been shown to be distinct from heat shock proteins, to be present mostly in the plasma membrane fraction of tumour cells, and to be increased in Bn5T cells (transformed rat embryo cells- see Materials and Methods, p68) by a factor of 2.5-5 fold following HSV-2 infection (Hewitt *et al.*, 1991). The characteristic of U90 in tumour cells which facilitates its immunoprecipitation from transformed but not control cells has been shown to be an increased half-life in tumour cells (13 hours compared to 33 minutes; Grassie *et al.*, 1993).

A 40kDa polypeptide with an identical peptide map to the 40kDa polypeptide identified above has been shown to be recognised by the sera of patients with cervical cancer, and both TBS and an antiserum raised against HSV-2 infected cells recognised an antigen specifically in tumour cells in sections of cervical carcinoma (Macnab *et al.*, 1992). The 40kDa polypeptide has been identified as a form of mitochondrial aspartate aminotransferase (mAspAT) (Lucasson, PhD Thesis 1992), and been shown to be increased at the protein (Lucasson *et al.*, 1994) and mRNA levels (Lucasson *et al.*, 1994; see *'Results: Chapter 4'* of this thesis) by infection with HSV-2. The induction of mAspAT in normal (RE), immortalised (BHK C13), and transformed (Bn5T) cells, and a possible role in the transformation process are the subject of this thesis.

1.3 MITOCHONDRIAL ASPARTATE AMINOTRANSFERASE.

1.3.1 INTRODUCTION.

Mitochondrial aspartate aminotransferase (mAspAT; L-aspartate:2-oxoglutarate aminotransferase, EC 2.6.1.1, also called glutamic oxaloacetic transaminase (mGOT)) catalyses the fully reversible transfer of an amino group from aspartate to α-ketoglutarate within the mitochondrion to form glutamate and oxaloacetate.

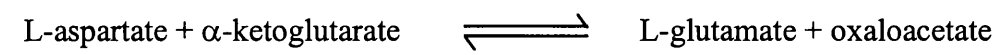

A closely related cytosolic aspartate aminotransferase (cAspAT) perfoms the same reaction in the cytosol. The details of the reaction mechanism are discussed in Section 1.3.3 below.

Mitochondrial aspartate aminotransferase (mAspAT) from rat liver was first purified by Huynh *et al.*, (1980), and shown to be very similar to other purified AspAT enzymes from, for example, pig and human heart tissue. The molecular weight of mAspAT was estimated by gel filtration and analytical ultracentrifugation to be 90kDa, corresponding to a dimer of approximately 45kDa per monomer. The same group later reported the full amino acid sequence of mAspAT, and determined it to contain 401 amino acids and have a predicted molecular weight of 44.358kDa (Huynh *et al.*, 1981). Comparison of this sequence with that of pig heart mAspAT showed the two to be 94% similar at the amino acid level. Comparisons between mAspAT and cAspAT within the same species show 50% homology at the nucleotide level, whilst a higher degree of similarity (80%) is observed when comparing each isoenzyme from different species (Pavé-Preux *et al.*, 1988).

The mitochondrial and cytoplasmic isozymes are transcribed from separate nuclear genes and synthesised on free polysomes in the cytoplasm (Sonderegger *et al.*, 1982). mAspAT is synthesised as a precursor containing a mitochondrial targetting pre-sequence and is translocated to the mitochondrion, where the signal sequence is cleaved (Joh *et al.*, 1985). The complete cDNA sequence of the precursor form of rat liver mAspAT has been published (Mattingley *et al.*, 1987) and the predicted amino acid sequence was shown to differ from the actual sequence obtained by Huynh *et al.*, (1981) at 13 positions. The amino terminal presequence is predicted to be 29 amino acids in length with a predicted molecular weight of 2.807kDa. The presequence contains 4 basic and no acidic residues and was thought to contain all the necessary information for binding to mitochondrial membranes, penetration/translocation across the membrane and proteolytic cleavage within the mitochondrial matrix (Morino *et al.* 1990), although additional residues are now thought to be involved (see Section 1.3.2, p59). The first possible translation initiation site in the cDNA is at nucleotide 90, and the open reading frame proceeds to nucleotide 2362, encoding a protein of 430 amino acids (Mattingley *et al.*, 1987). The predicted transcript size has been confirmed by the detection of a 2.4kKb

mAspAT transcript in rat cells (Pavé-Preux *et al.*, 1988). The mAspAT cDNA also contains a 3' untranslated region of 946 nucleotides. Expression of the cloned mAspAT cDNA in bacteria (Mattingley *et al.*, 1987) yielded a polypeptide of molecular weight approximately 47kDa, consistent with the presence of a 44kDa mature enzyme and a 3kDa translated pre-sequence.

1.3.2 PROTEIN FOLDING AND MITOCHONDRIAL IMPORT OF pre-mAspAT.

mAspAT has been much studied as a model for the transport and processing of mitochondrial matrix proteins. The precursor form of the mAspAT enzyme ('pre-mAspAT') contains the mitochondrial targetting presequence, and has been isolated as a soluble, dimeric, active enzyme in the cytoplasm which is able to be processed to the mature form by incubation with intact mitochondria (Altieri *et al.*, 1989). The folding of *in-vitro* translated protein demonstrated a slow conversion from a trypsin sensitive (unfolded) state to a trypsin resistant, fully active enzyme that was unable to traverse the inner mitochondrial membrane (Mattingley *et al.*, 1993). As the presence of the 29 amino acid presequence did not prevent 'bulk folding' of the protein, it was suggested that a 'mitochondrial molecular chaperone' (reviewed by Stuart *et al.*, 1994) might maintain the newly synthesised pre-mAspAT in a transport competent conformation. Evidence supporting this proposal has been obtained *in-vitro*. The refolding of acid denatured mAspAT is prevented by the presence of GroEL (hsp70 homologue), while the addition of both GroES (hsp60 homologue) and Mg^{2+} to the mixture was essential to promote correct folding (Mattingley *et al.*, 1993). Artigues *et al.*, (1997) similarily reported that refolding of denatured mAspAT could be stopped by addition of hsp70, while cAspAT is unaffected, and demonstrated that mAspAT undergoes two sequential first order folding reactions. The overall refolding mechanism includes a fast collapse to a form with 80% of the secondary structure found in the active dimer, followed by a slow isomerisation to produce assembly competent monomers that rapidly associate to form an inactive dimer prior to a final structural rearrangement to form active dimers. It appears that only the first collapsed state of mAspAT can bind hsp70 and that the inability of cAspAT to bind hsp70 might explain its single phase rapid refolding. Further

evidence of an interaction of mAspAT with hsp70 is provided by experiments in which the mAspAT presequence was fused to the cAspAT mature protein (Lain *et al.*, 1995). pre-mAspAT interacts with hsp70 early during translation while cAspAT does not interact with hsp70 at any time; in the fusion protein, hsp 70 binding was only observed once the enzyme had achieved the mature conformation. Furthermore, swapping the amino terminal portion of mAspAT for the equivalent cAspAT sequence but leaving the presequence intact eliminated binding of hsp70. The N-terminal region therefore contains signals that allow association with hsp70 in addition to those present in the presequence. The interaction of mAspAT with GroEL has recently been studied at the molecular level- this work showed that the N-terminal half of mAspAT is more flexible and lies at the mouth of the central cavity of GroEL while the more compact C-terminal region (200 amino acids) which contains residues at the subunit interface of mAspAT appears to be hidden in the cavity of GroEL (Torella *et al.*, 1998).

Further evidence that the presequence is not uniquely required for the interaction with molecular chaperones to promote entry into mitochondria is demonstrated *in-vitro* by the mitochondrial targetting of dihydrofolate reductase (DHFR) fusion proteins containing the N-terminal 10 or 191 amino acids of the mature mAspAT polypeptide (Giannattasio *et al.*, 1994). The import of a mAspAT protein containing a deletion within the presequence into mitochondria has also been reported (Azzariti *et al.*, 1995). Berezov *et al.*, (1994, 1996) have demonstrated using fluorescence probes that binding of pre-mAspAT to anionic phospholipid vesicles locks pre-mAspAT in an altered, partially unfolded conformation which may be important for membrane translocation and results in the loss of the catalytic activity of the enzyme. This interaction is thought to be mediated by the positively charged residues within the presequence. They also demonstrated that the interaction of each subunit of the dimer with lipid (via interaction with N-terminal pre-sequence) perturbs the structure of only that half of the molecule.

To summarise, mAspAT is synthesised as a precursor in the cytoplasm and interacts very early in translation with a chaperone protein, hsp70 (GroEL). This interaction is mediated by the presequence and some amino-terminal portions of mAspAT, and maintains the protein in a partially unfolded, transport competent conformation. The

interaction of the exposed N-terminal portion of mAspAT with mitochondrial membrane lipids contributes to the maintenance of a partially unfolded state, (perhaps in the GroEL/hsp70 complex?) and facilitates membrane transport.

1.3.3 TRANSAMINATION BY mAspAT.

1.3.3.1 Reaction mechanism.

mAspAT contains a pyridoxal phosphate (PLP) co-enzyme at its active site which is essential for mAspAT function. The PLP co-enzyme forms an internal aldimine bond with the ε-amino group of Lysine 258 within the active site (see figures 1.9A and 1.10A), and is tethered to the active site by electrostatic interactions with active site residues, which also regulate the electron distribution within the coenzyme-substrate complex (Morino *et al.* 1990). The aldimine bond between Lysine 258 and PLP undergoes a pH dependent protonation/deprotonation, with the environment surrounding the aldimine bond giving it a lower protolytic pK_a value than for a normal aldimine bond to PLP (Morino *et al.* 1990). The co-enzyme acts an electron sink that stabilises the reaction intermediates during catalysis (Seaman *et al.*, 1991). The interaction of the active site residues (e.g. Arg 292 and 386) with the co-enzyme-substrate complex determines the conformational orientation of the complex and positions the complex such that stereo-electronic effects favour removal of the substrate α- proton (Seaman *et al.*, 1991). Malashkevich *et al.*, (1993) determined the x-ray structure of a ketimine reaction intermediate (see mechanism, Figure 1.9B). The α-H was orientated almost perpendicular to the plane of the pyridine ring suggesting that sigma-pi (σ-π) orbital overlap is involved in removal of this proton. This conformation confers specificity to the reaction, favouring transamination rather than racemisation or decarboxylation (Seaman *et al.*, 1991).

The proposed transamination reaction mechanism is illustrated in Figure 1.9. Briefly, the internal aldimine bond between lysine 258 and the PLP co-enzyme is transferred to the amino group of the di-carboxylic amino acid substrate (aspartate/glutamate) (Figure 1.9A and 1.10A). Specific de-protonation at the α-carbon of the amino acid substrate produces a quinonoid intermediate which undergoes protonation of the aldimine bond (Figure 1.9B, and 1.10A which shows

Figure 1.9. Proposed transamination reaction mechanism of mAspAT.

A)

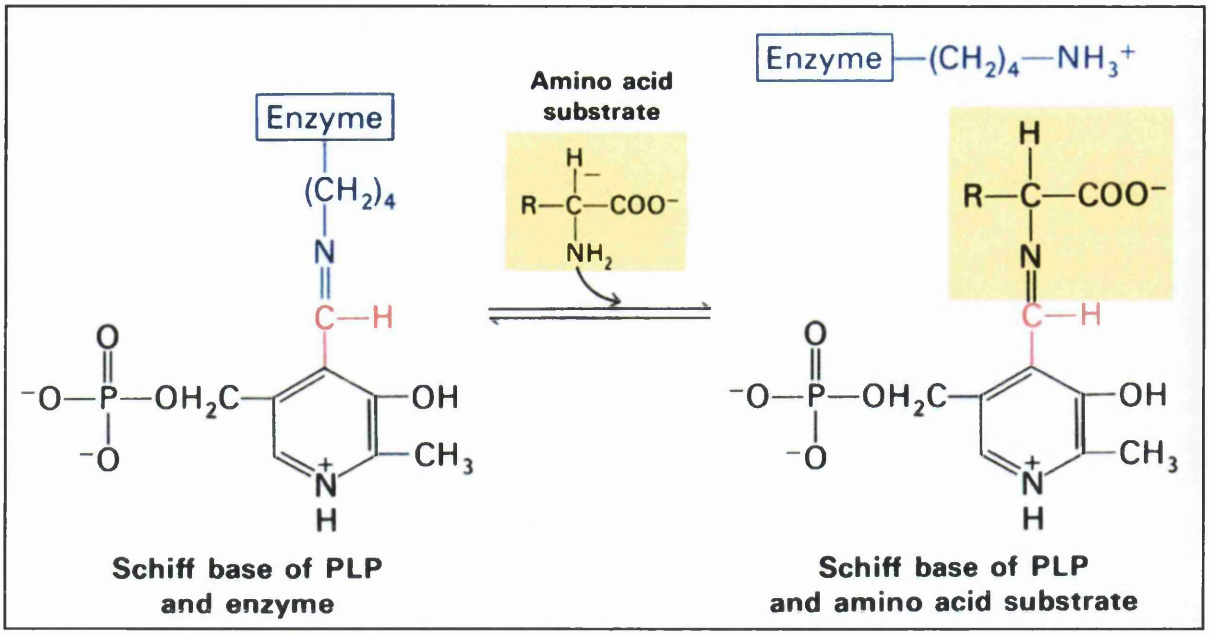

Legend. The pyridoxl phosphate co-enzyme forms an internal aldimine bond with Lysine 258 of the enzyme (shown in blue). On addition of the amino acid substrate (yellow box) the covalent link between the enzyme and co-enzyme is broken, and an aldimine is formed between the substrate and the co-enzyme.

B)

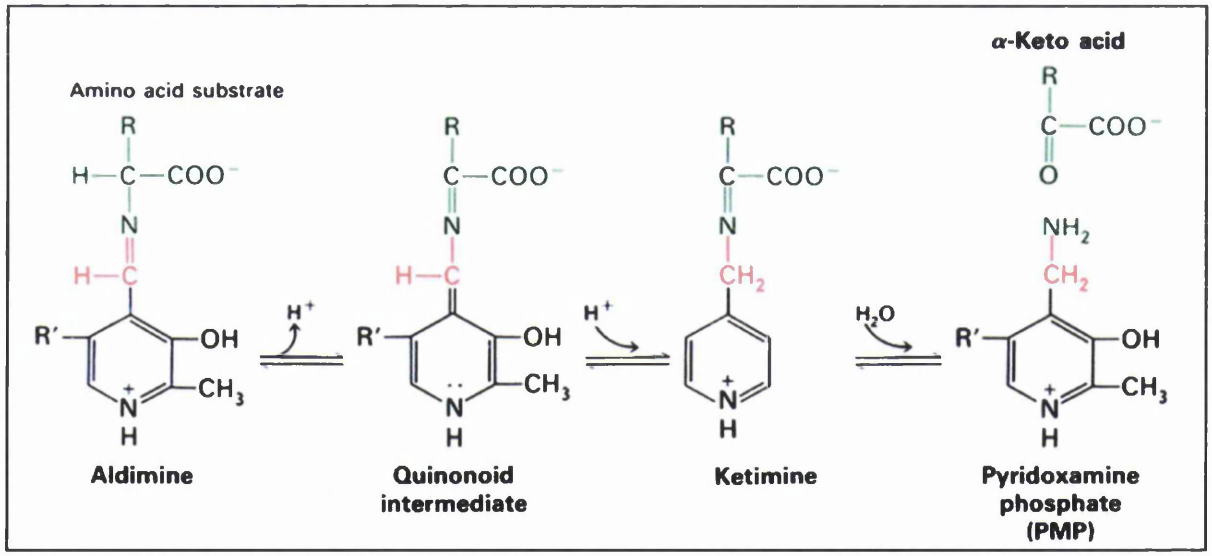

Legend. Deprotonation of the α-carbon of the amino acid substrate in the aldimine reaction intermediate forms a quinonoid intermediate. This species is re-protonated (at the carbon atom shown in red) to form a ketimine intermediate. Hydrolysis of this molecule releases the α-keto acid product, and leaves the co-enzyme in the pyridoxamine form, ready to catalyse the reverse reaction. See Section 1.3.3.1 for further details.

(Diagrams from Stryer, 1988)

Figure 1.10A. The arrangement of active site residues of aspartate aminotransferase stabilises the substrate- pyridoxal phosphate co-enzyme complex in an orientation favouring transamination.

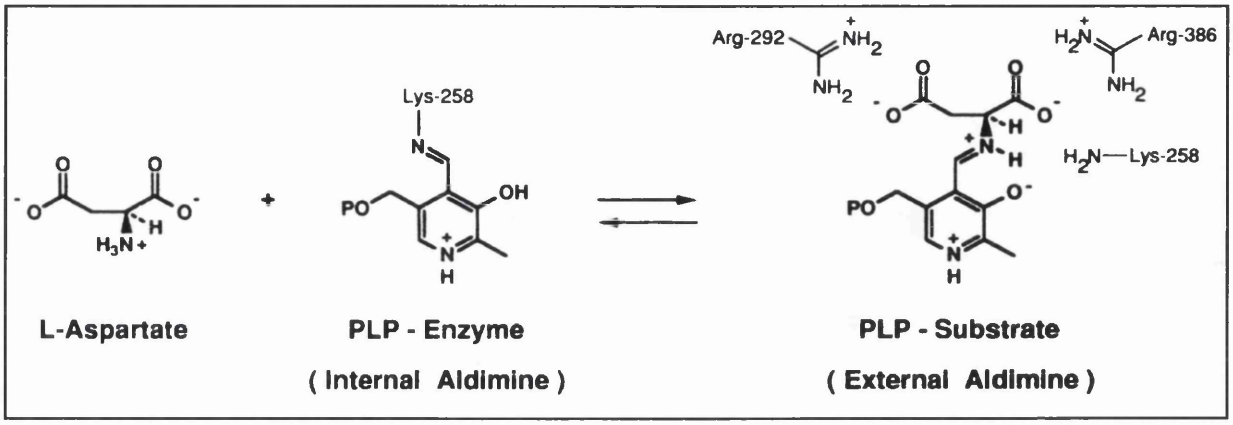

Reference: Seaman *et al.*, 1991.

Figure 1.10B. Molecular model of aspartate aminotransferase with bound pyridoxamine phosphate coenzyme.

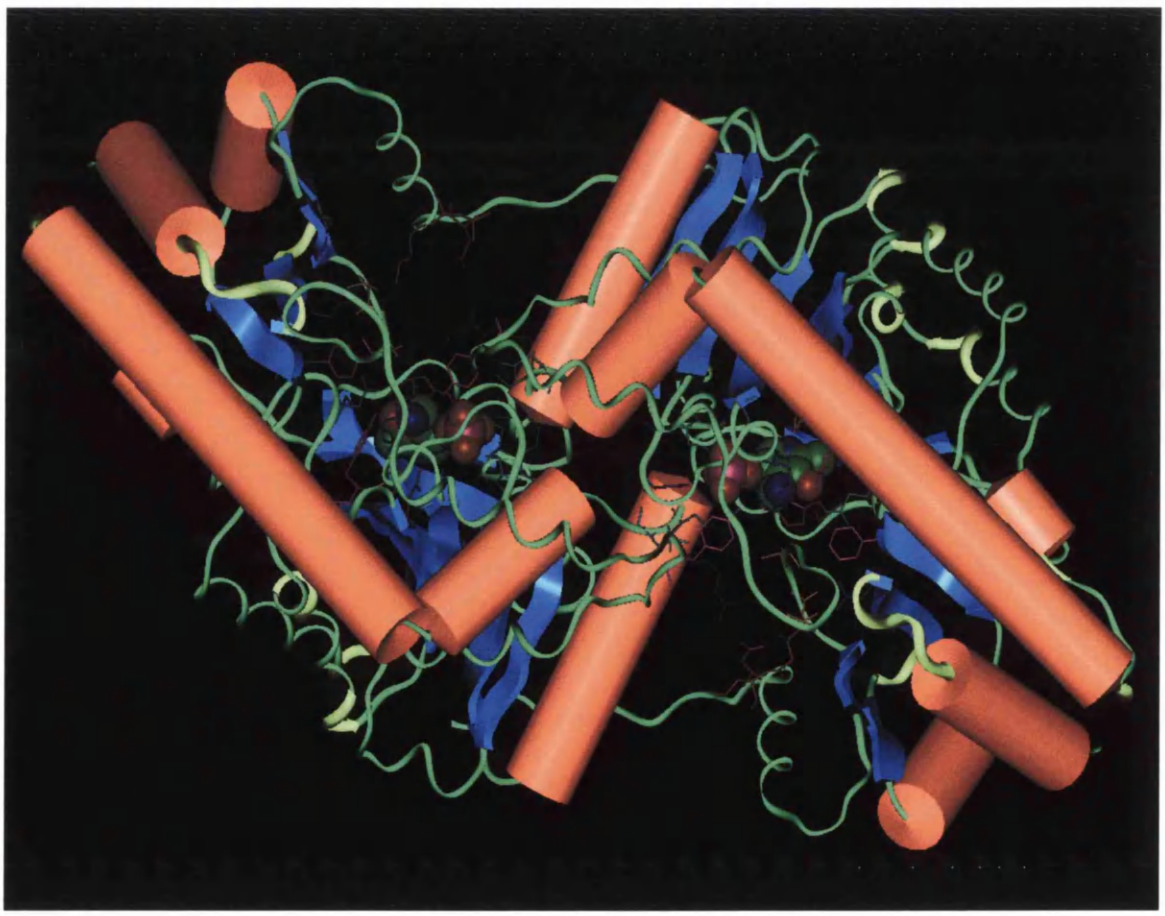

Co-enzyme= space filling model; Sticks = active site residues.
Model from Brookhaven Protein Structure Databank- 9AAT.

the spatial arrangement of active site residues that stabilise the co-enzyme-substrate complex in the correct orientation). Hydrolysis of this aldimine bond releases an α-keto acid and leaves the co-enzyme in the pyridoxamine phosphate form (PMP). This reaction represents half of the transamination reaction catalysed by mAspAT (i.e. L-glutamate conversion to α-ketoglutarate), and is fully reversible. The binding of a second α-keto acid to the pyridoxamine (PMP) form of the co-enzyme initiates the reverse reaction with the formation of an amino acid and the regeneration of the PLP form of the enzyme (i.e. the conversion of oxaloacetate to aspartate).

1.3.3.2 Structural studies of mAspAT enzyme mechanism.

Much work has centred on determining the three dimensional structure of aspartate aminotransferase enzymes alone and in complexes with various inhibitors (e.g. McPhalen *et al.*, 1992a; Malashkevich *et al.*, 1993; Miyahara *et al.*, 1994) in order to confirm details of the reaction mechanism described above, and to identify important active site and interdomain residues. McPhalen *et al.*, (1992b) compared the structure of chicken mAspAT with bound PLP co-enzyme (holo-enzyme) to the structure of the holo-enzyme in a complex with a strong inhibitor of mAspAT, the substrate analogue α-methyl-aspartate. The active enzyme is a dimer of two identical subunits. Each subunit consists of a small and a large domain with the active site positioned in a cavity between the domains and near the subunit interface (Figures 1.10B, and 1.11A). Each subunit contains one active site and their activities are independent of each other. In the liganded form, the large and small domains close around the substrate (analogue) and close the active site. This involves a rotation of the small domain relative to the large, and is discussed further below (illustrated in Figure 1.11B).

The subunit of the chicken mAspAT enzyme consists of a small domain (consisting of 2 small two stranded β-sheets, and 5 α-helices), and a large domain (a central seven stranded β-sheet surrounded by eleven α-helices that pack around the β-sheet). A long α-helix forms part of both subunits. The active site is formed by residues from both domains of the subunit and a few residues from the other subunit. These features can be seen in Figure 1.10B. An N-terminal arm from each subunit can be seen to extend across the large domain of its subunit partner (Figure 1.11B). On

Figure 1.11A. Space filling model of chicken mitochondrial aspartate aminotransferase homodimer.

Legend. A space filling model of a homodimer of chicken mAspAT is shown. This has an almost identical 3-D structure to the mammalian and *E. coli* enzymes. The large and small domains of the right hand monomer are labelled, as is the N-terminal arm which packs across the large domain of the left hand subunit (monomer). The active site is marked and sits at the interface of the left and right monomer subunits and between the large and small domains of the right hand monomer. A second, independent active site is formed in a similar way in the other monomer.

Figure 1.11B. Model of domain closure on substrate binding to chicken mAspAT monomer.

Legend. The peptide backbone of a single monomer of chicken mAspAT is shown, with the large and small domains shown in Panel A labelled to allow orientation of the two models. The solid line represents the structure of the mAspAT backbone without bound substrate, and the dotted line shows the position of the peptide backbone following binding of the inhibitor α-methylaspartate, a substrate analog. The major alterations in the structure are a rotation of 13.6° around the labelled axis of rotation (which lies almost perpendicular to the plane of the paper), and a shift of 0.7Å along this axis. In addition helix 1 undergoes further rearrangement and moves to cover the active site. For further discussion, see main text.

70* represents the active site residue Tyrosine 70 from the subunit shown; 292* represents the position of the active site residue Arginine 292 which is part of the other subunit.

Reference: McPhalen *et al.*, (1992b).

Figure 1.11. Substrate induced domain closure in mAspAT.

A) Space filling model of chicken mAspAT homodimer.

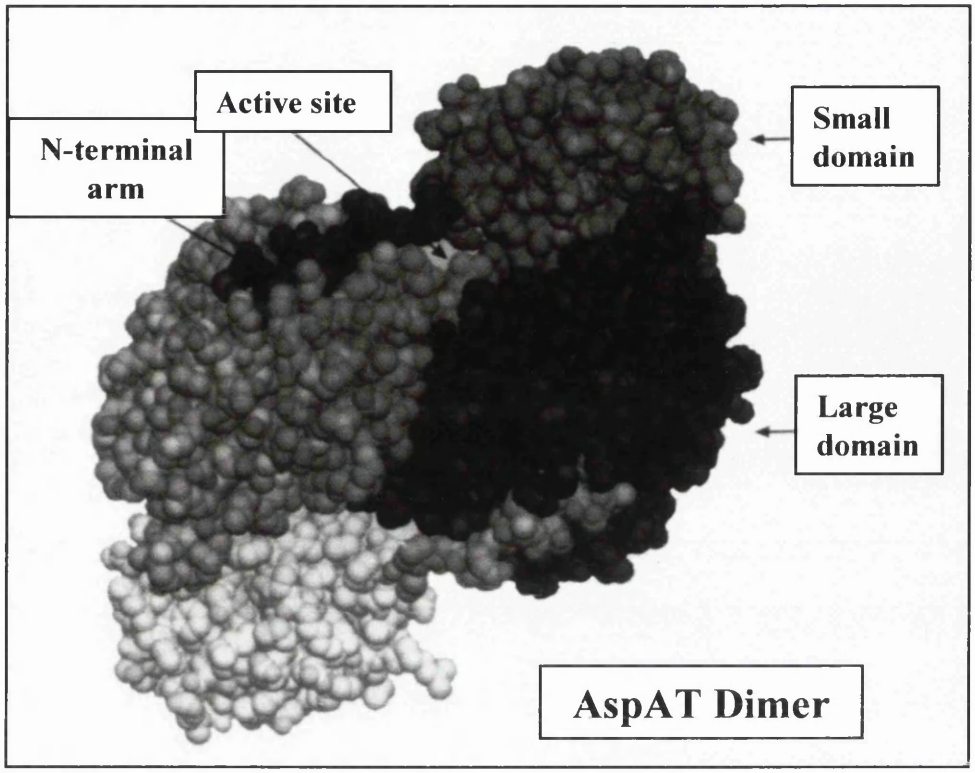

B) Model of domain closure on substrate binding in chicken mAspAT monomer.

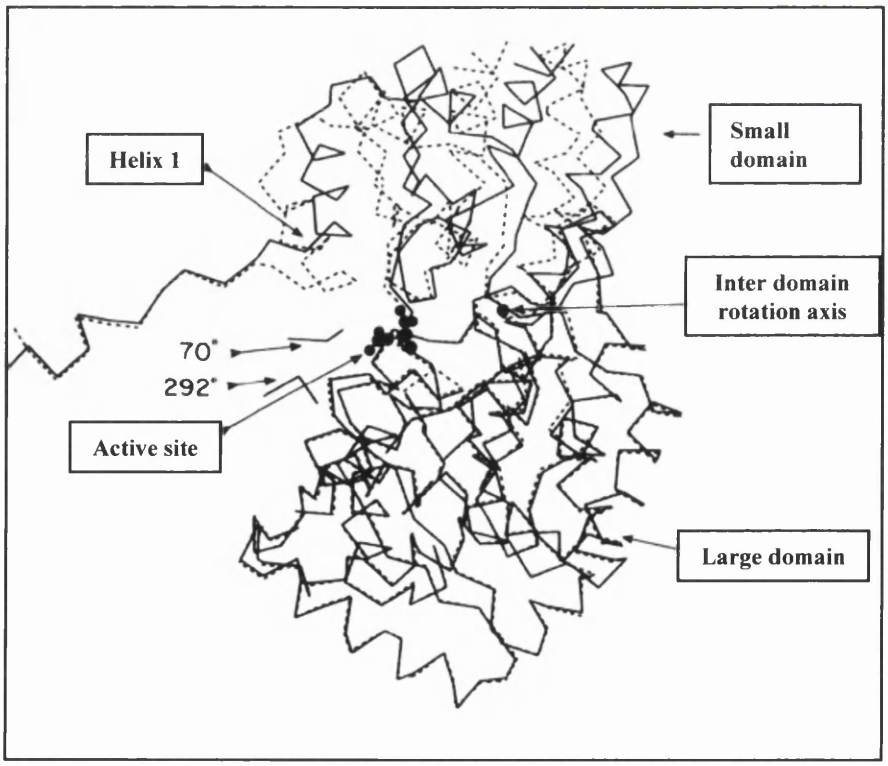

binding to substrate, the core of the small domain moves relative to that of the large domain, described as a "rotation of 13.6° and a shift of 0.7Å along the axis of rotation" (McPhalen *et al.*, 1992b; see Figure 1.11B). In addition, there are subtle compensatory changes within the internal structure of the domains, and in the interdomain and intersubunit contacts. Two of these changes occur in the peptides linking the two domains (an increase in the kinking of the long interconnecting helix 13, and smaller changes at the other link point). Helix 1 (illustrated in Figure 1.11B) moves considerably upon substrate binding, so that it makes considerable new contacts with the large domains of both subunits of the enzyme. This motion effectively closes the active site, and is accommodated by movement of the N-terminal linking arms (McPhalen *et al.*, 1992b). The function of the domain closure in mAspAT is to restructure the active site around the substrate, with the interactions of the active site residues and the substrate providing the driving force for domain closure. The salt bridges between Arg 292* (residue from the other subunit) and the β-carboxylate of the substrate, and Arg 386 with the α-carboxylate play a central role in domain closure, and these residues undergo large conformational changes to bind the substrate and position it near to the co-enzyme. Domain closure also moves three hydrophobic residues near the mouth of the active site to form a hydrophobic plug over the active site, removing the active site from solvent contacts, completely burying the substrate and facilitating catalysis (McPhalen *et al.*, 1992b; Miyahara *et al.*, 1994). The salt bridges between the two arginine side chains and the substrate hold the substrate tightly in the active site and confer stereo-specificity on the reaction (Miyahara *et al.*, 1994); both carboxylate groups of the substrate have been demonstrated to be essential for stabilising the closed conformation of the enzyme (Markovichousley *et al.*, 1996). Studies using electron spin resonance spectroscopy to probe the conformation of mAspAT using a spin label attached to Cys166 showed that substrate binding to the PLP form of mAspAT shifted the conformational equilibrium of the enzyme towards the closed conformation, an effect not seen with the PMP form of the enzyme (Sterk *et al.*, 1994). This evidence from enzyme studies in solution supports the induced domain closure model proposed from the crystallographic studies.

1.3.4 THE METABOLIC FUNCTIONS OF ASPARTATE AMINOTRANSFERASES.

The AspAT isoenzymes have a central role in cellular metabolism, playing an important role in the synthesis and degradation of amino acids, and being involved in the link between the Urea and tricarboxylic acid (TCA) cycles (illustrated in Figure 1.12). They also play an essential role in the transfer of reducing equivalents across the mitochondrial membrane (Pavé-Preux *et al.*, 1988). This latter role is discussed below. In addition, cAspAT has a role in the production of glutamate, the immediate precursor of the neurotransmitter γ-aminobutyrate (GABA) in the cell body and axons of GABAergic neurons (Kaneko and Mizuno, 1994).

1.3.4.1 The malate-aspartate shuttle.

NADH is synthesised during glycolysis in the cytoplasm of cells, but the next stage of oxidative respiration involves the electron transport chain within the mitochondria. The inner mitochondrial membrane is totally impermeable to both NADH and NAD^+. The transport of reducing equivalents across the inner mitochondrial membrane is therefore accomplished by means of shuttles- the 'glycerol phosphate shuttle' and the 'malate-aspartate shuttle'. The malate-aspartate shuttle is illustrated in Figure 1.13. The shuttle consists of both the cytoplasmic and mitochondrial forms of aspartate aminotransferase and malate dehydrogenase (MDH), and two membrane transporter proteins. Electrons are transferred from cytoplasmic NADH to oxaloacetate to form malate in a reaction catalysed by cMDH. Malate is then transported into the mitochondrial matrix, and is re-oxidised by NAD^+ to form NADH and oxaloacetate (catalysed by mMDH). A transamination reaction is necessary to facilitate the export of the oxaloacetate formed by this reaction out of the mitochondria. This reaction is catalysed by mAspAT. This shuttle is readily reversible (unlike the glycerol phosphate shuttle) and can therefore only transfer NADH into the mitochondrial matrix if the NADH/NAD^+ ratio is higher in the cytoplasm than in the matrix. The net effect of the malate aspartate shuttle is shown below.

NADH cytoplasmic + **NAD^+** mitochondrial $\rightleftharpoons$ **NAD^+** cytoplasmic + **NADH** mitochondrial

Figure 1.12. Aspartate aminotransferase is involved in amino acid metabolism, and in the link between the tricarboxylic acid and Urea cycles.

A) Amino acid metabolism.

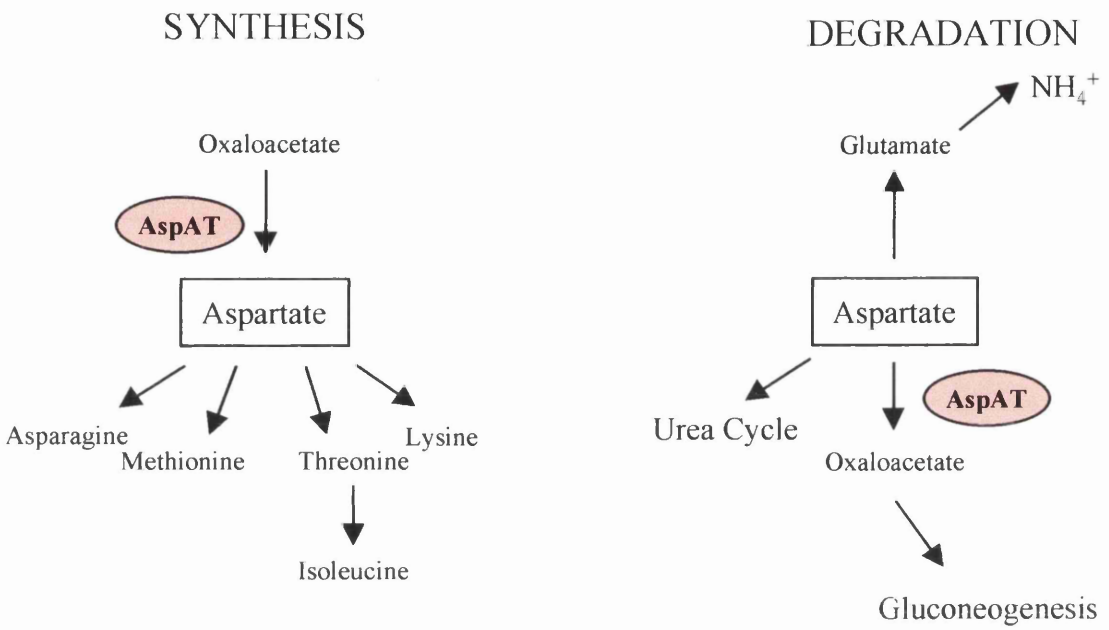

B) The TCA and the Urea Cycle are linked by Aspartate and Fumarate.

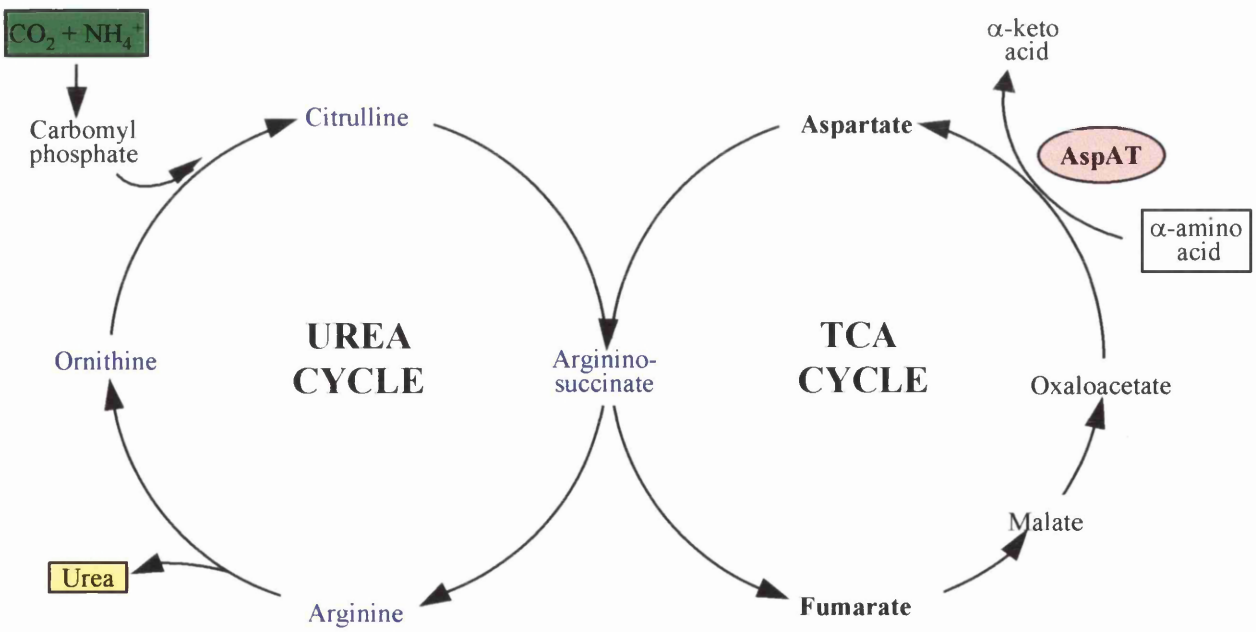

Figure 1.13. The malate-aspartate shuttle.

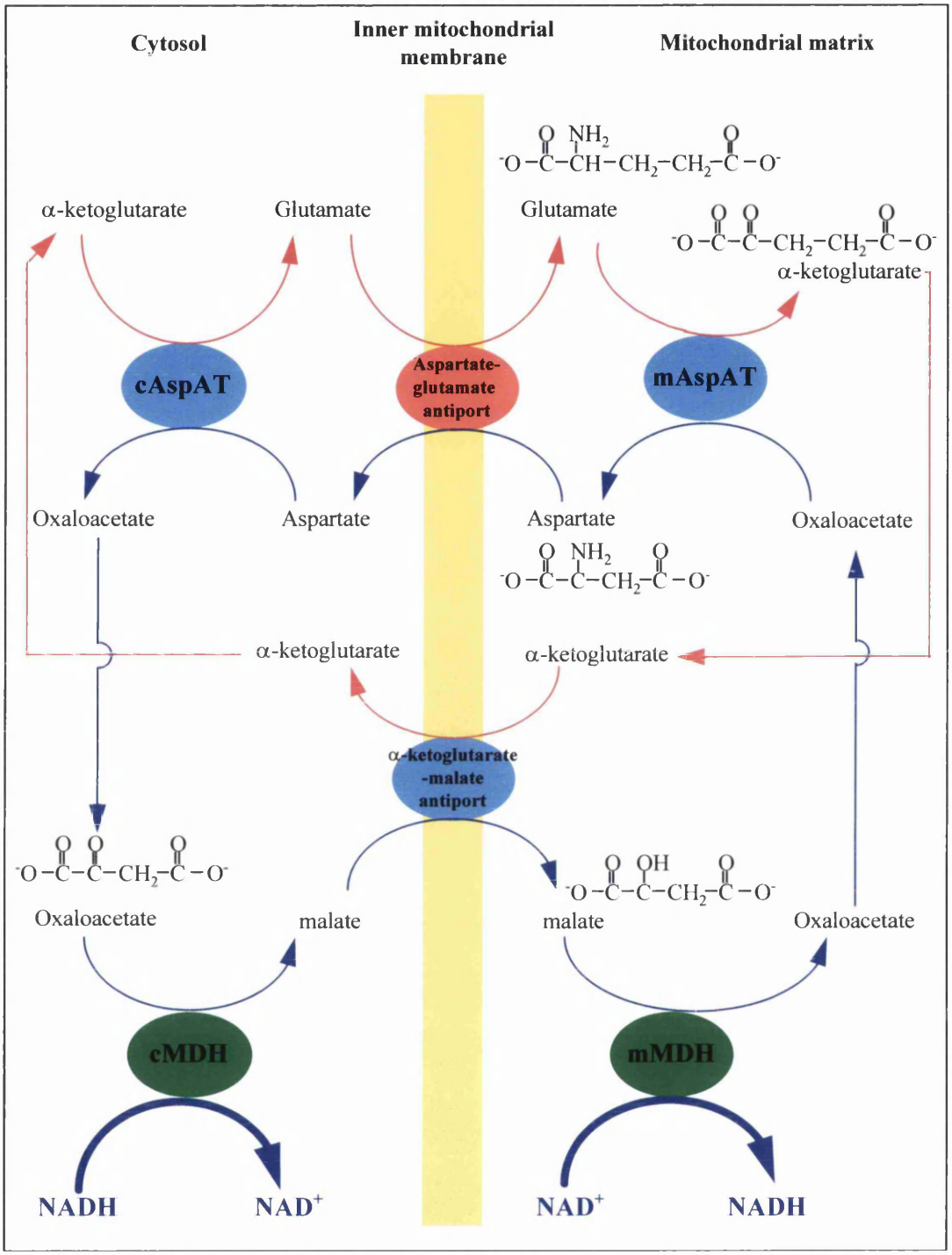

Legend. In heart and liver tissue the malate aspartate shuttle is the major mechanism for the transfer of reducing equivalents from the glycolytic pathway in the cytoplasm to the electron transfer chain in the mitochondrial matrix. Two parallel coupled reactions, catalysed by cytoplasmic and mitochondrial aspartate aminotransferase (cAspAT/mAspAT) and cytoplasmic and mitochondrial malate dehydrogenase (cMDH/mMDH) are involved. Essentially, electrons are transferred from cytoplasmic NADH to oxaloacetate, forming malate which translocates the inner mitochondrial membrane, and is then reoxidised by NAD^+ in the matrix to form NADH (represented by the blue lines in the lower portion of this figure). The resulting oxaloacetate cannot traverse the inner mitochondrial membrane, and is therefore transaminated to form aspartate which can be transported to the cytosolic side (red lines at top part of this figure). As this shuttle is readily reversible it can only transport NADH into the mitochondria if the NADH/NAD^+ ratio is higher in the cytosol than in the mitochondrial matrix.

Setoyama *et al.*, (1990) studied the malate aspartate shuttle in mouse cells, and found that the levels of all four enzymes were approximately equal, suggesting that expression of the components of the shuttle might be co-ordinately regulated. However, cAspAT and c/mMDH promoters were found to contain binding sites for the RNA polymerase II transcription factor CTF/NF, while this site was missing from the mAspAT promoter. The mAspAT promoter does however have an SP1 site, in common with other 'house-keeping' genes. This suggested that cAspAT/MDH and mAspAT genes are regulated differently. Indeed, following glucocorticoid stimulation, the levels of cAspAT mRNA, protein and enzyme activity are significantly elevated, while the corresponding levels of mAspAT remain unchanged (Pavé-Preux *et al.*, 1988). This effect was tissue specific, occuring in cells capable of gluconeogenesis (e.g. liver and kidney) but not in heart or brain cells. The structure of the cAspAT promoter has been further studied (Garlatti *et al.*, 1993) and found to interact with CCAAT/enhancer binding protein related proteins. The promoter is unusual in displaying features of both house-keeping and inducible genes. It lacks a TATA box, and is G+C rich (house-keeping) but has several CCAAT boxes and glucocorticoid response elements (inducible), and thus demonstrates a basal level of transcription that can be elevated by hormone signals in a tissue specific manner. The mAspAT promoter has also been shown to be inducible (e.g. Franklin *et al.*, 1987), and contains androgen response elements (Juang *et al.*, 1995); this and other possible effects of mAspAT up-regulation will be discussed in the 'General Discussion' section with respect to the work presented in this thesis.

2. MATERIALS AND METHODS.

2.1 MATERIALS.

2.1.1 CHEMICALS AND REAGENTS.

All chemicals were AnalR® grade obtained from BDH (Poole, Dorset) with the exception of those listed below.

3-[cyclohexylamino]-1-propane-sulphonic acid (CAPS).	Aldrich Chemical Co., Gillingham, Dorset, UK.
ECL Western blotting reagents; ECL molecular weight markers; Megaprime™ DNA labelling system; Rainbow molecular weight markers.	Amersham International Plc., Buckinghamshire, UK.
Ampicillin sodium B.P. (Penbritin®).	Beecham Research Laboratories.
Electrophoresis grade reagents: Tris; acrylamide; DATD; gelatin; SDS; N,N,N',N'-tetramethylenediamine (TEMED); N,N'-methylenebis-acrylamide; ammonium persulphate; HRP colour development reagent (4-chloro-1-napthol) ; Coomassie brilliant blue R250.	Bio-Rad Laboratories, Richmond, California, USA.
Tris; DOTAP transfection reagent.	Boehringer Mannheim GmbH, Germany.
Pansorbin (formalin fixed *S. aureus* type A cells).	Calbiochem, LaJolla, California, USA.
Trypsin; bacto-tryptone; yeast extract; bacto-agar.	Difco Ltd.
Formaldehyde; formamide.	Fluka Biochemicals. Gillingham, UK.

Tissue culture reagents: 7.5% sodium bicarbonate solution; L-glutamine solution; penicillin/streptomycin solution; DMEM; 1x and 10x BHK medium; new-born and foetal calf serum (NCS and FCS).	Gibco-BRL BRL, Paisley, UK.
Isopropyl thiogalactoside (IPTG); 5-bromo-4-chloro-3-indolyl β-D-galactoside (X-gal).	Life Technologies, Gaithersburg, USA.
Glycerol; ultrapure ethanol; glacial acetic acid; hydrochloric acid; methanol.	May and Baker Ltd., Dagenham, UK.
Ecoscint™ scintillation fluid; Sequagel acrylamide solution.	National Diagnostics, Manville, NJ, USA.
Sephaglas® Bandprep kit.	Pharmacia, Uppsala, Sweden.
Rnasin® Ribonuclease inhibitor.	Promega Corp., Wisconsin, USA.
Plasmid purification kit.	QIAGEN GmbH, Germany.
Tween 20; Triton X-100; agarose; lysozyme; guanidine thiocyanide; Ficoll 3350; polyvinylpyrollodine 360 (PVP); phenylmethylsulphonyl fluoride (PMSF); dithiothreitol; diethyl pyrocarbonate (DEPC); lyophilised salmon sperm DNA; protein-A FITC conjugate; DNAse free RNAse A (type IA); chloramphenicol; S-lauryl-sarcosine; Antifoam A; ultrapure phenol; ethidium bromide (solid); isoamylalcohol.	Sigma Chemical Co., UK.

2.1.2 RESTRICTION AND DNA MODIFYING ENZYMES.

Restriction enzymes ($10U\mu l^{-1}$) supplied with appropriate reaction buffers at a 10X concentration were purchased from Boehringer-Mannheim GmbH, Germany. T4 polynucleotide kinase, T4 DNA polymerase and Taq DNA polymerase ($5U\mu l^{-1}$) were obtained from the same source.

MoMLV Reverse transcriptase ($200U\mu l^{-1}$ with 5x buffer) and T4 DNA ligase were obtained from Gibco-BRL, Paisley, UK.

2.1.3 RADIOCHEMICALS.

Radiochemicals were supplied by Amersham International Plc. (Bucks., UK.).

[^{35}S] L-methionine.	SA 800 $Cimmol^{-1}$ ($15\mu Ci\mu l^{-1}$)
[α^{35}S] dATP.	SA 1000 $Cimmol^{-1}$ ($10\mu Ci\mu l^{-1}$)
5'[α^{32}P] dCTP and 5'[α^{32}P] dGTP.	SA 3000 $Cimmol^{-1}$ ($10\mu Ci\mu l^{-1}$)
5'[γ^{32}P] ATP.	SA 5000 $Cimmol^{-1}$ ($10\mu Ci\mu l^{-1}$)
14.3-200kDa ^{14}C methylated protein molecular weight markers.	SA $5\mu Ci\mu l^{-1}$

2.1.4 OTHER MATERIALS AND APPARATUS.

Hybond-N hybridisation membrane.	Amersham International, Bucks., UK.
Tissue culture plasticware.	Becton Dickinson Ltd., UK.
Mini Protean® protein gel kit; Mini Trans-Blot cell.	Bio-Rad Laboratories, Richmond, USA.
Sorvall RC5B, RT6000B centrifuges.	DuPont UK., Hitchin, Herts., UK.
Hybridisation oven and glass hybridisation tubes.	Hybaid,
XS-1 (x-ray film); Biomax MR x-ray film.	Kodak, UK.
PD-10 desalting (Sephadex G-25) columns.	Pharmacia Fine Chemicals, Uppsala, Sweden.
FPLC system; MonoQ HR 5/5 column.	Pharmacia LKB, Uppsala, Sweden.
Polaroid 667 film.	Polaroid UK.

0.5 and 1.5 ml micro-centrifuge tubes.	Sarstedt Ltd., Leicester, UK.
Stratalinker™ UV cross-linker.	Stratagene, USA

2.1.5 CELLS.

The following cell lines were used in the experiments described in this thesis.

BHK 21 clone 13 cells:- A fibroblast cell line derived from baby hamster kidney cells (Macpherson and Stoker, 1962), and maintained within the Institute of Virology, Glasgow.

RE cells:- Rat embryo fibroblasts prepared from 16-17 day old sibling embryos of inbred Hooded Lister rats, as described in Section 2.2.2.2 below.

Bn5T cells:- Derived from the *in vitro* culture of a tumour induced by injection of Bn5 cells, which were RE cells transformed by the cloned BglIIN fragment of HSV-2 strain HG52 (Cameron *et al.*, 1985; Macnab *et al.*, 1985).

NRK 536 cells:- Normal rat kidney fibroblast cell line used for colony formation assays, and obtained from B. Matz (University of Freiberg, Germany).

2.1.6 VIRUS STRAINS.

Virus stocks were provided by Mrs. Mary Murphy (Institute of Virology, Glasgow), except where stated below.

Herpes simplex virus type-1 (HSV-1) strain 17^+ (Brown *et al.*, 1973) and HSV-2 strain HG52 (Timbury, 1971) were used as wild type virus in all experiments.

The intertypic recombinant viruses Bx1, Fx9 and R12-5 were obtained from Mrs. Mary Murphy.

HSV-1 strain F was provided by Dr. A. Maclean, and HSV-2 strain MS was provided by Dr. J.C.M. Macnab, both of the Institute of Virology, Glasgow.

HSV-1 1217, a spontaneous mutant which fails to induce dUTPase activity, and HSV-1 1218, an insertional dUTPase mutant (Fisher and Preston, 1986) were kindly provided by Dr. V. Preston, Institute of Virology, Glasgow.

2.2 METHODS.

2.2.1 GENERAL PROCEDURES.

2.2.1.1 pH measurement.

The pH of aqueous solutions was measured using a Whatman PHA300T hand held pH meter fitted with a HI 1295 amplified electrode.

2.2.1.2 Autoclaving and Glassware sterilisation.

Equipment and solutions were sterilised at 15psi for 20 minutes by staff in the washroom, Institute of Virology, Glasgow. Glassware was sterilised by baking in an oven at 180 ° C for at least 12 hours.

2.2.1.3 Filter sterilisation.

Heat-labile solutions were sterilised by filtration through a Whatman syringe filter (pore diameter 0.2 μm) into a sterile tube.

2.2.2 TISSUE CULTURE.

2.2.2.1 General Solutions.

The following solutions were prepared by staff in the Media Department, Institute of Virology, Glasgow.

Sterile Deionised Water. De-ionised water obtained from a 'Milli-Ro 60 plus' de-ioniser (Millipore, USA) and sterilised by autoclaving.

Phosphate Buffered Saline (PBS-A). PBS-A (170mM NaCl, 3.4mM KCl, 1mM Na_2HPO_4, 2mM KH_2PO_4, pH 7.2) was sterilised by autoclaving.

Trypsin. Trypsin was dissolved at a concentration of 0.25% (w/v) in Tris-saline containing phenol red and adjusted to pH 7.5 with $NaHCO_3$. Aliquots were stored at -20 ° C.

Versene (ethylenediaminetetra-acetic acid, EDTA). 0.6mM EDTA dissolved in PBS-A containing phenol red, sterilised by autoclaving and stored at room temperature.

Trypsin/Versene (T/V). 5ml of trypsin solution 0.25% (w/v) was added to 20ml versene immediately prior to use, and stored for a maximum of 3 days at 4 ° C.

Carboxy-methyl Cellulose (MC). 3% carboxy-methyl cellulose dissolved in ddH_2O and sterilised by autoclaving.

The solutions below were purchased from Gibco-BRL, Paisley, UK.

Dulbecco's Modified Eagles Medium (DMEM). Stored at 4 ° C. Supplemented with 100U/ml penicillin, 100μgml^{-1} streptomycin (referred to as supplemented DMEM from now on) and NCS/FCS as stated for each cell type.

Glasgow modified Eagle's medium (1x BHK medium). Stored at 4 ° C. Supplemented with 100U/ml penicillin, 100μgml^{-1} streptomycin, 5% tryptose phosphate broth and 10% NCS.

Sodium Bicarbonate ($NaHCO_3$). A 7.5% w/v $NaHCO_3$ solution was stored at 4 ° C for up to 2 weeks.

Newborn Calf Serum (NCS) and Foetal Calf Serum (FCS). Mycoplasma tested and virus screened NCS and FCS was stored in 20ml aliquots at -20 ° C.

L-Glutamine. L-glutamine was supplied at a concentration of 200mM and stored in aliquots at -20 ° C.

Penicillin/Streptomycin (PS) solution. A solution containing concentrations of 1% w/v streptomycin, 10^4Uml^{-1} penicillin was dispensed into aliquots for storage at -20 ° C.

2.2.2.2 Preparation of primary rat embryo cells

Primary rat embryo cells were prepared from 16-17 day old embryos from an inbred colony of Hooded Lister rats which was maintained within the Institute of Virology, Glasgow by brother-sister mating for over 20 years. This colony has no history of susceptibility to form spontaneous tumours (Macnab, 1979). Embryos from a single litter were removed from the uterus of a pregnant rat, washed with versene, eviscerated and again washed with versene before being finely chopped. To obtain a single cell suspension, cells were treated with 0.25% trypsin for 30 minutes at 37 ° C. The supernatant was removed and the remaining cell clumps were treated with fresh trypsin. Newborn calf serum was added to a final concentration of 5% (v/v) to inactivate the trypsin. The supernatant was centrifuged at 1000rpm for 10 minutes at 4 ° C. The cell pellet was resuspended in supplemented DMEM containing 5% NCS.

$2x10^8$ cells were seeded in a $850cm^2$ plastic tissue culture roller bottle. Cells were grown at 37 °C until 80% confluent, and thereafter at 31 °C with weekly medium changes. Cells were viable for approximately four weeks, and were routinely used at second passage.

2.2.2.3 Maintenance of cell lines.

Bn5T and ***RE*** cells were maintained in $850cm^2$ plastic tissue culture roller bottles at 37 °C in supplemented DMEM containing 5% NCS in an atmosphere containing 5% CO_2. Confluent Bn5T and RE cells were split 1:5 to 1:10 and 1:3 or 1:4 respectively, depending on growth rates observed.

BHK C13 cells were maintained in roller bottles in 1x BHK medium (Gibco BRL) containing 10 % NCS in an atmosphere containing 5% CO_2, and were split 1:10 as required.

NRK 536 cells were cultured in $175cm^2$ flasks in DMEM containing 10% FCS, at 37 °C in an atmosphere containing 5% CO_2 and were split 1:5 when confluent.

The medium on all cells was replaced every 3-4 days. Cells were split by washing three times in versene, and then briefly in trypsin/versene (1:5). Released cells were pelleted at 1000rpm for 5 minutes to remove the trypsin before reseeding.

2.2.2.4 Cell harvesting.

Cells required for large scale protein purification were washed in ice cold PBS-A three times before being scraped into PBS-A using a rubber policeman. Cells were pelleted at 2000rpm for 10 minutes at 4 °C. The supernatant was removed and the cell pellet was either used immediately or was stored dry at -70 °C for later use.

Cell lysates for Western blotting experiments were prepared by the addition of 1ml of 3xBM *(Section 2.2.5.6)* to the cell monolayer.

2.2.2.5 Preparation and storage of cell stocks.

Actively growing cells (~2 $x10^8$) were trypsinised and the cells pelleted at 1000rpm for 10 minutes at 4 °C. The cell pellet was resuspended in 1ml of supplemented DMEM containing 10% FCS and 10% DMSO (v/v), and frozen slowly overnight at -70 °C before transfer for long term storage in liquid nitrogen (-196 °C).

Aliquots of stock cells were resuscitated periodically to replace existing cultures to

prevent the accumulation of alterations within the cell lines due to continuous passage. To recover frozen cells, 1ml stocks were thawed rapidly and seeded into $25cm^2$ flasks and incubated at 37°C in the appropriate medium. The medium was changed the following day to remove the DMSO and non-adherent cells from the culture.

2.2.2.6 Mock infection and infection of cells with HSV.

The growth medium was removed from the cells and serum free medium containing no virus or the appropriate amount of HSV was added; cells were incubated at 37°C for 1 hour. The innoculum was removed and replaced with normal medium, and the infection allowed to continue for defined periods of time, usually overnight.

2.2.2.7 Transfection with plasmid DNA.

2.2.2.7.1 Calcium Phosphate precipitation.

HEBS: 137mM NaCl, 5mM KCl, 0.2mM NaH_2PO_4, 9mM D-glucose, 21mM Hepes pH 7.5.

A modification of the method of Stow and Wilkie (1976) was used to transfect plasmid DNA into BHK C13 cells. 1-5μg of plasmid DNA was added to 1ml HEBS containing $5\mu gml^{-1}$ calf thymus DNA and 70μl 2M $CaCl_2$. Following mixing, this solution was added to 60mm plates of sub-confluent BHK C13 monolayers from which the medium had been removed. Following incubation at 37°C for 45 minutes, the cells were overlayed with 4ml of 1x BHK medium containing 5% NCS. 4-6 hours later, the medium was removed and the cells washed with serum free medium. 1ml of 20% (v/v) DMSO in HEBS was added to each plate and incubated at room temperature for exactly 4 minutes. The DMSO was removed and the cells washed twice with serum free medium before addition of 4ml of serum containing medium and incubation at 37°C.

2.2.2.7.2 Lipofection with DOTAP.

HBS: 20mM Hepes, 150mM NaCl, pH 7.4.

N-[1-(2,3-Dioleoyloxy)propyl]-N,N,N-trimethyl-ammoniummethysulphate (DOTAP) as an aqueous dispersion ($1mgml^{-1}$) was used to introduce plasmid DNA containing the mAspAT cDNA into NRK 536 cells. 60mm plates of sub-confluent NRK 536 cells were transfected with up to 5μg of plasmid following the manufacturers' instructions (Boehringer Mannheim).

30µl of the transfection reagent was diluted to 100µl in HBS. The DNA (5µg) was diluted separately to 100µl in HBS. The solutions were mixed and incubated at room temperature for 10 minutes. 4ml of tissue culture medium (containing serum) was added to the DOTAP-DNA mixture, and mixed gently, before addition to tissue culture cells from which the medium had been aspirated. The cells were incubated at 37 ° C for periods of time ranging from 6 hours to overnight, and the medium removed and replaced with normal tissue culture medium. The cells were incubated at 37 ° C and were ready for further experimentation.

2.2.3 VIRUS.

2.2.3.1 Virus stock production.

Stocks of HSV-1 strain 17 and HSV-2 HG52 were produced by the infection of 20 sub-confluent 850cm^2 roller bottles of BHK C13 cells with virus at a multiplicity of infection of 1:300. The virus was added in serum free BHK medium for 30 minutes, before removal of the virus and addition of 20ml of normal BHK medium to each bottle. Cells were incubated at 31 ° C for 4-7 days, until the cells were falling off the substrate.

To harvest HSV-1, cells were shaken from the roller bottle using sterile glass beads and the medium poured into 250ml sterile Falcon™ tubes. After centrifugation of the tubes at 2000g for 10 minutes at 4 ° C (A), the supernatant was removed to a Sorvall tube and centrifuged at 12,000g for 2 hours at 4 ° C (B). The pellet from each tube was resuspended in 5ml of supernatant in a universal tube and stored at -70 ° C. Each stock was checked for sterility by streaking on blood agar plates which were incubated at 37 ° C for 5 days. The first pellet (A) contains cell associated (CA) virus which was released by 2 cycles of sonication, freeze-thawing and centrifugation at 2000g. The supernatant from each stage was stored in aliquots at -70 ° C. The virus released into the supernatant (B) was sonicated once and stored in aliquots at -70 ° C.

HSV-2 infection produces mainly cell associated virus which is harvested as described for cell associated HSV-1 (A) above.

2.2.3.2 Titration of Virus stocks.

Sub confluent BHK C13 cells were routinely used to determine the titre (pfu/ml) of HSV. 1x 10^6 cells were seeded into sterile 60mm diameter tissue culture plates which were incubated at 37 ° C overnight in a humidified 5% CO_2 incubator.

Serial ten-fold dilutions of the virus stocks were made in serum free BHK medium. The growth medium was aspirated from the cells and 200µl of each virus dilution was added to a dish. The cells were then incubated at 37 ° C for 1 hour to enable virus adsorption. The inoculum was removed and to prevent secondary plaque formation the plates were overlayed with 5ml of a 1:1 mixture (v/v) of 2xBHK medium and 3% carboxy-methyl cellulose solution. A plate infected with each dilution was incubated at 31 ° C and another at 37 ° C for 2-3 days until plaques were visible. The cells were fixed by the addition of 5ml Giemsa stain to each plate. After staining at room temperature for 1-2 hours the plates were rinsed gently in cold water and allowed to dry. Visible plaques were counted with a low power binocular light microscope and the titre of the virus stock calculated.

2.2.4 ANTISERA.

2.2.4.1 Production of tumour bearing serum (TBS).

TBS was produced by Dr. Joan Macnab (Institute of Virology, Glasgow) by the subcutaneous injection of 8 week old Hooded Lister rats with 1x 10^7 Bn5T cells. Tumours generally developed within 1-2 months. Blood was collected by cardiac puncture, allowed to clot overnight at 4 ° C and centrifuged at 2000rpm for 10 minutes at 4 ° C before removal of the serum. 1ml aliquots of serum were stored at -20 ° C.

2.2.4.2 Raising an antiserum against the 40 kDa polypeptide.

The 40kDa polypeptide was purified by ammonium sulphate fractionation and FPLC anion exchange chromatography as described in Section 2.2.5.5. The 40kDa polypeptide was identified on an SDS-PAGE gel by comparison with a TBS immunoprecipitation, and excised from the dried gel with a sterile scalpel blade. The backing paper was removed from the gel slice, which was ground up in a small homogeniser and mixed with incomplete Freund's adjuvant. The immunogen was injected into a rabbit by Dr. J.C.M. Macnab, Institute of Virology, Glasgow,

followed by regular booster innoculations. Blood was collected by Mr David Miller, Institute of Virology, Glasgow, and the serum collected as described above.

2.2.4.3 Raising antibody to mAspAT.

Antibody to mAspAT was raised by injection of pre-mAspAT purified from *E.coli* (gift of J.R. Mattingley, University of Missourri) into a rabbit by Dr. J.C.M. Macnab. Serum was collected as previously described.

2.2.4.4 Antibody to HSV UL49.

An antiserum against the HSV UL49 gene product, p43 was kindly provided by J. Leslie, Institute of Virology, Glasgow.

2.2.4.5 Antibody to HSV dUTPase.

An antiserum against the HSV dUTPase was kindly provided by Dr S. Caradonna, Molecular Biology Department, Medical and Dental University of New Jersey, USA.

2.2.5 PROTEIN PURIFICATION AND ANALYSIS.

2.2.5.1 Solutions.

100X Protease inhibitors: 300mgml^{-1} benzamidine, 340mgml^{-1} PMSF, 100mgml^{-1} phenanthroline in ethanol.

WF buffer: 20mM Tris-acetate, 20mM NaCl, 0.5mM EDTA, 10mM β-mercaptoethanol, pH 7.4 (Welch and Feramisco, 1985).

RIPA: 0.1% (w/v) SDS, 1% (w/v) sodium deoxycholate, 1% (w/v) triton X-100, 150mM NaCl, 10mM Tris-HCL pH 7.4 (Docherty *et al.*, 1981).

2.2.5.2 Radiolabelling polypeptides with [^{35}S] L-methionine.

Cellular polypeptides were labelled with [^{35}S] L-methionine *in vitro* by growing cells in medium lacking methionine for at least 1 hour prior to the addition of 50μCiml^{-1} of [^{35}S] L-methionine to the medium. Radiolabelling was carried out at 37 ° C overnight, the cells washed twice with PBS-A and harvested for immunoprecipitation or protein purification, as described in Sections 2.2.5.4 and 2.2.5.5 respectively.

2.2.5.3 Measurement of incorporation of radiolabel into polypeptides.

A 1µl aliquot of cell lysate was spotted onto a DEAE filter disk, and the proteins precipitated by two washes in 5% TCA. The disk was rinsed in acetone, and dried under a heat lamp before scintillation counting in a vial containing 4ml of Ecoscint®.

2.2.5.4 Immunoprecipitation.

Immunoprecipitation of radiolabelled polypeptides was used to identify the 40kDa polypeptide in protein purification experiments. Radiolabelled cells were lysed by sonication and incubation for 30 minutes on ice in radioimmunoprecipitation assay buffer (RIPA) containing protease inhibitors. The incorporation of radiolabel was determined and $4x10^6$ cpm of [^{35}S] L-methionine labelled polypeptides were immunoprecipitated with 10µl of tumour bearing serum for 1 hour at 4 ° C in a total volume of 100µl. 60µl of Pansorbin® was added and the sample incubated on ice for 1 hour. The pansorbin was pelleted by centrifugation at 13krpm, washed twice with 1ml of RIPA, and once in Tris-saline. 50µl of SDS-PAGE sample buffer (Section 2.2.5.6) was added, and immune complexes dissociated by heating at 70 ° C for 10 minutes. After the Pansorbin® was pelleted the supernatant was loaded onto an SDS-PAGE gel, or stored at -20 ° C until required.

2.2.5.5 Purification of the 40kDa polypeptide.

2.2.5.5.1 Cell lysis.

Bn5T cells (approximately $4x10^9$) were rinsed twice, scraped into 40ml of ice cold PBS-A and pelleted at 1500rpm (Sorvall RTB-6 centrifuge). The pellet was resuspended in 20ml of WF buffer containing protease inhibitors, sonicated for 5 minutes in a sonibath and centrifuged at 10krpm (Sorvall SS34 rotor). The supernatant was taken to a fresh tube.

2.2.5.5.2 Ammonium sulphate fractionation.

Solid ammonium sulphate was ground in a pestle and mortar and added to the cell lysate with continuous stirring at room temperature. When the ammonium sulphate was completely dissolved, the solution was stirred on ice for 1 hour. The solution was then centrifuged at 10krpm (Sorvall SS34 rotor) to pellet the precipitated

polypeptides. Ammonium sulphate was added to concentrations of 30%, 60% and 90% in turn. The 40kDa polypeptide was precipitated in the 90% fraction.

2.2.5.5.3 Desalting.

The polypeptides precipitated in the 90% ammonium sulphate fraction were desalted into 50mM Tris-HCl pH 8.0 using a PD-10 column, containing 10ml of Sephadex G25. The polypeptides were eluted in a volume of 3.5ml and concentrated to half this volume in a speedivac.

2.2.5.5.4 Anion exchange chromatography.

A MonoQ prepacked HR 5/5 FPLC column was equilibrated with 50mM Tris-HCl, pH 8.0. The samples were centrifuged at 13krpm in a micofuge to pellet any debris, and loaded onto the column. A gradient of 0-1.0M NaCl in buffer followed by elution with 2M NaCl was used to elute the polypeptides. 1ml fractions were collected and desalted using a FastDesalt® column into 10mM ammonium bicarbonate, and concentrated to 1/10th volume in a speedivac for loading on an SDS-PAGE gel.

2.2.5.6 SDS-PAGE.

The SDS-PAGE system first described by Laemelli (1970) was used to analyse protein samples. The concentration of acrylamide in the resolving gel ranged from 9% to 15%. Acrylamide was crosslinked by the addition of 1:40 N-N'-methylenebisacrylamide (w/w), and polymerised with 0.04% (w/w) APS and 0.04% (w/w) TEMED. The gel was overlayed with butan-2-ol which was removed after polymerisation was complete. Stacking gel containing 5% acrylamide was crosslinked with 1:40 (w/w) N-N'diallyl-tartar-diamide (DATD) and polymerised as above.

Samples were heated at 70°C for 10 minutes in boiling mix before loading. Large (15cm x 15cm) gels were run at 35mA at 4°C, and mini gels at 200V at room temperature.

Following electrophoresis, polypeptides were visualised by staining with Coomassie blue for 30 minutes, and destaining with several washes in destain at 37°C. Gels were dried at 80°C under vacuum prior to autoradiography or exposure to a phosphorimager screen.

Samples for Western blotting were not stained, as this inhibited the electrophoretic transfer of the polypeptides to the membrane.

The solutions used are detailed below.

Solution	Acrylamide	DATD	bis-acrylamide	ddH_2O
Stacking gel mix (30%)	58.44g	1.56g	-	200ml
Resolving gel mix (30%)	55g	-	5g	200ml

Solution	Tris-HCl	SDS	ddH_2O	pH
Resolving gel buffer	181.5g	4g	1000ml	8.9
Stacking gel buffer	59g	4g	1000ml	6.7

Solution	Tris	Glycine	SDS	ddH_2O
Tank buffer	6.32g	4g	1g	1000ml

Boiling Mix (3xBM): 30% stacking gel buffer, 30% glycerol, 12.5% SDS, 15% β-mercaptoethanol.

Stain: 50% methanol, 7% acetic acid, 0.2% Coomassie blue R250 in ddH_2O.

De-stain: 10% methanol, 7% acetic acid in ddH_2O.

2.2.5.7 Western Blotting.

2.2.5.7.1 Solutions.

Transfer buffer: 10mM CAPS pH 11, containing 10% (v/v) methanol.

TBS-T: 20mM Tris-HCl, 500mM NaCl, pH 7.5 containing 0.1% (v/v) Tween 20.

Blocking solution: 3% (w/v) gelatin in TBS-T.

Antibody diluent: TBS-T containing 1% (w/v) gelatin and 0.1% sodium azide.

Stripping solution: 100mM β-mercaptoethanol, 2% (w/v) SDS, 62.5 mM Tris-HCl pH 6.7.

Ponceau S stain: 2% Ponceau S (w/v), 1% acetic acid (v/v) in ddH_2O.

2.2.5.7.2 Protocol.

Polypeptides separated by SDS-PAGE were transferred to Hybond-N™ membrane by electrophoretic transfer in a BioRad mini transfer kit at 50V for 2 hours. The efficiency of transfer was determined by analysis of transferred Rainbow molecular weight markers and by reversibly staining the membrane with Ponceau S.

The membrane was blocked by gentle shaking at 37 ° C in blocking buffer, washed three times in TBS-T and the primary antibody added in antibody diluent. After incubation for 1 hour, the membrane was washed again, and a 1/1000 dilution of secondary antibody conjugated to horse radish peroxidase (HRP) was added and the blot incubated for 1 hour. Final washing of the blot was with several changes of tris buffered saline without detergent. When biotinylated ECL molecular weight markers were used, streptavidin-HRP was added to the secondary antibody solution.

Detection of polypeptides was with ECL reagents (Amersham). An equal volume of each reagent was added to a tube, mixed and poured over the membrane. After 1 minute the excess reagent was removed and the membrane placed in a polythene bag. The blot was exposed to X-ray film for between 5 seconds and 1 minute.

The antibody could be stripped from the membrane and the samples reprobed with a different antiserum by treatment of the membrane with 'stripping solution' for 1 hour at 55 ° C and extensive washing in TBS-T.

2.2.6 INDIRECT IMMUNOFLUORESCENCE (FITC).

2.2.6.1 General Solutions.

Tris Buffered Saline (TBS). 0.606g Tris hydroxymethyl methylamine and 8g NaCl were dissolved in 600ml sterile ddH_2O and 38ml 1M HCl added. The volume was made up to 1L and the pH adjusted to 7.6 with 2M HCl. This produces a 5mM solution with respect to Tris.

Triton X100. A 0.25% v/v Triton X100 solution was made aseptically in PBS-A and stored at 4 ° C.

Antibody Diluent. A 1% w/v bovine serum albumin (BSA) solution was made in sterile PBS-A. 20µl of a 10% w/v sodium azide solution (Sigma) was added to 100ml of the BSA solution and the mixture was stored at 4 ° C in 10ml aliquots.

Tris-HCl. Tris was dissolved in deionised water to a final concentration of 2M and the pH adjusted as required with 2M HCl. The solution was sterilised by autoclaving and diluted with ddH_2O to the appropriate concentration for use.

Blocking Solution. FCS was added aseptically to sterile PBS-A or TBS to a final concentration of 5% v/v.

2.2.6.2 Antibodies.

The primary antibody was a 1/500 dilution of a rabbit antiserum raised against the precursor of mAspAT.

Secondary detection was with a Protein A-FITC conjugate, used at a dilution of 1/200. All dilutions were made with antibody diluent.

2.2.6.3 Cells.

Glass microscope coverslips were washed in a 0.1% (w/v) SDS and rinsed thoroughly with de-ionised water. Coverslips were rinsed in 70% ethanol, dried at 50 ° C, polished and sterilised by dry heat at 180 ° C for 2 hours. Coverslips were placed into tissue culture plates prior to cell seeding. After overnight incubation, coverslips were rinsed in PBS-A and then fixed in pre-cooled (-20 ° C) mixture of 3:1 methanol:acetone.

2.2.6.4 Immunofluorescence.

All procedures took place at room temperature. Fixed coverslips were placed in a holder and cells rehydrated in 10ml PBS-A for 2 minutes. The PBS-A was drained from the coverslips which were then washed 3x in 10ml PBS-A (5 minutes each). The coverslips were placed in a moist box and 50µl of blocking solution added to each. Blocking solution was drained from the slides just prior to addition of 10µl of primary antibody and the samples incubated for a minimum of 30 minutes. Cells were then placed into a slide holder, rinsed 3x in 10ml PBS-A (5 minutes each) and returned to the moist box. All subsequent procedures were performed in the dark whenever possible. 10µl of secondary antibody dilution was added to each coverslip and the samples were then incubated for a minimum of 30 minutes. The coverslips were again washed 3x in 10ml PBS-A, mounted onto slides using PBS:glycerol (50:50), and the edges of the coverslip sealed with clear nail polish. Cells were visualised using a Nikon Microphot-SA fluorescent microscope.

2.2.7 RIBONUCLEIC ACID EXTRACTION FROM EUKARYOTIC CELLS.

2.2.7.1 Solutions and equipment for RNA work.

All solutions were made from separate stocks of molecular biology grade chemicals used only for RNA work. Solutions were treated with 0.1% (v/v) diethyl pyrocarbonate (DEPC) overnight at room temperature and then autoclaved. Solutions containing Tris-Cl were made with distilled water pre-treated with DEPC. Glassware was treated with DEPC and sterilised. Sterile disposable plasticware was used whenever possible.

Ribonucleoside vanadyl complexes (RVC). RVCs were purchased as a 200mM solution at -20 ° C (Sigma), and used at a working concentration of 20mM in RNA solutions not containing SDS or EDTA to inhibit the action of RNases. They do not affect production of cDNA by reverse transcription of mRNA, and can be removed from the solution by phenol extraction.

Solution D ('denaturing'). 4M guanidinium thiocyanate, 50mM Tris-HCl (pH 7.5), 0.5% (w/v) S-lauryl-sarcosine, 2mM EDTA (pH 7.5), 0.1M β-mercaptoethanol.

100ml of solution D was made by dissolving 50g guanidinium thiocyanate, 0.5g sarkosyl, 0.33ml AntifoamA, 2.5ml 2M Tris-HCl pH 7.5, and 0.8ml 250mM EDTA pH 7.5 in sterile ddH_2O to a final volume to 99.3ml, prior to sterilisation by autoclaving. Following autoclaving, 0.7 ml of β-mercaptoethanol was added and the solution stored at 4 ° C for up to 1 month.

Ethidium Bromide (EtBr). EtBr was dissolved in ddH_2O to give a final concentration of $10mgml^{-1}$ and stored in a foil wrapped 20ml universal in a designated lockable cupboard. Extreme care was taken when preparing and using EtBr solutions which are known to be carcinogenic.

Sodium acetate (pH 4.0)(NaOAc). Solid sodium acetate was dissolved in sterile ddH_2O to a final concentration of 2M, and the pH adjusted to 4.0 with glacial acetic acid, prior to filter sterilisation, and storage in aliquots at 4 ° C.

Chloroform:Isoamylalcohol (CHCl$_3$/IAA). Chloroform and isoamylalcohol (isopentylalcohol, 95% v/v 3-methyl-1-butanol) were mixed to give solutions of 24:1 and 49:1 as required.

Ultrapure Phenol (φ). Solid ultrapure (UP) phenol was immersed in sterile ddH_2O and warmed to 65 ° C prior to equilibration with sterile ddH_2O or TE pH 7.5-8.0. The saturated phenol was allowed to settle, aliquoted into dark bottles (taking some of the aqueous phase) and stored at -20 ° C.

2.2.7.2 Single Step Extraction of total cellular RNA from tissue culture cells.

Protocol. This method is adapted from that of Chomczynski and Sacchi (1987). The volumes given refer to purification of total RNA from 10^6 cells and were scaled up accordingly. This method uses guanidinium isothiocyanate as a protein denaturant but omits the ultracentrifugation step that most guanidinium RNA extraction methods require (Chirgwin *et al.,* 1979), allowing rapid processing of multiple samples.

Cell pellets were harvested and stored at -70 ° C until required, or else cell monolayers were treated *in situ* following 2 washes in ice cold PBS-A. 100µl of solution D was added to the cell pellet or monolayer and mixed. 10µl 2M NaOAC (pH 4.0), 100µl of phenol (pH 7.6), and 20µl chloroform:*iso*-amyl alcohol (v/v, 49:1) were added with mixing after each addition. After incubation on ice for 15 minutes, and centrifugation at 12,000g at 4 ° C for 15 minutes, the aqueous phase was transferred (avoiding the debris at the interface) to a clean tube containing 100µl isopropanol. The RNA was precipitated at -20 ° C for 1 hour, followed by centrifugation at 12,000g at 4 ° C. The RNA pellet was resuspended in 300µl solution D, and re-precipitated by addition of 300µl of isopropanol. The RNA pellet was resuspended in 200µl RNase free ddH_2O and 20µl 3M NaOAc. EtOH (600µl) was added and the sample stored at -70 ° C until required. Before use the RNA was pelleted at 12,000g for 15 minutes at 4 ° C, washed twice with 70% EtOH and air dried before resuspension in a suitable volume (10-200µl) of RNAse free ddH_2O. The purity of the preparation was estimated by measuring the absorbance at 260nm and 280nm. A pure preparation was taken as having an A_{260}/A_{280} ratio of 1.8-2.0. All aqueous RNA preparations were stored at -70 ° C.

2.2.7.3 Isolation of polyA$^+$ RNA.

2.2.7.3.1 Oligo(dT)$_{25}$-Dynabeads®.

PolyA$^+$ RNA isolation from total cellular RNA (section 2.2.7.2) was carried out using oligo(dT)-Dynabeads® (Dynal, Oslo) according to the manufacturers instructions as indicated briefly below. Oligo(dT)$_{25}$-Dynabeads® bind approximately 2μg PolyA$^+$ RNA per mg of beads. A typical mammalian cell contains about 10^{-5}μg total RNA, of which 1-5% is mRNA.

Solutions. 2x Binding 20mM Tris-HCl, 1mM LiCl, 2mM EDTA, pH 7.5
1x Washing 10mM Tris-HCl, 150mM LiCl, 1mM EDTA, pH 7.5
1x Elution 2mM EDTA, pH 7.5

Protocol. Except where stated procedures were carried out at 4 ° C to reduce the effect of RNases. Separation of the Dynabeads® from solution was performed by inserting the microfuge tube into the Magnetic Particle Concentrator (MPC®) for at least 30 seconds, and removing the supernatant with the tube in the MPC®.

75μg of total RNA in 100μl of DEPC treated ddH_2O was added to a microfuge tube containing 1mg oligo(dT)$_{25}$-Dynabeads® which had been equilibrated in 100μl 2x Binding buffer. The solutions were mixed gently, and hybridisation allowed to proceed for 5 minutes at room temperature. The tube was placed in the MPC® and the supernatant removed. Two washes with 200μl washing buffer were followed by careful removal of all the supernatant before resuspension in 5-10μl elution buffer. Elution of the PolyA$^+$ RNA was facilitated by heating the sample to 65 ° C for 2 minutes and immediately transferring the tube to the MPC®. The polyA$^+$ RNA solution was removed to a fresh tube and stored at-70 ° C.

2.2.7.4 Nucleic acid precipitation.

Nucleic acids were generally precipitated by the addition of NaOAc (pH 5.2) to a final concentration of 0.3M, followed by the addition of two volumes of ice-cold 100% EtOH. DNA precipitation was aided by storing the samples at -20 ° C for 1 hour.

In precipitations where *iso*-propanol was used (plasmid preps and RNA extraction), addition of 0.6 volumes of alcohol was sufficient to precipitate the nucleic acid. In these cases, samples were centrifuged immediately to recover the nucleic acid.

Nucleic acid pellets were washed twice in 70% EtOH, centrifuged briefly, air dried and resuspended in an appropriate volume of ddH_2O or TE pH 8.0.

2.2.7.5 Quantification of DNA and RNA.

A sample of the nucleic acid solution to be quantified was diluted 1/100 in sterile ddH_2O. The absorbance of the solution was measured at 260nm and 280nm against a ddH_2O blank. An absorbance at 260nm (A_{260}) of 1 was assumed to indicate the following nucleic acid concentrations:

Type and form of nucleic acid	*Concentration (μgml^{-1}) of sample*
Double stranded DNA	50
Single stranded DNA and RNA	40
Oligonucleotides	20

2.2.8 ELECTROPHORESIS OF NUCLEIC ACID.

2.2.8.1 General Solutions.

10X TAE Buffer.

Tris-HCl pH 8.0	400mM
NaOAc pH 5.2	50mM
EDTA pH 8.0	10mM

The solution was stored at room temperature and diluted 1:10 with deionised water on use.

10X TBE Buffer.

Tris-HCl pH 8.0	900mM
Orthoboric acid	900mM
EDTA pH 8.0	25mM

The solution was checked to ensure that the pH was 8.0, then stored at room temperature and diluted 1:10 with deionised water on use.

10X MOPS Buffer (3-[N-morphpolino] propane sulphonic acid).

MOPS (Sigma)	200mM
EDTA	50mM
NaOAc	10mM
NaOH	to pH 7.0

The solution was autoclaved stored at room temperature in dark bottles, and diluted 1:10 with sterile DEPC-treated H_2O on use.

RNA Loading Buffer. This was prepared freshly on the day of use from 300µl ultrapure formamide, 60µl 10X sterile MOPS, 100µl formaldehyde and 140µl sterile DEPC-treated `AnalaR' water. This buffer was used for denaturing RNA gels only and separate stocks of the constituents were kept exclusively for RNA work.

DF Loading Dye. DF loading dye consisted of 0.25% (w/v) bromophenol blue 0.25% (w/v) xylene cyanol and 25% (w/v) ficoll 400 in sterile ddH_2O. This was used as loading dye for DNA agarose and polyacrylamide- urea gels.

2.2.8.2 Agarose gel electrophoresis.

2.2.8.2.1 Denaturing electrophoresis of RNA.

The method used for formaldehyde-agarose denaturing gels for northern hybridisation analysis was based on that described by Lehrach *et al.*, (1977). An appropriate amount of agarose (1.0 -1.5g) was added to 10ml of 10x MOPS buffer and 73ml of DEPC treated ddH_2O. The agarose suspension was heated in a microwave oven until the agarose had dissolved. The volume was adjusted to 83ml and the solution cooled to 50 ° C. 17ml of formaldehyde (37% v/v) was added and the gel was mixed by swirling prior to pouring. After a period of 30 minutes to allow the gel to set the gel was covered with 1x MOPS running buffer. The RNA sample (10-40µg) was prepared in a solution of 50% (v/v) formamide, 1x MOPS, and 5.92% formaldehyde (v/v) to a volume not exceeding 100µl. This solution was heated to 65 ° C for 15 minutes, cooled on ice and 0.1 volumes of RNA loading buffer added. The sample was immediately loaded onto the gel and run at $5Vcm^{-1}$ until the bromophenol blue had migrated approximately two thirds of the distance down the gel. The gel was washed in DEPC-treated ddH_2O for 15 minutes to remove the formaldehyde and then the RNA transferred to Hybond-N™ by capillary transfer.

A marker track containing a 0.24-9.5kb RNA ladder was cut from the gel and stained in $1\mu gml^{-1}$ EtBr for 20 minutes, destained in water for 20 minutes and observed under UV-light. Alternatively, the marker track was transferred with the RNA samples and the membrane stained reversibly with methylene blue (Section 2.2.9.3.6) to determine the efficiency of the transfer.

2.2.8.2.2 Electrophoresis of DNA.

The appropriate amount of agarose (0.5- 1.5% w/v low EEO or 1% low EEO + 3% w/v NuSieve GTG (FMC Bioproducts, USA)) was added to the required volume of 1X TBE or 1X TAE and heated in a microwave oven until all the agarose had dissolved. The agarose solution was then allowed to cool to around 50 ° C before addition of ethidium bromide to a final concentration of $1\mu gml^{-1}$. The gel solution was poured into the electrophoresis apparatus and allowed to set for 30 minutes. Sufficient 1x TBE or 1x TAE running buffer was added to cover the gel. The DNA samples were mixed with one-tenth volume of DF loading buffer and gels were run at $5Vcm^{-1}$ until the bromophenol blue had migrated two-thirds of the way down the gel. 30cm long 1.5% agarose gels were used to isolate closely sized DNA fragments in the 2kb size range. The gel was then washed in ddH_2O for 15 minutes and visualised under UV light. Long wave UV (630nm) was used to visualise DNA fragments that were to be further manipulated, to reduce radiation induced DNA damage.

2.2.8.2.3 Marker DNA and RNA.

Marker DNA and RNAs were run on agarose gels (as appropriate) to estimate the size and quantity of the DNA/RNA that was being analysed. Most frequently used for DNA gels was λ DNA digested with *EcoR*I and *Hind*III or a single *Hind*III digest (both Sigma), and occasionally a 123bp ladder (Gibco-BRL).

For the analysis of RNA gels, a synthetic 0.24 - 9.5Kb RNA ladder (Gibco-BRL) was run in the outer lane of the gel.

2.2.8.3 Acrylamide Gels.

Polyacrylamide gels were used to purify oligonucleotides which were synthesised on a Cruachem PS250 synthesiser, and removed from the matrix by treatment with ammonia (35% pure, specific gravity 0.88) at 55 ° C for 5 hours. The lyophilised oligonucleotide was resuspended in 20μl formamide and 5μl of 10x TBE. The sample was electrophoresed on a denaturing polyacrylamide gel (15% polyacrylamide cross linked with 4% (w/v) N,N'-methylenebisacrylamide in 1x TBE containing 8M urea; Sequagel reagents). Polymerisation was catalysed by the addition of 0.05% (w/v) APS and 0.1% (w/v) TEMED. The oligonucleotides were visualised by UV shadowing with short wave UV light, and excised from the gel. Oligonucleotides were recovered as described below (Section 2.2.8.4.2).

2.2.8.4 DNA Recovery from Gels.

2.2.8.4.1 Agarose Gels.

Sephaglas® Kit. DNA fragments were isolated from solution or from agarose gels using the Sephaglas® kit following the manufacturers' instructions. The DNA sample was run on a TBE gel to separate the DNA of interest from contaminating DNA. The DNA band was identified by illumination of the gel with long-wave UV light (λ= 630nm) and excised with a sterile scalpel blade. The agarose slice was weighed and 1µl gel solubiliser per mg of agarose added. The agarose was dissolved by incubation at 60 ° C for 10 minutes. 5µl of Sephaglas® per µg of DNA was added, the contents mixed and allowed to stand at room temperature for 5 minutes with occasional mixing. After pelleting of the Sephaglas® at 10,000*g* for 30 seconds the supernatant was removed and the pellet washed three times with 40µl wash buffer. The DNA was eluted by resuspension of the pellet in 20 µl elution buffer and incubation at 55 ° C for 3 min.

Elution by centrifugation. DNA fragments were excised from gels as described above, the gel slice cut into smaller pieces and placed in a 0.5ml microfuge tube which had a hole in its base covered by a siliconised glass wool plug. This tube was placed inside a 1.5ml microfuge tube and centrifuged at 6,000rpm for 10 minutes. The DNA in solution passed through the small tube into the larger one, leaving the solid agarose behind. The eluate was extracted twice with an equal volume of φ/$CHCl_3$ (see Section 2.2.10.1.2) and once with $CHCl_3$, before precipitation with 0.1 volumes of 5M NH_4Ac and 2 volumes of EtOH overnight at -20 ° C. The DNA was pelleted by centrifugation at 13,000rpm at room temperature for 10 minutes, washed in 70% v/v EtOH then absolute EtOH and air-dried. The DNA was resuspended in TE pH 8.0, the concentration estimated and the solution stored at -20 ° C.

2.2.8.4.2 Acrylamide Gels.

Elution into TE. Gel fragments containing oligonucleotides undergoing purification were excised as described above (Section 2.2.8.3) and placed in 1.5ml microfuge tubes. They were mashed using the end of a pipette tip, covered with TE and incubated on a rotating wheel at 37 ° C overnight. The tubes were centrifuged at 6,000rpm at room temperature for 10 minutes to pellet the acrylamide and the supernatants transferred to fresh microfuge tubes. The volume of each supernatant was noted and 0.1 volumes of 5M NH_4Ac and 2 volumes of EtOH was added to the tubes and the sample mixed well.

The tubes were incubated at -20 ° C for at least 3 hours and the DNA pelleted by centrifugation at 13,000rpm at room temperature for 10 minutes. The DNA pellets were washed with 70% v/v EtOH, absolute EtOH, and were air-dried prior to resuspension in TE pH 8.0, spectrophotometric analysis and storage at -20 ° C.

2.2.9 HYBRIDISATION.

2.2.9.1 General Solutions.

20X SSC Buffer. 3M NaCl, 0.3M Na_3Citrate dissolved in sterile ddH_2O at pH 7.0. The solution was stirred with gentle heating to aid solvation.

100x Denhardt's Solution. Ficoll 400, BSA and polyvinyl pyrolidone 360 were dissolved in sterile ddH_2O to final concentrations of 2% w/v of each constituent. The solution was filter sterilised through a 0.45µm filter and stored at -20 ° C in 20ml aliquots.

Denatured Salmon Sperm DNA. Lyophilised salmon sperm DNA was added to a beaker of sterile ddH_2O to give a final concentration of 5mgml^{-1}. The beaker was heated at 37 ° C for 1-2 hours with stirring. The solution was periodically pushed through a 5ml syringe with a 21G syringe needle attached. The solution was sonicated for 3 minutes and aliquoted into 1.5ml microfuge tubes for storage at -20 ° C.

Pre-hybridisation solution. 25ml of pre-hybridisation solution was prepared from stock solutions as follows: 3.13ml 20x SSC, 0.625ml 100x Denhardts and 0.313ml 20% SDS were mixed with ddH_2O to a volume of 12.5ml. An equal volume of formamide was added and mixed. The solution was sterilised by filtration through a 0.45µm filter and denatured salmon sperm DNA added at a concentration of 100µgml^{-1}. The solution was made on the day of use.

2.2.9.2 Radiolabelling of DNA probes.

2.2.9.2.1 Preparation of the DNA to be labelled.

The DNA fragment to be labelled was excised from the host plasmid using the appropriate restriction enzyme(s) and purified using Sephaglas® as described in section 2.2.8.4.1. The amount of insert DNA was estimated spectrophotometrically.

2.2.9.2.2 Random priming of dsDNA.

DNA fragments to be used as probes were labelled with 5'[α-^{32}P]dCTP with the Megaprime™ DNA labelling kit using random nona-nucleotides to prime synthesis on denatured DNA. Approximately 25ng of DNA was made up to a volume of 10µl and 5µl of primer solution (random nona-nucleotides) was added. The solutions were mixed in a 1.5 ml microfuge tube and heated to 95 °C for 5 minutes. The tube was put on ice and 10µl of buffer solution (dATP, dGTP, dTTP), 50µCi 5'[α-^{32}P]dCTP, 2µl of enzyme solution (2U DNA polymerase 1 'Klenow' fragment) and 18µl of ddH_2O were added. The tube was incubated at 37 °C for 10 minutes. The reaction was stopped by the addition of 5µl of 0.5M EDTA and a further 45µl of ddH_2O. 100µg of denatured salmon sperm DNA was added as carrier DNA, and the probe precipitated with 2 volumes of EtOH and 0.1 volume of NH_4Ac. After washing with 70% EtOH, the probe was resuspended in 250µl ddH_2O, denatured by boiling for 5 minutes and used immediately.

Incorporation of radiolabel into probe was determined as described in Section 2.2.9.2.5.

2.2.9.2.3 Labelling of dsDNA by nick-translation.

Nick Translation buffer (1x): 50mM Tris-HCl pH 7.8, 5mM $MgCl_2$, 1mM DTT, 5mgml^{-1} BSA.

DNA was labelled with 5'[α-^{32}P]dCTP and 5'[α-^{32}P]dGTP by nick-translation using a method based on that of Rigby *et al.*, (1977). 500ng of DNA probe was denatured by boiling and mixed with 20µCi of each labelled nucleotide, equal amounts of unlabelled dATP and dTTP, 1µl DNaseI (10^4 Uml^{-1}) and 2U *E. coli* DNA polymerase I in 1x nick translation buffer. The reaction was incubated at room temperature for 1 hour, and stopped by addition of 5µl of 1M EDTA. Separation of radiolabelled DNA from unincorporated radionucleotides was achieved by ethanol precipitation in the presence of carrier DNA.

2.2.9.2.4 End labelling.

This method was used to attach 5'[γ-^{32}P]dATP to the 5'-end of oligonucleotides. A reaction mix containing 100-200ng oligonucleotide in 5µl ddH_2O, 2.5µl 1M Tris-HCl pH 7.6, 5µl 50mM $MgCl_2$ and 2.5µl 200mM βME was prepared. Sterile stocks of all these solutions were stored at -20 °C. 2µl T4 polynucleotide kinase (PNK) and 5µl 5'[γ-^{32}P]dATP were added and the reaction incubated at 37 °C for 1 hour. The reaction

mixture was then diluted to 200µl with TE and the incorporation of ^{32}P label measured. The probe was denatured by boiling for 2 minutes, snap-cooled on ice, and was immediately added to the hybridisation reaction.

2.2.9.2.5 Measurement of the incorporation of radionucleotides into DNA probes.

1µl of the DNA probe mix was spotted onto each of two 2.5cm diameter filters of Whatman DEAE paper and dried under a heating lamp. 1 piece of DEAE paper was put into a scintillation vial and covered with 500µl of EcoScint® fluid. The other was washed twice for 3 minutes in 5% trichloroacetic acid (TCA) and once in acetone before drying under a lamp. The DEAE paper was put into a scintillation vial and covered with 500µl EcoScint® fluid. The counts per minute (cpm) were counted in a scintillation counter. The unwashed DEAE paper gave total ^{32}P cpm in 1µl of probe mix and the washed DEAE paper gave the incorporated ^{32}P counts. The percentage of radiolabel incorporated and the specific activity (cpmµg^{-1} probe) were calculated.

2.2.9.3 RNA Hybridisation.

2.2.9.3.1 Samples and gel electrophoresis.

RNA samples were prepared as described in Section 2.2.7.2, and electrophoresed on a denaturing gel as described in section 2.2.8.2.1.

2.2.9.3.2 RNA Transfer.

RNA was transferred to a Hybond-N™ nylon filter by capillary transfer (Alwine *et al.*, 1977). A 'bridge' was constructed over a tray containing 20x SSC and a strip of 3MM paper moistened in 20x SSC was laid across it as a 'wick'. Two further layers of 3MM paper were placed on top of the wick and then the denaturing gel was laid on top. A nylon filter (pre-wetted in 20x SSC) of exactly the same size was placed on top of the gel, ensuring that no air bubbles were trapped between the gel and the filter. One piece of 3MM paper cut to the exact size was moistened in 20x SSC and carefully placed on top of the filter. Five more exact sized pieces of dry 3MM paper and approximately 10cm height of absorbent paper towels were added. A gasket of polythene was put around the gel to prevent 'short-circuiting' of the 20xSSC around the gel. A weight of 500g was placed on top of the stack of towels and the nucleic acid transferred overnight.

The apparatus was dismantled and the RNA was fixed to the Hybond-N™ membrane by UV-irradiation in a Stratalinker™ set to 'Auto-crosslink'. The fixed blots were either prehybridised immediately or wrapped in clingfilm and stored wet at -20 ° C.

2.2.9.3.3 Hybridisation and washing.

RNA filters were prehybridised for at least 2 hours in 12.5ml pre-hybridisation solution, at 42 ° C in glass hybridisation tubes. Denatured probe was added and hybridised overnight at 42 ° C in a hybridisation oven. The filter was washed twice with 2X SSC, 0.1% SDS at room temperature for 10 minutes; then with 1X SSC, 0.1% w/v SDS at 65 ° C for 10 minutes. Control probed blots were further washed with 0.1X SSC, 0.1% w/v SDS at 65 ° C for 10 minutes. The filter was monitored at each washing step with a Geiger-Müller counter.

2.2.9.3.4 Autoradiography.

The hybridised filter was wrapped in clingfilm and exposed to pre-flashed X-OMAT S x-ray film in a cassette containing an intensifying screen at -70 ° C, or to a phosphorimager screen. The film was developed in an X-omat processor model ME3. All procedures involving X-ray film were carried out in a darkroom under a safe-red light. Phosphorimager images were generally obtained after an overnight exposure.

2.2.9.3.5 Stripping filters of bound radioactive probe.

After hybridisation and autoradiography the bound probe was removed by pouring a boiling solution of 0.1% (w/v) SDS over the filter. The solution was then allowed to cool to room temperature, and the process was repeated a further two times. The filter was wrapped in cling film and exposed to a phosphorimager screen overnight to confirm removal of the bound probe. The continued presence of RNA on the filter after stripping could be confirmed by methylene blue staining as described below.

2.2.9.3.6 Staining of filter-bound RNA/DNA with methylene blue.

This method was described by Herrin and Schmidt (1988). The filter containing the bound RNA/DNA was placed in 0.04% methylene blue (w/v), 0.5 M NaOAc (pH 5.2) for 5 to 10 minutes. The filter was washed in DEPC-treated ddH_2O until the RNA bands appeared as blue bands on a white background. The stain could be removed by washing the filter in 20% (v/v) acetic acid until the bands were no longer visible.

2.2.10 BACTERIOLOGY AND MANIPULATION OF PLASMID DNA.

2.2.10.1 The amplification and purification of plasmid DNA.

2.2.10.1.1 Media and supplements.

All media were provided pre-sterilised by the Media department within the Institute of Virology, Glasgow unless otherwise stated.

Liquid media.

L-Broth (LB): 1% bacto-tryptone (w/v), 1% NaCl (w/v), 0.5% yeast extract (w/v), pH 7.2. LB was sterilised by autoclaving and supplemented with the appropriate antibiotic for the culture of *E.Coli* strains.

2YT-broth (2YT): 0.5% NaCl, 1.6% bacto-tryptone, 1% yeast extract pH 7.2 in ddH_2O. Used for the preparation of competent *E. coli* XL1-Blue (Stratagene, Cambridge, UK), JM101 and NM522 strains using the TSB method.

Solid media.

'Bottom' Agar (LB-A): L-broth containing 1.5% (w/v) bactoagar (Difco) was used for plating out *E. coli* and as the base agar for plating M13 phage.

To make agar plates, LB-A was melted in a microwave and cooled to 50 °C. The appropriate antibiotic was added prior to pouring into sterile plastic petri dishes. Air bubbles at the surface of the agar were removed by brief flaming with a bunsen burner. The plates were allowed to set, dried at 37 °C for 30 minutes and stored inverted at 4 °C until needed (maximum 2 weeks). LB-A plates containing $100\mu gml^{-1}$ ampicillin were termed LB-A(amp) plates.

Top Agar (TA): Top agar for use in plating M13 phage was prepared by addition of 1% (w/v) bacto-agar and 10mM $MgSO_4$ to L-broth.

Antibiotics and selection agents.

Ampicillin (Amp). Ampicillin was dissolved in sterile ddH_2O to a concentration of 100 $mgml^{-1}$. This stock solution was dispensed into 1ml aliquots and stored at -20°C. When required in LB-A(amp) plates or LB/ 2YT overnight cultures, stock ampicillin was diluted to a final concentration of $100\mu gml^{-1}$.

Isopropyl thiogalactoside (IPTG). IPTG was made as a 1mM stock in ddH_2O and used at a final concentration of 0.1mM. The stock solution was stored at -20 °C.

5-bromo-4-chloro-3-indolyl β-D-galactoside (X-Gal). X-Gal was made as a 20mgml^{-1} stock in dimethylformamide (DMF) and used at a final concentration of 50μgml^{-1}. The stock solution was stored at -20 ° C.

2.2.10.1.2 Solutions.

All the following solutions were made with molecular biology grade chemicals.

TE Buffer (10x):- 100mM Tris-HCl pH 8.0, 10mM EDTA pH 8.0.

The solution was sterilised by autoclaving.

STE Buffer:- 10mM Tris-HCl pH 7.8, 1mM EDTA pH 8.0, 100mM NaCl.

The solution was checked to ensure that its pH was between 7.8 and 8.0 and then sterilised by autoclaving.

Lysis Buffer:- 25mM Tris-HCl pH 8.0, 10mM EDTA pH 8.0, 50mM Glucose.

The solution was made up aseptically and stored at 4 ° C.

Lysozyme Solution. Lysozyme solution was prepared on the day of use by dissolving lysozyme in lysis buffer to a final concentration of 16mgml^{-1}.

Chloramphenicol Solution. Chloramphenicol was prepared as a 34mgml^{-1} solution in EtOH and stored at -20 ° C.

Ribonuclease A (RNase A). 200μgml^{-1} RNase A was added to a solution of 10mM Tris-HCl pH 7.5 and 15mM NaCl, boiled for 20 minutes then cooled to room temperature and stored in 100μl aliquots at -20 ° C.

Ammonium Persulphate (APS). This was made as a 1% w/v APS solution in ddH_2O and stored at 4 ° C for a maximum of 2 weeks.

Potassium Acetate (KOAc). 5M KOAc pH 4.8 was made by addition of 11.5ml glacial acetic acid and 28.5ml sterile ddH_2O to 60ml of sterile filtered 5M KAc solution. The resulting solution was inverted sharply, incubated on ice for 10 minutes and the pH of 4.8 checked. This produced a solution that was 3M with respect to potassium (K) and 5M with respect to acetate (OAc).

Ammonium Acetate (NH_4OAc). NH_4OAc was dissolved in ddH_2O, the pH adjusted to 4.0 with glacial acetic acid, and the volume adjusted to give a final concentration of 5M prior to filter sterilisation.

Sodium Acetate (NaOAc). Anhydrous NaOAc was dissolved in ddH_2O to produce a 3M solution. The pH was adjusted with glacial acetic acid and the solution sterilised by filtration.

SDS Solution. SDS was added to sterile ddH_2O to a final concentration 20% w/v. The solution was warmed to 65 ° C until the solid dissolved and stored at room temperature. If necessary the 20% SDS solution was warmed slightly to redissolve any precipitated solid before use.

Phenol/Chloroform ($\varphi/CHCl_3$). This was made by mixing water saturated phenol with an equal volume of chloroform (24:1 with amyl-alcohol) and stored at -20 ° C.

NaOH/SDS Solution. 10% w/v SDS and 2M sodium hydroxide solution (NaOH) were diluted in ddH_2O to give final concentrations of 1% w/v SDS and 0.2M NaOH. This solution was prepared freshly on the day of use.

2.2.10.1.3 Bacterial strains and cloning vectors.

Plasmids were maintained and amplified in *E. coli* JM101 or NM522 which were also used for subsequent amplification and plating of isolated clones.

M13 mp19 was used for cloning PCR fragments and subsequent DNA sequencing, and was propagated in *E. coli* XL-1 Blue.

pBSKS-mAspAT: This plasmid is pBS-KS (Stratagene) containing the cDNA for rat mAspAT (Mattingley *et al.*, 1987).

pCMV10: A pUC derived plasmid which contains the HCMV major immediate early promotor and SV40 polyadenylation signal, and was used to express cloned DNA in eukaryotic cells. Obtained from Dr. N. Stow, Institute of Virology, Glasgow.

pSV2Neo: A plasmid containing the gene conferring resistance to the antibiotic G418 (Southern and Berg, 1982).

px11r1R: A plasmid containing the cDNA for X. Laevis 28S rRNA, used as a control probe in Northern blotting experiments. Obtained from Professor B.E.H. Maden, University of Liverpool, UK.

2.2.10.1.4 Preparation of competent bacterial cells.

2.2.10.1.4.1 Calcium Chloride method.

Preparation.

100ml of L-broth was innoculated with 1ml of an overnight culture of *E. coli* JM101, XL-1 Blue or NM522 and incubated at 37 ° C to an optical density (O.D.) of 0.3-0.5 at 630nm. The bacteria were pelleted at 3000rpm at 4 ° C for 10 minutes in a benchtop centrifuge, and the cells resuspended in 50ml of ice cold 100mM $CaCl_2$, for 2 hours. The bacteria were re-pelleted and resuspended in 1ml of 100mM $CaCl_2$. The cells were used within 1 hour.

Transformation.

This procedure was based on that described by Maniatis (1989). Up to 50ng of plasmid DNA was added to 200µl of competent bacteria in sterile 1.5ml 'Eppendorf' tubes and the sample mixed very gently. The tubes were incubated on ice for 30 minutes, and the bacteria heat shocked at 42 ° C for 2 minutes. 500µl of LB at 37 ° C was added, mixed gently and the tubes incubated for 45-60 minutes at 37 ° C. 200µl of bacterial suspension was plated onto LB-A plates containing 100µgml^{-1} ampicillin, spread with a sterile glass rod and left to dry for approximately 10 minutes. Plates were inverted and incubated overnight at 37 ° C. Individual colonies present on the plates next day were streaked onto fresh LB-A plates with sterile toothpicks. These plates were incubated overnight at 37 ° C and individual colonies from these plates used for plasmid DNA extraction.

2.2.10.1.4.2 TSB Method.

Transformation and Storage Buffer (TSB; Chung and Miller, 1988) was prepared by addition of sterile 10mM $MgSO_4$ and 10mM $MgCl_2$, 10%(w/v) PEG 3300 and 5%(v/v) DMSO to L-broth. The solution was filter sterilised and stored at 4 ° C in 20ml aliquots.

Preparation

A single colony of *E. coli* strain JM101, NM522 or XL-1 Blue was inoculated into 5ml of 2YT (without antibiotic) and grown up overnight at 37 ° C. 100ml of fresh 2YT broth was inoculated with 1ml of the overnight culture and was shaken at 37 ° C for approximately 100 minutes ($O.D._{630}$ 0.4 - 0.6). 50ml of this culture was transferred to a

sterile 50ml Falcon™ tube. The cells were pelleted by centrifugation for 10 minutes at 3000rpm at 4 ° C and the supernatant decanted. The cell pellet was resuspended in 5ml of ice-cold TSB and incubated on ice for 20 min. The cells were ready for transformation and could be kept on ice for a maximum of 2 hours without significant loss of transformation efficiency. Excess competent cells could be stored at -70 ° C with slightly diminished transformation efficiency.

Transformation.

A maximum of 1μg of plasmid DNA or ligation mix was added to 100μl of TSB-competent bacteria, mixed gently and incubated on ice for 30 minutes. 900μl of TSB containing 20mM glucose and 5% (v/v) DMSO was added and the mixture incubated at 37 ° C with shaking for 1 hour. 10μl and 100μl of this mix was plated onto LB-A plates and incubated overnight.

2.2.10.2 Preparation of plasmid DNA.

2.2.10.2.1 Plasmid Isolation: 'Mini-Prep'.

The method used is based on that of Birnboim and Doly (1979) as decribed by Maniatis (1989).

A single bacterial colony was used to inoculate 5ml of L-broth or 2YT containing ampicillin in a universal tube. The cultures were incubated overnight at 37 ° C with vigorous shaking.

The next day 1.5 ml of the culture was centrifuged at 12,000*g* in a microcentrifuge at 4 ° C for 30 seconds. The supernatant was carefully removed and the pellet was resuspended in 100μl of ice-cold lysis buffer by vortexing. 200μl of a freshly prepared solution of 0.2M NaOH and 1% SDS was added to the resuspended pellet and mixed by gentle agitation. The lysate was stored on ice before the addition of 150μl ice-cold 3M KOAc (pH 4.8). The sample was mixed gently and incubated on ice for 5 minutes and then centrifuged at 12,000*g* for 5 minutes at 4 ° C. The supernatant was removed to a fresh microfuge tube and extracted twice with an equal volume of φ/$CHCl_3$, and the upper aqueous layer transferred to new tubes. Plasmid DNA was precipitated with an equal volume of isopropanol at -20 ° C for at least 30 minutes. The plasmid DNA was pelleted by centrifugation at 13krpm at room temperature for 10 minutes. The supernatant was aspirated from the pellet, which was washed in 1ml 70% EtOH. The

pellet was left to air dry for 10 minutes and the DNA resuspended in 50µl of TE containing 20µgml^{-1} of DNase-free RNase. Miniprep DNA was stored at -20 ° C.

2.2.10.2.2 Plasmid Isolation: QIAGEN® Midi-Prep.

The QIAGEN® midi plasmid isolation kit purifies up to 100µg of pure super-coiled plasmid DNA by preferential binding to a resin following an alkaline lysis procedure (Birnboim and Doly, 1979). The method was as described in the handbook accompanying the kit and is described briefly below.

A single colony was inoculated into 5ml LB-amp and grown overnight, before addition of 1ml to 100ml L-broth containing 100µgml^{-1} ampicillin. After overnight growth the bacterial cells were harvested by centrifugation.

The final yield was determined spectrophometrically and by analysis on an agarose gel with standard markers of known concentration. Samples taken during the purification procedure were also run on the gel to allow trouble-shooting if the purification was poor.

Buffer	Composition	Storage
P1	100µgml^{-1} RNaseA, 50mM Tris-HCl, 10mM EDTA pH 8.0.	4 ° C
P2	200mM NaOH, 1% SDS	RT
P3	3M KAc, pH 5.5	4 ° C
QBT	750mM NaCl, 50mM MOPS, 15% EtOH,	
	0.15% Triton X-100, pH 7.0	RT
QC	1.0M NaCl, 50mM MOPS, 15% EtOH, pH 7.0	RT
QF	1.25M NaCl, 50mM Tris-HCl, 15% EtOH, pH 8.5	RT
TE	10mM Tris-HCl, 1mM EDTA, pH 8.0	RT
STE	100mM NaCl, 10mM Tris-HCl, 1mM EDTA, pH 8.0	RT

Protocol. The bacterial pellet from a 100ml culture was resuspended in 4ml P1 buffer. 4ml P2 buffer was added, mixed by inversion and incubated at RT for 5 minutes. 4ml chilled P3 buffer was added and mixed by inversion prior to incubation on ice for 15 minutes. The lysate was centrifuged at 30,000*g* for 30 minutes at 4 ° C, and the supernatant removed promptly. A 250µl sample was taken.

A QIAGEN®-tip 100 was equilibrated with 4ml QBT buffer, allowing gravity flow to empty the column. The cleared lysate was added and allowed to enter the resin by gravity flow. A 250µl sample was taken.

The column was washed with 2x 10 ml QC buffer and a 500 µl sample taken, prior to elution of the plasmid DNA with 5ml of buffer QF. A 100µl sample was taken for the analytical gel. The DNA was precipitated by addition of 3.5ml isopropanol at room temperature, and centrifuged immediately at 9000rpm in a Sorvall SM24 high speed rotor. The glassy pellet was rinsed with 5ml 70% EtOH, air dried, and resuspended in 500µl TE pH 8.0 to a final concentration of approximately 200µgml^{-1}.

For the analytical gel, each sample was precipitated with 0.7 volumes of isopropanol at room temperature, rinsed in 70% EtOH, and resuspended in 5µl TE pH 8.0. 1µl of each was run on a 1% agarose gel with molecular weight markers and visualised by UV-illumination following staining with ethidium bromide.

2.2.10.3 Restriction Enzyme Digestion of DNA.

Plasmid DNA digests were performed in 0.5ml Eppendorfs for 1-2 hours at 37°C. Digestion mixes contained 2U enzyme/µg DNA, 0.1 volumes of enzyme buffer, 0.1 volumes RNase A (miniprep DNA samples only) and ddH_2O to a total volume of 10µl. Digests performed to check plasmid identity used 0.5-1µg DNA and for probe preparation used 1-4µg DNA depending on the size of the inserted fragment. When two different restriction enzymes were used, the digestion was conducted simultaneously if the reaction buffers were compatible (in a volume large enough to dilute out the glycerol from the enzyme stock). However, if the buffers were not compatable, the DNA was digested with the first enzyme, precipitated and resuspended in the required buffer containing the second enzyme.

2.2.10.4 Ligation.

The vector backbone was linearised with the appropriate restriction enzyme and to prevent recircularisation 1U of calf intestinal phosphatase (CIP) was added to the reaction. The DNA insert was excised from the host plasmid with the required restriction enzymes, and both insert and vector were purified by agarose gel electrophoresis and Sephaglas® purification. The DNA fragments were precipitated with PEG 6000, and ligations set up containing ratios of vector:insert ranging from 1:3 to 3:1. Ligations were carried out in a final volume of 20µl containing 2U T4 DNA

ligase in ligation buffer (50mM Tris-HCl, 10mM $MgCl_2$, 1mM DTT, 1mM ATP, 25% (w/v) PEG 6000, pH 7.8). Incubation was performed for a minimum of 2 hours at 16 °C in a 0.5ml microfuge tube in a thermo-cycler.

2.2.11 REVERSE TRANSCRIPTASE-PCR.

2.2.11.1 Buffers.

5xRT buffer: 250mM Tris-HCl pH8.3, 375mM KCl, 15mM $MgCl_2$

10xPCR buffer: 670mM Tris-Cl pH 8.8, 67mM $MgCl_2$, 1.7mgml^{-1} BSA, 166mM $(NH_4)_2SO_4$

2.2.11.2 Protocol.

Amplification of mAspAT transcripts was achieved using a single tube to carry out both cDNA synthesis and the subsequent amplification procedure, based on a method described by Steinthorsdotir and Mautner, (1991). Briefly, 3-5µg of total RNA extracted from tissue culture cells as described above *(Section 2.2.7.2)* was mixed in a 0.5ml Eppendorf® tube with 50pmol of 3' primer (9302), 1µl of dNTP mix (10mmol of each), 2µl 5xRT buffer and sufficient ddH_2O to make a final volume of 9.5µl. After incubation at 80 °C for 1 minute and cooling to 37 °C, 0.5µl MoMLV-RT (200Uµl^{-1}) was added and mixed, before incubation at 37 °C for 30 minutes. The tube was placed on ice, before addition of 5µl 10x PCR buffer, 50pmol of 5' primer (9301) and 33.5µl ddH_2O. After mixing, the reaction mixture was overlaid with light mineral oil and heated to 94 °C for 2 minutes before addition of 0.5µl Taq DNA polymerase (5Uµl^{-1}) and incubation in a thermocycler as described below.

1.	94 °C	1 minutes	Denaturation
2.	60 °C	1 minutes	annealing
3.	72 °C	2 minutes	extension

Cycle back to step 1 for 25- 40 cycles

4.	72 °C	10 minutes	final extension
5.	4 °C	∞	

The number of cycles of PCR amplification used varied. For production of double stranded cDNA for cloning 40 cycles were used. To analyse the relative level of RNA

transcripts by semi quantitative RT-PCR *(Results-Section 4.3)* 20 cycles of amplification were used to ensure that the final yield of product was proportional to the initial input of mAspAT mRNA (Kang *et al.*, 1995).

Each experiment contained negative and positive controls at the PCR stage. 200 ng of plasmid containing the mAspAT cDNA was included as the positive control, allowing identification of the correct sized product after agarose gel electrophoresis. The negative control contained all reagents except the RNA.

2.2.12 DIDEOXY DNA SEQUENCING.

DNA was sequenced using Sequenase® Version 2.0 enzyme and kit obtained from United States Biochemicals (Ohio, USA).

2.2.12.1 Template preparation.

Phage precipitation solution: 3.75M ammonium acetate pH 7.5, 20% PEG 8000.

Protocol. Single-stranded template DNA was prepared from M13 phage as follows. A 3ml overnight culture of *E. coli* XL-1 blue was innoculated with a single plaque of recombinant M13. After incubation with shaking at 37 ° C for 6-8 hours, the cells were pelleted by centrifugation at 13krpm for 15 minutes. The supernatant was removed and centrifuged again, before addition of 0.25 volumes of phage precipitation solution on ice for 30 minutes. Phage were pelleted by centrifugation at 13krpm for 15 minutes, and resuspended in 400µl TE. The phage were extracted with an equal volume of chloroform:isoamyl alcohol, and then with φ/$CHCl_3$ until there was no material present at the interface. The DNA in the upper aqueous phase was precipitated with 2 volumes of EtOH and 0.5 volumes 7.5M ammonium acetate at -20 ° C for 30 minutes. The DNA was pelleted at 13krpm for 15 minutes, rinsed in 70% EtOH and resuspended in 20µl of ddH_2O.

2.2.12.2 Annealing of template and primer.

Reaction buffer: 0.2M Tris-HCl pH 7.5, 0.1M $MgCl_2$, 0.25M NaCl.

The single stranded M13 template DNA (1µg) was resuspended in 7 µl H_2O and 2 µl reaction buffer and 1 µl (2.5 ng) of sequencing primer added. Annealing was accomplished by heating the sample to 65 ° C for 2 minutes, then cooling it slowly to room temperature. The tube was briefly centrifuged to collect the sample.

2.2.12.3 Labelling and termination reactions.

Labelling mix 1.5 µM dGTP, 1.5 µM dCTP, 1.5 µM dTTP

Stop solution: 50% formamide (v/v)

To the annealed template-primer was added: 1µl 0.1 M DTT, 2µl diluted labelling mix, 0.5µl (5µCi) [α-^{35}S]dATP (1000Ci mmol^{-1}) and 2µl of diluted Sequenase® 2.0. The contents were mixed and incubated for 2-5 minutes at room temperature. Four rows of a microtitre plate were labelled A, C, G and T and 2.5µl of the appropriate termination mix added. The plate was prewarmed for 5-10 minutes at 37 ° C. On completion of the labelling reaction, 3.5 µl of the reaction mix was placed into each of the termination mixes. Termination reactions proceeded for 3-5 minutes at 37 ° C after which time 4 µl of stop solution was added. The plate was stored at -20 ° C prior to electrophoresis. Samples were denatured by heating to 75-80 ° C for 2 minutes before loading on the gel.

2.2.12.4 Sequencing gel electrophoresis.

Gels of dimension 20cm x 40cm x 0.4mm were prepared using Seqagel™ reagents *(6% (w/v)acrylamide:bisacrylamide (38:2), 7M urea, 1x TBE)*, to give a final gel concentration of 6% acrylamide. The gels were pre-run for 20 minutes at a constant power of 100W before the samples were loaded. Gels were run for 2-2.5 hours at a constant power of 100W. After electrophoresis the gel plates were removed from the gel kit and separated. The gel was transferred onto Whatman 3MM paper directly and dried on a slab gel-drier at 80 ° C for 1-1.5 h. Gels were autoradiographed overnight without intensifying screens at room temperature using Kodak Biomax MR film, and re-exposed for a longer period of time if neccessary.

2.2.12.5 Sequence analysis.

DNA sequence was read by eye, and entered manually into a datadase using the SEQED sequence editor program of the GCG Wisconsin Package, Version 9.0. Subsequent analysis used the sequence alignment and editing programs from this same package.

2.2.13 TRANSFORMATION ASSAYS.

2.2.13.1 Growth in soft agar.

This assay is based on a method first described by Macpherson and Montagnier, 1964.

2.2.13.1.1 Soft agar.

Noble 3.2% (w/v) agar was melted and stored at 48 °C, and added to tissue culture medium (as described below) pre-warmed to 45 °C immediately prior to addition of the cells.

100ml Base agar (0.6%): 35ml ddH_2O, 26.3ml 3.2% (w/v) noble agar, 13.3ml FCS, 6.7ml TP broth, 2.7ml glutamine, 1.3ml Penicillin/streptomycin, 4.7ml sodium bicarbonate and 10ml of 10x DMEM.

100ml top agar (0.3%): as above except 48ml ddH_2O, 13.2ml 3.2% (w/v) noble agar.

2.2.13.1.2 Protocol.

Plates (60mm) of NRK 536 cells lipofected with mAspAT expressing plasmid or a control plasmid overnight *(Section 2.2.2.7.2)* were washed twice with PBS-A, and 1ml of Trypsin/Versene added. Cells were collected and pelleted at 1000rpm for 10 minutes at room temperature (Heraeus variable speed microfuge). The cells were resuspended in 2ml of tissue culture medium, and vortexed to obtain a single cell suspension. 0.2ml and 0.4ml of cell suspension was put into labelled tubes, and 1.5ml of top agar added at 45 °C. The cells were mixed by inversion (with care being taken to avoid bubbles forming) and quickly poured onto a base agar plate. The plates were immediately transferred to a 37 °C incubator containing a tray of sterile ddH_2O to humidify the atmosphere.

2.2.13.2 Loss of contact inhibition.

Cells were transfected and prepared as described above *(Section 2.2.13.1.2)*, and 0.2ml or 0.4ml of the single cell suspension added to a 60mm tissue culture plate containing 4ml of medium. The tissue culture medium was replaced every 2 days and the plates observed for the formation of piles of cells.

2.2.13.3 Tumourogenicity in nude mice.

Athymic nude mice were injected sub-cutaneously at the back of the neck with $1x10^6$ NRK 536 cells lipofected with plasmid as detailed above *(Section 2.2.13.1.2)*. All live animal work was performed by Dr. J.C.M. Macnab, Institute of Virology, Glasgow. Assessment of tumour formation was performed by examination of the size of induced tumours by external examination of the sacrificed mice and excision of the tumours, and by a search for secondary tumours and metastases.

3. PURIFICATION OF THE 40kDa POLYPEPTIDE AND PRODUCTION OF AN ANTISERUM.

3.1 INTRODUCTION.

Macnab *et al.* (1985) immunoprecipitated a set of polypeptides from the transformed Bn5T cell line with the sera of rats with tumours induced by injection of Bn5T cells. These polypeptides had molecular weights of 200kDa, 90kDa (doublet of U90 and L90), 40kDa and 32kDa. This set of polypeptides were also immunoprecipitated by antisera raised in rats and mice to HSV-2 infected cells (Hewitt *et al.*, 1991). However, the polypeptides were not immunoprecipitated from control RE cells.

A monoclonal antibody (TG7A) raised against the DNA binding proteins of HSV-2 infected BHK C13 cells (Macnab *et al.*, 1985) immunoprecipitated a similar set of polypeptides from Bn5T but not RE cells. These polypeptides were transformation specific, and were also immunoprecipitated from rat cells transformed with Rous sarcoma virus or adenovirus 12 (Macnab *et al.*, 1985). This demonstrated that the polypeptides were transformation specific and not HSV encoded. These findings suggested that certain cellular polypeptides induced by HSV-2 infection were related to polypeptides expressed at increased levels in transformed cells, and that these polypeptides might therefore play a role in the transformation process.

The result of a similar experiment is shown in Figure 3.1. Mock infected, HSV-1 and HSV-2 infected Bn5T and RE cell lysates labelled with [^{35}S]-L-methionine were immunoprecipitated with a rat tumour bearing serum (TBS). The precipitated polypeptides were electrophoresed on a 9% SDS-PAGE gel and autoradiographed. The 90kDa polypeptide is labelled with a diamond and the 40kDa polypeptide with a filled rectangle on the gel. Neither the 40kDa ('40') or 90kDa ('90') polypeptides were visible in the mock infected RE track, but were induced by HSV infection (lanes 3 and 4). Both the '40' and '90' were present in all the transformed Bn5T samples (including the mock infected sample). In this experiment the L90 band was only just detectable in the TBS ip and Bn5T mock infected samples (lanes 5 and 8). The 200kDa polypeptide was detectable in all samples except the RE mock infected sample. These results are not consistent with those reported by Macnab *et al.*(1985) and Hewitt *et al.* (1991) where the 40kDa polypeptide was shown to be specific to

Figure 3.1. Immunoprecipitation of a 40kDa polypeptide from infected control and transformed cells (Phosphorimager image).

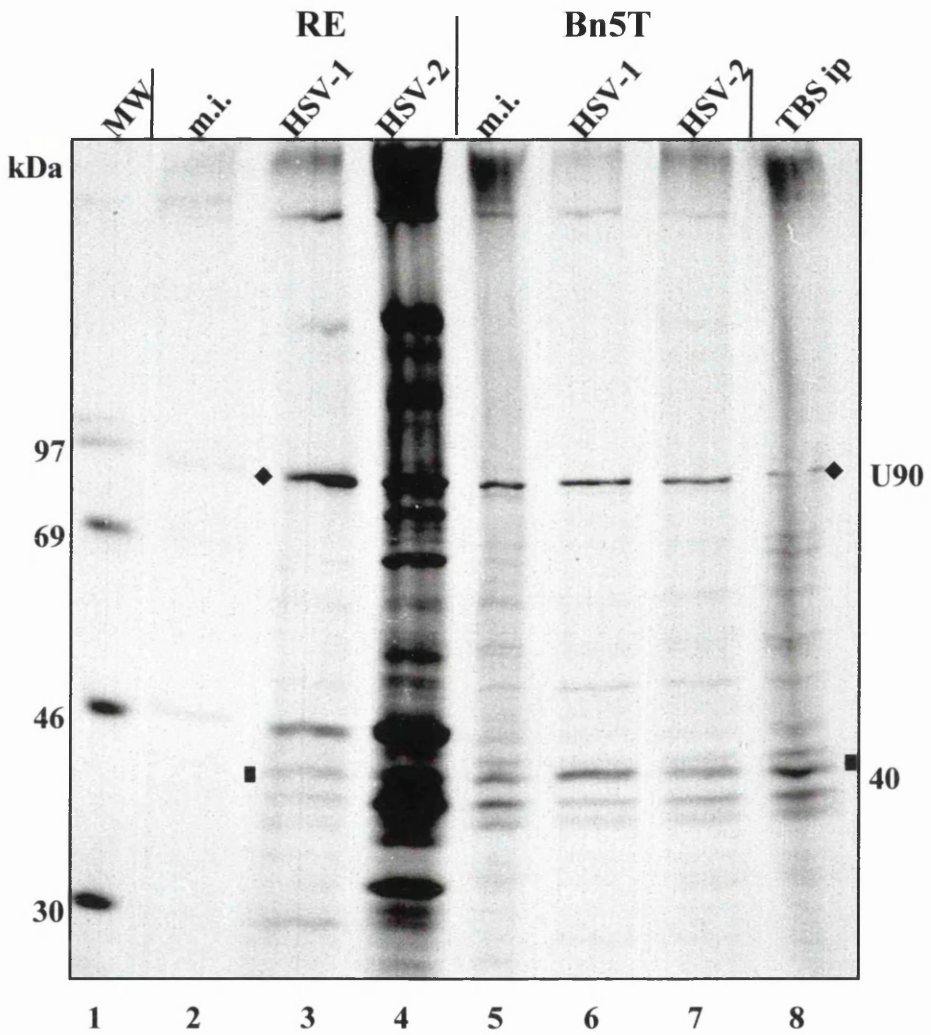

Legend. RE and Bn5T cells were infected overnight with HSV-1 strain 17 or HSV-2 strain HG52, or mock infected in tissue culture medium containing [^{35}S]-L-methionine. Cells were lysed in RIPA buffer and immunoprecipitated with a rat TBS (see Materials and Methods). The immunoprecipitated polypeptides were electrophoresed on a 9% SDS-PAGE gel with ^{14}C-labeled molecular weight markers (lane 1) and a control immunoprecipitation (lane 8) provided by J-F. Lucasson which was known to produce a clear 40kDa band for comparison. The dried gel was exposed to a phosphorimager screen overnight.

The '40' and '90' (marked ▪ and ◆ respectively) are not present in the mock infected RE sample (lane 2), but are induced in RE cells by infection with HSV-1 and HSV-2 (lanes 3 and 4). (A faint band representing U90 may be present in the mock infected RE sample- (Grassie *et al*, 1993) see section 3.1). Both the '40' and '90' are present in mock infected and HSV infected Bn5T cells (lanes 5-7). The L90 is only just detectable in the TBS ip and Bn5T HSV-1 tracks in this experiment (lanes 8 and 6 respectively). A clearer immunoprecipitation showing the full set of HSV induced polypeptides described by Macnab *et al*, (1985) is presented in Figure 3.4 (labelled TBS).

the transformed cell, and was induced by HSV infection. This may be due to variation in the RE cells or to the specific TBS used in this particular experiment. The quality of the TBS was previously noted to be variable (see below).

Grassie, (1993) raised an antiserum that was mono-specific for the U90 polypeptide, and used this to study in detail the biological properties of the U90 polypeptide. The induction of U90 by HSV was shown not to be dependent upon functional Vmw175 by infection with temperature sensitive mutants (tsK, tsD and tsT) and the deletion mutant (In1411) viruses. This antiserum was also used to detect a homologue of U90 in the control RE cells and demonstrate that this is increased in RE cells by HSV infection (a faint band is visible in the RE m.i. track in Figure 3.1). The increased level of the U90 detected in transformed cells compared to control RE cells was shown to be the result of the greatly extended half-life of the U90 polypeptide in the transformed cells (Grassie *et al.*, 1993).

The purification and raising of a mono-specific antiserum to the 40kDa polypeptide would facilitate the characterisation, and possibly identification of this polypeptide. Tumour bearing sera, the only tool available at the time to study the 40kDa polypeptide were of variable quality and detected many polypeptides other than the 40kDa polypeptide (for example, see figure 3.1, lane 4). The following work describes the purification of the 40kDa polypeptide, and an attempt to produce a mono-specific antiserum.

3.2 PURIFICATION OF THE 40kDa POLYPEPTIDE FROM Bn5T CELLS

The 40 kDa polypeptide was purified from Bn5T cells essentially as described by Lucasson (1992) and in Materials and Methods. Twenty plastic roller bottles (850 cm^2) of cells were grown at 37°C until almost confluent, washed several times with PBS-A to remove contaminating serum proteins, and harvested using a sterile scraper. Cells were collected in a total volume of ice cold PBS-A of approximately 200ml, and pelleted by centrifugation at 1000g. 50ml of ice cold hypotonic lysis buffer (WF) was added and the pellet dispersed by gentle agitation. $5x10^7$ cells labelled with [^{35}S]-L-methionine were added at this stage to facilitate the subsequent identification of the 40kDa polypeptide. The cell suspension was homogenised with

a dounce homogeniser, and sonicated. The solution was incubated on ice for 5 minutes, prior to centrifugation at 1000g to pellet cellular debris.

The clarified extract was then subjected to ammonium sulphate precipitation of the polypeptides by the gradual addition of solid ammonium sulphate to final concentrations of 30, 60 and 90% with stirring on ice. At each stage the precipitated polypeptides were collected by centrifugation at 30,000g at 4°C and stored on ice. The polypeptides precipitated at 90% saturation were resuspended in 2ml of 50mM Tris-HCl pH 8.0 and desalted using a PD-10 column.

The polypeptides were purified by FPLC, using a Mono-Q anion exchange column equilibrated with 50mM Tris-HCl buffer pH 8.0. The proteins were eluted using a 0-2M NaCl gradient in 50mM Tris-HCl. Figure 3.2 shows a typical FPLC trace from the MonoQ column, with the elution of polypeptides detected by absorbance at 260nm. The increasing salt gradient is illustrated below the trace. The 40kDa polypeptide was known to elute from the column in the 'flow-through' volume (Lucasson, 1992), indicating that it did not bind to the anion exchange resin at pH 8.0 in the Tris-HCl buffer used.

Fractions containing the protein peak from the 'flow-through' were desalted using a FastDesalt column on the FPLC into a buffer containing 10mM ammonium bicarbonate. This allowed the polypeptides in the fractions to be concentrated by lyophilisation in a vacuum dryer without increasing the salt concentration of the sample. Ammonia and carbon dioxide are given off during the lyophilisation process. The fractions were resuspended in a small amount of buffer before electrophoresis on a 9% SDS-PAGE gel. The gel was dried and exposed to a phosphorimager screen. Figure 3.3 shows the phosphorimager image of a preparative gel. An immunoprecipitation reaction with a tumour bearing serum known to produce a good 40kDa band (J-F. Lucasson, pers. comm.) was included on the gel to allow the 40kDa band in the FPLC fractions to be identified. Overlaying the phosphorimager image on the Coomassie Blue stained gel allowed the 40kDa polypeptide band to be excised from the dried gel with a sterile scalpel blade. The 40kDa polypeptide is marked on the gel with an arrow. The majority of the 40kDa polypeptide eluted in fractions 3-7 from the MonoQ column.

Figure 3.2. FPLC trace from MonoQ anion exchange column: 0- 2.0 M NaCl gradient.

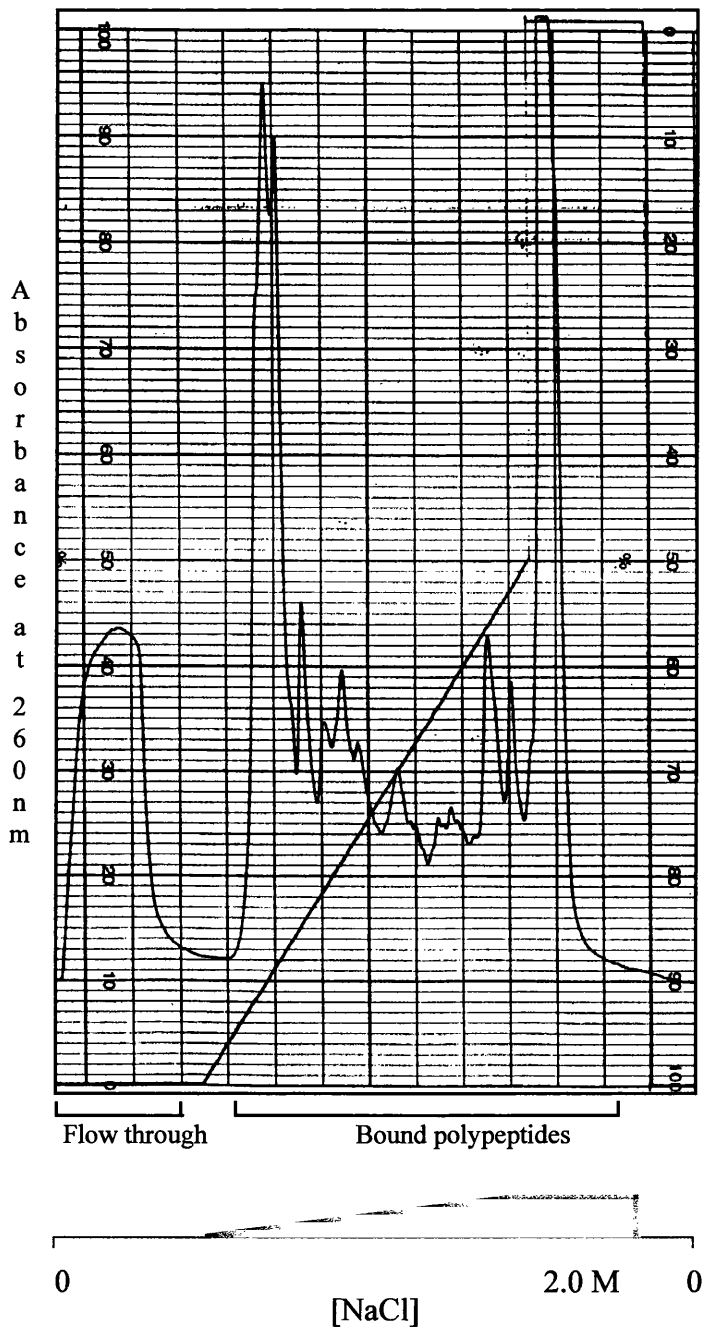

Legend. Polypeptides precipitated by 90% $(NH_4)_2SO_4$ fractionation of a Bn5T cell lysatewere seperated by anion exchange chromatography on a 1ml MonoQ FPLC column. Samples were loaded in 1ml of 50mM Tris-HCl buffer at pH 8.0, and eluted from the column with an increasing gradient of NaCl. The salt gradient is illustrated below the trace. The '40' was known to elute in the 'flow-through' from the column, and this peak is marked on the trace. The '40' is therefore purified by the removal from the lysate of those polypeptides that bind to the column.

Vertical lines represent 1ml intervals. Absorbance at 260nm was used to detect polypeptides as they eluted from the column (FSD= 0.2).

Figure 3.3. Preparative SDS-PAGE gel for purification of the 40kDa polypeptide

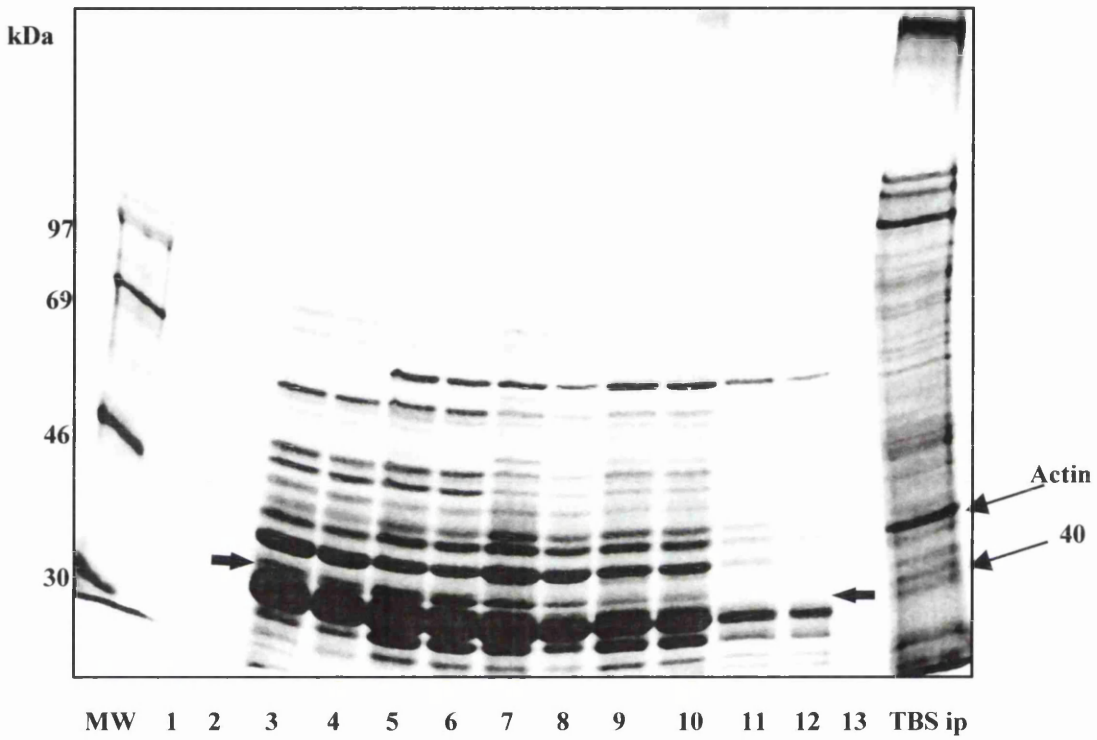

Legend. Fractions from the 'flow-through' (lanes 1-13) of an FPLC purification experiment using a MonoQ column equilibrated at pH 8.0 in 50mM Tris-HCL buffer were desalted and lyophilised. The fractions were resuspended in ddH_20 and electrophoresed on a 9% SDS-PAGE gel. A TBS ip known to produce a good '40' band was included to facilitate the identification of the '40' in the FPLC fractions. The radiolabelled polypeptides were detected using a phosphorimager. The sizes of the ^{14}C-labelled molecular weight markers are shown at the left of the gel. The '40' is present in fractions 3-10, and is labelled ➡ . Actin and the '40' are labelled in the TBS ip lane used to identify the 40kDa polypeptide. The '40' was excised from the SDS-PAGE gel by comparison with this phosphorimager printout.

3.3 IMMUNISATION OF A RABBIT WITH THE 40kDa POLYPEPTIDE AND TESTING OF ANTISERUM

The excised protein band containing the 40 kDa polypeptide was rehydrated, the paper backing removed and the polyacrylamide gel slice ground up in a small homogeniser. This suspension was mixed with Freunds incomplete adjuvant and injected into a rabbit by Dr. J.C.M. Macnab, Institute of Virology, Glasgow. Booster injections were initially given at 2 week intervals, but the animal did not produce a significant antibody response. Further booster injections were given over a period of 6 months. In western blotting experiments with whole cell lysate from HSV-2 infected Bn5T cells, this antiserum failed to detect the 40kDa polypeptide (data not shown), even when enhanced chemiluminescence detection reagents were used.

The rabbit was sacrificed after 6 months, and the serum collected. This serum (92A) was tested in immunoprecipitation assays to determine whether antibody to the 40kDa polypeptide had been induced. Between 10 and 95µl of serum 92A were included in standard immunoprecipitation assays as described in Materials and Methods. Pre-immune control immunoprecipitations, and a TBS immunoprecipitation known to produce a good 40kDa band (J-F. Lucasson, pers. comm.) were included on a 9% SDS-PAGE gel. Figure 3.4 shows the phosphorimager image of this experiment. The 40kDa polypeptide is clearly visible in the TBS immunoprecipitation track (labelled with a star in lane 2), as are the 200kDa, U90 and L90 and 32kDa polypeptides previously identified in Bn5T cells and increased by HSV-2 infection (Macnab *et al.*, 1985). All are labelled as described in the legend to Figure 3.4. A faint, diffuse band of the same molecular weight as the 40kDa polypeptide is present in the 92A immunoprecipitations (lanes 3-5, 7) but this is also present in the pre-immune serum (lanes 6 and 8). The only polypeptide detected in the 92A immunoprecipitations that is not present in the pre-immune reactions is a 67kDa polypeptide (labelled with a fat arrow in lanes 5 and 7). This band is also present in the TBS i.p. track (lane 2). This polypeptide remains unidentified, but as this was a denaturing gel it is unlikely to be a dimer of the 40kDa polypeptide. It appears that no specific antibody to the 40kDa polypeptide was induced in this animal. Indirect immunofluorescence experiments using this antiserum displayed diffuse fluorescence at the cell surface but this was not

Figure 3.4. Immunoprecipitations to test the rabbit antiserum 92A raised against purified 40kDa polypeptide

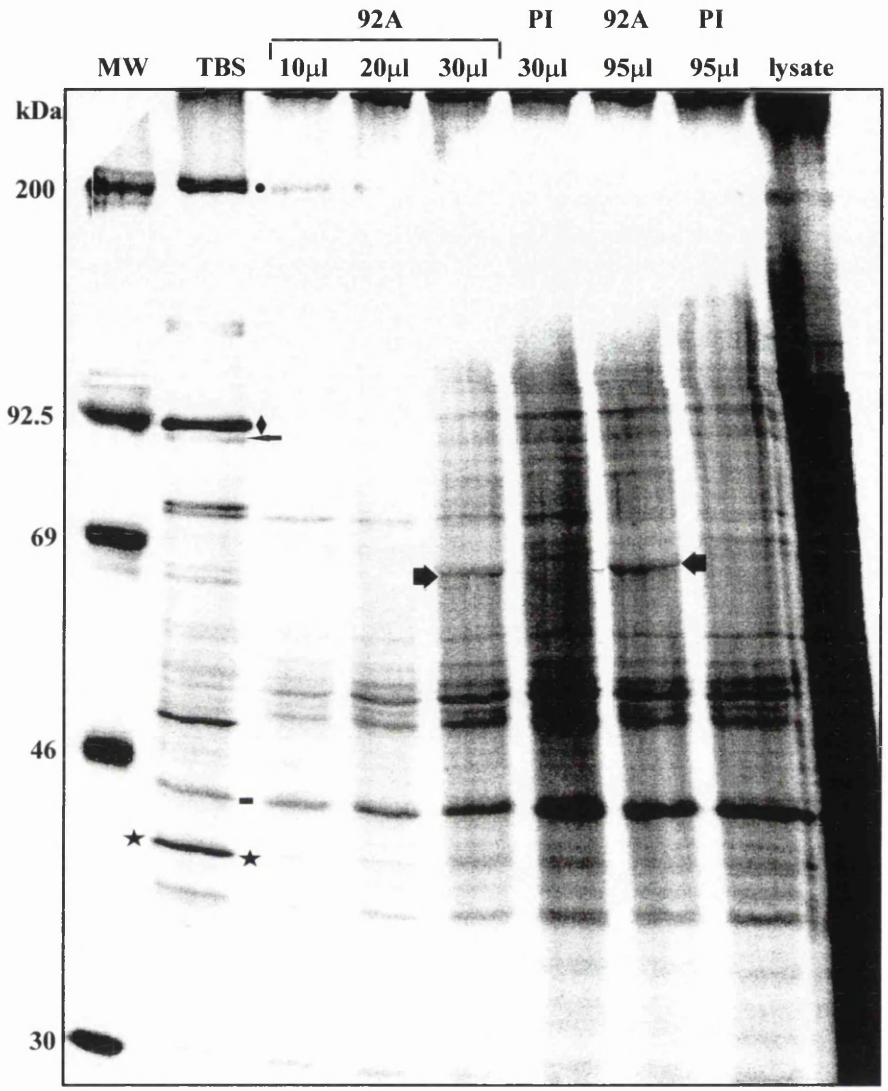

Legend. $4x10^6$ cpm of [α^{35}S]-L-methionine labelled polypeptides were immunoprecipitated from a Bn5T cell lysate with a TBS which produces a good '40' band, the rabbit antiserum raised against the '40' purified as described in sections 3.2 and 3.3 (92A), or pre-immune serum (PI). ECL molecular weight markers are shown to the left of the gel. The lysate lane contains 1µl of the Bn5T lysate used in the immunoprecipitations. The volume of antiserum used in each immunoprecipitation with 5µl of lysate in a total volume of 100µl is indicated above the lanes. The '40' is marked with a star in the TBS ip lane, and a diffuse faint band is present at this position in all of the samples, including the pre-immune serum reactions. The only polypeptide that is detected by the 92A serum that is absent in the pre-immune serum lane is of approximately 67kDa, and is labelled with a 'fat' arrow. In the TBS ip lane the group of polypeptides identified by Macnab *et al*, (1985) (see section 3.1) are labelled as described in the key below.

• 200	⬅ L90	▬ Actin
♦ U90	➡ unknown	★ '40'

significantly different to the result obtained with the pre-immune serum (Dr. J.C.M. Macnab, pers. comm.).

3.4 DISCUSSION

The 40kDa polypeptide was partially purified from infected Bn5T cells by ammonium sulphate fractionation and anion exchange chromatography as described by Lucasson (1992) *(Section 3.2)*. The purification obtained was fairly crude, but all polypeptides that bound to the MonoQ column were removed from the sample. However, the purification was sufficient to allow the separation of the 40kDa polypeptide from contaminating polypeptides (displayed in Figure 3.3). The 40kDa polypeptide was excised from the 9% SDS-PAGE gel. Lucasson (1992) included a further ion exchange purification step, but although the degree of purification was greater, the overall yield of the 40kDa polypeptide was somewhat reduced. Experiments to further purify the 40kDa from the 'flow-through' fractions were performed using a heparin affinity chromatography column on the FPLC. The same buffers used with the MonoQ column were used. The FPLC trace in Figure 3.5 shows the elution profile of polypeptides from the heparin column eluted with a 0-2.0M NaCl gradient. Two peaks were observed - a 'flow-through' peak of proteins which did not bind to the column, and a second broad peak eluting at 0-0.4M NaCl. The 40kDa polypeptide eluted in the 'flow-through' peak, but the purification obtained was not sufficient to overcome the reduced recovery of the 40kDa polypeptides as a result of the extra step (data not shown).

The 40kDa polypeptide purified from the MonoQ column and excised from a SDS-PAGE gel was therefore used to immunise a rabbit. A similar method of producing an immunogen had been successfully used in this laboratory to raise a mono-specific antibody to the U90 polypeptide immunoprecipitated from transformed cells (Macnab *et al.*, 1985; Grassie, 1993; Grassie *et al.*, 1993). However, as described above (*Section 3.3*), there was no significant antibody response detected by immunoprecipitation (*Figure 3.4*), Western blotting or immunofluorescence experiments (data not shown). The lack of reaction in immunoprecipitation experiments could be explained because the immunogen consisted of denatured polypeptide, and conformational epitopes from the native polypeptide would therefore not be displayed. The negative Western blotting results could not however

Figure 3.5. FPLC trace from Heparin affinity chromatography column

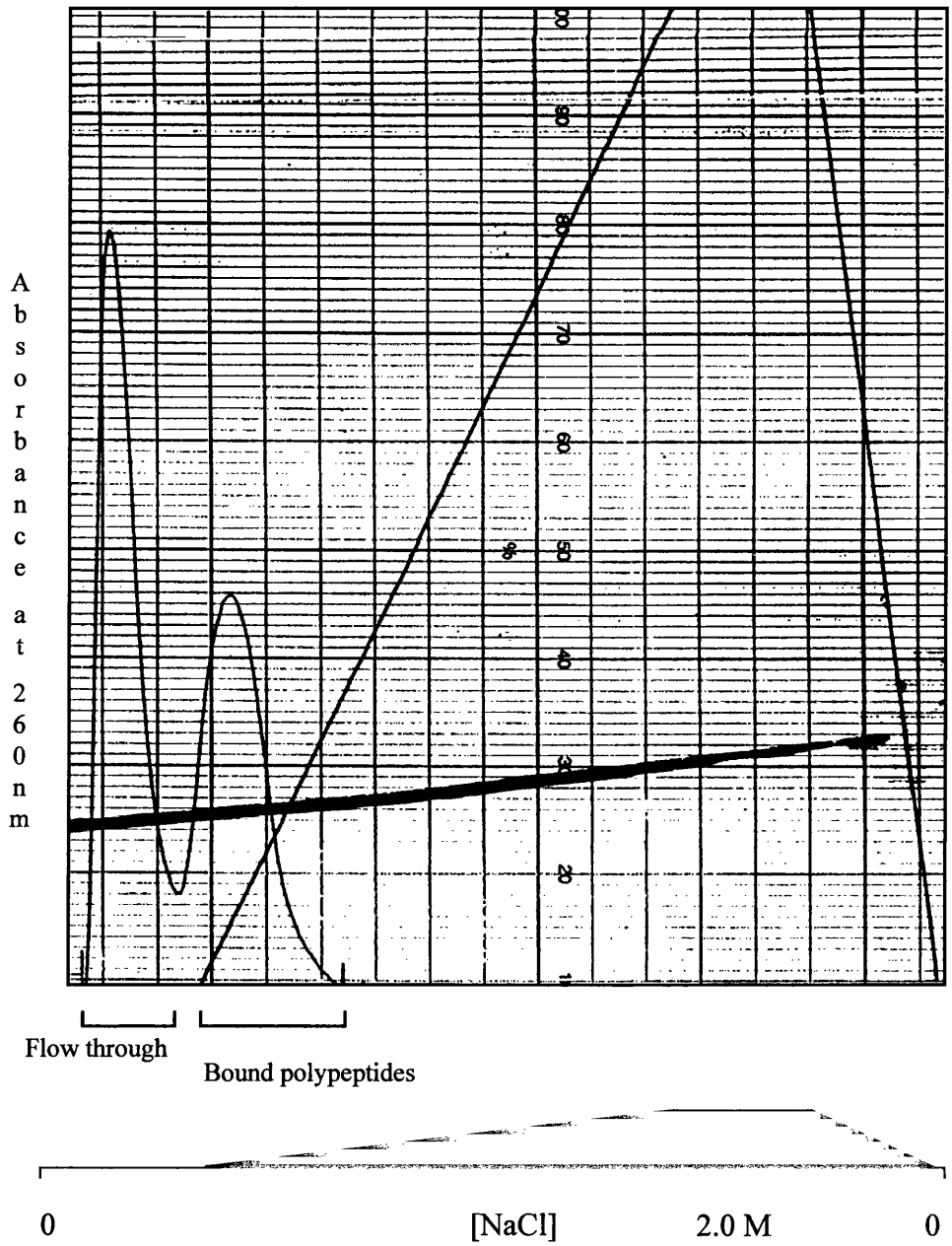

Legend. The polypeptides purified from the 'flow-through' of the MonoQ column described in Section 3.2 (Figure 3.2) were pooled and concentrated in a 'speedivac' prior to loading on a 1ml Heparin affinity chromatography column. The column was equilibrated in 50mM Tris-HCl pH 8.0, and polypeptides were eluted with a salt gradient as illustrated below the trace. The '40' eluted in the flow through of the column at pH 8.0, indicating that it did not bind to heparin under the experimental conditions used. The second peak represents polypeptides that bound to the column. The additional purification of the '40' obtained from this column was minimal.

Vertical lines represent 1ml volume intervals. Absorbance at 260nm was used to detect the eluted polypeptides (FSD= 0.2).

be explained in this way. Lucasson (1992) attempted to raise an antiserum in rabbit using 40kDa polypeptide from a second ion exchange experiment at pH 9.5. This also failed to elicit an immune response. Why the 40kDa polypeptide purified from a transformed rat cell line should fail to induce an immune response in rabbit is unclear. The 40kDa polypeptide could be highly conserved between species, or may have an intrinsically low immunogenicity. Furthermore, the amount of polypeptide in the immunogen was quite low, as the 40kDa polypeptide has a low abundance even in HSV infected Bn5T cells. Alternative adjuvant and immunisation regimes may have elicited an immune response, but these were not tested for reasons detailed in the following paragraph.

During the process of this work, the 40kDa polypeptide was identified as a form of mitochondrial aspartate aminotransferase by internal peptide sequence analysis and immunological characterisation (Lucasson, 1992). A mono-specific antiserum to mAspAT was available (Mattingley *et al.*, 1987), and a polyclonal rabbit antiserum was produced by Dr. J.C.M. Macnab using immunogen provided by Mattingley (University of Missouri). This serum immunoprecipitated the 40kDa polypeptide (Lucasson, 1992), and therefore no further attempt was made to produce an antiserum to the 40kDa polypeptide purified from Bn5T cells. The ease with which a rabbit antiserum was raised against bacterially expressed rat mitochondrial aspartate aminotransferase suggests that the immunogen purified from Bn5T cells above (Section 3.2) was of low abundance and/or of poor quality.

4 THE EFFECT OF HSV-2 INFECTION ON THE STEADY-STATE LEVEL OF mAspAT mRNA IN A TRANSFORMED CELL LINE.

4.1 INTRODUCTION

Lucasson *et al.* (1994) identified the 40kDa polypeptide which is increased in tumour cells by infection with HSV-2 (Macnab *et al.*, 1985) as a form of mitochondrial aspartate aminotransferase (EC 2.6.1.1). We reported a fourfold increase in the level of mAspAT polypeptide present in Bn5T cells following infection with HSV-2 (Lucasson, 1992; Lucasson *et al.*, 1994) determined by slot-blot immunoblotting with two different antisera raised against mAspAT (Mattingley *et al.*, 1987). Further experiments investigating the effect of HSV-2 infection of Bn5T cells on the mAspAT enzyme activity (for a fixed amount of total cellular protein) showed a mean increase in the activity of 2.5 fold compared to control Bn5T cells over 3 determinations (Lucasson *et al.*, 1994).

These results could arise from altered control of protein synthesis and processing, or by alterations in the stability of the polypeptide molecule. Specific stabilisation of a polypeptide molecule has been observed in HSV transformed cells. The U90 member of the group of polypeptides that are increased in tumour cells (Macnab *et al.*, 1985) has an increased half life in transformed cells (13 hours compared to 33 minutes in control cells) (Grassie *et al.*, 1993).

An increase in the steady-state level of mAspAT mRNA following HSV-2 infection of the transformed Bn5T cell line could also lead to an increase in the absolute amount of protein present, independently of direct effects at the protein level. This could occur by transcriptional activation of the mAspAT gene, as has been reported for the HSV-2 induced TI56 protein (Patel *et al.*, 1986; Kemp and Latchman, 1988). Possible mechanisms include the activation of upstream regulatory sequences by HSV-2 transactivation factors, or the activation of previously hidden promotor elements. Alternatively, the mAspAT mRNA could be preferentially stabilised following HSV-2 infection. This would contrast the UL41 (*vhs*) mediated destabilisation of most host cell and viral mRNA that normally accompanies infection (Kwong *et al.*, 1987; Oroskar & Read, 1989), although it should be noted that the HG52 strain of HSV-2 used in the following work has an inactive *vhs*

function (Everett and Fenwick, 1990). Both of these mechanisms would lead to an accumulation of mAspAT mRNA.

Preliminary Northern blotting experiments suggested that there was an increase in the steady state level of the mAspAT mRNA in transformed cells after infection with HSV-2. Further investigation of this possibility is described below.

4.2 SLOT-BLOT AND NORTHERN BLOT EXPERIMENTS TO ANALYSE THE EFFECT OF HSV-2 INFECTION ON THE STEADY STATE LEVEL OF mAspAT RNA IN THE Bn5T TRANSFORMED CELL LINE.

4.2.1 Northern blotting

Northern blotting experiments were performed using total cellular RNA from Bn5T cells infected with 10 pfu/cell HSV-2 for 17 hours at 37°C, or from mock infected Bn5T cells. An adaptation of the single step acid guanidinium thiocyanate-phenol-chloroform extraction procedure of Chomczynski and Sacchi (1987) (described in Materials and Methods) was used. Equal quantities of total RNA (determined spectrophotometrically as described in Materials and Methods) were loaded onto a 30cm long 1.5% agarose-formaldehyde gel and electrophoresed until the bromophenol blue dye was near the end of the gel. The gel was rinsed in ddH_2O and blotted by capillary transfer as described in Materials and Methods. The transferred nucleic acid was fixed to the Hybond-N™ membrane by UV-irradiation in a Stratalinker™. 1µl of a synthetic RNA ladder (Gibco BRL) was run on a track alongside the RNA samples to facilitate a) an estimation of the size of the mAspAT transcript detected and b) analysis of the integrity of the RNA following fixation to the membrane by methylene blue staining as described in Materials and Methods.

4.2.2 mAspAT cDNA probe labelling

The blots were initially hybridised with a 2.3kb mAspAT cDNA probe. This probe was purified by gel electrophoresis following excision from either pBS-KS-mAspAT (Mattingley *et al.*, 1987) or pCMV-mAspAT1 (see Chapter 6, *Section 6.2*) by digestion with EcoRI. The probe was labelled to high specific activity (>$2x10^8$ cpm/µg) by nick translation, or using the Megaprime™ random priming kit (Amersham International), as described in Materials and Methods. A control strip containing dots of denatured mAspAT cDNA insert, ranging from 60ng to 0.6pg

fixed to Hybond-N™ membrane was included in each hybridisation experiment to determine the effectiveness of the hybridisation procedure.

4.2.3 Optimisation of washing protocol

The washing protocol following hybridisation with the mAspAT probes was optimised by checking the counts remaining on the blot with a Geiger-Muller counter after washes of increasing stringency. It was noted that washing at a stringency greater than 1x SSC, 65°C, for 30 minutes caused the counts retained on the blot to fall to a level indistinguishable from background. A long exposure to the phosphorimager screen was required to detect any bound probe. Final washing of blots probed with the mAspAT probes was therefore restricted to a maximum stringency of 1x SSC at 65°C for 30 minutes. Blots were wrapped in cling film and exposed to the phosphorimager screen overnight at room temperature.

Following analysis of the overnight exposure, blots were stripped by three washes with 1 litre of boiling 1% SDS(w/v) solution and checked to ensure complete stripping by exposure to the phosphorimager screen. If stripping was complete the blots were re-hybridised with a control probe.

4.2.4 Probing with a control probe

The control probes used to normalise the amount of RNA loaded in each track of the Northern blotting experiments were either a γ-actin cDNA (Leader *et al.*, 1985), or an X. laevis 28S rDNA clone in plasmid pX11r1R (Maden *et al.*, 1987). The level of γ-actin had previously been shown to be unaffected by HSV-2 infection in rat fibroblasts (Dr. J.C.M. Macnab, pers. comm.) and MCF-7 cells (Offord *et al.*, 1989). The 28S rRNA has been widely used as a control in Northern blotting experiments. As a major constituent of cellular RNA the 28S rRNA levels have been shown to be generally unaffected by cellular differentiation or proliferation (Barbu & Dautry, 1989).

4.2.5 Calculation of the relative increase of mAspAT mRNA levels

All Northern and slot-blot experiments were analysed using a Phosphorimager (Molecular Dynamics Inc., running ImageQuant™ (Version 1) software). The number of counts detected in each RNA sample when probed with the mAspAT cDNA was measured and compared to the number of counts detected in each sample

when probed with the one of the control probes. This allowed a correction to be made for errors which may have occurred whilst preparing and loading the RNA samples. The calculation is described by the following equation, and was performed on samples from mock infected and HSV-2 infected Bn5T cells.

$$\frac{counts\ with\ mAspAT\ probe}{counts\ with\ control\ probe} = ratio\ of\ counts\ for\ RNA\ sample$$

The ratio obtained from the mock infected Bn5T cell RNA samples was then compared to the ratio obtained from the HSV infected samples. This allowed the overall relative increase in the level of mAspAT mRNA following HSV-2 infection to be calculated.

These calculations are illustrated in the sample calculation shown in Figure 4.1 and described in section 4.2.6 below.

4.2.6 Representative calculation of altered mAspAT mRNA levels.

Figure 4.1 presents the raw data obtained from the phosphorimager and a representative calculation of the altered level of mAspAT mRNA following HSV-2 infection. The actual image of the Northern blot used in this calculation is presented in Figure 4.2. Bn5T cells were infected with 10 pfu/cell of HSV-2 for 17 hours. 40μg of total RNA from mock infected Bn5T cells and from Bn5T cells infected with HSV-2 was electrophoresed on a 1.5% agarose-formaldehyde gel, transferred to Hybond-N™ and probed sequentially with mAspAT and γ-Actin probes as described in Sections 4.2.1-4.2.4 above.

Panel A shows the results obtained when this blot was probed with the mAspAT cDNA. The ratio of counts in the HSV-2 infected track compared to the mock infected sample is 5.85 or 4.43, depending on the method used to delineate the boundary of the samples. Both a grid and free-drawn rectangles were used to delineate the area to be examined. This reduces the errors introduced by the positioning of the regions to be counted for analysis with the ImageQuant™ software. Combination of these results gives a mean 5.14 fold relative increase in the counts in the HSV-2 infected sample compared to the mock infected track

Panel B shows results for the same blot probed with the control γ-Actin probe. In this experiment the mean result was a 2.04 fold increase in the counts in the HSV-2 infected track compared to the control track. This result most likely represents a

Figure 4.1. Comparison of steady-state level of mAspAT mRNA in Bn5T cells before and after infection with HSV-2. Analysis of data from Northern blot illustrated in Figure 4.2A.

Panel A

mAspAT probed blot- phosphorimager results (Rectangles)

Sample	counts detected	% of counts	Ratio HSV /mock
Bn5T	2308	14.6	5.85 **(A)**
Bn5T HSV-2	13505	85.4	

mAspAT probed blot- phosphorimager results (Grid)

Sample	counts detected	% of counts	Ratio HSV /mock
Bn5T	3566	5.63	4.43 **(B)**
Bn5T HSV-2	15798	24.93	

Mean ratio of counts in HSV-2/mock infected samples = **5.14x (C)** [1]

Panel B

γ-Actin probed blot- phosphorimager results (Rectangles)

Sample	counts detected	% of counts	Ratio HSV /mock
Bn5T	90565	21.93	2.03 **(D)**
Bn5T HSV-2	184728	44.73	

γ-Actin probed blot- phosphorimager results (Grid)

Sample	counts detected	% of counts	Ratio HSV /mock
Bn5T	86523	32.7	2.05 **(E)**
Bn5T HSV-2	178185	67.3	

Mean ratio of γ-Actin counts in HSV-2/mock samples = **2.04 (F)** [2]

Overall Result [3]

Increase of mAspAT mRNA relative γ-Actin observed following infection of Bn5T cells with HSV-2 = **2.52x**

Calculations

[1] **C= ((A+B)/2)**

[2] **F= ((D+E)/2)**

[3] **= (C/F)**

Figure 4.2. Northern blot and slot blot experiments with HSV-2 infected Bn5T cell RNA reprobed with a γ-Actin cDNA probe after hybridisation with a mAspAT probe.

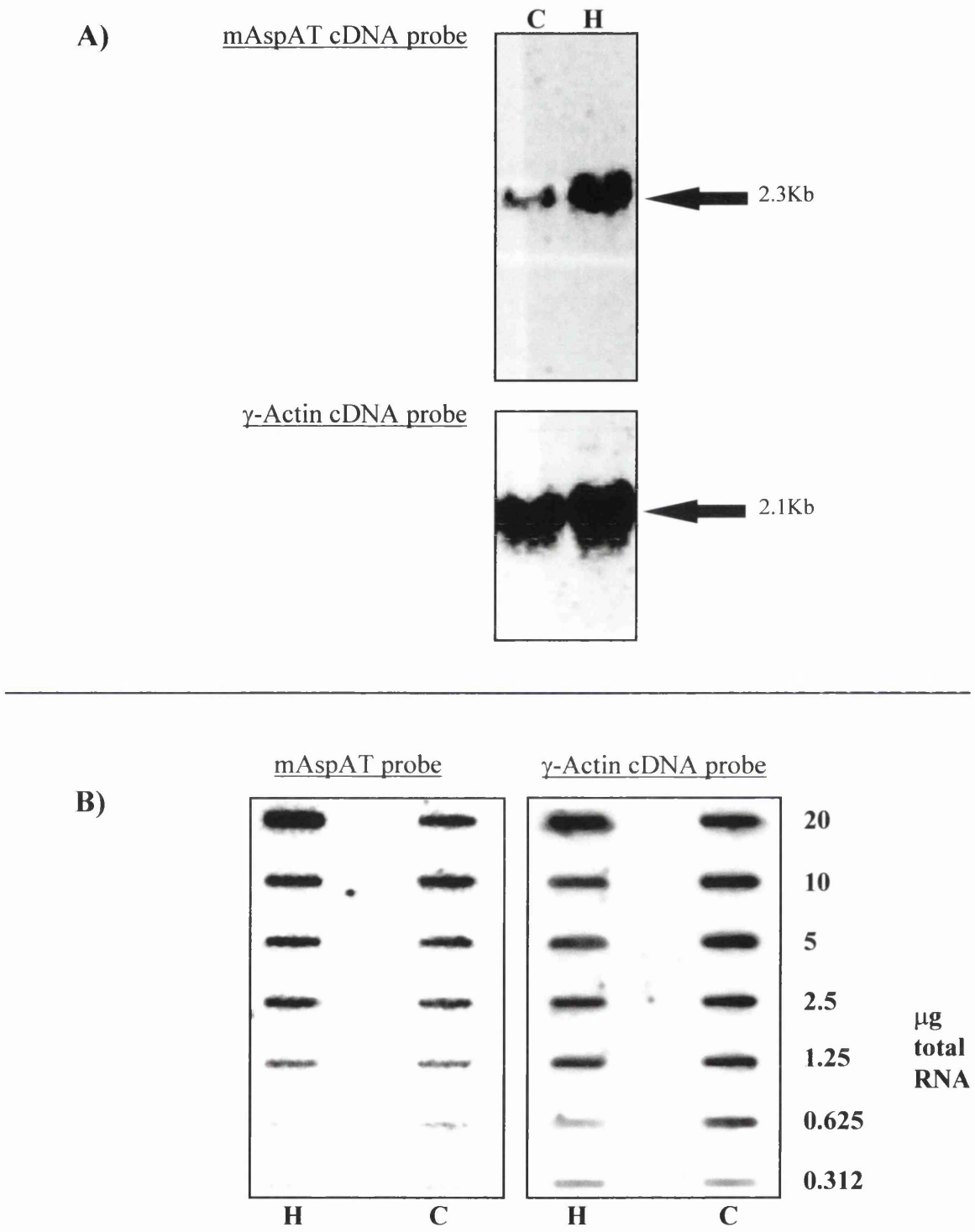

Legend. Panel A shows a Northern blot of 40μg of total RNA from mock infected (**C**) and HSV-2 infected (**H**) from Bn5T cells. The top phosphorimager image was obtained when the blot was probed with a mAspAT probe, and the lower image following reprobing with a γ-Actin probe. A single transcript was detected with each probe. The calculated increase in the relative level of mAspAT following HSV-2 infection was 2.52 fold. (Experiment 2 in Table 4.1). Panel B shows a slot blot of similar mock infected or HSV-2 infected RNA, probed with the same probes. The samples containing 20-1.25μg of total RNA were analysed with the phosphorimager and showed a mean relative increase over all samples of 1.49 fold (Experiment 3 in Table 4.1).

loading or sample preparation error. Approximately twice as much total RNA (as detected by the level of γ-Actin) was present in the HSV-2 infected Bn5T cell sample than in the mock infected sample in this particular experiment. This is despite the RNA being quantitated spectrophotometrically prior to denaturation and electrophoresis.

By dividing the HSV-2 infected counts/mock infected counts ratio calculated in Panel A by the ratio obtained in Panel B, the alteration in the level of mAspAT mRNA was corrected for the loading variations which were detected on the γ-Actin probed blot. The overall result (see footnotes to Figure 4.1 for a summary of the calculations performed) is a 2.52 fold increase in the steady state level of mAspAT mRNA in Bn5T cells after infection with HSV2.

4.2.7 Increased mAspAT mRNA levels - cumulative results.

A total of eight experiments were performed to confirm the increase in the steady state level of mAspAT mRNA previously reported in Figures 4.1 and 4.2. These results are presented in Table 4.1. Each experiment showed an increase in the mAspAT mRNA level relative to the γ-actin or 28S rRNA controls following infection with HSV-2. However, there was a range of 1.07 to 2.69 in the increase of mAspAT mRNA observed. Statistical analysis of these results using the 'descriptive statistics' function of Microsoft Excel® 5.0 calculated a mean value of 1.748 for the increase in the mAspAT mRNA following infection of Bn5T cells with HSV-2. The standard error was calculated as 0.255 (14.5%). An example of an RNA slot blot (Figure 4.2B) reprobed with a γ-Actin probe, and a Northern blot (Figure 4.3) reprobed with a 28S rRNA probe are shown. The results of these experiments are presented in Table 4.1 (experiments 3 and 7 respectively). A single 2.3kb transcript is detected in the mAspAT probed blot of Figure 4.3 (labelled in Panel B), which validates the results from the slot-blot experiments.

4.3 SEMI-QUANTITATIVE RT-PCR TO EXAMINE THE ALTERED LEVEL OF mAspAT mRNA IN HSV-2 INFECTED Bn5T CELLS.

Further experiments were performed to confirm the increase in the level of mAspAT mRNA following HSV-2 infection which was observed in the Northern blotting experiments described in Section 4.2. A semi-quantitative reverse transcriptase polymerase chain reaction (RT-PCR) method was used to assess the amount of

Table 4.1. The effect of HSV-2 infection on the relative level of mAspAT mRNA in Bn5T cells. Cumulative results of eight experiments.

A) Ratio of increases in mAspAT mRNA observed in eight experiments

Experiment		Increase in mAspAT mRNA[A]	Notes
1	8/12/92	2.69	Northern
2	16/12/92	2.52	Northern
3	12/01/93	1.49	Slot-blot- mean of 5 results
4	12/01/93	1.07	Northern-mean of 2 results
5	16/01/93	1.17	Northern-mean of 2 results
6	23/02/93	1.19	Northern
7	8/03/93	1.26	Northern-mean of 2 results
8	12/05/93	2.60	Slot-blot- mean of 5 results

B) Statistical Analysis of the results from eight experiments[B]

Mean	1.748
Standard Error	0.254

Mean overall increase in the relative level of mAspAT mRNA following HSV-2 infection of Bn5T cells

$$1.748 \pm 0.25$$

Legend. The results of eight separate Northern blotting and slot-blot experiments to determine the effect of HSV-2 infection on the level of mAspAT mRNA relative to an internal control mRNA are presented in Section A. In each experiment Bn5T cells were infected with 10pfu/cell of HSV-2 HG52 or were mock infected overnight. Total cellular RNA was extracted and Northern blotted as described in Materials and Methods. The number of separate samples analysed in each experiment are displayed in the 'Notes' section.
In section B the results presented in Section A were subjected to statistical analysis using Microsoft Excel. The mean and calculated standard error of the mean are presented.
The images of a Northern blot (experiment 2) and slot blot (experiment 3) reprobed with a γ-Actin probe are shown in Figures 4.2A and 4.2B. The image of a Northern blot reprobed with the 28S rRNA probe (experiment 7) is shown in Figure 4.3.

[A] *Results calculated relative to internal control as described in Figure 4.1*

[B] *Calculated using MS Excel 'descriptive statistics' package*

Figure 4.3. Northern blot to show increase in the level of mAspAT RNA (relative to 28S rRNA) following infection of Bn5T cells with HSV-2.

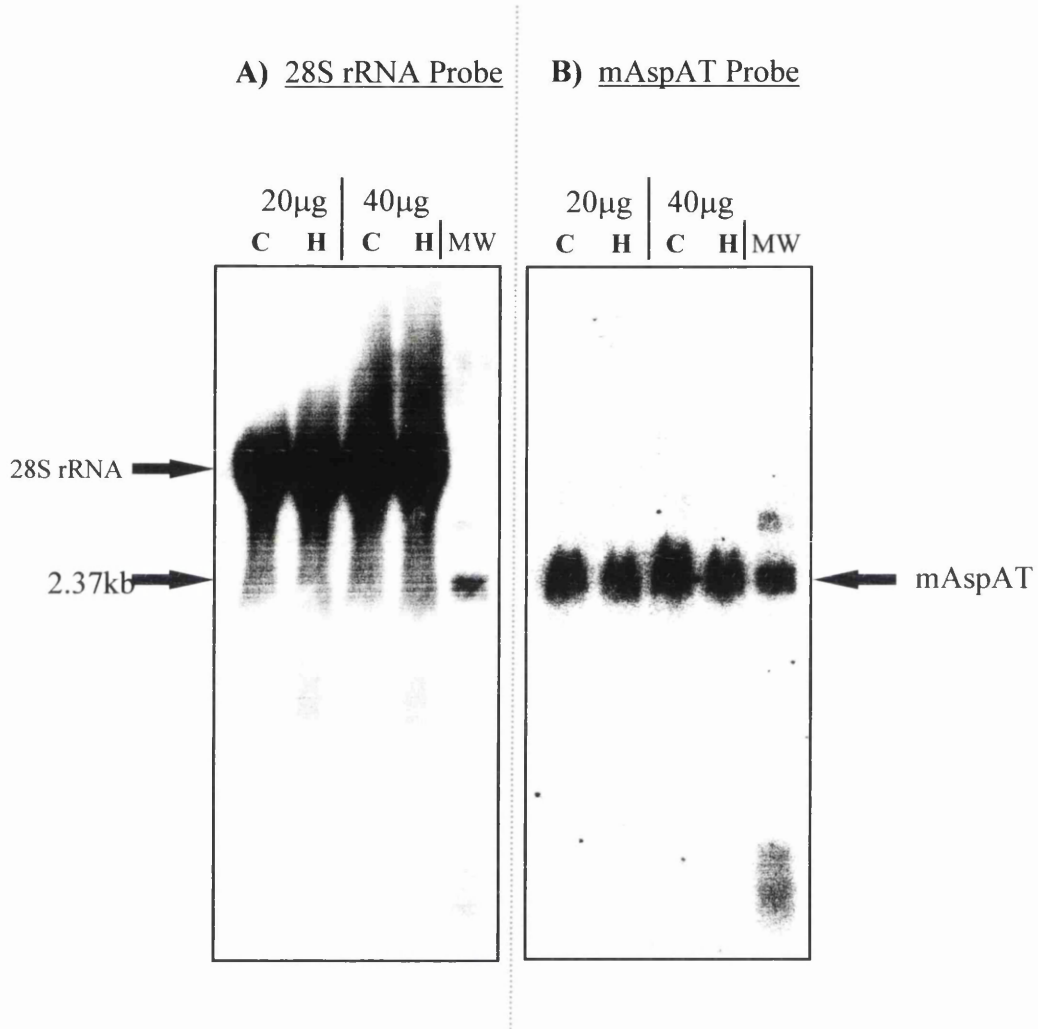

Legend. Total RNA was extracted from Bn5T cells which had been mock infected (**C**) or infected with 10 pfu/cell of HSV-2 HG52 (**H**) overnight. 20µg and 40µg were electrophoresed on a 1.5% formaldehyde-agarose gel and transferred to Hybond-N membrane. Panel B shows the phosphorimager image of the blot probed with the mAspAT probe. A single transcript of 2.3 kb is observed (co-migrating with the molecular weight marker marked to the left of panel A). Panel A shows this same blot reprobed with a 28S rRNA probe. Again a single band is detected, although the background is somewhat higher. The amount of radiolabel in both the 20µg and 40µg tracks was analysed with the phosphorimager software and showed a mean increase in the level of mAspAT mRNA in infected cells of 1.26 fold Experiment 7 in Table 4.1).

The presence of a single transcript in the mAspAT probed blot in this gel confirms the validity of the slot blot results illustrated in Figure 4.2 and Table 4.1.

The molecular weight markers were a synthetic RNA ladder (0.24-9.5kb, Gibco BRL) which fortuitously reacted with both of these probes, allowing direct visualisation of the size of the detected transcripts.

mAspAT mRNA present in samples of total RNA from HSV-2 infected and mock infected Bn5T cells.

Oligonucleotide primers were synthesised to the 5' and 3' ends of the mAspAT cDNA clone sequenced by Mattingley *et al.* (1987), and are illustrated in Figure 4.4. Primer 9301 (5' end) represents nucleotides 29-51 of the published sequence, upstream of the ATG initiation codon. Primer 9302 (3' end) represents nucleotides 1431-1450, downstream of the mAspAT stop codon within the long 3' untranslated region. The 9302 primer was used to prime cDNA synthesis in the RT reaction. To maintain the PCR reaction within the linear portion of the amplification curve (Kang *et al.*, 1995) a maximum of 20 cycles of PCR were performed following cDNA synthesis. The amount of total RNA added (3μg) to the reverse-transcriptase reaction was limited relative to the amount of primers, Taq DNA polymerase and deoxynucleotides included in the subsequent PCR reaction to ensure the linear phase of the amplification reaction was maintained (Kidd & Ruano, 1995).

The results presented in Table 4.2 were obtained from two separate RT-PCR experiments in which the primer 9302 was end-labelled with 5'[γ^{32}P]-dATP using T4 polynucleotide kinase as described in Materials and Methods. This facilitated the quantification of the PCR product by agarose gel electrophoresis of an equal volume of each sample.

In the top rows of Table 4.2, the results were obtained by phosphorimager analysis of the 1.4kbp product on a dried 1% agarose gel. The results show an approximate two-fold (1.967x) increase in the amount of radiolabel incorporated into the major PCR product in the HSV-2 infected Bn5T RNA track compared to the mock infected track.

The RT-PCR experiment was repeated, and equal volumes of the labelled PCR reaction mix from the HSV-2 infected and mock infected Bn5T RNA samples were electrophoresed on a 1% agarose gel. The major band (1.4kbp) was visualised by ethidium bromide staining and short wave UV illumination of the gel. The 1.4kbp product was excised from each track of the gel and added to a scintillation vial containing 5ml of Ecoscint™. The results from the scintillation counter are presented in the bottom rows of Table 4.2. These results again show a two-fold increase (2.01x) in the number of counts in the HSV-2 infected sample compared to

Figure 4.4. Oligonucleotide primers used in semi-quantitative RT-PCR experiments to determine the relative level of mAspAT mRNA in Bn5T cell samples.

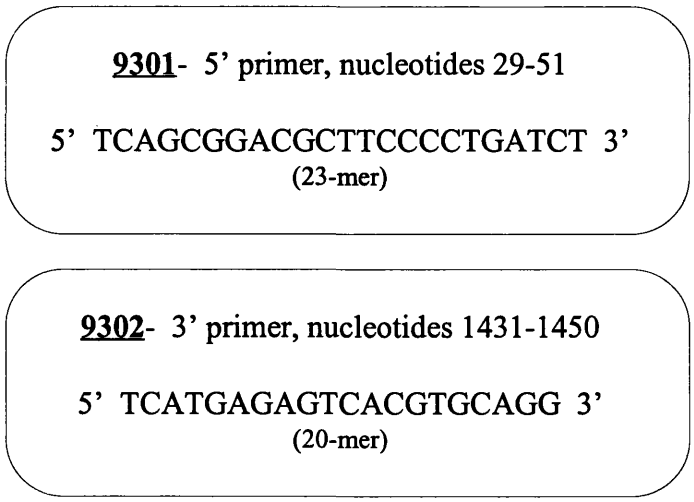

Legend. Sequence of the oligonucleotide primers used in the semi-quantitative RT-PCR experiments to determine the effect of HSV-2 infection on the level of mAspAT mRNA in the transformed Bn5T cell line. The primers were designed using the published sequence of rat mAspAT cDNA and the nucleotide positions within the sequence are shown (Mattingley *et al.*, 1987). Primer 9302 is complementary and reversed with respect to the published sequence, and was used to prime the reverse transcriptase reaction.

Table 4.2. RT-PCR analysis of mAspAT mRNA levels

SAMPLE	COUNTS INCORPORATED	RATIO HSV/CONTROL	DETECTION METHOD
Mock Infected Bn5T RNA Bn5T HSV-2 RNA	5935 11676	1.967	Phosphorimager
Mock Infected Bn5T RNA Bn5T HSV-2 RNA	29562 59452	2.011	Scintillation counter

Legend. The number of counts in equal volumes of RT-PCR reaction mixtures from HSV-2 and mock infected Bn5T cells allowed a calculation of the increase in mAspAT mRNA levels. The increases observed in these experiments are consistent with those presented in Table 4.1.

the mock infected sample. These results are combined with those from the Northern blotting experiments in Section 4.4 below.

4.4 COMBINED RESULTS OF NORTHERN BLOTTING AND RT-PCR EXPERIMENTS ON THE EFFECT OF HSV-2 ON mAspAT mRNA LEVELS.

The mean of the results from the Northern blotting and RT-PCR experiments (described in sections 4.2.7 and 4.3 respectively) is calculated as 1.865, with a standard error of 0.08. These results confirm that there is an approximate twofold increase in the level of mAspAT mRNA in Bn5T cells following infection with HSV-2. This increase is consistent with the increase in enzyme activity (two-fold) and absolute protein levels (~4 fold) observed following infection of Bn5T cells with HSV-2 (Lucasson *et al.*, 1994).

4.5 EXPERIMENTS TO CONFIRM THAT THE PHOSPHORIMAGER CAN RELIABLY DETECT A 2-FOLD INCREASE IN THE AMOUNT OF RADIOACTIVITY PRESENT IN DNA AND RNA SAMPLES.

To validate the results of the Northern and slot blot experiments which showed a two-fold increase in the level of mAspAT RNA following infection of Bn5T cells with HSV-2 (Section 4.2) it was necessary to confirm that the Phosphorimager could reliably detect a two fold increase in the amount of radiolabelled RNA or DNA loaded onto an agarose gel. An estimation of the error involved in the phosphorimager detection of a two or three-fold increase in the amount of labelled nucleic acid could also be made. Two different experiments were performed.

4.5.1 Agarose gel electrophoresis of 5'[γ-^{32}P] labelled DNA molecular weight markers.

1µl of λ DNA *HindIII* molecular weight markers (Sigma) were end labelled with 5'[γ-^{32}P] ATP using T4 polynucleotide kinase and ethanol precipitated with 5µg of salmon sperm DNA as carrier. The DNA pellet was resuspended in 50µl of ddH_2O. An equal volume of sucrose gel loading buffer was added. The sample was denaturated by boiling and rapid cooling on ice. A 1.5% agarose gel was loaded as described in Table 4.3 below and electrophoresed at 100 Volts until the dye front reached three-quarters of the way down the gel.

Table 4.3. Volume of 5'[γ-^{32}P] labelled DNA molecular weight markers loaded onto an agarose gel to test the sensitivity of Phosphorimager analysis.

DNA Loading	Volume of markers loaded (µl)
1x	10
2x	20
3x	30

The results from this experiment are presented in Table 4.4 and Figures 4.5 & 4.6.

The gel was rinsed in ddH_2O to remove free radioactivity, dried and exposed to the phosphorimager screen overnight. The results were analysed using ImageQuant software. Figure 4.5 shows the phosphorimager image of this gel, and includes the rectangles (labelled 001- 008 but excluding 002) which delineate the areas used for the analysis of the counts in each track of the molecular weight markers.

Table 4.4A presents the number of counts detected by the phosphorimager in each of the seven molecular weight marker bands for each loading level (1x, 2x, 3x referred to in Table 4.3). In Table 4.4B the results in the 2x and 3x tracks have been normalised with respect to the number of counts in the 1x track for each molecular weight marker analysed. The mean increase across all seven samples in the 2x track was 2.36 fold, and for the 3x track the increase was 3.5 fold (Table 4.4C). The standard error of the mean for each of the data series was 3.52% and 1.94% respectively. The individual results for each marker band are represented graphically in Figure 4.6, with trendlines and standard error bars marked on the chart. The error in these results is probably due to a systematic pipetting error, as the required volume of labelled markers was loaded by repeated loading of 10µl samples. This would cause a cumulative error in the 2x and 3x lanes of the gel. Other potential errors arise from the positioning of the rectangles during phosphorimager analysis. This introduces variation in the number of counts detected and therefore in the final ratios obtained. However, as the overall result is derived from the results of seven samples the effect of this positioning effect is reduced.

Figure 4.5. Phosphorimager image of a 1.5% agarose gel of 5'[γ-^{32}P] labelled λ *HindIII* molecular weight markers.

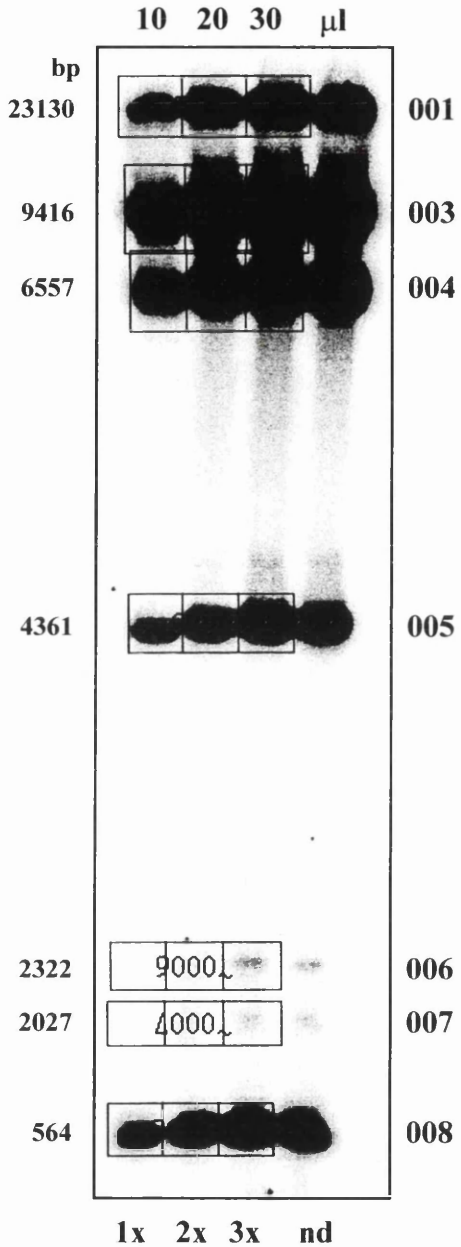

Legend. λ *HindIII* molecular weight markers were labelled with 5'[γ-^{32}P] using T4 polynucleotide kinase and 10, 20 and 30 µl of this was electrophoresed on a 1.5% agarose gel (1x, 2x, 3x) as described in the main text. The dried gel was analysed with the phosphorimager and the number of counts in each molecular weight band (labelled at left hand side) analysed in each of the tracks. The grids used to delineate the regions analysed by the phosphorimager are labelled to the right of the gel. The counts in each track were compared with each other as described in Table 4.4. The results confirmed that the phosphorimager can accurately determine a two or three fold increase in the amount of radiolabelled DNA on an agarose gel.
(nd). Band not analysed as this distorted the grid shape and would have invalidated the results for the other 3 lanes.

Table 4.4. Confirmation of linearity in Phosphorimager detection of 5'[γ-^{32}P] radiolabelled nucleic acid.

A) Total counts in selected bands of λ molecular weight markers

	Molecular weight marker band						
Loading	001	003	004	005	006	007	008
1x	184093	590486	323347	105010	6306	4395	162753
2x	433092	1406101	756892	258582	12433	11966	388347
3x	629787	2189675	1120164	387645	21075	14278	597199

B) Ratio of counts in tracks relative to 1x loading counts

	Molecular weight marker band						
Loading	001	003	004	005	006	700	008
1x	1.00	1.00	1.00	1.00	1.00	1.00	1.00
2x	2.35	2.38	2.34	2.46	1.97	2.72	2.38
3x	3.42	3.70	3.46	3.69	3.34	3.24	3.66

C) Mean and standard error of the mean of data from Table 3.2 B.

DNA loading	Mean of increase for all bands	Standard error of the mean[a]	% error (SEM/mean x 100)
1x	1.00	n/a	n/a
2x	2.36	0.083	3.52%
3x	3.50	0.068	1.94%

[a] Standard error of the mean calculated as shown in the equation below:-

$$SEM = \frac{\sqrt{\frac{\sum_{i=1}^{N}(x_i - \bar{x})^2}{N-1}}}{\sqrt{N}}$$

Legend. Analysis of data obtained from an experiment to determine the validity of Phosphorimager detection of changes in the level of RNA by Northern blotting. 5'[γ^{32}P] labelled λ DNA molecular weight markers were loaded onto a 1% agarose gel in multiples of 10μl. The total counts obtained from the phosphorimager (Section A) were used to calculate a value for each loading level relative to the counts in the standard 1x loading for each marker (Section B). The mean increase across all seven molecular weight markers for each loading level is highlighted in Section C. A systematic error has occurred in this experiment- see main text for further discussion.
n/a- not applicable.

Figure 4.6. Linearity of phosphorimager detection of radiolabelled nucleic acid

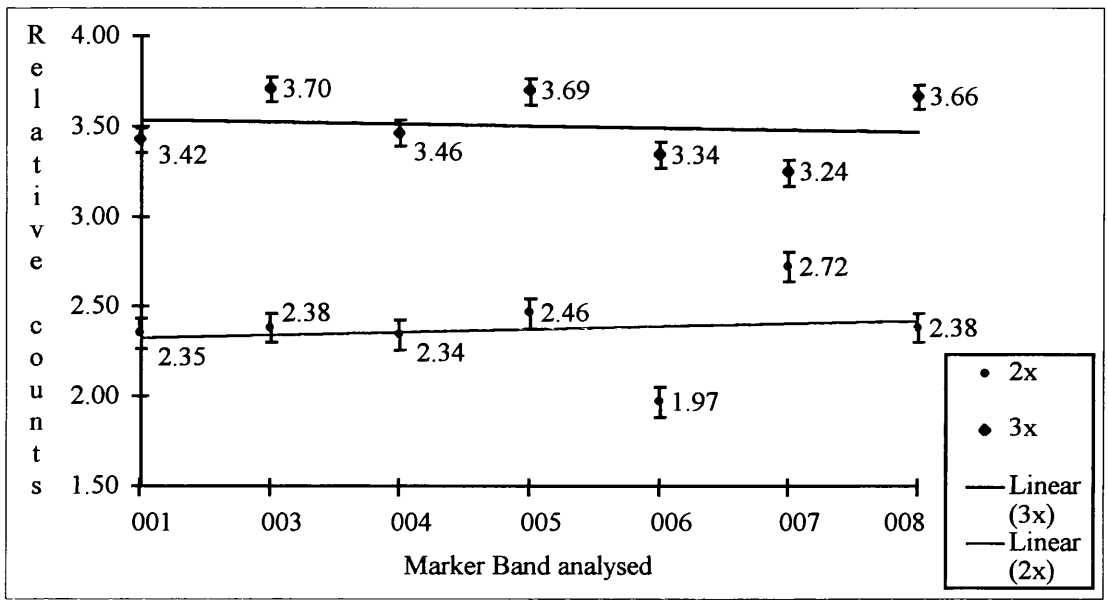

Legend. Graph of data illustrated in table 4.4. The ratio of counts in each marker band (y-axis) relative to those in the 1x loading track are plotted for each marker band (x-axis). This experiment confirms that a linear increase in the amount of a radiolabelled nucleic acid can be detected by phosphorimager analysis. The y-axis represents the relative loading of marker DNA as determned by the number of counts detected in each marker band (001-008 excluding 002), labelled 1 to 7 on the x-axis. Although the response is relatively linear, a systematic error in the loading of the samples is responsible for the result not being exactly 2.00 and 3.00x respectively. See main text for discussion of this point.

The errors determined in this experiment are sufficiently small (+/- 4%) to allow the detection of a 2-fold change in the level of RNA present in Northern and slot blot experiments with confidence.

4.5.2 *In vitro* transcription analysis.

To independently confirm that the experimental system could detect two-fold increases in the radiolabel content of RNA samples, and that increases in radiolabel in RNA were detected as effectively as increases in the amount of label in a DNA sample, *in vitro* transcription experiments were performed by Dr. Joan Macnab, (Institute of Virology, Glasgow.) The plasmid pBS-KS containing the mAspAT cDNA (Mattingley *et al.*, 1993) under the control of the T3 promotor was *in vitro* transcribed in the presence of [α-^{32}P]-ATP and the product electrophoresed on an agarose gel. The number of counts in a track loaded with one volume of sample was compared by phosphorimager analysis with those in a track loaded with two volumes of the same sample. The results were 6438 and 13002 counts respectively (Lucasson *et al.*, 1994) an approximate two-fold increase (2.02x). This experiment confirmed that the phosphorimager was capable of detecting a twofold increase in radiolabelled RNA as well as DNA.

4.6 DISCUSSION.

A series of eight Northern blotting experiments *(Section 4.2.7)* showed that the level of mAspAT mRNA was increased by a factor of 1.748 +/- 0.26 in HSV-2 infected Bn5T cells compared to mock infected cells. These results were standardised by comparison with the level of the γ-Actin transcript or 28S rRNA present in the samples.

Offord *et al.* (1989) determined that the level of γ-actin mRNA was unaffected by infection of MCF-7 cells (an estrogen responsive breast cell line) with either HSV tsK or HG52. The level of the γ-actin transcript in the Bn5T cells which were used in the experiments described in this chapter has also been shown to be unaffected by HSV-2 infection (J.C.M. Macnab, pers. comm). However, Latchman (1988) reported that the level of actin mRNA was decreased both at the transcriptional and post-transcriptional levels following HSV-2 strain 333 infection of BHK C13 cells. The probe he used hybridised to both β and γ-actin mRNAs, and as dot blot rather than Northern blot experiments were performed, it would not be possible to determine

whether this decrease was due to a decline in the transcription of just one class of actin gene. As previously noted, the HG52 strain of HSV-2 used in my experiments has a defective host shutoff function (Everett and Fenwick, 1990) and one might not therefore expect to detect a decrease in the level of γ-Actin in cells infected with this virus. In my experiments a similar increase in mAspAT mRNA was also observed relative to 28S rRNA, and therefore I have confidence in the use of the γ-actin probe as an internal control in these experiments.

There is a relatively large range and standard error observed in this data series. This could be due to variation in the efficiency of infection of Bn5T cells with HSV-2. Different vials of HSV-2 HG52 stocks were used during these experiments, although the infection was always performed at 10pfu/cell. A more likely reason is the varying passage number of the Bn5T cells used. It was previously noted that Bn5T cells become refractory to infection with HSV-2 after extended passage. After extended passage (around passage number 50), infection with HSV-2 HG52 resulted in a less effective infection, as determined by examination of the cytopathic effect on cell morphology. When the typical rounding of the cells was not exhibited in infected cells examined microscopically, it was noted that the level of increase in mAspAT mRNA was much reduced, for example down to a 1.07 fold increase (Table 4.1, experiment 4). A similar effect has been reported on examination of the effect of HSV-2 infection of Bn5T cells on the enzymatic activity of mAspAT (Lucasson *et al.*, 1994). Only when the cytopathic effect was visible and infection with HSV-2 was confirmed by the immunological detection of HSV-2 coded polypeptides (generally the large subunit of ribonucleotide reductase, (RR1)) was an increase in the enzyme activity observed. Productive infection therefore appears to be necessary for the alterations in the levels of mAspAT mRNA, protein and enzyme activity observed following HSV-2 infection. (*See also Section 5.9.1*)

Estridge *et al.* (1989), have previously noted that HSV-2 gene expression is required for the increase in the level of a cellular protein they term p40, a DNA binding protein purified from transformed cells and from dyskaryotic cells from cervical smears. The increase they observed following HSV-2 infection was dependent upon HSV-2 immediate early gene expression.

The HSV gene products required for the increase in mAspAT mRNA were not studied in detail in this work. Attempts were made to assess the requirement for specific temporal classes of HSV genes using inhibitors of viral protein and DNA synthesis (ara-C, PAA, ActinomycinD and cycloheximide), and by infection of cells with UV-inactivated HSV-2. However the RNA purified from these cells was of poor quality, and the Northern blots were difficult to interpret. No conclusions could be drawn from these experiments. Grassie (1993) has shown that functionally active Vmw 175 is not necessary for the induction of the U90 member of this group of polypeptides that are specifically induced in transformed cells (Macnab *et al.*, 1985). Furthermore, U90 was not induced by virus attachment to the cell surface (UV inactivated HSV-2) but was increased in the presence of cellular and viral DNA synthesis. It is possible that these results may hold true for the 40kDa polypeptide from this group, now known to be a form of mitochondrial aspartate aminotransferase (Lucasson *et al.*, 1994).

Reverse transcriptase PCR experiments confirmed the two-fold increase in the level of mAspAT mRNA present in Bn5T cells after HSV-2 infection. The experimental conditions were such that the reaction was maintained in the linear phase, and the result was for the same initial amount of total cellular RNA (3μg) in the RT reaction mix. No internal controls were included in this experiment. Ideally, primers which would amplify an mRNA known not to be altered by HSV infection should be included at the reverse transcriptase stage of these experiments. Two sets of primers to the γ-actin sequence were synthesised, but did not amplify a product in these experiments. As a control to ensure the amplification was linear in each reaction tube performed at the same time, a fixed amount of a synthetic template derived from the mAspAT cDNA sequence containing an internal deletion should be added to each PCR reaction. This template would contain the same 9301 and 9302 primer sequences, and amplification should result in the production of an equal amount of a smaller distinguishable PCR product in each reaction. This would control for effects such as thermocycler block temperature variations.

The results from the northern blotting and RT-PCR experiments were consistent with each other, and the cumulative result of a 1.865 fold increase on HSV-2 infection is

consistent with the enzyme activity (two-fold) and protein (approximately four-fold) increases reported previously by Lucasson *et al.* (1994).

Offord *et al.,* (1989) have reported a similar degree of increase (between 1.5 and 2 fold (+/- 0.5)) in the level of estrogen receptor mRNA in HSV-2 infected MCF-7 cells relative to mock infected cells. These cells are an estrogen responsive transformed cell line, and increased expression of the estrogen receptor at the cell surface may have implications for the growth regulation of these cells. mAspAT is known to be identical to the fatty acid binding protein (mFABP) which has a role in the uptake of long chain fatty acids at the cell surface (Stump *et al.*, 1993). Increased expression of mAspAT at the cell surface could therefore affect cellular metabolism by introducing an imbalance in the metabolic pools within the cell. Alterations in cellular metabolism could also occur by aberrant expression of mAspAT within the mitochondria, affecting the malate-aspartate shuttle. These possibilities are discussed further in the general discussion (Chapter 8) at the end of this thesis.

4.7 CONCLUSIONS.

The level of mitochondrial aspartate aminotransferase mRNA is increased in the transformed rat fibroblast cell line Bn5T following infection with HSV-2.

Northern blotting experiments quantify the level of this induction as 1.748 fold, and RT-PCR experiments as 1.98 fold.

The overall mean increase was observed as 1.865 fold, consistent with results previously reported from our laboratory on the induction of mAspAT protein and enzyme activity following HSV-2 infection (Lucasson *et al.*, 1994).

5. IDENTIFICATION OF A POLYPEPTIDE IN HSV INFECTED CELLS WHICH CROSS-REACTS WITH AN ANTISERUM RAISED AGAINST mAspAT.

5.1 INTRODUCTION

Whilst working on the upregulation of mAspAT as a result of HSV-2 infection, a colleague in the Institute of Virology, Dr. Jean-Francois Lucasson reported a fourfold increase in the mAspAT protein level detected by slot-blot immunoblotting. The enzyme activity of mAspAT in Bn5T cells was also elevated approximately two-fold (Lucasson, 1992; Lucasson *et al.*, 1994). The experiments described below were performed to further investigate this increase in the level of mAspAT protein observed following infection with HSV-2.

5.2 INITIAL INVESTIGATION

In an initial Western blotting experiment, a 9% polyacrylamide gel was run with samples of Bn5T cell polypeptides following an 18 hour infection with HSV-1 or HSV-2 at 10 pfu/cell, or a mock infection. Samples were produced by lysis of the cells in hypotonic WF buffer (Welch & Feramisco, 1985), sonication and pelleting of the cellular debris by centrifugation, essentially as described in Materials and Methods and Section 3.2. Following electrophoretic transfer to Hybond-N™, the polypeptides were probed with a 1/50 dilution of a rabbit antiserum raised against the pre-mAspAT polypeptide expressed in *E. coli* (kindly provided by J. R. Mattingley (Mattingley *et al.*, 1987)), and detected using anti-rabbit Ig-HRP conjugate. The blot was developed using colour reagent as described in Materials and Methods.

Although the staining of this blot was faint, it appeared that an additional lower molecular weight band might be present in the infected cell tracks that was absent from the mock infected track (data not shown). This additional lower molecular weight band appeared to vary in size; the additional polypeptide in the HSV-1 infected sample appeared to have a larger molecular weight than the additional polypeptide in the HSV-2 infected sample.

There were several possible explanations for the results described above. HSV-1 and HSV-2 may be inducing different forms of mAspAT, or the lower molecular weight polypeptides might be HSV induced degradation products of mAspAT. Another possibility was that the antiserum might be detecting a cross-reacting HSV coded polypeptide with a slightly different molecular weight depending on the HSV type

used to infect the cells. These possibilities are investigated in the following experiments.

5.3 OPTIMISATION OF EXPERIMENTAL CONDITIONS

5.3.1 Gel electrophoresis conditions

The presence of the induced lower molecular weight polypeptides and the size difference between the two virus types were not clearly resolved on a 9% SDS-PAGE gel. 15% SDS-PAGE gels were therefore used in all subsequent experiments to increase the separation of polypeptides in the 35-50kDa range. Rainbow molecular weight markers (Amersham Life Sciences) were used to follow the migration of the polypeptides during electrophoresis. This allowed the gels to be electrophoresed further after the bromophenol blue marker dye had run off the gel, without losing the polypeptides of interest. Increased resolution was obtained in the 35-50kDa molecular weight region of the gel. Figure 5.1 shows an example of a Western blot obtained using the optimised conditions described in this section, with HSV-2 and mock infected samples of rat embryo and Bn5T cells.

5.3.2 Cell lysis conditions

Degradation during cell lysis was unlikely to be the cause of the presence of the lower molecular weight polypeptides as no lower molecular weight polypeptide was detected in the mock infected samples (Figure 5.1, lanes 1 & 3). However, to reduce protein degradation during lysis to a minimum, cells were lysed by the addition of 500µl of SDS-PAGE sample loading buffer (3xBM) directly to the cell monolayer on the tissue culture plate. This lysis method produced a higher protein concentration in the lysate than lysis in hypotonic WF buffer (data not shown). However, the lipid content of these samples was also elevated, and to avoid smearing of the gel care had to be taken not to overload the samples.

5.3.3 Western blotting

A final optimisation step was the use of enhanced chemiluminescence (ECL, Amersham Life Science) reagents to develop Western blots. These reagents are at least 10x more sensitive than the colour reagent and produce high contrast results, allowing detection of minor bands using lower amounts of primary antibody. A 1/200 dilution of the anti-mAspAT antibody was used in subsequent experiments to reduce the background on the blots. ECL reagents have the added advantage that blots can be stripped of all bound antibody and re-probed several times with different

Figure 5.1. Optimised Western blot to show detection of an additional polypeptide in Bn5T and RE cells after infection with HSV-2.

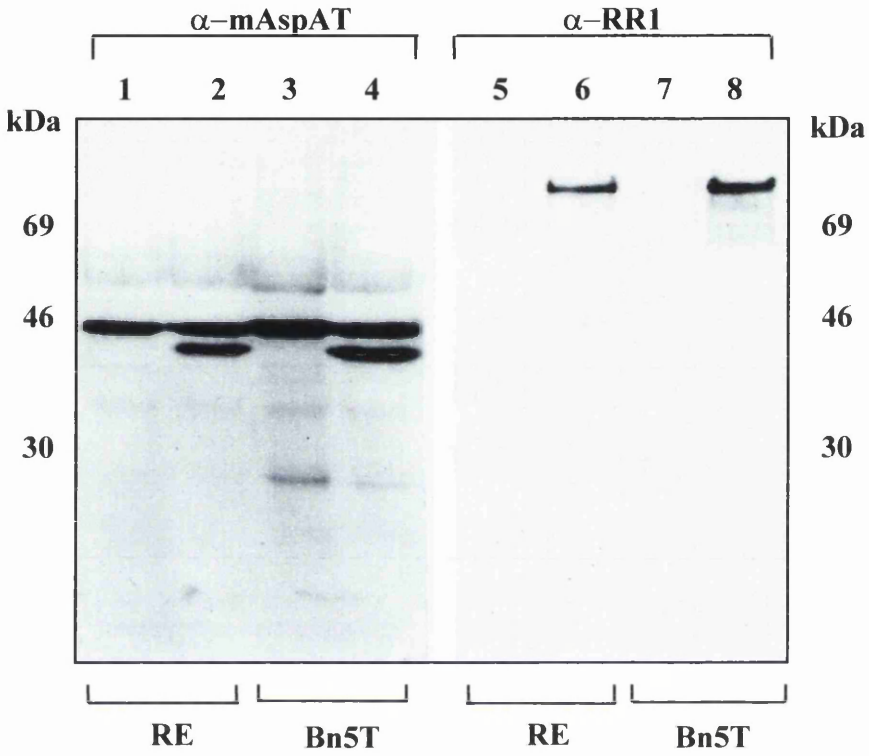

Legend. Bn5T and RE cells were infected at 10pfu/cell with HSV-2 HG52 or mock infected overnight, and lysed directly into SDS-PAGE sample loading buffer (3xBM). Samples were electrophoresed on a 15% SDS-PAGE minigel, transferred to Hybond-N membrane and Western blotted with 1/200 dilution of an antiserum raised against rat mitochondrial aspartate aminotransferase (α–mAspAT, lanes 1-4) or an antiserum against the large subunit of HSV-1 ribonucleotide reductase (α–RR1, lanes 5-8). Enhanced chemiluminescence reagents were used to detect bound antibody. The position of the molecular weight markers is indicated at the sides of the gel.

An additional polypeptide is detected by the α-mAspAT antiserum in the HSV-2 infected samples (lanes 2 & 4) compared to the mock infected samples (lanes 1 & 3). Infection of the samples with HSV-2 is confirmed by the presence of ribonucleotide reductase (lanes 6 & 8). There is no reaction with the anti-RR1 antiserum in the mock infected tracks.

This gel shows that the additional polypeptide detected by α-mAspAT antiserum is specific to HSV infection, and that in addition to Bn5T cells the polypeptide is also induced in primary rat embryo (RE).

primary antibodies without significant loss of sensitivity. This allows polypeptides of similar molecular weight to be detected sequentially in the same sample. ECL molecular weight markers were added to allow direct visualisation of markers on the Western blot.

In all the following experiments, the blots were stripped and reprobed with a polyclonal antiserum raised against the large subunit of HSV-1 ribonucleotide reductase (RR1, 124kDa) to confirm that productive infection had occurred (Figure 5.1, lanes 6 & 8). The mock infected samples did not display any reactivity with the anti-RR1 antiserum (Figure 1, lanes 5 & 7).

The following experiments were performed using the optimised procedures described above.

5.4 THE EFFECT OF HSV INFECTION ON MASPAT LEVELS IN BHK C13 CELLS

This experiment was performed using BHK C13 cells to determine whether the lower molecular weight polypeptides detected in RE and Bn5T cells following HSV infection were also present in HSV infected BHK C13 extracts. BHK C13 cells, which are used to propagate HSV are permissive for productive virus infection, whilst Bn5T cells are sometimes refractory to infection. If the lower molecular weight polypeptides are induced by HSV infection and were present in infected BHK C13 cells these cells could be used in future experiments to provide more reproducible results.

BHK C13 cells were infected at 10 pfu/cell with HSV-1 or HSV-2 overnight and lysed directly in 500µl 3xBM. This lysate was diluted 3:2 with 1xBM but remained too concentrated and resulted in an overloaded gel with poor resolution of the polypeptides (data not shown). The lysate was further diluted 1:2 with 1xBM to prevent overloading of the gels. 50µl and 100µl of each sample were loaded onto a full size 15% SDS-PAGE gel, and electrophoresed until the 21kDa molecular weight marker only just remained on the bottom of the gel. Following electrophoretic transfer to Hybond-N™, the blot was probed with a 1/200 dilution of anti-mAspAT antiserum and detected using ECL reagents.

Figure 5.2 shows the presence of an additional polypeptide band following infection with either HSV -1 (lanes 2 & 5), or HSV-2 (lanes 3 & 6), which is not present in the mock infected track (tracks 1 & 4). The additional band clearly has a different

Figure 5.2. Induction of HSV type specific additional polypeptides following infection of BHK C13 cells with HSV-1 and HSV-2.

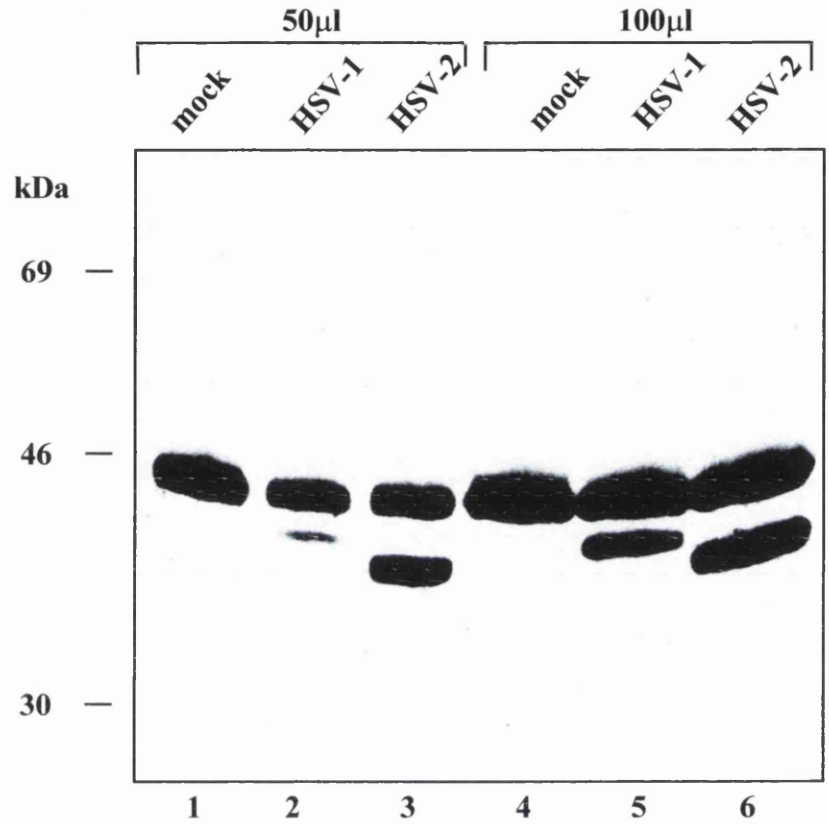

Legend. BHK C13 cells were infected at 10 pfu/cell HSV-1 strain 17 or HSV-2 strain HG52 overnight and lysed directly into 3xBM. 50µl and 100µl samples were electrophoresed on a large 15% SDS-PAGE gel and blotted as described in Materials and Methods. The Western blot was probed with an antiserum to mAspAT.
In the mock infected cell samples (lanes 1 & 4), a single polypeptide is detected, representing the constitutively expressed cellular mitochondrial aspartate aminotransferase. There is a single additional polypeptide detected in the samples infected with HSV-1 (lanes 2 & 5), and a different additional polypeptide detected in the samples infected with HSV-2 (lanes 3 & 6). The bands detected in HSV infected cells are clearly of differing molecular weights dependent upon the HSV type .

molecular weight in HSV-1 and HSV-2 infected BHK C13 cell samples, with the HSV-1 band having a slightly greater molecular weight. The apparent molecular weights of the HSV-1 and HSV-2 induced lower molecular weight polypeptides on this gel were 37.7 kDa and 35.5kDa respectively.

In this experiment the apparent molecular weight of the cellular mAspAT on a 15% SDS-PAGE gel is 41.1kDa, compared to the predicted molecular weight of 44.358kDa for rat mAspAT (Huynh *et al.*, 1981) which corresponds to the observed molecular weight on SDS-PAGE gels (Huynh *et al.*, 1980; Mattingley *et al.*, 1987). This molecular weight difference may be due to different gel electrophoresis conditions or to altered post-transcriptional processing of the mAspAT transcript (or post-translational alterations to the polypeptide) in the BHK C13, Bn5T and RE cells used in these experiments. The constitutive cellular mAspAT was of similar molecular weight in all three cell types used in these experiments. Mattingley *et al.*, (1987) do not report their experimental conditions or the derivation of the processed 44kDa mAspAT polypeptide used as a control in his experiments. No conclusions can be drawn without further information. mAspAT is highly conserved in eukaryotes with high sequence homology at both the DNA and amino acid level (*see Appendix 1*). The variation between prokaryotic and eukaryotic proteins is greater, although the homology is still extensive. If the variation is biological rather than due to different experimental conditions, some form of cell type dependent processing is the most likely cause of the variation, for example altered glycosylation.

5.5 ARE THE LOWER MOLECULAR WEIGHT POLYPEPTIDES CELL ASSOCIATED?

An experiment was performed to determine whether the lower molecular weight polypeptides detected by the antiserum to mAspAT were cell associated (either intracellular or membrane associated), and not serum contaminants from the tissue culture medium or secreted cell coded polypeptides. BHK C13 and RE cells were infected with 10pfu/cell HSV-1 or HSV-2 or were mock infected as previously described. An additional plate of each cell type was infected with HSV-1, and the cells on this plate were washed three times with 10ml ice-cold PBS-A to remove secreted polypeptides or serum contaminants prior to lysis in 3xBM. The other plates were lysed directly into 3xBM. The polypeptides extracted from the cells on

the washed plate were compared on a Western blot with those from the plates lysed directly in 3xBM.

The samples from the RE cells were included to compare the induction of the lower molecular weight polypeptides induced following HSV infection in a primary cell with that observed in immortalised cell lines.

Figure 5.3 confirms the appearance of the lower molecular weight polypeptides specific to each HSV type following infection of BHK C13 cells (lanes 1-4). A similar result is observed in RE cells (lanes 5-8). The lower molecular weight polypeptides are probably cell associated, as washing the plate with PBS-A did not visibly reduce the level of polypeptide detected (compare track 2 with 3, and 6 with 7).

The amount of the lower molecular weight polypeptides induced in RE cells is reduced in comparison to the level of those induced by infection of BHK C13 with HSV. The level of the cellular mAspAT is comparable in both cell lines. The reduced level of induced polypeptides may be because RE cells are less permissive for HSV infection than BHK C13 cells, and therefore lower amounts of viral polypeptides are produced. This would have an effect whether the detected polypeptides were virally coded or required a viral polypeptide for their induction. The result could also be due to the different nature of the cells types. BHK C13 cells are a continuous cell line whilst RE cells are primary cells. The induction of the additional polypeptides is greater in the immortalised cells (Figure 5.3, lanes 1-4). This is in agreement with the levels of the TBS-40kDa polypeptide immunoprecipitated from transformed Bn5T and primary RE cells (Figure 3.1) where the observed increase following HSV infection is greater in the Bn5T cells.

5.6 THE LOWER MOLECULAR WEIGHT POLYPEPTIDES ARE NOT DEGRADATION PRODUCTS

An experiment was performed to confirm that the lower molecular weight polypeptides were not degradation products caused directly by the lysis procedure, or by cellular proteases released during lysis, and were induced specifically following HSV infection.

60mm plates of RE and BHK C13 cells were mock infected (as described in Materials and Methods) and incubated at 37 ° C overnight. The cell monolayers were washed, harvested by scraping into PBS-A and pelleted before lysis by sonication in

Figure 5.3. Experiment to determine whether the HSV induced polypeptides are cell associated, secreted or serum contaminants.

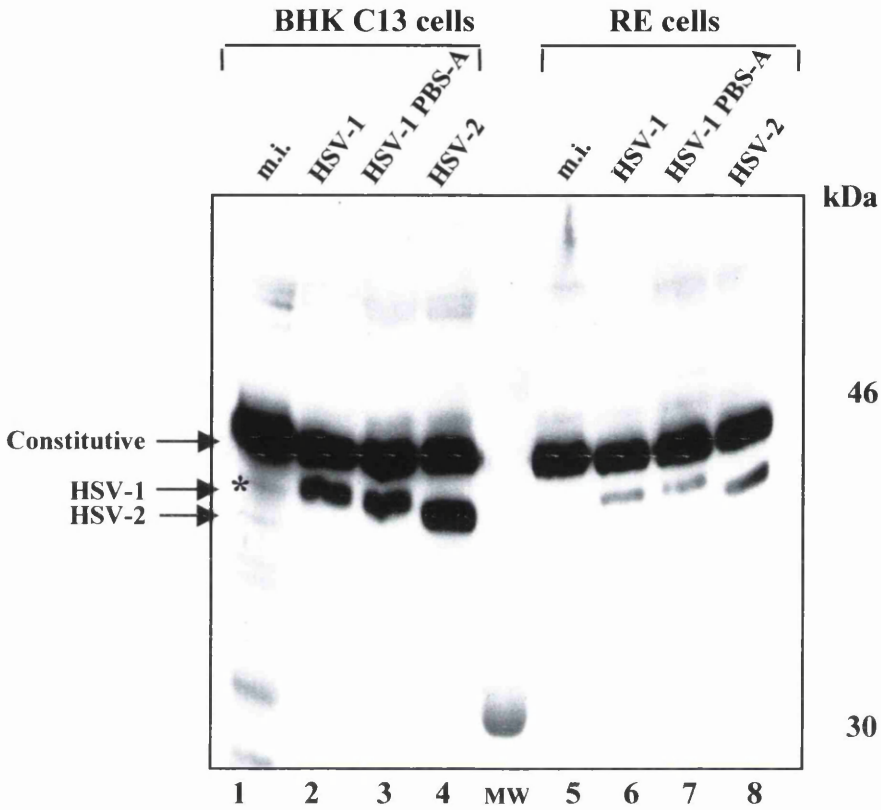

Legend. BHK C13 and RE cells were infected for 17 hours with 10pfu/cell HSV-1 strain 17 or HSV-2 strain HG52. 50 µl samples were electrophoresed on a large 15% SDS-PAGE gel prior to blotting. The blot was probed with an antiserum to mAspAT, and visualised using ECL reagents. The position of the molecular weight markers is indicated to the right of the gel.

Lanes 1-4 contain BHK C13 samples and lanes 5-8 the corresponding samples from RE cells. Lanes 1 & 5 contain samples from mock infected cells; lanes 2 & 6 contain HSV-1 infected cell samples lysed directly into 3xBM; lanes 3 & 7 contain HSV-1 infected samples washed with PBS-A to remove contaminating polypeptides prior to lysis in 3xBM; lanes 4 & 8 contain HSV-2 infected samples lysed directly into 3xBM.

There is an additional polypeptide detected in HSV-1 and HSV-2 infected C13 and RE cells (lanes 2-4 and 5-8), which is absent from the mock infected cells (lanes 1 & 5). The faint band in lane 1 (marked with an asterisk) is due to the high background in this track. Washing of the infected plates with PBS-A prior to lysis has no effect on the level of lower molecular weight polypeptide present (lanes 3 & 7) compared to the directly lysed cells (lanes 2 & 6). This suggests that the additional polypeptide is cell associated, and is not secreted into the medium. Neither is it a serum contaminant. The level of the induced bands is somewhat reduced in the primary rat embryo cell samples (RE, lanes 6-8) compared to the levels in the C13 samples. See main text for further discussion.

1ml hypotonic WF buffer. 100µl samples of the lysate were incubated at room temperature for periods of time ranging from 0 to 48 hours from the time of lysis. At the relevant time point, 50µl of 3xBM was added to each sample, which was then stored at -20 ° C until all the samples had been collected for analysis.

Figure 5.4 shows an ECL western blot of a full size 15% SDS-PAGE gel run with these samples. The normal cellular mAspAT band is present at approximately 42kDa in all the samples (BHK C13 samples in lanes 1-7; RE samples in lanes 8-14). No lower molecular weight polypeptide bands were visible in the region where the additional bands normally run on this type of gel following HSV infection. There were some much smaller molecular weight polypeptides present at the foot of the gel, which increased in abundance with incubation time (not visible in this figure). These bands may be caused by the degradation of a small proportion of the mAspAT by cellular proteases during the incubation period. There are no intermediate molecular weight bands present at earlier time-points in this experiment, suggesting that this degradation occurs at specific proteolytic sites within the polypeptide molecule. However, this degradation is not responsible for the presence of the lower molecular weight polypeptides which appear following HSV infection.

This experiment confirms that the lower molecular weight polypeptide bands described in this chapter are specifically induced by HSV infection, and are not degradation products caused during the lysis procedure or subsequent manipulations.

5.7 TIMECOURSE OF INDUCTION OF THE LOWER MOLECULAR WEIGHT POLYPEPTIDES

A timecourse experiment was carried out to examine the induction of the lower molecular weight polypeptides following infection with HSV.

60mm plates of BHK C13 cells were infected at 10pfu/cell of HSV-1 for 4, 8, 12 and 24 hours. A plate of mock infected cells was harvested at 24 hours. Cells were harvested directly by addition of 500µl of 3xBM to the plates and 10µl samples were loaded onto a 15% SDS-PAGE mini-gel for Western blotting with the α-mAspAT antiserum.

Figure 5.5A shows that the HSV-1 induced lower molecular weight polypeptide is just detectable using ECL reagents at 12 hours post-infection (marked with an arrow in lane 3), and accumulates during infection (lane 4). The normal cellular mAspAT level remains relatively constant. Neither of the mock infected samples (lanes 5 & 6)

Figure 5.4. Western blot to demonstrate that the additional polypeptide detected by anti-mAspAT antiserum is not due to non-specific proteolytic degradation.

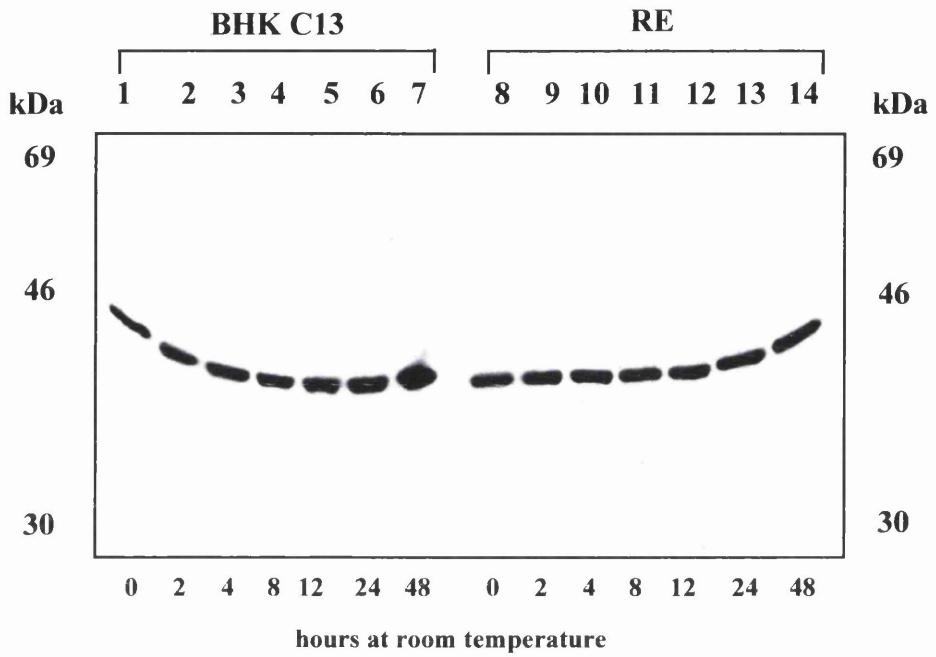

Legend. 60mm plates of BHK C13 and primary rat embryo (RE) cells were mock infected and incubated overnight. The plates were washed with PBS-A, and a lysate prepared by scraping into WF buffer and sonication (as described for large scale protein purification in Materials and Methods). 100µl samples of the lysate were incubated at room temperature for 0, 2, 4, 8, 12, 24 and 48 hours (lanes 1-7 and 8-14), before addition of 50µl of 3xBM. Samples were then analysed by Western blotting as described in the main text.

The constitutive mAspAT band is present at approximately 41kDa in all of the samples from both BHK C13 (lanes 1-7) and RE cells (lanes 8-14), but the additional polypeptide bands previously detected following HSV infection are absent from all samples.

This experiment therefore confirms that the additional polypeptides are specific to HSV infected cells, and are not breakdown products caused by cellular proteases released during the lysis procedure.

Figure 5.5A. Timecourse of induction of HSV-1 specific band detected by an antiserum to mAspAT.

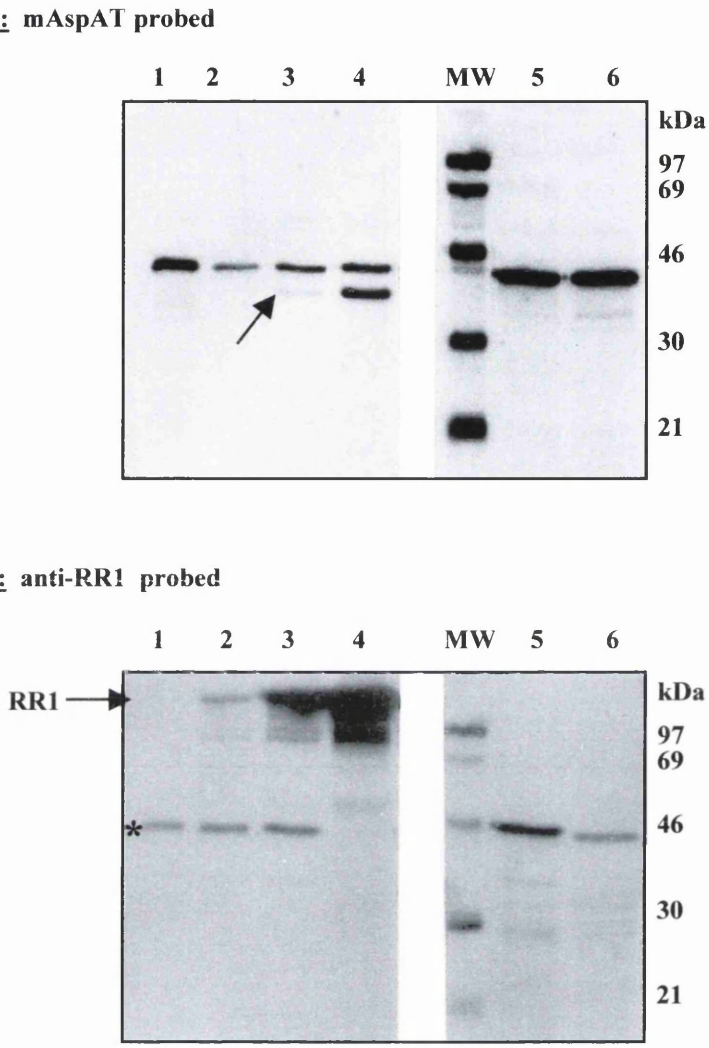

Legend. BHK C13 cells were infected with 10pfu/cell of HSV-1 strain 17, and samples were taken at 4, 8, 12 and 24 hours post-infection (lanes 1-4). A mock infected C13 cell sample (lane 5) and mock infected RE cell sample (lane 6) were included. Cells were lysed in 3xBM, and Western blotted as described in Materials and Methods. ECL molecular weight markers (MW) are labelled at the side of the gels.

Panel A shows a blot probed with a rabbit antiserum raised against bacterially expressed rat mitochondrial aspartate aminotransferase. The lower molecular weight band is just visible at 12 hours post-infection (marked with an arrow in lane 3), and increases during the course of infection. The additional polypeptide is not present in either C13 or RE mock infected samples (lanes 5 & 6).

Panel B shows the same blot stripped and re-probed with an antiserum against the large subunit of HSV-1 ribonucleotide reductase (RR1). RR1, an early (β) HSV-1 gene, is detectable in the 8 hour post-infection sample (lane 2), and increases as the infection proceeds (lanes 3 & 4). No RR1 is detectable in the mock infected samples (lanes 5 & 6). The appearance of the additional polypeptide in the mAspAT probed blot parallels the expression of RR1.

The extra band in Panel B (marked with an asterisk) represents the constitutive mAspAT and is due to incomplete stripping of the blot prior to re-probing with the anti RR1 antiserum.

contained detectable amounts of the lower molecular weight polypeptide at 24 hours post-infection.

Figure 5.5B shows a Western blot of a full size 15% SDS-PAGE gel, loaded with 100µl samples from a 24 hour timecourse of infection of BHK C13 cells with HSV-1, to further investigate the result shown in figure 5.5A. A mock infected sample was taken at each time-point. In this blot, due to the greater amount of sample loaded, the lower molecular weight polypeptide is more readily detectable. A faint band is detectable at 6 hours post-infection, and is clearly present by 8 hours post-infection. This polypeptide accumulates during infection, whilst only the constitutively expressed cellular mAspAT band is present in the corresponding mock infected samples.

These results suggest that the lower molecular weight polypeptide is induced early during HSV infection, in the early (β) stage of the viral replicative cycle.

5.8 EXPERIMENTS TO IDENTIFY THE HSV INDUCED POLYPEPTIDES.

5.8.1 Infection of cells with HSV-1/HSV-2 intertypic recombinant viruses.

As previously shown (in Figures 5.2 and 5.3), HSV-1 and HSV-2 induce slightly differently sized lower molecular weight polypeptides in infected BHK C13, Bn5T and RE cells. If the lower molecular weight polypeptides are viral polypeptides rather than HSV induced cellular polypeptides, this difference in the molecular weights of the induced polypeptides could provide a method of identifying the lower molecular weight polypeptides. The following experiments are similar to those of Wohlrab *et al.*,(1982) and Williams and Parris (1987), who used HSV intertypic recombinants to map the region of the HSV-1 genome encoding the dUTPase (see *Section 5.9.2* of Discussion for more details).

Three HSV-1/HSV-2 intertypic recombinants (obtained as detailed in Materials and Methods) were used to map the region of the HSV genome encoding these lower molecular weight polypeptides. Comparison of the size of the particular lower molecular weight polypeptide produced in cells following infection with each intertypic recombinant (i.e. HSV-1 or HSV-2 like), and reference to the genome maps of these intertypic viruses would enable the region of the HSV genome encoding these polypeptides to be identified.

The recombinant viruses used in this experiment were Bx1, Fx9 and R12-5. Approximate genome maps of these viruses are shown in Figure 5.6. HSV-1 strain F

Figure 5.5B. Timecourse of induction of the HSV specific polypeptide detected by an antiserum to mAspAT in infected cell extracts (large gel).

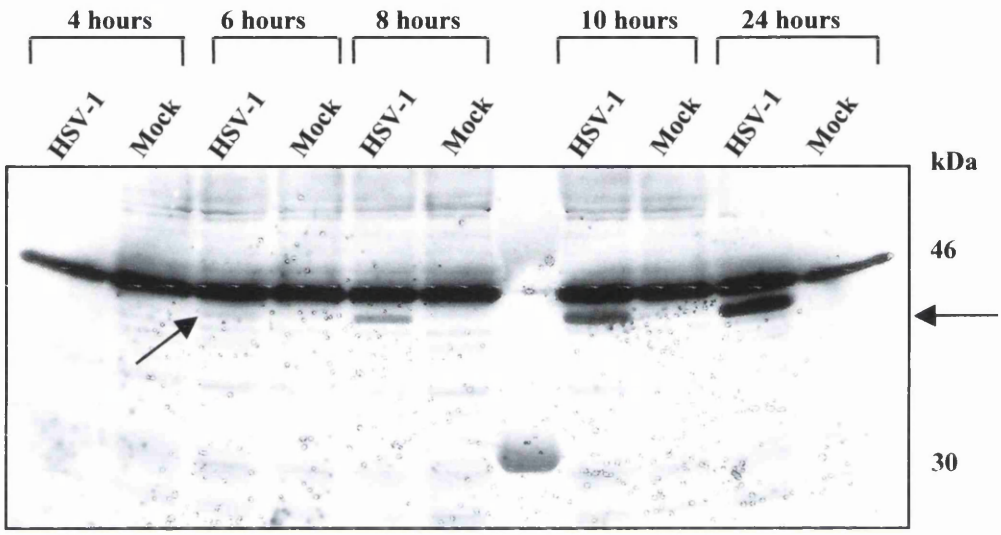

Legend. BHK C13 cells were infected with 10pfu/cell of HSV-1 strain 17 for periods of time ranging from 0 to 24 hours as labelled above the tracks. A mock infected sample was collected at each time point. Cells were lysed directly into 3xBM, and equal volumes (100µl) of lysate loaded onto a large 15% SDS-PAGE gel. After transfer to Hybond-N membrane, the polypeptides were detected by immunoblotting with an anti- mAspAT antiserum.

The HSV-1 specific band is not visible in the 4 hour post-infection track, but is just detectable at 6 hours p.i.(labelled with an arrow in the 6 hour track). The HSV-1 band is clearly visible in the 8 hour p.i. HSV-1 track, but is absent from the mock infected lane. The intensity of the band increases during infection as the polypeptide accumulates, but is present at no stage in the mock infected tracks. This suggests that the polypeptide is either an HSV coded protein, or is induced specifically by infection with HSV. (See main text for further discussion).

and HSV-2 strain MS were used in addition to HSV-1 strain 17 and HSV-2 strain HG52. The latter were controls to identify the benchmark size of the HSV-1 and HSV-2 type lower molecular weight polypeptides.

60mm plates of BHK C13 cells were infected at 10pfu/cell with one of the intertypic recombinants, virus subtypes or control viruses for 18 hours at 37 ° C. The cells were lysed directly into 3xBM, electrophoresed on a 15% SDS-PAGE mini-gel and blotted as described previously (section 5.7). The blot was developed with ECL reagents and is shown in Figure 5.7. The blot was reprobed with an antibody to RR1 to confirm HSV infection.

In this experiment HSV-1 strain F produced the lower molecular weight polypeptide typical of HSV-1 strain 17 (Figure 5.7, lanes 1 & 2), and HSV-2 strain MS induced the typical HSV-2 HG52 type polypeptide (lanes 3 & 4). The recombinant viruses Bx1 and R12-5 (lanes 5 & 7) induced the lower molecular weight polypeptide characteristic of infection with HSV-1 strain 17 (lane 1). The recombinant Fx9 (lane 6) induced the HSV-2 type band.

Examination of the approximate genome maps of the intertypic recombinants (Figure 5.6) revealed that the determinant was located in the region mapping between approximately 0.64 and 0.83 m.u. (shaded in Figure 5.6). Examination of the predicted molecular weights for the unprocessed virus coded polypeptide chains from the 0.64-0.83 m.u region (Figure 5.8 and Table 5.1) of the HSV-1 genome (McGeoch *et al.*, 1988) suggested two candidate polypeptides with molecular weights of approximately the correct size (30-40kDa). These were the products of the UL49 and UL50 open reading frames, which lie within the region defined by the recombinant virus studies. Both of these genes are early (β) HSV genes (Wagner, 1994), which correlates with the observations from the timecourse experiments described in Section 5.7, where the additional polypeptides are detectable at 6 hours post-infection.

5.8.2 The UL49 gene product (p43) is not the induced polypeptide.

UL49 encodes the tegument protein p43 (VP22). It is a major structural component of the virion (Heine *et al.*, 1974) and is extensively post-translationally modified. Indirect immunofluorescence studies demonstrated that VP22 has a perinuclear localisation (Elliot & Meredith, 1992), and later studies that VP22 binds stably to the activation domain of VP16 (Elliot *et al.*, 1995), suggesting a role in virus assembly.

Figure 5.6. Genome maps of the intertypic HSV recombinants Fx9, R12-5 and Bx1.

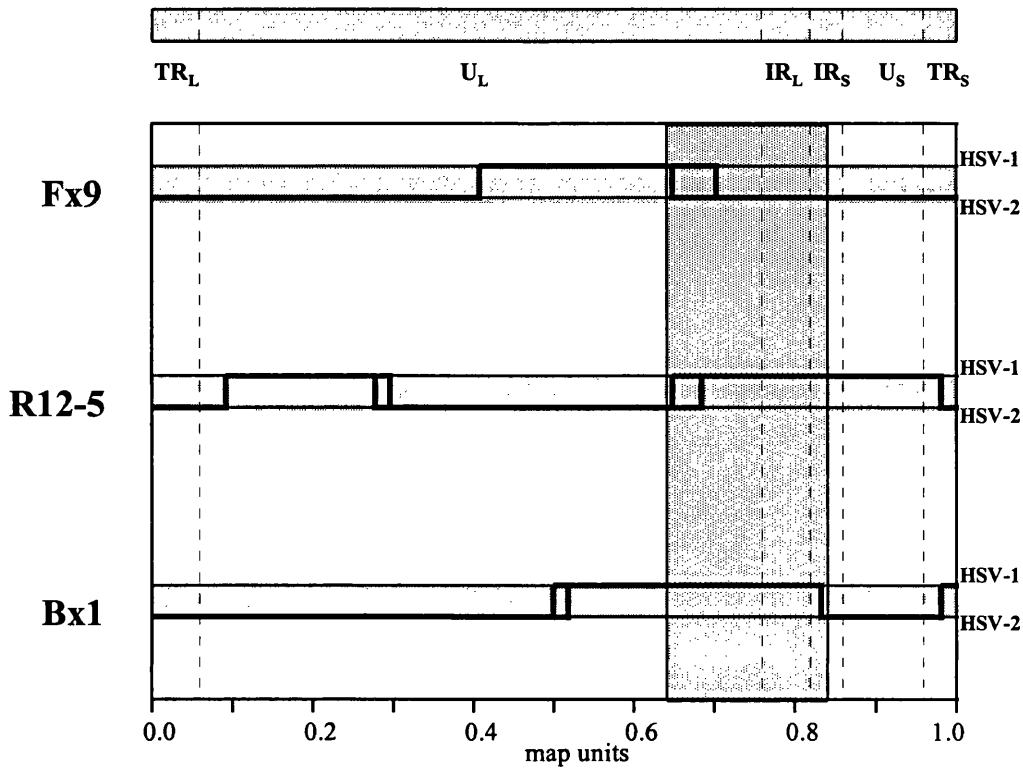

Legend. Approximate genome maps of the intertypic HSV-1/HSV-2 recombinant viruses used in the mapping of the lower molecular weight polypeptide induced by HSV in infected cells. The genome map is marked in 0.1 map unit divisions. The genome of the recombinant is shown as a bold line. For each recombinant the top line represents HSV-1 sequences, and the bottom line HSV-2 sequences. Where there is uncertainty about which type of HSV genome is present at the region of overlap, both HSV-1 and HSV-2 sequences are shown in bold.

On infection of BHK C13 cells, the recombinant viruses Bx1 and R12-5 induced the type 1 lower molecular weight polypeptide, and the Fx9 recombinant virus a type 2 polypeptide (Figure 5.7). The region of the HSV genome delineated by these experiments is shaded grey. The surrounding region (between 0.64 to 0.83 map units) of the HSV-1 genome was examined for potential polypeptides of the correct molecular weight.

(Recombinant virus data provided by Dr. H. Marsden, Institute of Virology, Glasgow).

Figure 5.7. Intertypic recombinant HSV viruses induce different molecular weight polypeptides in infected cells. Mapping of the genome region responsible and identification of the polypeptide as the HSV dUTPase.

A) Probed with anti mAspat antiserum

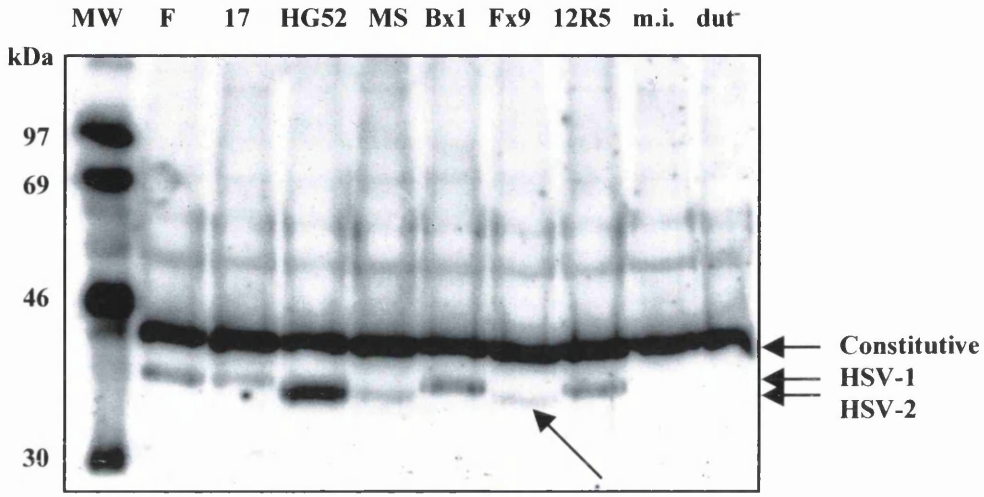

B) Reprobed with anti RR1 antiserum

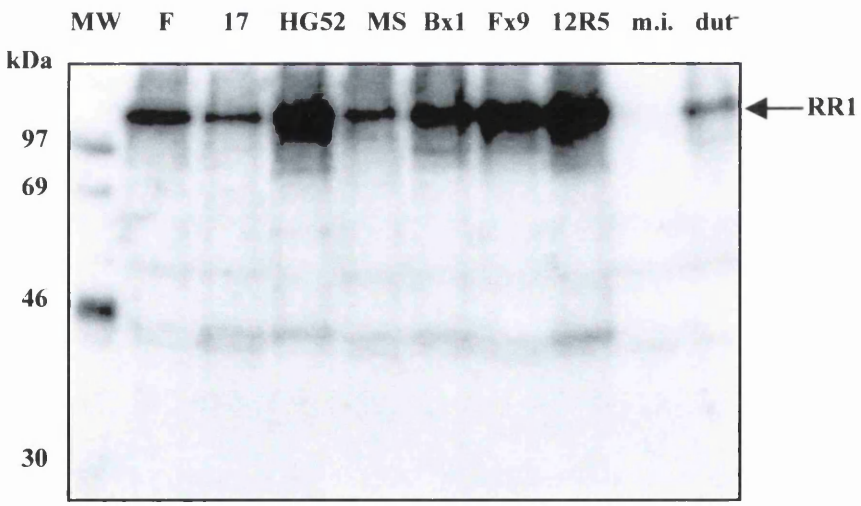

Legend. BHK C13 cells were infected with 10pfu/cell of HSV-1 strains 17 and F, HSV-2 strains HG52 and MS or one of the intertypic recombinant viruses, Bx1, Fx9 or R12-5. A mock infected sample was included. Samples were Western blotted as previously described. Both F and 17 induce the type 1 lower molecular weight polypeptide, and HG52 and MS the type 2 polypeptide. The recombinant viruses Bx1 and R12-5 induce the a type 1 polypeptide by comparison with F and HG52. The Fx9 recombinant induces a type 2 polypeptide (marked by an arrow). The blot was reprobed with an antiserum to RR1 to confirm that infection had occurred in the recombinant virus samples. (See Section 5.8.1 for further discussion).

The track labelled dut$^-$ contains a sample infected with the dUTPase deficient mutant 1218, and fails to induce any lower molecular weight polypeptide. (See Section 5.8.3 and Figure 5.9).

Figure 5.8. Layout of the genes in the region 0.6-0.83 m.u. of the genome of HSV-1

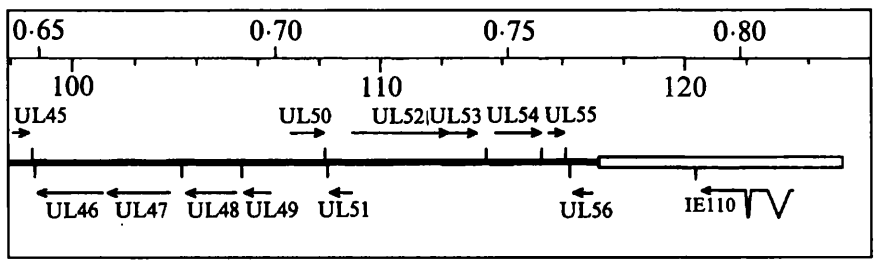

Legend. Layout of the genes in the genome of HSV-1 in the region 0.64-0.83 map units. The sizes and orientation of the proposed functional ORFs are shown by arrows. Locations of proposed transcriptional polyadenylation sites are indicated as short vertical bars. (Derived from McGeoch *et al.*, 1988).

Table 5.1. Function of genes mapping within the 0.6- 0.83 m.u. region of the HSV-1 genome.

Gene	No of residues		M_r*	Function/properties
UL45	172		18178	Hydrophobic N-terminus
UL46	718		78239	Tegument protein VP11/12
UL47	693		73812	Tegument protein VP13/14
UL48	490		54342	Major tegument protein. Activates IE genes
UL49	301	◆	32252	p43 tegument protein (VP22)
UL50	371	◆	39125	dUTPase
UL51	244		25468	Unknown function
UL52	1058		114416	Component of helicase primase
UL53	338		37570	Glycoprotein K
UL54	512		55249	Vmw63- post-transcriptional regulator
UL55	186		20491	Unknown function
UL56	197		21182	role in virulence
RS1	1298		132835	Vmw175- transcriptional regulator

* M_r for unprocessed polypeptide chain

Legend. The proposed functions and molecular weights of the gene products in this region were compared with the molecular weight of the polypeptide induced by HSV-1 infection of BHK C13 cells. The two polypeptides with suitable molecular weights within the genome region delineated in figure 6, (see section 1.8) are highlighted and marked ◆ (UL49 & UL50). gK was excluded on the basis of its' classification as a βγ gene (see discussion for details). (Derived from McGeoch *et al.*, 1988).

Analysis of a western blot of HSV-1 and HSV-2 infected BHK C13 cell polypeptides probed with an anti-mAspAT antiserum and then stripped and re-probed with an antibody against p43 (provided by J. Leslie, MRC Virology Unit, Glasgow) showed that the antisera recognised different polypeptides. The anti-p43 antibody recognised a polypeptide with a molecular weight intermediate between the constitutive cellular mAspAT and the HSV induced forms (Figure 5.9). This experiment confirmed that the lower molecular weight band induced by HSV infection is not p43 (VP22), the gene product of UL49.

5.8.3 HSV mutants in the dUTPase gene fail to induce the lower molecular weight polypeptides in infected cells.

The HSV-1 UL50 gene encodes the viral dUTPase. Preston and Fisher (1984) have mapped the HSV-1 dUTPase gene within genome map coordinates 0.69-0.70. The enzyme catalyses the hydrolysis of dUTP to prevent incorporation of dUTP into newly synthesised viral DNA by DNA polymerase (Ostrander and Cheng, 1980). The HSV-1 dUTPase has a molecular weight of 46kDa compared to 53kDa for the HSV-2 encoded enzyme determined by non-denaturing PAGE (Williams, 1984). This contradicts the size variation observed between the induced polypeptides in my experiments, where the HSV-1 polypeptide is the larger with an apparent molecular weight of 37.7kDa compared to 35.5kDa for the HSV-2 induced polypeptide (Figures 5.2 & 5.3, *Section 5.4*). The predicted molecular weight of the unprocessed polypeptide chain of HSV-1 dUTPase is 39.1kDa (McGeoch *et al.*, 1988).

To determine whether the viral dUTPase was the HSV induced lower molecular weight polypeptide, two mutant dUTPase-deficient HSV-1 viruses were used to infect BHK C13 cells prior to analysis by Western blotting as previously described. HSV-1 1217 is a spontaneous mutant which does not induce dUTPase activity and 1218 is a dUTPase-deficient (*dut*$^-$) mutant obtained by insertional mutagenesis (kindly provided by Dr. Val Preston, Institute of Virology, Glasgow (Preston and Fisher, 1986)).

A sample from BHK C13 cells infected with HSV-1 1218 was probed firstly with anti-mAspAT antiserum and subsequently with an antiserum to HSV RR1 (kindly provided by Dr. Ann Cross, Institute of Virology, Glasgow) as a marker of positive infection. This is shown in Figure 5.7, lane 9 (labelled *dut*$^-$) alongside the

Figure 5.9. The additional polypeptides recognised by the mAspAT antiserum are not the product of the HSV UL49 genes.

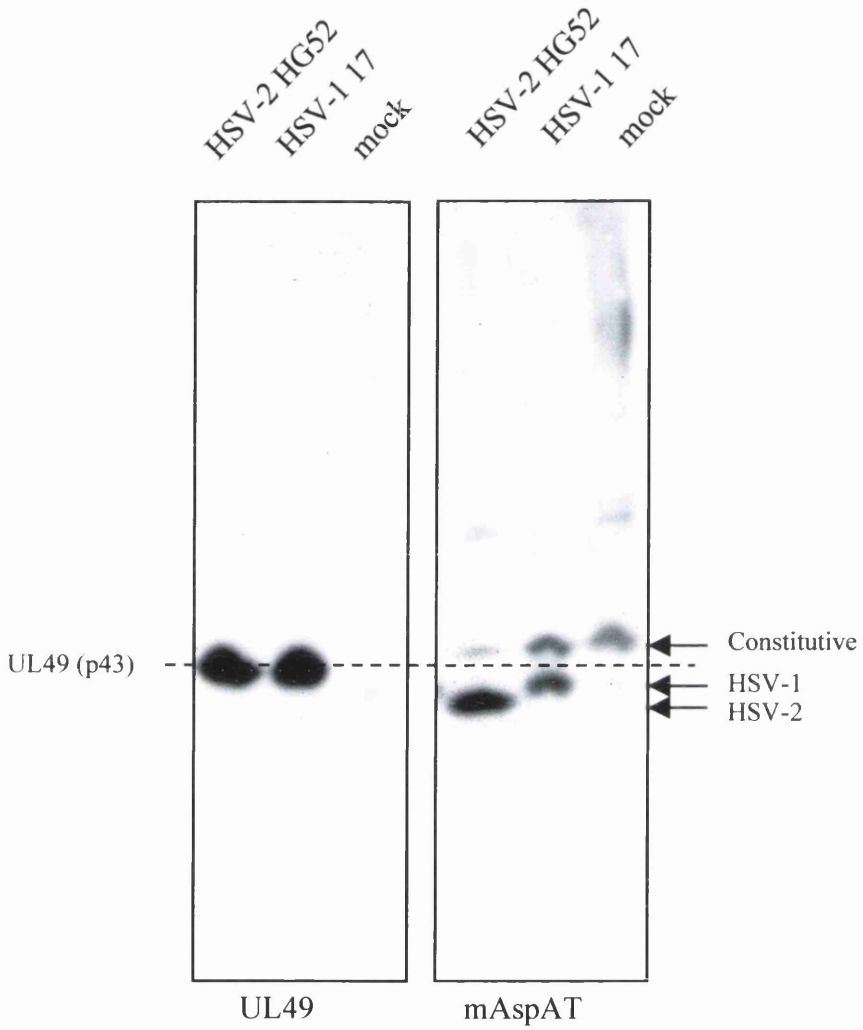

Legend. BHK C13 cells were infected with 10pfu/cell of HSV-1 or HSV-2 overnight, prior to Western blotting as previously described. The blot was first probed with the anti-mAspAT antiserum (right hand panel) and then stripped and re-probed with an antiserum to p43, the polypeptide product of the HSV UL49 gene (left hand panel). Lining up the two blots illustrates that the polypeptide detected by the anti-p43 serum has a molecular weight intermediate between the constitutive cellular mAspAT and the HSV induced cross-reacting species (marked by the dashed line). The cross-reacting species is therefore not the product of the UL49 gene.

recombinant intertypic virus samples. There is a significant absence of a lower molecular weight band in the track infected with HSV-1 1218 (lane 9) compared to HSV-2 HG52 and HSV-1 17 controls (lanes 2 & 3 respectively), despite clear evidence of productive HSV infection as assayed by the presence of RR1 in the lysate.

A repeat of this experiment was performed using Bn5T cells, as these were the cells in which the appearance of the lower molecular weight polypeptides were first observed. Bn5T cells were infected with HSV-1 strain 17, HSV-2 strain HG52, one of the *dut*⁻ viruses 1217 or 1218, or were mock infected overnight. Samples were electrophoresed and immunoblotted as previously described. The Western blot is shown in Figure 5.10. The constitutive cellular mAspAT is present in all the samples, and the HSV induced lower molecular weight polypeptides are present in the HSV-1 and HSV-2 infected samples. However, no additional polypeptides are detected in either of the dUTPase deficient virus infected samples.

These results demonstrate that the lower molecular weight polypeptides detected following infection with HSV-1 and HSV-2 by the antiserum against mAspAT represent the dUTPase enzymes of HSV-1 and HSV-2.

5.8.4 Western blotting with a dUTPase antiserum.

A western blot was performed using extracts from HSV-1 strain 17 and F , HSV-2 strains HG52 and 333 or mock infected BHK C13 cells. Blots were performed as previously described, but using an antiserum raised against HSV-1 dUTPase (kindly donated by Dr. V. Preston). The blot is shown in Figure 5.11. The HSV-1 lanes contain a single polypeptide band with a molecular weight slightly larger than the band detected in the HSV-2 samples. This result is consistent with the results previously described in Sections 5.8.2 and 5.8.3, and confirms the identification of the cross reacting species detected by the antiserum against mAspAT as the HSV dUTPase.

5.9 DISCUSSION.

5.9.1 Summary of Results.

As a result of the increased resolution obtained in the 30-50kDa region of SDS-PAGE gels by increasing the concentration of the gels to 15% polyacrylamide, and increasing the time of electrophoresis, an additional polypeptide was detected by

Figure 5.10. Infection of Bn5T cells with dUTPase deficient mutants of herpes simplex virus.

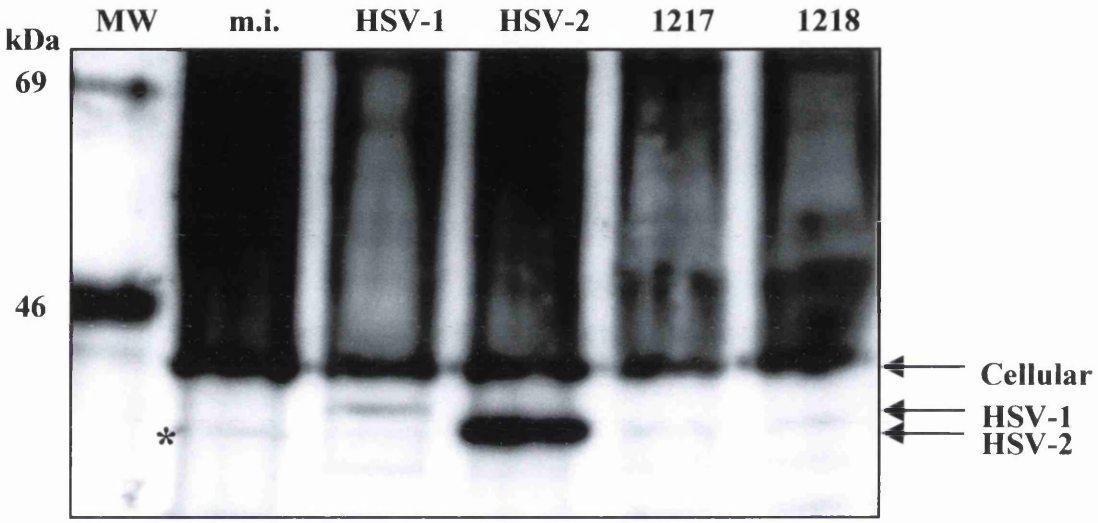

Legend. Bn5T cells were infected overnight with HSV-1, HSV-2, HSV 1217, HSV 1218 or were mock infected. HSV 1217 is a spontaneous mutant that fails to synthesise dUTPase, and 1218 contains an in frame insertion resulting in a larger protein product (Preston and Fisher, 1986). Samples were immunoblotted with an antiserum to mAspAT as previously described. The position of the induced polypeptides is marked by arrows to the right of the gel. Neither dUTPase mutant virus induces a lower molecular weight polypeptide of the type induced by wild-type infection. The faint band which migrates at the same position as the HSV-2 type band (labelled with an asterisk in the mock infected track) is due to the relatively high background in this blot, and is present in all the samples. This experiment confirms that the lower molecular weight polypeptides which cross-react with the anti-mAspAT antiserum represent the HSV dUTPase enzymes.

Figure 5.11. A dUTPase antiserum recognises different molecular weight polypeptide bands in HSV-1 and HSV-2 infected BHK C13 cells.

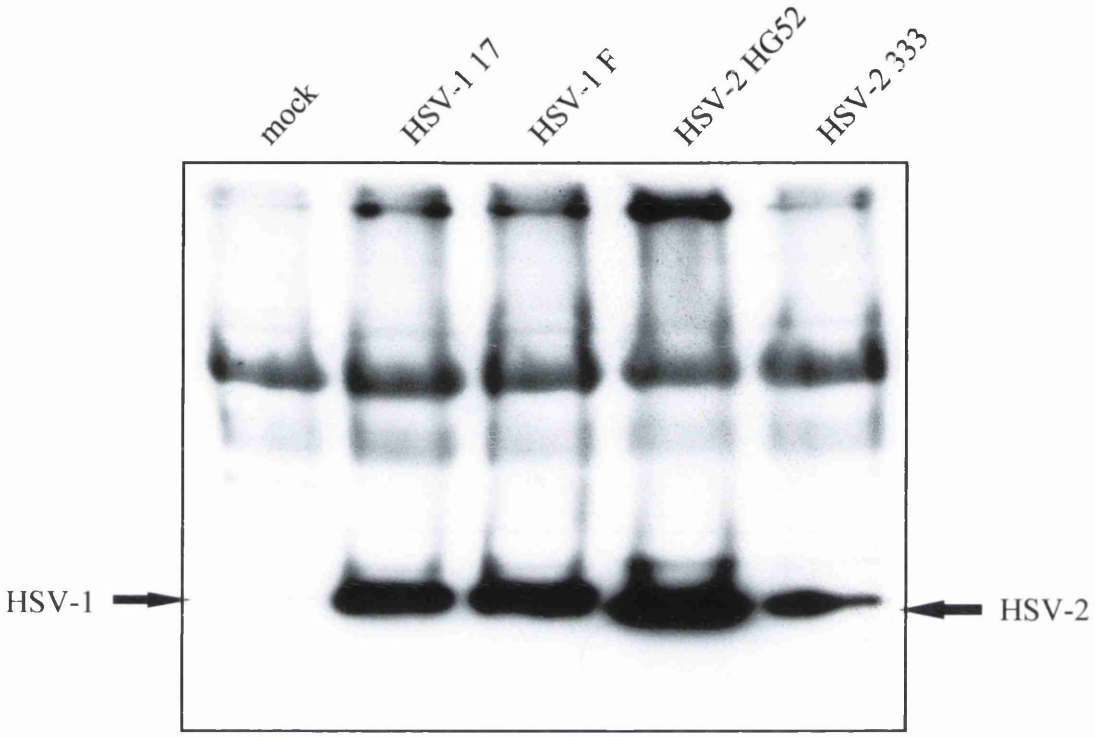

Legend. BHK C13 cells were infected with HSV-1 strains 17 and F, and with HSV-2 strains HG52 and 333, or were mock infected. Cell extracts were analysed by Western blotting with an antiserum to the HSV-1 dUTPase (donated by Dr S. Caradonna). The dUTPase antiserum detects bands of differing molecular weight in the HSV-1 and HSV-2 tracks, as previously noted for the additional polypeptide detected in HSV infected cells with the mAspAT antiserum. In conjunction with the recombinant intertypic mapping and dUTPase mutant virus studies, this result confirms that the cross-reacting species is the HSV dUTPase.

Western blotting with an antiserum to mAspAT in Bn5T tumour, BHK C13 and RE cells infected with HSV-1 and HSV-2 (*Sections 5.3 and 5.4*).

The increase in the level of this polypeptide was greater in the Bn5T cells than in the RE cells, and was also observed in the BHK C13 cell line. The BHK C13 cells were routinely used to propagate HSV within this Institute, and infect reproducibly. This was not the case with Bn5T cells which occasionally lose their ability to be infected after prolonged passage in tissue culture (J.C.M. Macnab, pers. comm). This effect was observed at passage numbers as low as 50, and was not predictable. Therefore BHK C13 cells were used for further experiments on the induction of the lower molecular weight polypeptides following HSV infection.

A series of experiments were performed to examine the induction of the lower molecular weight polypeptides. These experiments showed that the polypeptides were associated with the cell, as washing of the cell monolayer prior to lysis failed to remove the induced polypeptides (*Section 5.5*). The polypeptides could be either membrane associated or intracellular proteins. Furthermore, by prolonged incubation in the absence of protease inhibitors, it was demonstrated that the lower molecular weight polypeptides were not caused by degradation of the mature cellular mAspAT by proteases released during the lysis procedure (*Section 5.6*). This result was as expected, as the lower molecular weight polypeptides were present following lysis of the cells directly in SDS-PAGE sample loading buffer (3xBM). This solution contains high concentrations of both SDS and β-mercaptoethanol which would be expected to denature the cellular proteases released during lysis.

Analysis of the time-course of induction of the lower molecular weight polypeptides detected by the anti-mAspAT antiserum (*Section 5.7*) showed that they appeared approximately 6 hours post infection. If the induced polypeptides are viral encoded polypeptides this would place the gene(s) responsible into the early (β) temporal class of HSV genes (Honess and Roizman, 1974). Alternatively, if the additional polypeptides are cell coded and are induced following HSV infection, this induction may require HSV immediate early gene expression. Estridge *et al.* (1988) previously reported that HSV-2 IE gene expression was necessary for the induction of a 40kDa polypeptide purified from transformed cells and from dyskaryotic cells from cervical smears. However, Preston (1990) reported the induction of a 56kDa cellular polypeptide in HFL cells infected with the penetration deficient HSV ts1204. This

cellular polypeptide was present at 3.5 hours post infection, and it was suggested that viral attachment to the cell surface could be responsible for the induction. This could be the case for the induction of the lower molecular weight polypeptide detected by the anti-mAspAT antiserum.

The induced polypeptides were of different molecular weight depending on the HSV type used for the infection of the cells. Because of this, it was likely that the polypeptides were the product of an HSV gene or genes. If this was the case, it would be possible to approximately map the position of the gene(s) encoding these polypeptides by analysis of the phenotype displayed following infection with a panel of intertypic HSV-1/HSV-2 recombinants. These viruses contain delineated regions of the genomes of both HSV-1 and HSV-2, and express polypeptides of the relevant size for the HSV gene type present in the particular recombinant virus studied. I have demonstrated that HSV-1 and HSV-2 induce differently sized additional polypeptides in BHK C13, Bn5T and RE cells *(Section 5.4)*.

By infection of BHK C13 cells with intertypic recombinants and analysis of the phenotype of the induced lower molecular weight polypeptides, I was able to delineate the region of the HSV genome encoding the induced polypeptide. The three viruses used (Fx9, Bx1 and R12-5: *Section 5.8, Figure 5.6*) showed that the gene was in the region of the HSV genome between map co-ordinates 0.64 and 0.83m.u. The complete cDNA sequence and protein coding capacity of HSV-1 (McGeoch *et al.*, 1988) was examined and three potential genes which coded for polypeptides in the molecular weight range 30-50kDa identified. These were the UL49 (VP22), UL50 (dUTPase) and UL53 (gK) genes. The UL49 and UL50 are classified as β genes, whilst gK is a βγ gene (Wagner, 1994). I provisionally classified the gene encoding the induced polypeptides in my experiments as a probable β gene, on the basis of timecourse experiments (*Section 5.7*). gK was therefore excluded from further analysis.

The product of the UL49 gene is the tegument protein VP22 (p43) (Elliot and Meredith, 1992), which is of similar molecular weight to the induced polypeptide. However, in an experiment in which a blot of infected cell polypeptides was reprobed with an antiserum to p43, a single polypeptide was detected in each infected track. This was larger than the induced polypeptides and smaller than the

constitutive cellular mAspAT polypeptide. This excluded the UL49 gene from further consideration.

The remaining candidate polypeptide was the viral dUTPase, encoded by the UL50 gene (Preston and Fisher, 1984). The induced polypeptide in HSV infected cells was identifed as the dUTPase by infection of cells with two mutant HSV-1 viruses that fail to induce dUTPase activity; 1217 a spontaneous mutant, and 1218 an insertional mutant virus (Fisher and Preston, 1986). Infection with these viruses failed to induce the lower molecular weight polypeptides detected by the anti- mAspAT antiserum in cells infected with wild-type virus *(Section 5.8)*. Confirmation that infection had occurred was obtained by the presence in the HSV-1 1218 infected cell lysates of the large subunit of ribonucleotide reductase, also a β HSV gene product. The intertypic recombinant virus experiments are further discussed in Section 5.9.2 below.

The experiments described in this chapter have identified the cross-reacting species detected in HSV infected cells as the product of the HSV UL50 gene, the deoxyuridine triphosphatase. This result was confirmed by comparison of the polypeptides detected with an antiserum raised against the HSV-1 dUTPase with the additional bands detected by the anti- mAspAT antiserum in cells infected with HSV-1 or HSV-2 (*Figure 5.11*).

5.9.2 Mapping of the HSV induced lower molecular weight polypeptides using HSV-1/HSV-2 intertypic recombinants.

Wohlrab *et al.* (1982) used a panel of intertypic recombinant viruses to map the location of the HSV gene encoding the viral dUTPase to within genome co-ordinates 0.67 and 0.68 m.u., on the basis of the differential cellular localisation of the HSV-1 and HSV-2 enzymes (ratio of nuclear/cytoplasmic dUTPase activity of 0.66 and 0.13 respectively). More recently, Williams and Parris (1987) have repeated this experiment, and in addition to cellular localisation they used the differing mobility of the HSV dUTPases in non-denaturing PAGE experiments to classify the phenotype (type 1 or type 2) of the induced dUTPase. In both experiments they reported that the recombinant Bx1 virus exhibited a type 2 phenotype despite containing a type 1 genome in the 0.67 to 0.68 m.u. region. This contradicted the results of Wohlrab *et al.* (1982). In the work described here *(Section 5.8.1)*, where the dUTPase phenotype was assessed by denaturing SDS-PAGE electrophoresis, this recombinant exhibited a type 1 phenotype. This is consistent with the localisation of the type specific

determinant of dUTPase mapping within the right hand 33% of the genome, which includes the region previously reported by Wohlrab *et al.* (1982), and Preston and Fisher (1984). This result contradicts that of Williams and Parris (1987) who located the type specific determinant of HSV dUTPase to the left hand 20% of the genome (between either 0.06-0.1, or 0.148-0.204). Preston and Fisher (1984) cloned the region of the HSV-1 genome covering map co-ordinates 0.69-0.7 and demonstrated that this coded for a 1.5kb mRNA. The primary product of this transcript was a 39kDa polypeptide corresponding to the previously reported molecular weight of the purified HSV-1 dUTPase (Caradonna and Adamkiewicz, 1984). This polypeptide displayed dUTPase activity in transient assays, which was abrogated by insertional mutagenesis. In the light of these results, Williams and Parris (1987) suggested that whilst the structural gene may lie within the 0.69-0.7 m.u. region of the HSV-1 genome, an additional determinant located at the left end of the genome may determine type specificity *in vivo*.

Williams and Parris (1987) were unable to detect any dUTPase induction in cells infected with the R12-5 recombinant virus. In the work described here this virus induces a dUTPase with a type 1 phenotype; this virus contains HSV-1 genome representing approximately the regions 0.1-0.27m.u. and 0.64-0.98m.u. This result therefore fails to resolve the confusion surrounding the localisation of the type specific determinant of the dUTPase. The induction of a type 2 phenotype dUTPase by the recombinant Fx9 in these experiments is also inconclusive in this respect, as this virus has type 2 genome sequences at both the left hand region defined by Williams and Parris (1987) and the region between 0.69 and 0.7m.u. defined by the studies of Preston and Fisher (1986).

In summary, the recombinant virus studies described in this thesis fail to resolve the question of which region of the genome is responsible for the type specificity demonstrated by the dUTPase enzymes of HSV.

5.9.3 Discussion of the cross reactivity between HSV dUTPase and mAspAT.

5.9.3.1 Sequence comparison

The reason for the cross-reactivity of the HSV dUTPase with an antiserum raised against purified rat mAspAT was unclear. It was possible that there were antigenic epitopes in common between the two polypeptides. Analysis of the cDNA and derived amino acid sequences of the two enzymes performed using programs from

the GCG Wisconsin Package failed to detect any significant similarity. 'Bestfit' comparison, illustrated in Figure 5.12, calculated the highest degree of similarity at the amino acid level as 18/163 identical amino acids, with the longest continuous run of identical amino acids being two. At the nucleotide level, the comparison was 13/21 nucleotides, containing 5 contiguous nucleotides. Clearly it is unlikely that there is a linear epitope in common between these two polypeptides. Further analysis using the 'Gap' program (which aligns the full length of the two sequences by inserting gaps) and FASTA confirms that the similarity at nucleotide and amino acid level respectively is minimal.

The cross-reactivity may therefore be due to common conformational epitopes present in both polypeptides, perhaps a functional domain or co-factor binding site. A search was performed using the GCG 'Motifs' program to determine whether there were motifs in common. This program currently analyses only DNA sequences. Even within the motifs which were common to both sequences (2Fe2S Ferredoxin for example) the individual sequences within the motifs were very divergent. This analysis and the 'Gap' and FASTA analyses are presented in Appendices 2A to 2C.

5.9.3.2 Comparison of the structure and function of dUTPase and mAspAT

Consideration of the enzymatic function and structure of the two enzymes failed to provide an obvious explanation for the cross reactivity.

There appear to be two groups of dUTPase enzyme, classified here on the basis of their protein structure. The first of these contains the dUTPase enzymes from *E. coli* (Cedergren-Zeppezauer *et al.*, 1992); humans (Climie *et al.*, 1994); FIV (Prasad *et al.*, 1996); EIAV (Bergman *et al.*, 1995) and Vaccinia virus (Broyles *et al.*, 1993). The crystal structures of the *E. coli* (Cedergren-Zeppezauer *et al.*, 1992; Larsson *et al.*, 1996), human (Mol *et al.*, 1996) and FIV (Prasad *et al.*, 1996) dUTPases have been solved. Each is a trimer consisting of subunits ranging from 14.3 to 17.5kDa. Each trimer binds three substrate molecules (Larsson *et al.*, 1996), with the active sites being formed by residues from each of the subunits (Mol *et al.*, 1996). These active site residues come from four of the five conserved dUTPase motifs identified by McGeoch (1990) which are located at the interface between the subunits.

The second group contains the dUTPase enzymes of HSV-1 (Preston and Fisher, 1984), HSV-2 (Williams, 1984), BHV-1 (Liang *et al.*, 1993), EBV (Sommer *et al.*, 1996), PRV (Jons and Mettenleiter, 1996), MMTV (Koppe *et al.*, 1994) and that

Figure 5.12. Comparison of the nucleotide and amino acid sequences of rat mitochondrial aspartate aminotransferase and HSV-1 deoxyuridine triphosphatase.

A) Nucleotide sequence comparison

```
M18467 x Hsv1ul50.Seq

   1363 TTCACCAGGTCACCAAGTAATC 1384
        ::| || ||:||||| |: |:|
    255 UUCCCCGGGUCACCACGUUAUC 276
```

B) Amino acid sequence comparison

```
M18467.Pep x Hsv1ul50

     36 PVASSPGWLLPFTQALQPQPLPEPAPGGPMLKWDLQIPSWE*PKPSREIP 85
        |  . |  |  | |   | |         | |.  |  ||     |.|
    136 PALTEPISLRQFPQLAPPPPTGAGIREDPWLEGALGAPSVTTALPARRRG 185

     86 TARR*TWELVPTGT 99
         .     || |  |
    186 RSLVYAGELTPVQT 199
```

Legend. Nucleotide and amino acid sequence comparisons were made between the HSV-1 dUTPase (encoded by gene UL50) and rat mitochondrial aspartate aminotransferase (M18467.Em_ro), using the 'Bestfit' program of the Wisconsin GCG software suite.

The top row of each diagram represents the mAspAT sequence, and the lower row the dUTPase sequence. Limited homology is observed at both the nucleotide and amino acid level. The degree of homology observed in this diagram, and further analysis using other GCG programs is discussed in the discussion for this chapter (Section 5.9.3).

from Leishmania major (Camacho *et al.*, 1997). These enzymes consist of a single polypeptide chain ranging in molecular weight from 30kDa to 53kDa. McGeoch (1990) suggested a model to account for the presence of the conserved dUTPase motifs within the herpesvirus enzymes which suggests that the herpesvirus enzymes may have resulted from an intragenic duplication, resulting in a single chain enzyme containing the equivalent of two chains of the *E. coli* enzyme. Although the *E. coli* enzyme is now known to be trimeric, an adaptation of this model could still be valid, as the combined subunit molecular weights of the trimeric enzymes approximates the molecular weight of the single chain dUTPases of the herpesviruses. Comparison of the 3-D crystal structure of a single chain dUTPase with the overall (quaternary) structure of the *E. coli* or human enzyme may provide evidence to support this model.

Bjornberg and Nyman (1996) have reported that the dUTPase enzymes of HSV-1 and MMTV are less substrate specific than the *E. coli* enzyme. HSV-1 dUTPase has a higher reactivity with dCTP and dTTP, and MMTV with dTTP and UTP. This substrate promiscuity may be a result of the single chain structure of these enzymes compared to the potentially more mobile (and therefore discriminating) active sites of the trimeric enzymes.

dUTPases require the divalent cations Co^{2+} or Mg^{2+} for full activity, but have no cofactor requirement. They bind substrate by pseudo-Watson and Crick hydrogen bonding to main chain residues.

The structure and function of the mAspAT enzyme have been discussed in the introduction to this thesis (*Chapter 1, Section 1.3*), and only the salient points are discussed here. The enzyme has a highly conserved quaternary structure despite divergence at the amino acid and nucleotide sequence levels. The crystal structure of the *E. coli* enzyme has been solved in the presence of substrate (McPhalen *et al.*, 1992), inhibitors (Miyahara *et al.*, 1994) and reaction intermediates (Malashkevich *et al.*, 1993) and a Molecular Dynamics simulation of intramolecular motion within the enzyme performed (Kasper *et al.*, 1996). The *E. coli* enzyme is a dimer of identical 44kDa subunits, each of which consists of a small and a large domain. The active site lies in a cavity that is close to both the subunit interface, and the interface between the two domains. On binding substrate the domains close together and bury the substrate in the active site, moving two arginine residues into position to form

salt bridges with the substrate. These hold the substrate in proximity to the pyridoxal 5' phosphate co-factor in the correct orientation for catalysis of the transamination reaction (McPhalen *et al.*, 1992). Unhindered domain movement is required for full catalytic activity (Markovichousley *et al.*, 1996), and the presence of the α-carboxylate groups of both the L-glutamate and L-aspartate substrate molecules are required to promote domain closure (Kasper *et al.*, 1996), ensuring that the enzyme remains in the open conformation until catalysis can occur.

To summarise, the overall organisation of the dUTPase and mAspAT enzymes is very different, they have different co-factor requirements and bind different substrates via different electrostatic and hydrogen bonding interactions. It is difficult to imagine why there should be a cross-reactivity of the dUTPase with the mAspAT antiserum.

5.9.4 Possible contamination of the immunogen.

The antiserum used in the majority of this work was produced by Dr. Joan Macnab (Institute of Virology, Glasgow) by injection of purified pre-mAspAT polypeptide expressed in *E. coli* (gift of J.R. Mattingley, University of Missouri, USA). The initial experiments utilised an antiserum raised by Mattingley against the same immunogen. It was possible therefore that this immunogen could be contaminated with the *E. coli* dUTPase enzyme, and that this might cause the cross-reactivity with the HSV dUTPase enzyme. The purification procedure for pre-mAspAT involved lysis of the bacteria in 50mM Tris, 150mM NaCl and 0.5mM EDTA at pH7.5, followed by ammonium sulphate precipitation and serial anion and cation exchange chromatography at pH 8.0 (Altieri *et al.*, 1989). This procedure produced a single polypeptide band on silver stained SDS-PAGE gels, and immunoblotting with an antiserum to pig heart mAspAT detected the same single band.

The purification procedure for the HSV-2 dUTPase begins with lysis of infected cells in 10mM Tris-HCl, pH 8.0, and several rounds of chromatography at pH 6.0 and 8.0 (Williams and Parris, 1986). This is similar to the purification procedure described above for mAspAT. However, the pI values of the two proteins are very different, at 9.5-10.0 for mAspAT (Stremmel *et al.*, 1990) and 5.9 for the HSV-2 dUTPase (Williams, 1984). Furthermore, the *E. coli* dUTPase enzyme is a trimer of 14kDa subunits, which although likely to remain intact during the mAspAT purification procedure (as the mAspAT dimer does), would dissociate and be visible on the silver

stained SDS-PAGE gel. This is not the case, and it is therefore unlikely that the bacterially expressed mAspAT immunogen was contaminated with the *E. coli* dUTPase.

5.10 CONCLUSIONS.

HSV-1 and HSV-2 infection of a variety of cell types induces a lower molecular weight polypeptide which cross-reacts with an antiserum raised against rat mitochondrial aspartate aminotransferase. This polypeptide has been identified as the HSV deoxyuridine triphosphatase. No explanation for the cross reactivity was obvious.

6. CLONING OF THE mAspAT cDNA INTO A EUKARYOTIC EXPRESSION VECTOR AND CELLULAR TRANSFORMATION ASSAYS.

6.1 INTRODUCTION.

Macnab *et al* (1985) have reported that a set of cell coded polypeptides are present in increased amounts in transformed cells relative to control cells, and that these polypeptides were further increased following infection with HSV (Macnab *et al.*, 1985; Grassie *et al.*, 1992). The 40 kDa polypeptide from this group was identified as mitochondrial aspartate aminotransferase by comparison of partial amino acid sequence (Lucasson, 1992). Both the protein level and enzyme activity of mAspAT were increased in the transformed cells and were further increased following HSV infection (Lucasson *et al.*, 1994). Furthermore, in Chapter 4 of this thesis I have shown that the level of mAspAT mRNA is increased approximately two-fold in Bn5T cells by infection with HSV-2.

The 40kDa polypeptide was shown to be specifically induced in transformed cells, and as HSV-2 infection increased the level further, the following experiments were designed to examine whether increasing the level of the mAspAT enzyme in non-transformed cells by transfection of a mAspAT expressing plasmid would lead to an altered phenotype in these cells.

6.1.1 Cells.

NRK 536 cells, a rat fibroblast cell-line, were kindly provided by Bert Matz (University of Freiberg, Germany) who had previously used them in experiments to assess cellular transformation following plasmid transfection or viral infection. Vossbeck *et al.*, (1995) used these cells to assay the transforming effect of EGF and TGF-β treatment of cells in culture. Treatment of NRK 536 cells with TGF-β alone led to the formation of a small percentage of colonies in soft agar. Transformation could only be demonstrated by addition of TGF-β to individualised NRK 536 cells which were already plated into soft agar, as treatment of cell monolayers led to the induction of apoptosis in the newly transformed cells by neighbouring normal cells. Colony formation in soft agar indicates anchorage independent growth and is a standard assay to assess the induction of phenotypic alterations characteristic of

partial cellular transformation (MacPherson and Montagnier, 1964; Kusuhara *et al.*, 1992; Schultzcherry and Murphy-Ullrich, 1993).

6.1.2 Plasmids.

A full length cDNA clone of rat mAspAT (2362nt) containing the presequence (89 nucleotides representing a 29 amino acid signal peptide which is cleaved following targetting of the enzyme to the mitochondrion) inserted at the *EcoRI* site of the polylinker of pBS-KS (Figure 6.1A) was provided by J.R. Mattingley (Mattingley *et al.*, 1987).

A eukaryotic expression vector, pCMV10, (Figure 6.1A) containing the HCMV major immediate early promoter (HCMV-mIE) and the SV40 RNA processing and polyadenylation signals was in use within the Institute of Virology, Glasgow. This plasmid was constructed from pCMV19K as follows (White and Cipriani, 1989). The *BamHI* site downstream of the polyadenylation signal was destroyed by sequential cleavage, filling in and religation, and the *EcoRI-HindIII* fragment encoding the HCMV 19K protein was then replaced with the polylinker cloning site fragment of plasmid pTZ19U (Mead *et al.*, 1986). A stock was obtained from Dr N. Stow (Institute of Virology, Glasgow).

6.2 CLONING OF mAspAT cDNA INTO A EUKARYOTIC EXPRESSION VECTOR.

6.2.1 Directional cloning into pCMV10.

Initial attempts were made to clone the pre-mAspAT cDNA directionally into pCMV10. This should yield a high percentage (ideally 100%) of the recovered clones containing the mAspAT cDNA in the correct orientation to facilitate expression from the upstream HCMV mIE promoter.

pBS-KS mAspAT and pCMV10 were digested using *KpnI*, precipitated and then digested with *BamHI*. The 4kb pCMV10 vector backbone and the 2.3kb mAspAT cDNA insert were excised from a 1% agarose gel. The DNA fragments were purified using a Sephaglas kit (Pharmacia), ethanol precipitated and the concentration of each determined spectrophotometrically. Ligation mixes containing vector:insert ratios of 1:1, 1:2, 1:3, 2:1, 3:1 and positive and negative controls were incubated overnight at 16°C, as described in Materials and Methods. Competent JM101 bacteria were prepared using $CaCl_2$ and transformed with 1µl, 2µl or 5µl of the ligation mixes.

Legend. Maps of the plasmids used to clone the mAspAT cDNA into a vector for expression in eukaryotic cells are shown.

Figure 6.1 (facing page) shows the production of pCMV-mAspAT1 as described in Section 6.2.3. Plasmid pBS-KS containing the mAspAT cDNA inserted at the *EcoRI* site was kindly donated by J.R. Mattingley (Mattingley *et al.*, 1987) and is denoted pBS-KS-mAspAT. The mAspAT cDNA was excised from pBS-KS-mAspAT using *EcoRI* , and inserted into the *EcoRI* site of pCMV10 (provided by Dr. N. Stow, Institute of Virology, Glasgow) to produce pCMV-mAspAT1 . The orientation of the cDNA insert was determined by restriction of pCMV-mAspAT1 with SstI which cuts within the HCMV mIE promoter, and NcoI which cuts 89bp from the 5' end of the cDNA (see Figure 6.4).

Figure 6.1. Plasmids used in the construction of a eukaryotic vector expressing mAspAT.

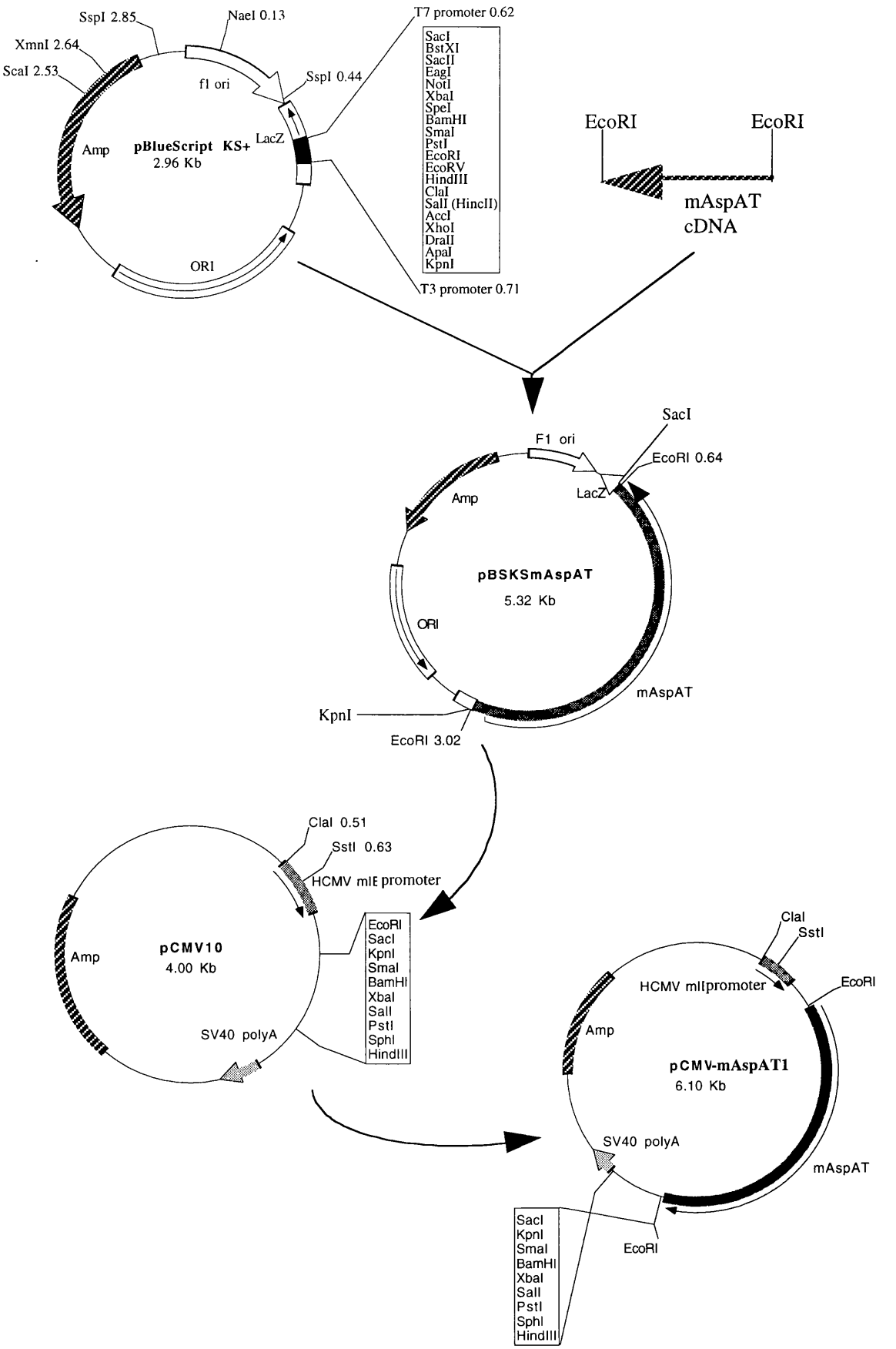

Colonies resistant to ampicillin were picked and minipreps made from overnight cultures of these bacteria. These DNA samples were digested with *KpnI* and *BamHI* to determine the size of the cDNA insert each contained. The efficiency of the ligation reaction was poor in many repeats of this experiment, and of the few colonies present on the ampicillin plates, none contained an insert of 2.3kb, representing the mAspAT cDNA. The positive transformation control produced many colonies indicating that this step was working efficiently.

In an attempt to determine the reason for the lack of recovery of recombinant plasmid in these experiments, various parameters were altered in turn. Firstly, fresh preparations of pCMV10 and pBS-KS mAspAT and restriction enzyme stocks were obtained, and used to produce the ligation precursors. The digested DNA was recovered from agarose gels by both Sephaglas extraction and by centrifugation of the excised DNA band through siliconised glass wool. Ligation conditions were varied and different sources of T4 DNA ligase used. Ligation for 72 hours at 16 ° C failed to produce colonies when transformed into competent JM101 bacteria ($CaCl_2$). A more efficient method (A. Maclean, pers. comm.) for making and transforming competent cells was used in later experiments (TSB, as described in Materials and Methods). No combination of these altered conditions resulted in correctly ligated pCMV10-mAspAT cDNA using the *KpnI* and *BamHI* sites.

6.2.2 Cloning non-directionally into pCMV10.

6.2.2.1 Introduction.

Because of the difficulties encountered trying to clone the mAspAT cDNA directionally into pCMV10 described above (*Sections 6.2.1)*, it was decided to clone the mAspAT cDNA non-directionally into the *EcoRI* site of pCMV10. This reduced the number of manipulations required in the preparation of ligation precursors, for example by removing an ethanol precipitation or linker ligation step. This reduced the chance of damage to the cDNA ends which appeared to be the most likely cause of the failed ligation experiments. However, non-directional cloning necessitated further selection for clones which contained the mAspAT cDNA insert in the correct orientation to facilitate expression from the HCMV-mIE promoter. Following confirmation of the insert size obtained from the recovered plasmids, the orientation

of the insert was determined. A restriction digest was designed to determine the orientation of the insert in the plasmid. This protocol is illustrated diagramatically in Figure 6.5, and discussed further in section 6.2.3.3

6.2.2.2 Ligation and bacterial transformation

pCMV10 and pBSKS-mAspAT were digested with 10U/μg of *EcoRI*. 1U of CIP was added to the pCMV10 restriction digest. The DNA fragments were separated by electrophoresis on a 1% agarose gel, and compared to the relevant uncut plasmid and λ *HindIII* molecular weight markers to allow identification of the required fragments. The 4kb pCMV10 vector backbone (linearised and phosphatased) and the 2.3kb mAspAT cDNA fragment were excised from the gel and purified using Sephaglas® as described in Materials and Methods. Figures 6.2A and 6.2B show 1% agarose gels of the purified fragments and subsequent ligations (see below), stained with ethidium bromide and visualised with UV light. Lanes 4 and 5 of each gel contain the Sephaglas® purified *EcoR1* digested pCMV10 plasmid and mAspAT cDNA insert respectively. Each DNA fragment has approximately the expected molecular weight.

Ligations were set up using the DNA fragments isolated as illustrated in Figure 6.2A and 6.2B above, as described in Materials and Methods. The fragments were extracted with phenol/chloroform and precipitated with PEG 3000. A negative vector only control and a positive transformation control (uncut pCMV10) were included. Figure 6.2A shows the results of a ligation analysed on a 1% agarose gel prior to the transformation of competent bacteria using the TSB transformation protocol. Additional DNA bands are visible in the tracks containing 1:2 and 1:1 ratios of pCMV10 vector: mAspAT insert (lanes 2 and 3 respectively). These bands are not present in the pCMV10 re-ligation control (lane 1). Figure 6.2B shows a different ligation reaction in which only two additional bands are present in the ligated samples (marked with arrows in lane 1). These bands are absent from both of the pCMV10 control tracks (lanes 3 and 4). Following linearisation of the ligated plasmids in lane 1 with *BamHI* a single larger band (labelled with a white arrow in lane 2) remains in addition to the pCMV10 backbone. Comparison with the molecular weight markers estimates the size of this DNA species as approximately 6.6KB. Comparison of the intensity of the higher molecular weight bands with the

Legend. Panel A shows the results of an experiment to ligate the mAspAT cDNA excised from pBS-KS-mAspAT with *EcoRI* (lane 5) into *EcoRI* digested pCMV10 (lane 4). Additional DNA bands are observed in the ligation mixtures containing a 1:1 ratio (lane 3) and 1:2 ratio (lane 2) of pCMV10:mAspAT cDNA insert. Lane 1 contains a pCMV10 re-ligation control to demonstrate that the extra DNA bands are not due to the intramolecular re-ligation of the pCMV10 backbone.

Panel B shows a separate experiment to ligate the mAspAT cDNA into pCMV10 using the *EcoRI* sites. Lanes 4 and 5 contain the pCMV10 and pBS-KS mAspAT cDNA ligation precursors respectively. The pCMV10 re-ligation control is shown in lane 3. The ligation reaction produced two extra DNA bands (labelled with arrows) in addition to the band of unligated pCMV10 plasmid. Following linearisation of the ligation products by restriction at the unique *BamHI* site within the polylinker, a single extra DNA band remains (marked with a white arrow in lane 2). This band has a molecular weight of approximately 6.6kbp determined by comparison with the molecular weight markers. The predicted molecular weight of pCMV-mAspAT1 is $\approx$ 6.3kbp (4 + 2.3).

Figure 6.2. Agarose gel analysis of ligation precursors and products for cloning mAspAT cDNA into pCMV10 expression vector.

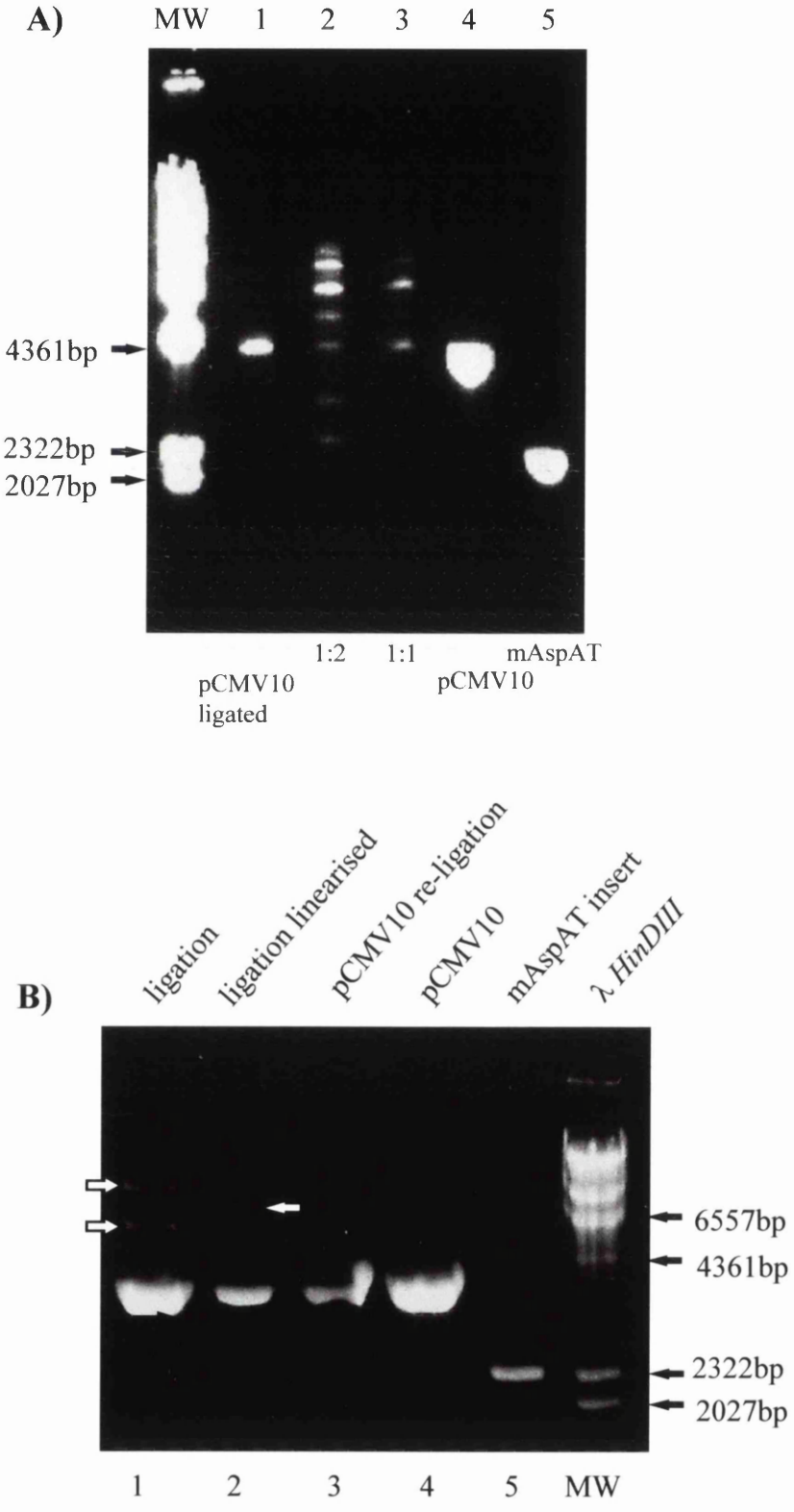

intensity of the pCMV10 remaining unligated backbone (Figure 6.2A, lanes 2 & 3; Figure 6.2B, lanes 1 & 2) shows that the overall efficiency of the intermolecular ligation reaction was low. However there was the potential to obtain positive clones from this ligation reaction, which was therefore transformed into TSB competent *E. coli* Jm101. Ampicillin resistant bacterial colonies were picked from antibiotic containing plates.

6.2.2.3 Restriction digest analysis of ligated plasmids

Minipreps were made from each of the potential positive colonies recovered from the transformation plates as described in Materials and Methods. The extracted plasmid DNA was digested with 1U *EcoRI* to determine which colonies contained the 2.3kb mAspAT insert cDNA. Figure 6.3 shows a 1% agarose gel of the miniprep digests. Only one of the ten clones analysed on this gel contains a 2.3kb insert (marked with an arrow in lane 1). This plasmid was subjected to further restriction analysis. The remaining colonies were false positives, perhaps due to incomplete dephosphorylation and subsequent re-ligation of the vector backbone.

To determine if this miniprep contained the mAspAT cDNA insert in the correct orientation to allow expression of the mAspAT cDNA from the HCMV mIE promoter, a restriction digest was performed using *SstI* and *NcoI*. The *SstI* site lies within the HCMV immediate early promoter and the *NcoI* site lies 89bp within the mAspAT cDNA. Figure 6.4 shows the digest schematically, and the fragments expected from the digestion with *SstI* and *NcoI* of:- a) plasmid with the mAspAT cDNA inserted in the correct orientation and of b) plasmid with the insert in the wrong orientation. These enzymes cut the plasmid in such a way as to determine the orientation of the cDNA insert with respect to the HCMV mIE promoter by analysis of the size of the fragments produced. A plasmid containing the cDNA insert in the correct orientation would produce fragments of approximately 6.2 and 0.15kb, whilst the opposite orientation would produce fragments of 3.8 and 2.4kb.

The number of bacterial colonies recovered which contained the mAspAT cDNA insert in the correct orientation to facilitate expression was low. One would expect a 1:1 ratio of each insert orientation to be obtained from this experiment, and the reason for the heavy bias towards the opposite orientation in this case is unclear. Statistically however, the number of colonies tested is small and the ratio might

Figure 6.3. Restriction digest analysis of pCMV-mAspAT plasmid clones.

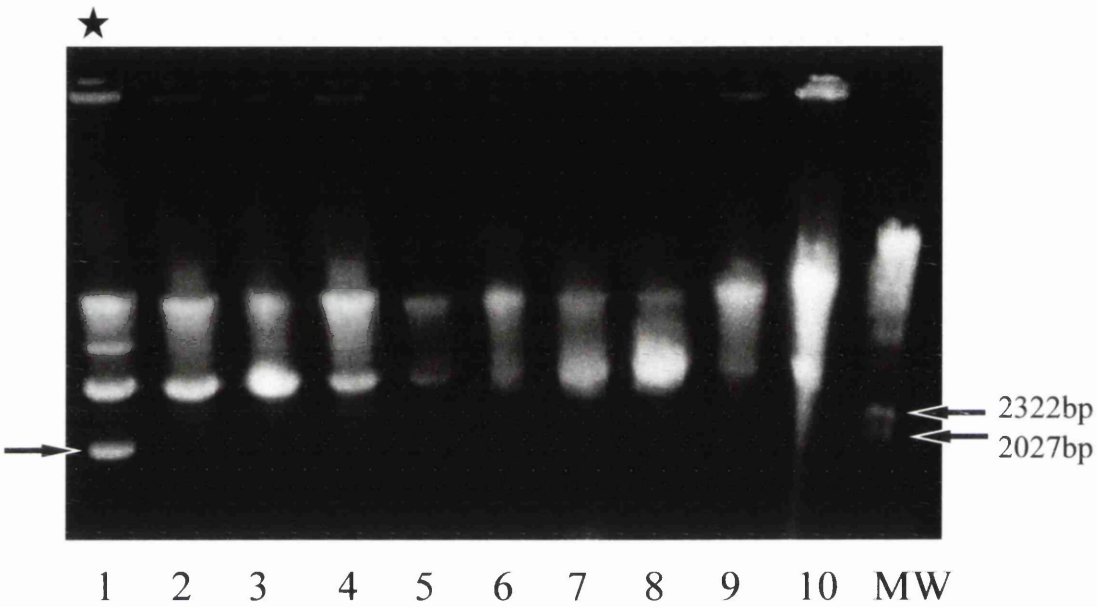

Legend. Plasmid DNA was extracted from colonies recovered from transfections of ligated pCMV10-mAspAT and digested with EcoRI. Digested DNA was electrophoresed on a 1% agarose gel to analyse the size of the cDNA insert contained. Only 1 of the 10 clones isolated in this experiment contained the correct insert (lane 1) marked with an arrow. The remaining clones appear to have no insert, and are probably re-ligated pCMV10, due to incomplete dephosphorylation of the vector backbone.

Figure 6.4. Restriction digest analysis of pCMV-mAspAT plasmid.

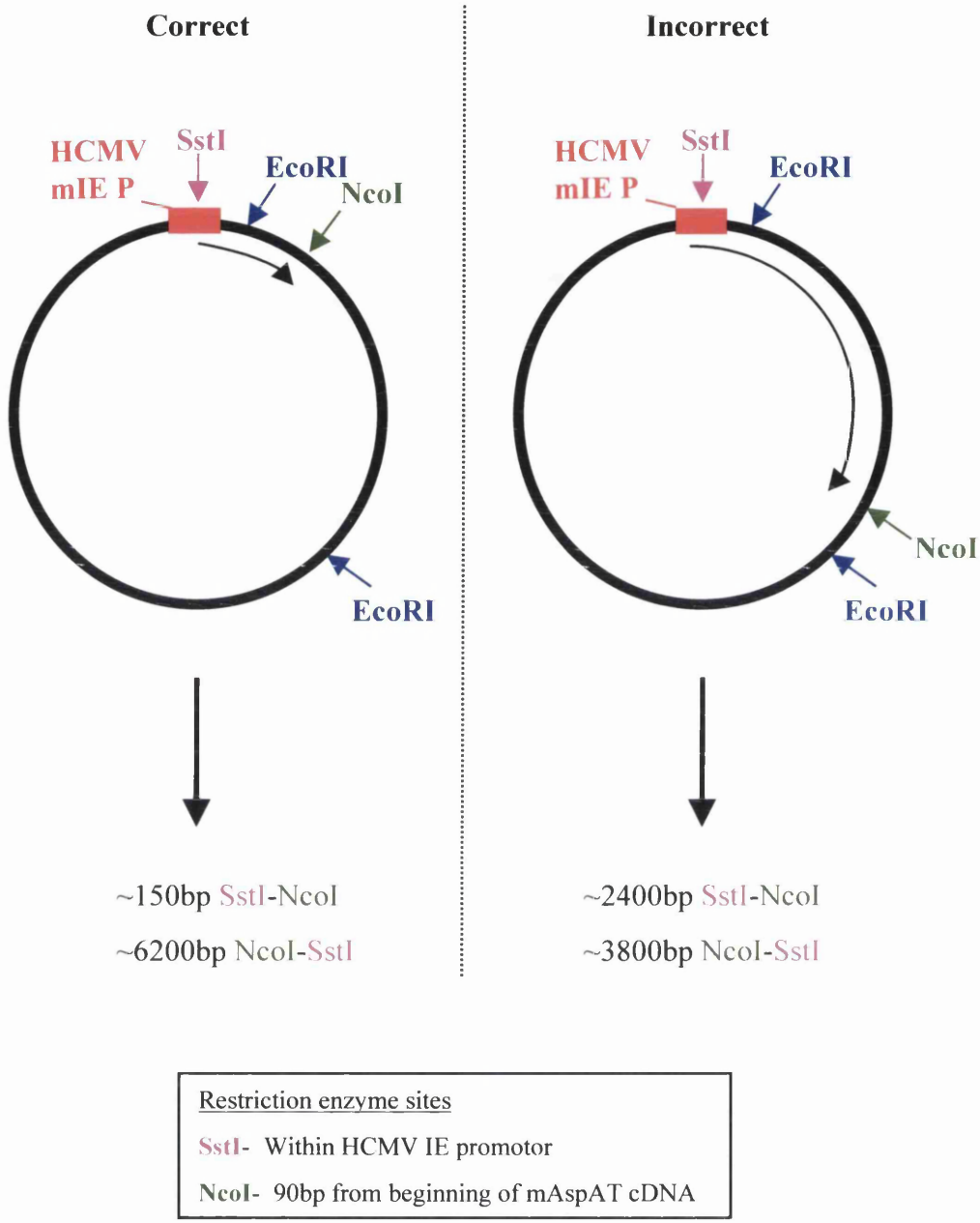

Legend. Schematic representation of a restriction enzyme digest designed to determine the orientation of the mAspAT cDNA insert within recovered pCMV-mAspAT clones.
mAspAT cDNA was excised from pBS-KS using *EcoRI* and ligated into the *EcoR1* site of pCMV10. Positive clones were recovered from transformed bacteria and plasmid DNA extracted. The plasmid DNA was digested with *SstI* which cuts within the HCMV immediate early promoter, and *NcoI* which cuts at position 89 of the mAspAT cDNA (the cleavage point for removal of the presequence). The digest allows clones containing the correct orientation of the mAspAT insert (to allow expression from the CMV immediate early promoter) to be selected by analysis of the digest on an agarose gel.

improve if more colonies were available for analysis. The plasmid recovered from this experiment was designated pCMV-AspAT1.

To confirm that this plasmid actually expressed mAspAT in transfected cells, immunofluorescence experiments were performed (Section 6.3 below).

6.3 CONFIRMATION OF mAspAT EXPRESSION FROM pCMV-mAspAT1.

6.3.1 Large scale preparation of pCMV-AspAT1

A 10ml overnight culture of a bacterial stock of pCMV-mAspAT1 was diluted into 100ml 2YT and grown overnight with shaking at 37 ° C. Plasmid DNA was extracted by following the protocol provided with the Qiagen tip 100® purification kit. Yields ranged from 70-90 μg of plasmid DNA. The plasmid DNA was stored at -20 ° C for use in subsequent experiments, and a bacterial stock containing the plasmid stored at -70 ° C.

6.3.2 Immunofluorescence experiments to confirm expression of mAspAT in transfected cells.

To confirm that mAspAT was being expressed from the HCMV mIE promoter on the pCMV-mAspAT1 plasmid, immunofluorescence experiments were performed with NRK 536 cells transfected with varying amounts of pCMV-mAspAT1. 60mm plates of 70% confluent cells were transfected with 1μg, 5μg or 10μg of pCMV-mAspAT1 and allowed to recover overnight at 37 ° C prior to trypsinisation and re-seeding of a small proportion into plates containing glass coverslips. After overnight incubation the coverslips were removed, washed three times in PBS-A and fixed for 15 minutes in 3:1 MeOH/Acetone. Coverslips were probed with a 1/200 dilution of a rabbit antiserum to mAspAT and a 1/85 dilution of FITC-anti rabbit conjugate. Coverslips were examined using a Nikon epi-fluorescence microscope, and micrographs are shown in Figure 6.5. Panels A, B and C show images at increasing magnification from cells on a single coverslip transfected with 1μg of pCMV-mAspAT1. The fluorescence is mainly cytoplasmic, with the nucleii appearing dark. However, within the cytoplasm the fluorescence is not homogeneous, and areas of stronger fluorescence are visible (see cells at the top of Panel C, Figure 6.5). Panels D, E and F show images from a coverslip from a plate of cells transfected with 10μg of the mAspAT expressing plasmid. A similar fluorescence pattern is observed, although there are many more rounded cells visible on this plate.

Legend. Immunofluorescence experiments were performed to confirm that the pCMV-mAspAT1 plasmid (Section 6.2.3) expressed mAspAT polypeptide in transfected cells. 60mm plates of NRK 536 cells were transfected with 1μg of pCMV-mAspAT1 or pCMV10 by calcium phosphate precipitation. After overnight incubation to recover from the transfection procedure, the cells were trypsinised and 1/10 were re-seeded in plates containing glass coverslips. After overnight incubation the cells were fixed in 3:1 MeOH:Acetone, probed with a 1/200 dilution of an anti-mAspAT antiserum and detected with an FITC-anti rabbit conjugate (1/85).

Panels A-C show increasing magnification of cells from one pCMV-mAspAT1 transfected plate. The fluorescence is mostly cytoplasmic, and the nuclei appear as dark ovals within the cell. Examination of the cell marked in Panel C with a white arrow suggests that the distribution of mAspAT throughout the cytoplasm is not homogeneous, although at this resolution it is not possible to determine what (if any) structures the mAspAT is associated with.

Panels D and E (overleaf) show 10x and 20x magnifications of cells from a different plate of cells, again transfected with the mAspAT expression plasmid (pCMV-mAspAT1). The fluorescence pattern is similar to that observed in Panels A-C.

Panels F and G (overleaf) show cells transfected with the parental control plasmid (pCMV10). Although there is a low background of fluorescence in these cells due to the normal cellular mAspAT enzyme, the level of fluorescence is much reduced in comparison to the cells transfected with pCMV-mAspAT1 (Panels A-E).

These experiments confirm that pCMV-mAspAT1 expresses mAspAT polypeptide in transfected cells.

Figure 6.5. Immunofluorescence in NRK 536 cells transfected with a mAspAT expressing plasmid.

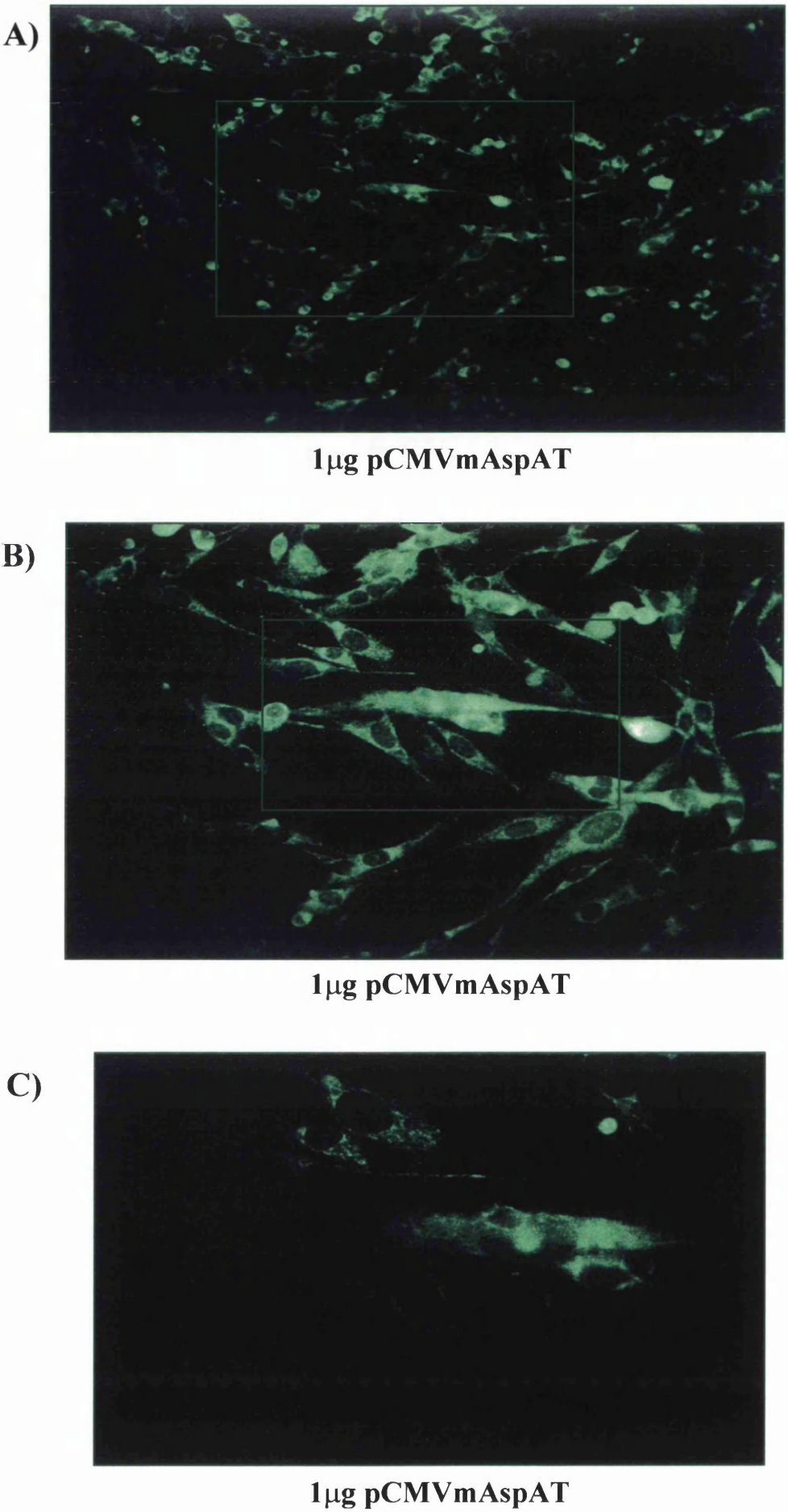

Figure 6.5. Continued.

D)

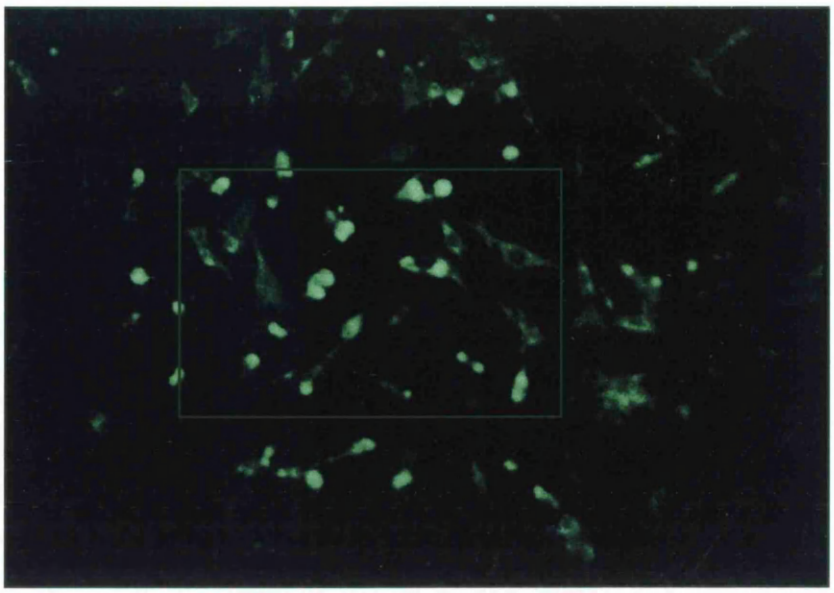

10x

10μg pCMVmAspAT

E)

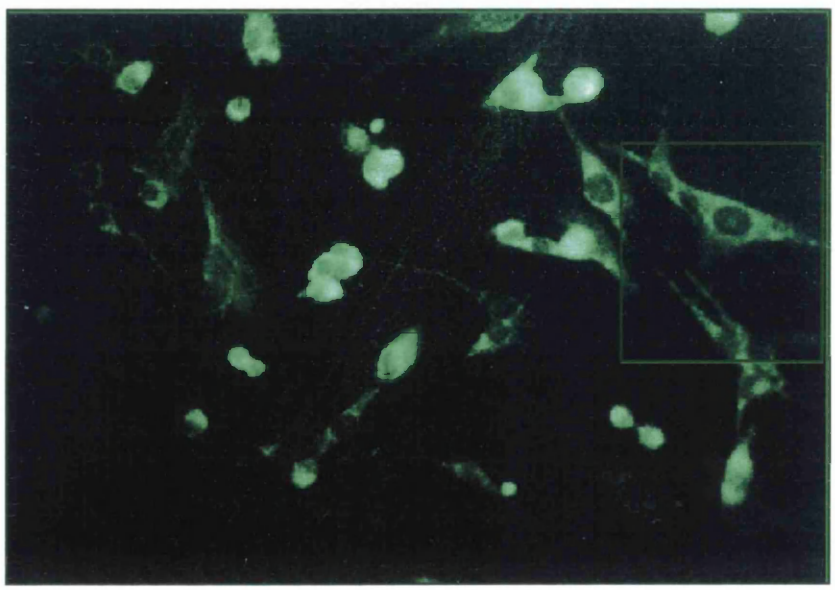

20x

10μg pCMVmAspAT

F)

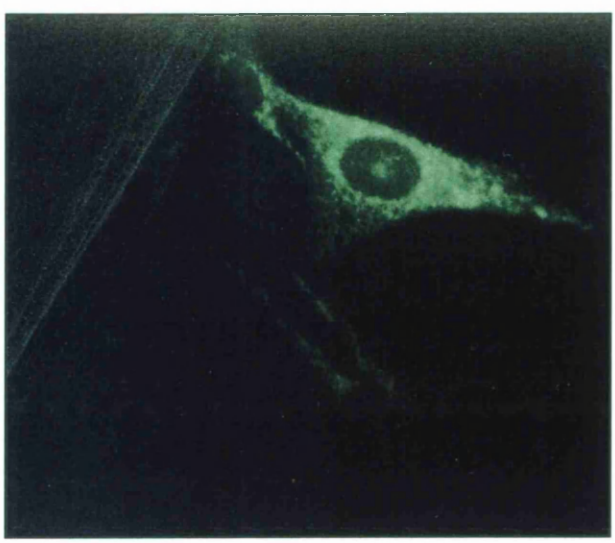

40x

10μg pCMVmAspAT

Figure 6.5. Continued.

G)

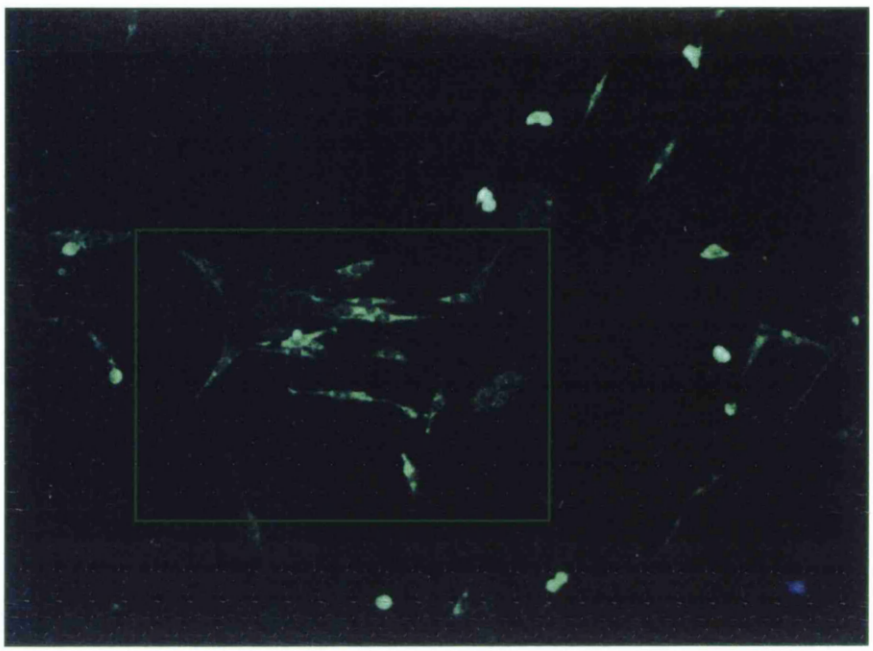

10x

1μg pCMV10 control

H)

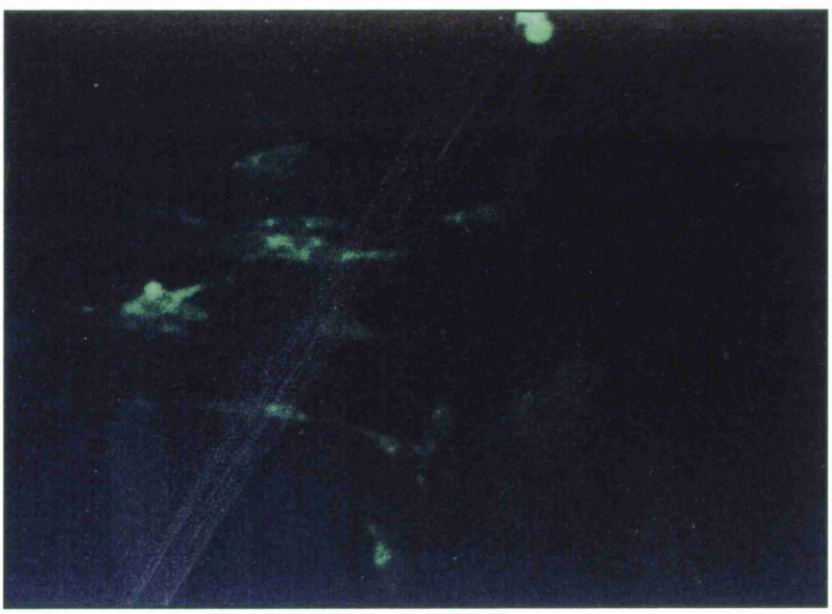

20x

1μg pCMV10 control

Panels G and H show cells transfected with the parental pCMV10 plasmid as a control. There is some background fluorescence in these cells, probably due to the presence of the constitutive cellular mAspAT enzmye. However, the number of cells displaying fluorescence is much reduced in comparison to the cells which contain the mAspAT expressing plasmid (Panels A-F). This experiment confirms that the pCMV-mAspAT plasmid expresses mAspAT in transfected NRK 536 cells.

6.4 LIPOFECTION OF CELLS WITH pCMV-AspAT1 AND TRANSFORMATION ASSAYS.

6.4.1 Lipofection.

NRK 536 cells were grown as monolayers in 60mm tissue culture plates as described in Materials and Methods. Cells were lipofected with varying amounts of pCMV-mAspAT1, pCMV10 or with the lipofection agent (DOTAP, Boehringer Mannheim) alone. In initial experiments, cells were co-transfected with a plasmid (pSV2Neo) expressing a neomycin resistance gene. 400μgml^{-1} of G418 was used to select transfected cells, whilst this was reduced to 100μgml^{-1} for maintenance of stably transfected cell lines. However, over extended passage (several weeks) even the initially selected cells appeared to be adversely affected by the G418 antibiotic and the viability of the mAspAT/pSV2Neo co-transfected cells was poor. Therefore in subsequent experiments, when cells were to be used in transformation assays, no selection procedure was used.

6.4.2 Colony formation in soft agar.

After overnight incubation at 37 ° C to allow the cells to recover from the lipofection procedure, cells were removed from the monolayer by trypsinisation. The cells were resuspended to make a single cell suspension and a proportion were replated on a 60mm tissue culture plate, or were suspended in soft agar for the colony formation assay, as described in Materials and Methods. The soft agar plates were examined next day to confirm that single cells had been seeded. Plates were incubated at 37 ° C in a humid atmosphere and were monitored to ensure that the agarose did not dry out. After 5 days at 37 ° C to allow the cells to recover, the plates were observed daily under the microscope to identify the formation of colonies in soft agar, or of foci of cells on the 60mm plates.

After approximately 14 days incubation, colonies of cells were visible in the soft agar plates. A colony was defined as a cluster of cells with a diameter greater than 100μm originating from a single progenitor cell. The plates were divided into eight sectors, and the number of colonies were counted in both the control and mAspAT transfected cell plates. The results are shown in table 6.1A.

Table 6.1B presents the data as the total number of colonies in each lipofected plate. The cells lipofected with all concentrations of pCMV-mAspAT1 produced more colonies than the control pCMV10 treated cells (mean 152 compared to 63 in the control for $4x10^5$ cells plated). There is however, a background level of colony formation with the NRK 536 cells used in these experiments. Treatment with DOTAP alone results in the formation of approximately 60 colonies per $2x10^5$ cells plated. In these experiments a control using NRK 536 cells that had received no treatment at all was not included. This would have provided a measure of the true basal level of colony formation of NRK 536 cells. Furthermore, there is a reduction in the number of colonies formed by transfection of cells with 10μg of pCMV-mAspAT1 compared to transfection with 4μg or 6μg. This may be an effect of the overexpression of mAspAT in these cells, perhaps due to disruption of normal cellular metabolism. This is discussed later in Section 6.6.

Figure 6.6 shows representative micrographs (bar = 100μm) of colonies formed in soft agar by cells lipofected with A) pCMV-mAspAT1 and B) pCMV10. There are more colonies present in the pCMV-mAspAT1 lipofected plate (A) than in the control plate (B). Some clumps of cells are visible in these pictures. These are due to the incomplete resuspension of the cells during trypsinisation and plating in the soft agar. They appear as fuzzy dead looking clumps (marked with an empty arrow in each image) and are obviously distinct from the growing colonies present in these pictures (marked with filled arrows in Figure 6.6A).

The appearance of colonies in soft agar following transfection with a mAspAT expressing plasmid reflects the loss of anchorage dependence and contact inhibition of these cells and is a measure of transformation. It is normal to calculate a transformation efficiency relative to the number of viable cells plated. However, as no determination of cell viability was made in these experiments, my results are calculated relative to the total number of cells plated. Table 6.2 shows the %

Legend. $1x10^6$ NRK 536 cells were lipofected with 2μg, 4μg,,6μg or 10μg of pCMV-mAspAT1, 10μg of the pCMV10 control plasmid, or with no plasmid DNA (DOTAP reagent alone). A proportion of the cells (0.2 or 0.4) were plated in soft agar and incubated at 37 °C. Colonies which had a diameter greater than 100μm were counted after approximately 14 days.

In Table **6.1A** the number of colonies counted in each of the eight sectors into which the plates were divided are presented for each plate. The total number of colonies in each plate is also presented. The plate labelling (e.g. 1.02) is as follows- the prefix refers to the treatment the cells received, as detailed in Table **6.1B**, and the suffix refers to the number of cells plated. $0.2=0.2x10^5$ cells.

The dotted line across the tables seperates the control treatments from the cells lipofected with various amounts of pCMV-mAspAT1.

The data from this experiment is summarised in Table **6.1B**. The number of colonies for each cell treatment for both numbers of cells plated is given. A calculation of the percentage transformation efficiency is presented in Table 6.2, and micrographs from pCMV-mAspAT1 and pCMV10 lipofected cells are shown in Figure 6.6.

Table 6.1A. Colony formation in soft agar. Transformation assay following lipofection of NRK 536 cells with a mAspAT expressing plasmid.

	Number of colonies of diameter >100μm in each sector								
Plate	1	2	3	4	5	6	7	8	Total
1.02	7	14	12	8	5	8	0[a]	0[a]	72[b]
1.04	18	13	14	13	21	12	12	7	110
2.04	6	12	10	5	6	8	8	0[a]	63[b]
3.02	11	11	6	9	9	11	9	10	76
3.04	16	13	17	20	19	17	16	0[a]	135[b]
4.04	17	16	18	28	19	16	24	21	159
5.02	6	5	12	8	8	0[a]	0[a]	0[a]	61[b]
5.04	32	24	18	20	27	15	0[a]	0[a]	181[b]
6.02	19	11	9	15	10	16	0[a]	0[a]	93[b]
6.04	30	15	12	12	10	15	15	22	131

a; Sectors had fungal contamination obscuring any colonies present, and were not counted.
b; Totals calculated by averaging results from sectors counted and multiplying by 8.

Table 6.1B. Total number of colonies obtained by transfection of various amounts of mAspAT expressing plasmids.

			Number of NRK 536 cells plated	
			2x 10^5	4x 10^5
Plate prefix	Cell treatment	μg plasmid	Corrected total number of colonies on plate	
1	DOTAP[c]	n/a	72	110
2	pCMV10		[d]	63
3	pCMV-mAspAT	2	76	135
4	pCMV-mAspAT	4	[d]	159
5	pCMV-mAspAT	6	61	181
6	pCMV-mAspAT	10	93	131

c; lipofection control
d; These plates were fungally contaminated and were not able to be analysed..

Figure 6.6. Colony formation in soft agar following transfection of NRK536 cells with a plasmid expressing mAspAT.

A)

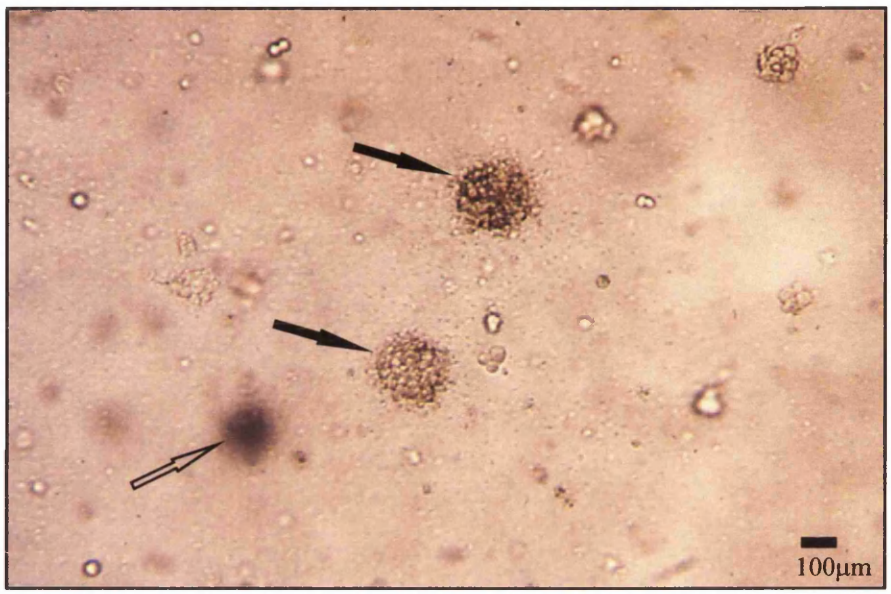

B)

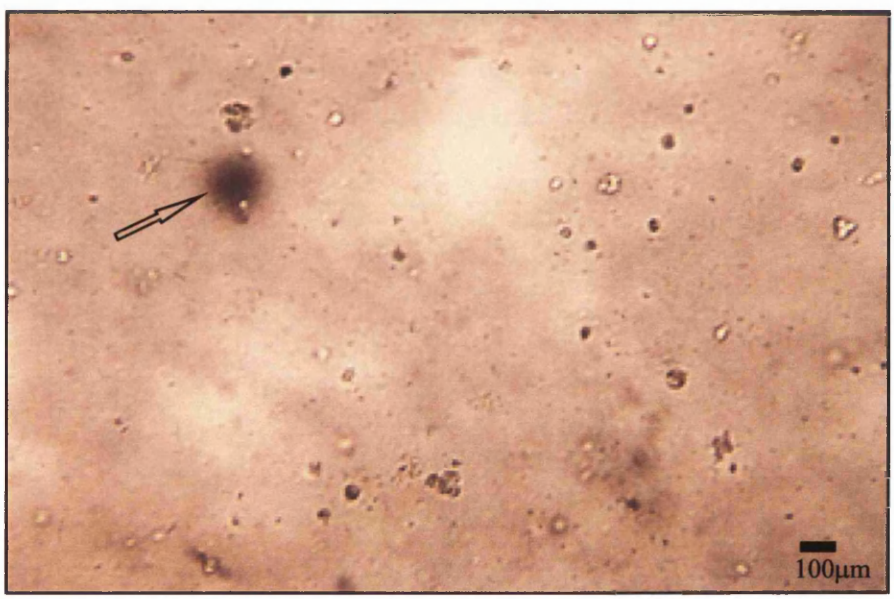

Legend. NRK 536 cells were transfected with a plasmid construct expressing mAspAT under the control of the HCMV mIE promotor (Panel A) or with the parental plasmid (Panel B).
Single cells were seeded into soft agar and incubated at 37C for 2-3 weeks while colonies formed. Colonies over the arbritary cut off size of 100μm were counted (labelled with filled arrows in Panel A) and the number of colonies in each sample compared-see Table 6.1B.
Some clumps of dead cells are apparent in both samples (labelled with an empty arrow), but these have an appearance distinct from colonies of viable cells.

Table 6.2. Percentage transformation efficiency for colonies obtained by lipofection of various amounts of mAspAT expressing plasmid into NRK 536 cells compared to control lipofections.

			Number of NRK 536 cells plated		
			2×10^5	4×10^5	
Plate prefix	Cell treatment	µg plasmid	% of cells that formed colonies >100µm diameter		Mean % of cells
1	DOTAP[c]	n/a	0.36	0.275	0.318
2	pCMV10	5	*d*	0.158	0.158
3	pCMV-mAspAT	2	0.38	0.338	0.359
4	pCMV-mAspAT	4	*d*	0.398	0.398
5	pCMV-mAspAT	6	0.305	0.453	0.384
6	pCMV-mAspAT	10	0.465	0.328	0.397

c; lipofection control

d; These plates were fungally contaminated and were not able to be analysed..

Legend. NRK 536 cells were lipofected with various amount of pCMV-mAspAT, with 5µg of the control plasmid or with no plasmid DNA. The cells were incubated at 37°C overnight to recover, and then 2 or 4×10^5 cells were plated into soft agar. Colonies which formed from a single progenitor cell with a diameter greater than 100mm were counted in each of the plates, and a calculation of the percentage of seeded cells that produced colonies was made. This is not a true 'Transformation efficiency' as the number of viable cells was not determined. This explains the low % transformation efficiency. The number of colonies in the plates transfected with the mAspAT expressing plasmid is approximately 2.5x greater than in the pCMV10 transfected plate. However, as the lipofection reagent alone increased the number of colonies present, no conclusions can be drawn from this experiment.

transformation efficiencies for each plate. The mean transformation efficiency for all mAspAT transfected NRK 536 cells was 0.38%, compared to 0.24% for the control lipofected and DOTAP treated cells. This level of colony formation represents a 1.58 fold increase, but is not statistically relevant without further repetition of this experiment.

The parallel experiment involving the transfected cells plated out for analysis of foci formation became contaminated prior to quantitative analysis, and no data was obtained from this experiment.

6.5 TUMOUROGENICITY IN NUDE MICE.

It had been planned to inject cells derived from the colonies which formed in soft agar into nude (athymic) mice to examine the tumourogenicity of these cells *in vivo*. Colonies were transferred from the soft agar plates to a tissue culture plate and dispersed using a sterile pasteur pipette. However, during the subsequent incubation period, fungal contamination became apparent. This necessitated the destruction of the cells obtained from the growth in soft agar experiments described above.

Nude mice had been purchased in order to assess the tumourogenicity of the cells which subsequently became contaminated. These animals have a limited life-span dependent to a large extent upon their exposure to pathogens, and within the Institute of Virology, these animals usually live for 3-5 months (Joan Macnab, personal communication). There is therefore a 'window of opportunity' in which to inject the mice, whilst allowing sufficient time for tumours to develop during the lifespan of the mouse. This period is up to about 10 weeks from the birth of the mouse. Due to the nature of these experiments, it was not possible to repeat the transfection and colony formation experiments and to grow up the transformed cells within this time period. It was therefore decided to repeat the lipofections of NRK 536 cells with the mAspAT expressing and control plasmids, and inject the lipofected cells, omitting the colony formation step.

NRK 536 cells were lipofected with pCMV-mAspAT1, pCMV10 and DOTAP as detailed in Table 6.3. Following an overnight incubation to recover from the lipofection procedure, the cells were harvested for sub-cutaneous injection into the nude mice. Approximately 10^6 cells (1x confluent 60mm plate) were injected sub-

cutaneously into the back of the neck of the nude mice by Dr Joan Macnab, Institute of Virology, Glasgow.

After 3-4 weeks tumours were observed in the mice. The mice were sacrificed prior to external examination of the morphology and size of the tumours present. This examination was performed 'blind'- at the time of the examination I was unaware which mouse had been injected with which of the lipofected cells. The results are presented in Table 6.3.

These results were inconclusive with respect to the effect of mAspAT expression on the tumourogenesis of NRK 536 cells. Tumours were present in animals injected with the pCMV10 lipofected control cells or cells treated with DOTAP alone. Analysis of the amount of tumour tissue present in the mice revealed that there was no correlation between the amount of pCMV-mAspAT1 transfected into NRK 536 cells and the tumourogenicity of the transfected cells *in vivo*. It was decided not to explant the tumours for tissue culture and further phenotypic analysis because these results were inconclusive. Time constraints unfortunately prevented the repetition of this series of experiments.

6.6 DISCUSSION.

Attempts were made to clone the mAspAT cDNA insert into a eukaryotic expression vector to facilitate analysis of the effects of over-expression of mAspAT in cells. Cloning directionally into pCMV10 (*Section 6.2.1*) failed. The reason for the failure with pCMV10 remains unclear.

The mAspAT cDNA was finally cloned non-directionally into pCMV10 at the unique *EcoRI* site. This protocol required fewer manipulations, and was in effect a direct sub-cloning of the mAspAT cDNA insert cloned into pBS-KS by Mattingley *et al.* (1987). The efficiency of the ligation reaction was still low, and in the experiment shown (*Section 6.2.3.3*) only one of the ten clones analysed contained the mAspAT cDNA insert. A restriction digest was designed to differentiate between the two possible orientations of the cDNA insert with respect to the HCMV mIE promoter. By analysis of the fragments recovered, a single clone was picked which had the mAspAT cDNA in the correct orientation. To confirm that this plasmid was at least transiently expressing mAspAT in transfected cells, the plasmid was transfected (calcium phosphate) into NRK 536 cells, and these were compared with

Table 6.3. Tumour formation in nude mice following sub-cutaneous injection of cells transfected with a mAspAT expressing plasmid.

Mouse	Treatment	µg plasmid	No of tumours	Dimensions	Gross morphology
A	pCMV-AspAT1	1	2	0.6x 0.4x 0.2cm 0.3x 0.3x 0.2cm	Flatish- spread out across back of neck
B	pCMV-AspAT1	5	1	0.9cm diameter	Single large round tumour
C	pCMV-AspAT1	10	3[a]	0.8x 0.3x 0.3cm	Lumpy flat tumour which may have nodules
D	pCMV10	10	3	0.6cm diameter 0.4cm diameter 0.2cm diameter	3 roundish tumours clumped together
E	Control	n/a	1	1.1cm diameter	Single large round tumour

***a**;either a single mass of tissue or 3 tumours closely grouped- could not distinguish without excision of tumours.*

Legend. Nude mice were injected with 1x 10^6 NRK 536 cells which had been lipofected the previous day with plasmid expressing mAspAT (A-C), with the native plasmid (D), or with cells treated with only the lipofection agent (E) as a control. The mice were injected sub-cutaneously behind the neck and tumours which formed were examined externally after the mice were sacrificed.

control cells by immunofluorescence using an antiserum to mAspAT. These experiments showed a greater fluorescence in the transfected cells than in the control cells (*Section 6.3.2*) indicative of expression from the plasmid. There is a background level of fluorescence in the control cells due to the constitutive cellular mAspAT. By cloning the mAspAT cDNA into an expression vector that expressed an epitope tag (for example the HCMV UL83 epitope used by Leslie (1996)) at the end of the inserted mAspAT cDNA the expression of the protein could have been detected without these background problems.

Lipofection of the mAspAT expressing plasmid into NRK 536 cells resulted in the formation of colonies in soft agar. However the increase in the number of colonies formed, and in tumour formation in nude mice was not significantly elevated in cells lipofected with the mAspAT expressing plasmid compared to controls. Ideally, the NRK 536 cells transfected with mAspAT should have been selected, to ensure that only cells expressing mAspAT were used in the soft agar assays. Cells were initially co-transfected with a plasmid conferring neomycin resistance, and resistant clones were selected. However, these cells failed to grow properly, and could not be grown up in large amounts. It appears that either the cells were adversely affected by the G418 antibiotic, or that the cells were not growing for another unrelated reason. Previous experiments using these cells to show the transformation of cells by treatment with TGF-β (Vossbeck *et al.*, 1995) showed that stably transformed cells could only be obtained by treatment of individualised cells. Treatment of the cells whilst in contact with neighbouring cells (i.e. as monolayers) before plating into soft agar led to induced apoptosis of the transformed cells. A similar apoptotic effect could be occurring in the experiments described in this chapter, but as the experiments required lipofection of a plasmid into the cells it would be impossible to treat individual cells in soft agar. Apoptosis of lipofected cells might explain the reduced number of colonies formed in the cells lipofected with 10μg of pCMV-mAspAT1 compared to those lipofected with 2μg, 4μg or 6μg of plasmid. However, a cellular DNA fragmentation ELISA kit (Boehringer Mannheim) which detects the fragmented DNA characteristic of apoptosis, failed to demonstrate apoptosis in any of the lipofected cells. The reduced number of colonies could also be a result of the overexpression of mAspAT in the cell. This could cause disruption of cellular

metabolism by disturbing the equilibrium of the malate-aspartate shuttle, which functions to transfer reducing equivalents (from NADH) into the mitochondria. Alternatively, the uptake of long chain fatty acids into the cell could be increased, as mAspAT has been shown to be identical to the fatty acid binding protein (Stump *et al.*, 1993). This is discussed further in the General Discussion at the end of this thesis.

7. AMPLIFICATION, CLONING AND DNA SEQUENCING OF A SMALLER mAspAT cDNA FROM HSV-2 INFECTED Bn5T CELLS.

7.1 INTRODUCTION.

During both the Northern blotting and RT-PCR experiments to examine the change in the level of the mAspAT mRNA in cells following infection with HSV, I noticed that an additional minor transcript or cDNA product was present in the samples from HSV infected cells. This minor species had a slightly lower molecular weight than the major transcript or cDNA product.

The presence of a smaller mAspAT transcript in HSV infected cells could explain the appearance of the 40kDa polypeptide (identified as a form of mAspAT by Lucasson, 1992) in transformed and HSV infected cells, in addition to the constitutive mAspAT polypeptide. To study the difference between this smaller transcript and the constitutive mAspAT mRNA, the minor transcript was amplifed to produce a cDNA by RT-PCR, cloned into M13 phage and subjected to DNA sequence analysis.

The mAspAT gene is highly spliced. The mouse mAspAT gene contains ten exons ranging in size from 20 to 59 amino acids, and spanning approximately 25kb of the genome (Morino and Shimada, 1990). The smaller transcript observed in HSV-2 infected Bn5T cells could be due to alternative splicing. Splicing out of one exon could result in the production of a truncated cDNA approximately 60bp to 180bp shorter. This would represent a polypeptide some 2 to 6kDa shorter. If the first exon (29 amino acids) containing the presequence (which encodes the mitochondrial targetting signal) was absent, this would cause aberrant expression of mAspAT within HSV infected cells. J.C.M. Macnab (personal communication) has previously noted the altered localisation of mAspAT in transformed cells observed by immunofluoresence. mAspAT fluorescence was visible at the cell surface in transformed, but not control cells.

The following work was designed to investigate the difference between the major and minor transcripts from HSV-2 infected cells by cloning and sequencing the minor transcript and comparing this with the published sequence of rat mAspAT (Mattingley *et al.*, 1987).

7.2 RT-PCR AMPLIFICATION USING PCR PRIMERS 9301 AND 9302 AND CLONING OF THE MINOR mAspAT TRANSCRIPT INTO M13.

An adaptation of the RT-PCR protocol used to analyse the amount of mRNA present in HSV infected and mock infected cells (*Section 4.3*) was used to produce cDNAs for subsequent cloning into the M13mp19 sequencing vector. Following reverse transcription of 3μg of total cellular RNA, 40 cycles of PCR amplification were performed using the primers 9301 and 9302 (Figure 4.4). Following amplification, samples of the PCR products from mock infected and HSV-2 infected Bn5T cell RNA were electrophoresed on a 30cm long 1.5% agarose gel at 100V overnight, to facilitate good separation of the closely related mAspAT cDNA products. To reduce damage to the cDNAs prior to cloning, the DNA bands were visualised by ethidium bromide staining and long wave ultraviolet irradiation of the gel for as brief a period of time as possible.

Figure 7.1 shows a representative gel from this experiment. A positive PCR control containing mAspAT plasmid as template, and a negative control (no template) were included (lanes 2 and 3). A single PCR product is present in the mock infected sample (lane 4), migrating just above the 1375bp molecular weight marker (lane 6). In the HSV-2 infected sample (lane 5) this product is more abundant, and an extra PCR product is visible. This has a molecular weight less than 1375bp, and is less abundant than the larger molecular weight band. Both PCR products from the HSV-2 infected sample are marked with arrows at the right of the gel.

The minor cDNA product and the larger constitutive cDNA were excised from the gel and the DNA was purified using Sephaglas®.

In initial experiments the ends of these purified cDNAs were filled in, and blunt end ligated directly into M13mp19 digested with SmaI as described in as described in Materials and Methods. However, this procedure proved to be very inefficient. The following alterations to the protocol were made.

7.3 RT-PCR AMPLIFICATION USING PRIMERS 9301ECORI AND 9302XBAI, AND CLONING INTO pGEM-T.

The RT-PCR experiment was repeated using the PCR primers 9301-EcoRI and 9302-XbaI (Figure 7.2) which were the same primers as previously described but with the relevant restriction enzyme site and 3 random nucleotides added to the end. Following amplification, the cDNA products were purified directly from the

Figure 7.1. Different sized mAspAT PCR products from HSV-2 and mock infected Bn5T RNA.

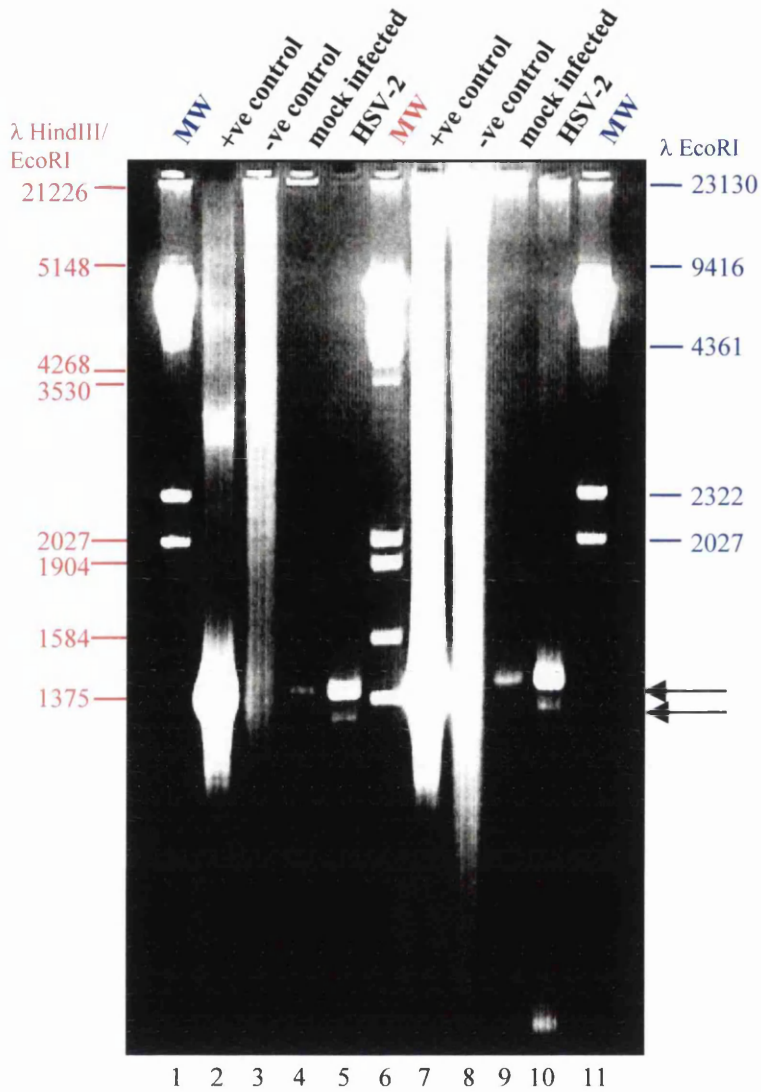

Legend. Agarose gel electrophoresis of RT-PCR products from Bn5T cell RNA. RNA from Bn5T cells mock infected or infected with 10 pfu/ml of HSV-2 HG52 was reverse transcribed and amplified by PCR as described in Materials and Methods. Lane 1 contains λ *HindIII* DNA markers. Lanes 2 and 3 contain positive and negative controls respectively. Lane 4 contains PCR products from mock infected Bn5T cell RNA, and shows a single product of approximately 1.4kbp. Lane 5 contains PCR products from HSV-2 infected Bn5T cell RNA, containing larger amounts of the product present in the mock infected sample, and an additional slightly smaller product (about 1.3kbp). These two products are marked with arrows to the right of the gel. The expected size of the PCR product is 1421bp. Lane 6 contains λ *HindIII/EcoRI* DNA markers. The samples in lanes 7-10 are as for lanes 2-5.

Figure 7.2. PCR primers containing restriction enzyme sites.

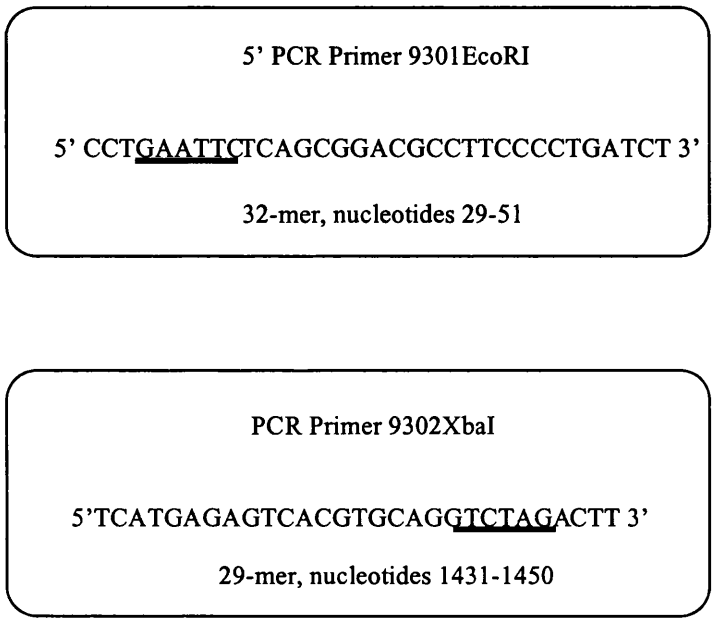

Legend. PCR primers were synthesised from the cDNA sequence of mAspAT (Mattingley et al., 1987), containing a restriction enzyme recognition site, and 3 extra nucleotides at the end of the primer. This was to ensure any errors introduced at the end of the PCR products did not abolish the enzyme sites. The primers are essentially the same as those presented in Figure 4.4.

RT-PCR reaction mixture using the Sephaglas® kit. The PCR products were digested with *EcoR1* and *XbaI* to remove the excess nucleotides from the cDNA ends and provide 'sticky ends' for ligation into PGEM-T, which was restricted with these same enzymes. *E. coli* JM101 competent bacteria were transformed with the ligation mixture and plated onto agar plates containing ampicillin and X-gal. Positive (white) clones were picked for further analysis. DNA minipreps were made from these colonies, and the DNA was digested with *EcoR1* and *XbaI*. Analysis on a 1.5% agarose gel (Figures 7.3A and 7.3B) allowed the isolation of clones containing smaller PCR products. In Figure 7.3A, the PGEM-T backbone migrates at about 3kbp as expected. Clones 1- 5 and 9-17 contain an insert of approximately 1.4kbp. The insert in clone 3 is slightly larger. The full length PCR product is expected to have a length of 1421bp. The clones marked with a star above the lanes were selected for sequence analysis.

In Figure 7.3B clones 41-61 contain an insert of about 800bp, and clones 11-31, 71, 72 and 74 an insert of about 2kb. The clones marked with a star were selected for analysis. A clone (57) from a different gel with a 1.4kbp insert was also selected for sequencing.

Single stranded DNA was produced directly from the PGEM-T clones and sequenced as described in Materials and Methods. However, the quality of the sequencing reactions was poor, and little information could be obtained from these sequencing gels. The cDNA inserts from the selected clones were therefore ligated into *EcoRI-XbaI* digested M13mp19. Single strand DNA preparation and sequencing using the Sequenase® kit (United States Biochemical) were performed as described in Materials and Methods. Sequencing from the M13 clones was successful. Synthetic oligonucleotide sequencing primers were made using the rat mAspAT cDNA sequence published by Mattingley *et al.* (1987), and were provided by Mr D. McNab in our laboratory. The M13 -40 primer and the primers used for the RT-PCR reaction were also used.

The DNA sequence obtained from each clone was analysed using the Wisconsin GCG package (version 9). Sequence was entered manually and aligned with the published cDNA sequence of rat mAspAT (Mattingley *et al.*, 1987).

Figure 7.3. Restriction analysis of PGEM-T clones recovered from RT-PCR of HSV-2 infected Bn5T cell RNA.

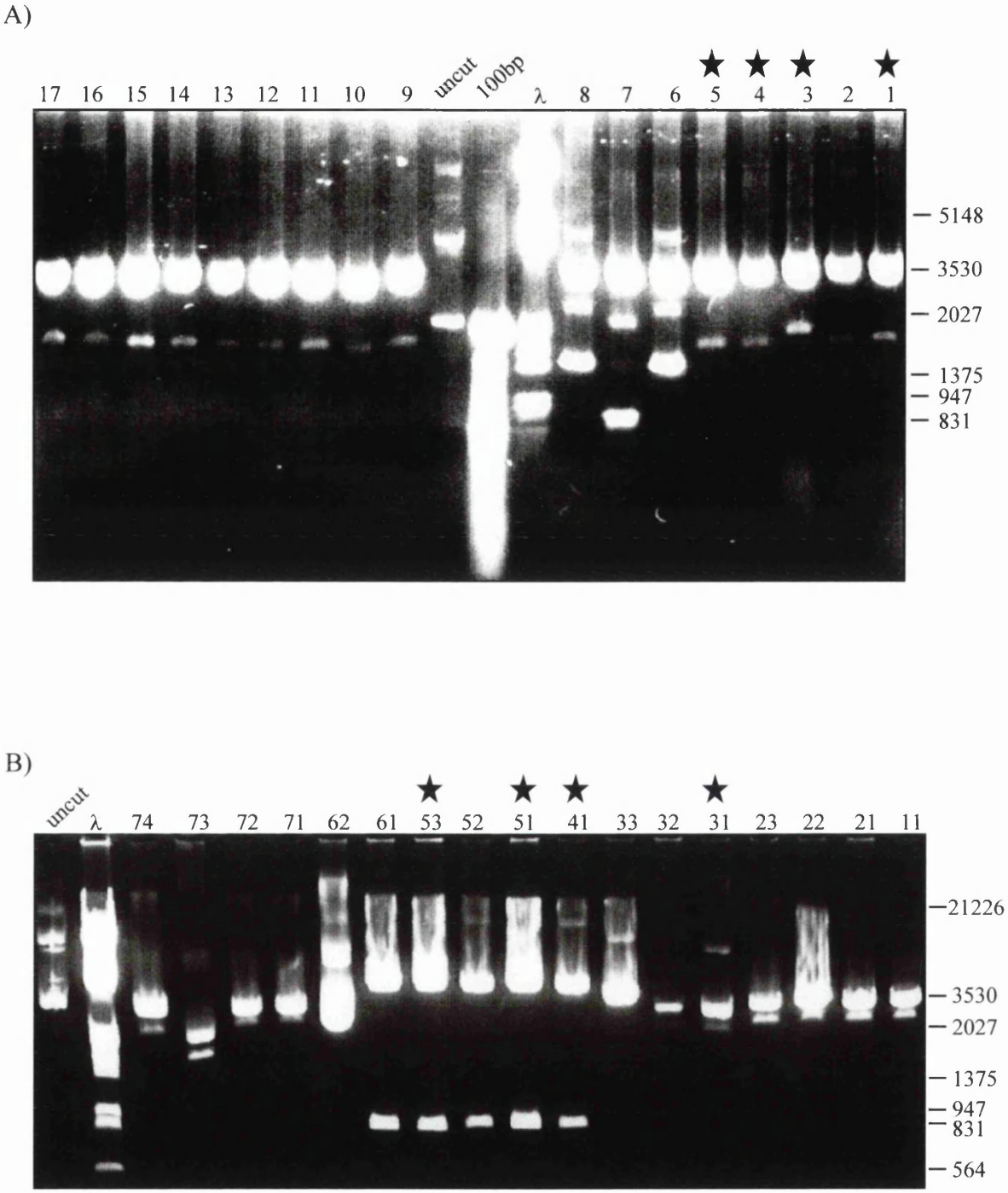

Legend. RT-PCR products from mock infected or HSV-2 infected Bn5T cell RNA were cloned into PGEM-T at the *EcoRI* and *XbaI* sites. The insert was excised from recovered clones with these same enzymes and electrophoresed on a 1% agarose gel. In Figure 7.3A, clones 1-5 and 9-17 contain cDNA inserts of approximately 1.4kbp, although clone 3 has a slightly larger insert than the others. In Figure 7.3B, clones 41-61 contain an insert of approximately 800bp, and 11-31, 71, 71 and 73 contain inserts greater than 2kbp in length. The clones marked with stars above the lane were selected for DNA sequencing.

Figure 7.4 shows the alignment of of the DNA sequence obtained from the 5' end of the PCR clones. The 5' untranslated region is shown in red, the initiation codon in green, and the pre-sequence is shown underlined in blue. The pre-sequence is encoded by a separate exon of 89nt, and codes for a 29 amino acid segment containing the mitochondrial targetting signal which is cleaved to release the mature protein. Differences from the consensus sequence are shown in black. No corrections have been made to the sequences shown. The homology between the sequence of the clones and mAspAT within the 5'UTR is good. There are a few differences, but these are likely to be gel reading errors, as the differences are not present in all clones which have the same size on agarose gels (see for example the 'a' at position 76 sequence 53p-40 and compare it to 51p-40 above). Within the first 40nt of the presequence, there are few differences between the obtained sequence and the consensus sequence. The sequence alignment for the remainder of the presequence contains a large number of gaps. This is due to problems reading the sequence from the top of the gels. The calculated consensus from this region is however identical to the mAspAT sequence. Few conclusions can be drawn from the limited data available, but it is interesting to note that the pre-sequence is likely to be present in both the 800bp (clones 51 and 53) and 1.4kbp (clones1-5, and 57) PCR products.

Table 7.1 shows a summary of all the sequence data available for all the clones analysed. No clone was sequenced completely, or from the opposite strand to confirm the data. An interesting observation concerning clone 53 can however be made. This clone has a size of around 800bp on an agarose gel (Figure 7.3B), yet contains sequence aligning with nucleotides 32-164 and 1051-1219 of the mAspAT sequence. There must therefore be an internal deletion within this clone, perhaps representing a splicing event. Completion of the sequencing of this clone would allow this possibility to be examined.

7.4 DISCUSSION.

RT-PCR experiments identified an additional product in Bn5T cells infected with HSV-2 compared to mock infected cells (*Section 7.2*). Clones were obtained in PGEM-T which contained differently sized PCR products (*Section 7.3*) from HSV-2 infected RNA. Two classes of PCR product were obtained- approximately 800bp

Figure 7.4. DNA sequence of PGEM-T clones of the smaller RT-PCR products from HSV-2 infected Bn5T cells.

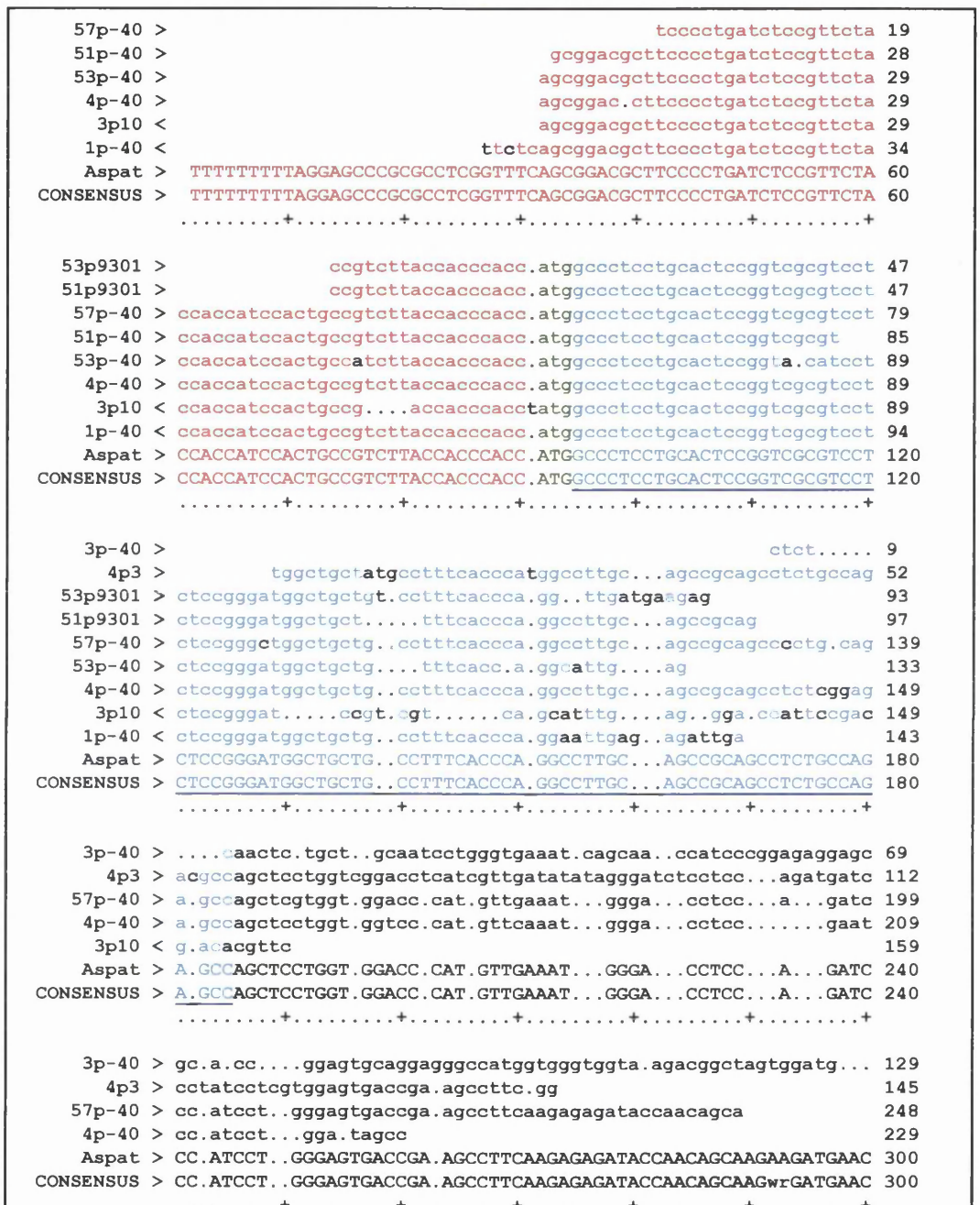

Legend. DNA sequence data obtained from the PGEM-T clones which contained shorter PCR products (see Figures 7.3A and B) was aligned with the cDNA sequence of mAspAT (Mattingley *et al.*, 1987) using programs from the GCG package. The 5' untranslated region is shown in red, and the ATG initiation codon in green. The pre-sequence of mAspAT is underlined and coloured blue. This region contains the mitochondrial targetting sequence and is cleaved to produce the mature protein. The consensus sequence is identical to the mAspAT sequence throughout this region. Differences from the consensus sequence in individual clones are coloured black. The sequence is labelled as follows- the number before the 'p' represents the clone and the number following the 'p' is the primer used.

Table 7.1. Summary of sequence data obtained from RT-PCR clones from HSV-2 infected Bn5T cells.

	PRIMER									
CLONE	-40	10	9301	3	41	31	23	21	26	25
1	26-169									
3	172-348	32-190								
4	33-260			129-273		471-708	493-591	823-1072		
5				748-936		478-667		789-912		
51	33-117		73-170		352-457					
53	32-164		73-166					1051-1219		
57	42-289				376-667				1178-1461	1222-1355
31					394-612					

Legend. The regions of the mAspAT cDNA sequence to which sequence data from the PGEM-T clones (Figure 7.3) was obtained is shown. The clone sequenced is shown in the first column, and sequence was obtained using the primers labelled in the top row. The full length of the PCR product is 1419bp. Clone 53 is interesting in that it contains sequence from both ends of the full length PCR product, but is only around 800bp long on agarose gels (Figure 7.3B). This must therefore represent an internal deletion within this cDNA, presumably representing different RNA splicing.
Primers used in sequencing represented the nucleotides of the published sequence of mAspAT as detailed below. **-40**= M13 -40 primer; **9301**= nt39-51; **3**= nt75-89; **41**= nt281-299; **31**= nt378-396; **23**= nt423-444; **21**= nt717-738; **26**= nt9909-1014; **25**= nt1128-1149.

long and a group containing inserts around 1.4kb. DNA sequence analysis from these clones showed that all clones contained the mAspAT presequence, and as such would be expected to locate to the mitochondria. One clone (53) appears to have an internal deletion(s) of about 400bp, and would be unlikely to code for a functional protein. This would be unlikely to be targetted to the mitochondria, as it has been shown that import into mitochondria is dependent upon the correct folding of the polypeptide chain, and interaction with specific chaperone proteins (Mattingley *et al.*, 1993).

Unfortunately no further conclusions can be drawn from this work without completing the sequencing of the smaller clones.

8. SUMMARY OF RESULTS AND GENERAL DISCUSSION.

8.1 SUMMARY OF RESULTS.

In this thesis I have demonstrated that:

1) The steady state level of mAspAT mRNA is increased approximately 1.8-2 fold in the Bn5T (transformed) cell line by infection with HSV-2 strain HG52 compared to HSV-2 infected control cells (*Chapter 4*). This value is consistent with the previously reported increases in the levels of mAspAT protein and enzyme activity (Lucasson , 1992; Lucasson *et al.*, 1994).

2) The HSV encoded dUTPase enzyme cross reacts with antisera raised against mAspAT, and that there were no obvious structural or sequence similarities between the two proteins to explain this cross-reactivity (*Chapter 5*). However, a link between chronic inflammation of the cervix or vagina and the development of cervical/vaginal cancer has been reported in pessary users (Schraub *et al.*, 1992), and Woodworth *et al.*, (1995) have reported that pro-inflammatory cytokines (IL-1α and TNF-α) specifically promoted the growth of HPV positive cervical cancer cell lines while inhibiting proliferation in normal cells. It is possible that the cross-reactivity between the HSV-2 dUTPase and cellular mAspAT (which is also expressed at the cell surface as FABP(pm)- see *Section 8.2.1*) might also lead to inflammation of the cervix and promote cervical disease.

3) The transient expression of mAspAT in NRK 536 cells led to an almost 1.6 fold increase in the number of cell colonies that formed in soft agar compared to NRK 536 cells transfected with a control plasmid (*Chapter 6*). Assays of tumour formation in athymic mice were inconclusive, although tumours did appear more rapidly in the mice injected with NRK 536 cells transfected with the mAspAT expression plasmid (J.C.M. Macnab, pers. comm.) than in those injected with control cells.

4) An additional smaller sized PCR product was obtained from RT-PCR experiments with HSV-2 infected Bn5T cell (transformed) RNA compared to mock infected Bn5T cell RNA. This product was not apparent in RE cells infected with HSV-2 (*Chapter 7*). The available sequence data demonstrated that all of the clones obtained from this smaller RT-PCR product contained the mitochondrial targetting pre-sequence, although little other information could be derived.

8.2 GENERAL DISCUSSION.

Mitochondrial aspartate aminotransferase has an important role in cellular metabolism, and increasing the level of the enzyme within the cell might therefore have an advantageous effect on the growth potential of the cell. In addition, mAspAT has been shown to be similar to a long chain fatty acid binding protein (FABP(pm)). The possible role of an elevated level of mAspAT is discussed with respect to these functions below.

8.2.1 PLASMA MEMBRANE FATTY ACID BINDING PROTEIN (FABP(pm)).

Evidence is accumulating that long chain fatty acid uptake into cells is at least partially mediated by a 40-43kDa plasma membrane fatty acid binding protein (FABP(pm); e.g. Turcotte *et al.*, 1997), while a 15kDa cytoplasmic FABP binds to long chain free fatty acids within the cell (e.g. Keler and Sorof, 1993). The level of FABP(pm) has been shown to be elevated in the red skeletal muscle of fasting rats, where free fatty acids provide the major source of energy for the cell (Turcotte *et al.*,1997), and increased fatty acid utilisation has been reported in tumour cells (Paradies *et al.*, 1983). In agreement with this observation, Keler and Sorof (1993) have demonstrated that increased expression of the cytoplasmic 15kDa FABP correlates with growth promotion of hepatoma cells.

Berk *et al.*, (1990) showed that FABP(pm) from rat liver cells was similar in amino acid sequence, purification characteristics and immunological cross-reactivity to mAspAT. Zhou *et al.*, (1995) demonstrated that FABP(pm) and mAspAT were related by physico-chemical properties, and also that uptake of long chain fatty acids into the cell could be abolished by treating the cells with antibodies to mAspAT. The transfection of mAspAT cDNA under the control of an inducible promotor into 3T3 cells resulted in an increase in the saturable uptake of long chain fatty acids into the

cell (>10-fold), and plasma membrane mAspAT fluorescence was observed in the transfected, but not control cells (Isola *et al.*, 1995). This evidence appears to show that mAspAT and FABP(pm) are closely related, if not identical (although Stremmel *et al.*, (1990) reported that the two proteins were not identical).

In our laboratory, increased immunofluorescence was observed at the plasma membrane in transformed (Bn5T) cells compared to controls (J.C.M. Macnab, unpublished results). This was thought to be due to aberrant localisation of mAspAT, perhaps due to the deletion of the mitochondrial targetting presequence. It is possible however, that this immunofluorescence may have been due to the expression of FABP(pm)/mAspAT in these cells, and that a subsequent elevated rate of uptake of long chain fatty acids might be important for transformed cell growth. How mAspAT can perform two very different functions at different localisations within the cell remains unclear, as mAspAT is generally targetted to the mitochondria by interaction with molecular chaperone proteins (see *Introduction, Section 1.3.2*), and it would be interesting to examine the cDNA of the FABP(pm) to discover if regions important for targetting mAspAT to the mitochondria were altered, or whether there were additional plasma membrane targetting signals present.

8.2.2 HORMONAL REGULATION OF mAspAT AND CITRATE SYNTHESIS.

Citrate production and accumulation is a characteristic function of the prostate gland, and has been shown to be upregulated by hormonal stimulation (Franklin *et al.*, 1987; 1997). Tissue specific stimulation of mAspAT activity in the rat ventral prostate by testosterone has been demonstrated (Franklin *et al.*, 1987); this effect is due to a rapid and direct increase in the transcription rate of the mAspAT gene and an increase in the half life of the mAspAT mRNA from 2 to 16 hours in both rat ventral prostate and pig prostate cells (Quian *et al.*, 1993). Prolactin and phorbol esters have also been shown to increase the transcription rate of mAspAT mRNA by a factor of 2.5 to 3-fold in pig prostate cells (Franklin *et al.*, 1992). The promotor of mAspAT lacks both TATA and CCAAT boxes, but is GC rich and contains regions with high homology to glucocorticoid/androgen response elements (GRE/ARE), and a divergent ARE sequence (Juang *et al.*, 1995). The modulation of mAspAT by testosterone was shown to depend on the presence of the two ARE sequences, and to be specific to the prostate, with testosterone having no effect on the level of

transcription of mAspAT in liver cells. Franklin and Costello (1985) proposed the existence of a 'glutamate-aspartate-citrate' pathway in the prostate to account for the high levels of citrate production in this tissue. The stimulation of mAspAT by testosterone (or prolactin) is proposed to increase the transamination of aspartate to oxaloacetate, which then condenses with acetyl CoA to form citrate within the prostate. In support of this model, Costello *et al.*, (1995) have demonstrated that pyruvate dehydrogenase E1α (which produces acetyl CoA) and mAspAT are coordinately upregulated in the rat lateral prostate by prolactin and in the ventral prostate by testosterone. The effect of testosterone treatment of two prostate cancer cell lines (LNCap and PC-3) has recently been studied (Franklin *et al.*, 1997). Both LNCaP and PC-3 cells responded with an increased intracellular citrate concentration (which accumulated in the tissue culture medium), increased mAspAT activity, increased steady state levels of mAspAT mRNA (consistent with the operation of the proposed 'glutamate-aspartate-citrate' pathway) and an increased rate of citrate oxidation in these cells. Interestingly, the more aggressive PC-3 carcinoma cell line has a higher rate of citrate oxidation than the LNCaP cell line, and as citrate metabolism is regulated by the levels of oxaloacetate and acetyl CoA, increased transamination of aspartate by mAspAT may correlate with more rapid cell growth and a more malignant phenotype.

8.2.3 INCREASED FLUX THROUGH THE MALATE-ASPARTATE SHUTTLE

Fahien *et al.*, (1989) have described the quaternary complex formed by mAspAT, α-ketoglutarate dehydrogenase, mitochondrial malate dehydogenase (mMDH) and glutamate dehydrogenase (GDH), and the kinetic advantages conferred by channelling of common ligands between members of such complexes. More mAspAT and mMDH are present in this quaternary complex than in the binary complexes formed between GDH and mAspAT or GDH and mMDH, facilitating enhanced glutamate-malate oxidation. The direct transfer of α-ketoglutarate from mAspAT to α-ketoglutarate dehydrogenase is especially important for the functioning of the malate-aspartate shuttle, as α-ketoglutarate is a potent inhibitor of aspartate production by mAspAT. The flux through the shuttle is increased in response to Ca^{2+} mobilising hormones, an effect which is thought to be mediated by

the activation of α-ketoglutarate dehydrogenase. High concentrations of citrate have been shown to dissociate mMDH and GDH from these complexes, (which would be expected to reduce the flux through the malate-aspartate shuttle), and so in fast growing tumour cells which have a lower mitochondrial citrate level these complexes will be more stable and flux through the shuttle maintained. Fahien *et al.*, (1989) suggest that the compartmentalised metabolism of glutamate and malate within these complexes may allow glutamate to be utilised as the major fuel source in these cells.

As mentioned above, Ca^{2+} mobilising gluconeogenic hormones (e.g. glucagon) increase the flux through the malate-aspartate shuttle by increasing the action of α-ketoglutarate dehydrogenase (Strzelecki *et al.*, 1988). Aspartate transport from the mitochondria is electrophoretically driven, and is far from equilibrium, favouring export to the cytoplasm. During gluconeogenesis, aspartate formed in the mitochondria from lactate, glutamate and glutamine enters the cytoplasm and is converted to phosphoenolpyruvate before entering the gluconeogenic pathway. The malate-aspartate shuttle is therefore essential for gluconeogensis. The aspartate-glutamate translocator protein interacts directly with mAspAT to channel aspartate directly to the cytoplasm. Lowering the level of oxaloacetate (OAA) in the cell increases the transamination of α-ketoglutarate to aspartate and therefore favours efflux. OAA levels are low when ADP levels within the cell are elevated, thus gluconeogenic flux through the shuttle is stimulated when energy levels are low. However, only if OAA is being produced in the cell can the transamination to aspartate occur, and therefore the level of pyruvate carboxylase must also increase- as this enzyme is inhibited by glutamate, and glutamate levels are reduced in response to gluconeogenic hormones, this activation of pyruvate carboxylase can occur.

The malate-aspartate shuttle is the major shuttle operating in a variety of tumour cells (Greenhouse and Lehninger, 1977), with approximately one third of the respiratory ATP generated through the electron flow originating from cytosolic NADH via the shuttle. Thomasset *et al.*, (1992) have used L-glutamic acid monohydroxamate (GAH) to inhibit flux through the malate-aspartate shuttle in L1210 leukaemia cells, resulting in cell death. They demonstrated an 8-fold increase in the cytoplasmic $NADH/NAD^+$ ratio following treatment of cells with 1mM GAH, and also demonstrated inhibition of mAspAT *in vitro*. Addition of 2-oxocarboxylic acids to

the cells protected them from this rise in the NADH/NAD^+ ratios, but only if they were substrates for the tumour lactate dehydrogenase, which uses up NADH, returning the NADH/NAD^+ ratio to near normal and preventing cell death. An increased NADH/NAD^+ ratio has also been induced by GAH treatment of a Burkitt lymphoma cell line and a Friend leukamia cell line. Thomasset *et al.*, (1992) propose a model in which increased levels of cytoplasmic NAD^+ initiate a chain of events leading to DNA synthesis, and that inhibition of the malate-aspartate shuttle reduces the NAD^+ level in the cytoplasm, prevents DNA synthesis and promotes cell death. The continuing function of the shuttle is therefore essential for tumour cell growth, especially as these cells often rely much more heavily on this shuttle than normal cells.

8.2.4 ENHANCED GLUTAMINE OXIDATION IN TUMOUR CELLS.

Bagetto (1992) has reviewed the metabolic pathways active in cancer cells. The main pathways operating in these cells are illustrated in Figure 8.1, and discussed briefly below. The majority of pyruvate produced by glycolysis in cancer cells is oxidised to form lactate, and only a small fraction enters the TCA cycle. Glutamine is the major source of energy in tumour cell lines (including HeLa cells), and enters a truncated TCA cycle following conversion to glutamate and a subsequent transamination to form α-ketoglutarate, a reaction catalysed by mAspAT. The TCA cycle is truncated because of the export of citrate to the cytoplasm to feed the cholesterol and fatty acid synthetic pathways, which are much more active in tumour cells than in normal tissue. Increased cholesterol concentration in the inner mitochondrial membrane is thought to increase the ability of the cell to synthesise ATP by decreasing the intrinsic permeability of the membrane to protons. In order to complete the truncated TCA cycle and fully oxidise glutamine, a source of acetyl CoA is required. This is provided by the presence in tumour cells of $NAD(P)^+$-malic enzyme, which converts extracellular malate into pyruvate, which is then decarboxylated to form acetyl CoA. It is possible that increasing the level of mAspAT in the cell could increase flux through the truncated TCA cycle, and provide more energy for the rapidly growing tumour cell. This assumes, of course that the mAspAT reaction is rate limiting for the overall functioning of this truncated TCA cycle.

Figure 8.1. Altered metabolic pathways operate in glycolytic tumour cells.

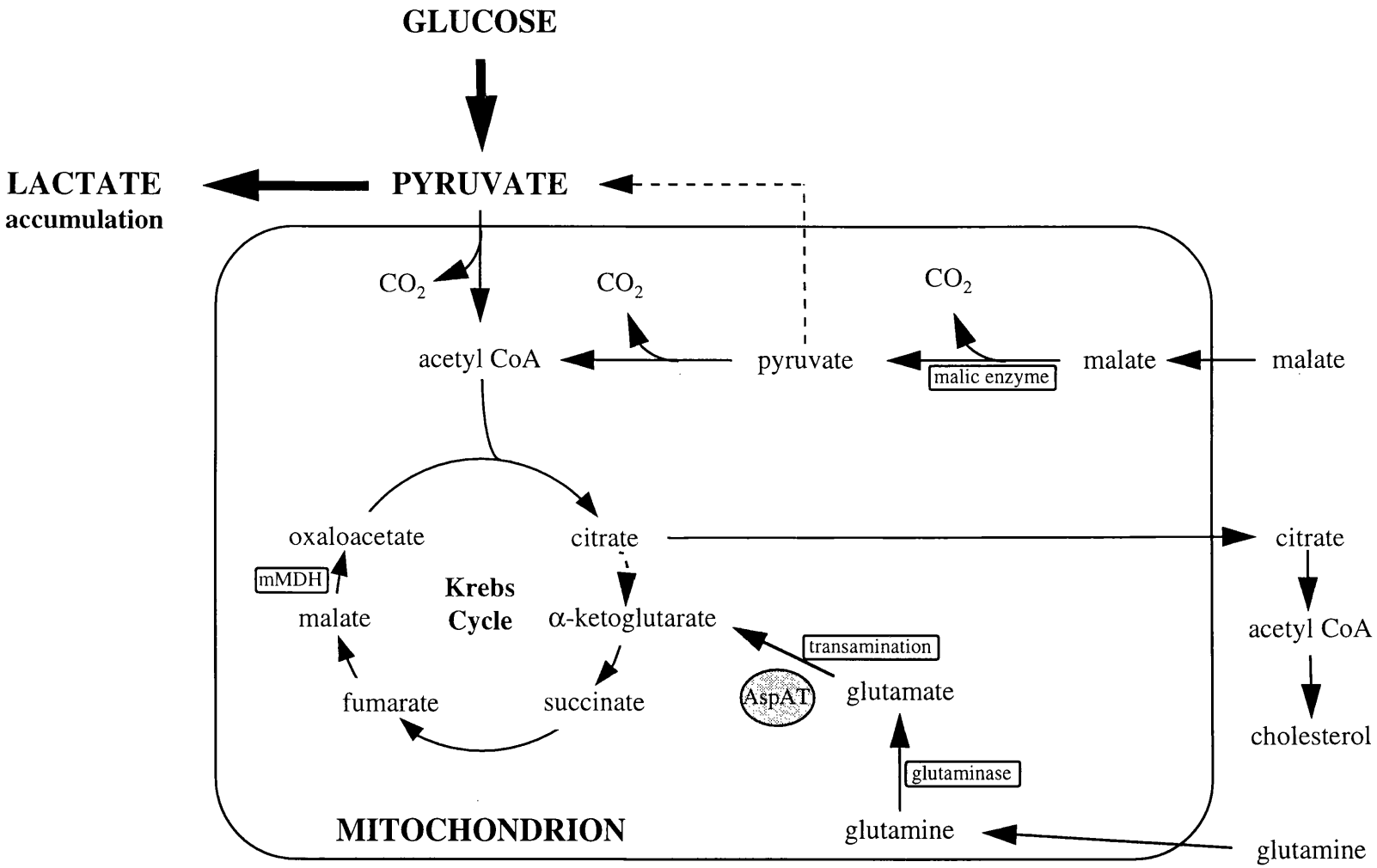

Legend. In tumour cells >90% of glycolytic pyruvate is metabolised to lactate in the cytoplasm. The remaining pyruvate enters a truncated Krebs Cycle, from which citrate is exported to fuel deregulated cholesterol and fatty acid synthesis. Glutamine is the major substrate for the 'tumour cell Krebs Cycle', entering via glutamate transamination by mAspAT to form α-ketoglutarate. Intracellular malate is oxidised to oxaloacetate, while imported malate is prefentially oxidised to pyruvate, providing a source of acetyl CoA to allow the complete oxidation of glutamine. (Reference: Bagetto, 1992).

A recent report has confirmed the importance of the truncated TCA cycle in HeLa cells (a cervical cancer derived cell line). Piva and McEvoy-Bowe, (1998) noted that a significant proportion of glutamate oxidation in these cells proceeded through mAspAT mediated transamination, and that if isolated mitochondria from HeLa cells were incubated in medium containing glutamine, glutamate or (glutamate+malate), aspartate was the major metabolite that accumulated. Furthermore, amino-oxyacetate (which inhibits mAspAT) inhibited respiration and aspartate efflux in these isolated mitochondria. This report demonstrates the importance of mAspAT in the metabolism of tumour cells.

8.3 CONCLUSIONS.

Mitochondrial aspartate aminotransferase is increased in a tumour cell line by infection with HSV-2, and transfection of a plasmid expressing mAspAT into NRK 536 cells resulted in an increased transformation efficiency, as assayed by colony formation in soft agar. This suggests that the HSV-2 induced increase in mAspAT levels may play a role in the transformation process.

mAspAT is involved in many of the metabolic pathways of the normal, and especially the transformed/cancerous cell. In normal cells mAspAT is involved in amino acid metabolism, the malate-aspartate shuttle, in linking the TCA and Urea cycles, and is also involved in prostate citrate synthesis and acts as a long chain fatty acid binding protein at the plasma membrane. In the transformed cell, in addition to these functions, mAspAT is involved in the 'glutaminolysis pathway'-truncated TCA cycle (*Figure 8.1*) which provides much of the energy for the transformed cell, and flux through the malate-aspartate shuttle is elevated.

The elevation of mAspAT levels by HSV-2 could affect one or all of these pathways to promote increased cell growth, and may therefore have a role in the progression of cervical cancer by promoting the growth of already abnormal cells (e.g. HPV infected cells). Further work will be required to determine the precise effect of the HSV-2 stimulated increase in mAspAT expression on the metabolism of tumour cells.

References

Addison, C., F.J. Rixon, J.W. Palfreyman, M. O'Hara and V.G. Preston (1984). Characterisation of an HSV type 1 mutant which has a temperature sensitive defect in penetration of cells and assembly of capsids. *Virology* **138**: 246-259.

Altieri, F., J.R. Mattingley, F.J. Rodriguez-Berrocal, J. Youssef, A. Iriarte, T. Wu and M. Martinez-Carrion (1989). Isolation and properties of a liver mitochondrial precursor protein to aspartate aminotransferase expressed in *Escherichia coli*. *Journal of Biological Chemistry* **264**: 4782-4786.

Altman, A., l. Gissmann and I. Jochmus (1994). Towards HPV vaccination. In: *Human Papillomaviruses and Cervical Cancer: Biology and Immunology*. pp71-81. Edited by Stern, P.L. and M.A. Stanley: Oxford University Press, Oxford.

Alwine, J.C., D.J. Kemp and G.R. Stark (1977). Method for detection of specific RNAs in agarose gels by transfer to diaminobenzylmethyl paper and hybridisation with DNA probes. *Proceedings of the National Academy of Sciences of the United States of America* **74**: 5350-5354.

Anthony, D.D., W.B. Wentz, J.W. Reagan and A.D. Heggie. (1989). Induction of cervical neoplasia in the mouse by herpes simplex virus type 2 DNA. *Proceedings of the National Academy of Sciences of the United States of America* **86**: 4520-4524.

Antinore, M.J., M.J. Birrer, D. Patel, L.Nader and D.J. McCance (1996). The human papillomavirus type 16 E7 gene product interacts with and transactivates the AP-1 family of transcription factors. *Journal of the European Molecular Biology Organisation* **15**: 1950-1960.

Arbuckle, M. I., and N.D. Stow (1993). A mutational analysis of the DNA binding domain of the Herpes Simplex Virus type-1 UL9 protein. *Journal of General Virology* **74**: 1349-1355.

Artigues, A., A. Iriate and M. Martinez-Carrion (1997). Refolding intermediates of acid-unfolded mitochondrial aspartate aminotransferase bind to hsp70. *Journal of Biological Chemistry* **272**: 16852-16861.

Azzariti, A., S. Giannattasio, S. Doonan, R.S. Merafina, E. Marra and E. Quagliarello (1995). Use of pronase sensitivity to probe the conformations of newly synthesised mutant forms of mitochondrial aspartate aminotransferase. *Bioch. Biophys. Res. Comm.* **215**: 800-807.

Bagetto, L.G., (1992). Deviant energetic metabolism of glycolytic cancer cells. *Biochimie* **74**: 959-974.

Bandarra, L.R., and N.B. LaThangue (1991). Adenovirus E1A prevents the retinoblastoma gene product from complexing with a cellular transcription factor complex. *Nature* **351**: 494-497.

Banfield, B.W., and F. Tufaro (1990). Herpes simplex virus particles are unable to traverse the secretory pathway in the mouse L-cell mutant gro29. *Journal of Virology* **64**: 5716-5729.

Barbu, V., and F. Dautry (1989). Northern blot normalisation with a 28S rRNA oligonucleotide probe. *Nucleic Acids Research* **17**: 7115.

Berezov, A., A. Iriate and M. Martinez-Carrion (1994). Binding to phospholipid vesicles impairs substrate mediated conformational changes of the precursor to mitochondrial aspartate aminotransferase. *Journal of Biological Chemistry* **269**: 22222-22229.

Berezov, A., A. Iriate and M. Martinez-Carrion (1996). Interaction of a dimeric mitochondrial precursor with phospholipid vesicles- direct association of each subunit with the membrane is required for loss of functionality. *Archives of Biochemistry and Biophysics* **336**: 173-183.

Berg, J.M., (1986). Potential metal binding domains in nucleic acid binding proteins. *Science* **232**: 485-487.

Bergman, A.C., O. Bjornberg, J. Nord, A.M. Rosengren and P.O. Nyman (1995). dUTPase from the retrovirus equine infectious anaemia virus- high level expression in *Escherichia coli* and purification. *Protein expression and Purification.* **6**: 379-387.

Berk, P.D., H.Wada, Y. Horio, B.J. Potter, D. Sorrentino, S.L. Zhou, L.M. Isola, D. Stump, C.L. Kiang and S. Thung (1990). Plasma membrane fatty acid binding protein and mitochondrial glutamic-oxaloacetic transaminase of rat liver are related. *Proceedings of the National Academy of Sciences of the United States of America* **87**: 3484-3488.

Birnboim, H.C., and J. Doly (1979). A rapid alkaline extraction procedure for screening recombinant plasmid DNA. *Nucleic Acids Research* **7**: 1513-1523.

Bister, K., (1986). Multiple cell derived sequences in single retroviral genomes. *Advances in Viral Oncology* **6**: 45-70.

Bjornberg, O., and P.O Nyman (1996). The dUTPases from herpes simplex virus type 1 and mouse mammary tumour virus are less specific than the *Escherichia coli* enzyme. *Journal of General Virology* **77**: 3107-3111.

Blaho, J.A., C. Mitchell and B. Roizman (1994). An amino acid sequence shared by the herpes simplex virus 1 α proteins 0, 4, 22 and 27 predicted the nucleotidylation of proteins encoded by the UL21, UL31, UL47 and UL49 genes. *Journal of Biological Chemistry* **269**: 17401-17410.

Block, T.M., and J.M. Hill (1997). The latency associated transcripts (LAT) of herpes simplex virus: still no end in sight. *Journal of Neurovirology* **3**: 313-321.

Bloom, D.C., J.G. Stevens, J.M. Hill and R.K. Tran (1997). Mutagenesis of a cAMP response element within the latency associated transcript promoter of HSV-1 reduces adrenergic reactivation. *Virology* **236**: 202-207.

Blyth, W.A., T.J. Hill, H.J. Field and D.A. Harbour (1976). Reactivation of herpes simplex virus infection by ultraviolet light, and possible involvement of prostaglandin. *Journal of General Virology* **33**: 547-550.

Boehmer, P.E., and I.R. Lehman (1993). Physical interaction between the Herpes Simplex Virus -1 origin binding protein and single stranded DNA binding protein ICP8. *Journal of Virology* **67**: 711-715.

Boehmer, P.E., I.R. Lehman (1997). Herpes Simplex Virus DNA Replication. *Annual Review of Biochemistry* **66**: 347-384.

Booy, F.B., W.W. Newcomb, B.L. Trus, J.C. Brown, T.S. Baker and A.C. Steven (1991). Liquid-crystalline, phage like packing of encapsidated DNA in herpes simplex virus. *Cell* **64**: 1-20.

Brock, B.V., S. Selke, J. Benedetti, J.M. Douglas and L. Corey (1990). Frequency of asymptomatic shedding of herpes simplex virus in women with genital herpes. *Journal of the American Medical Association* **263**: 418-420.

Brown, S.M., D.A. Ritchie and J.H. Subak-Sharpe (1973). Genetic studies with herpes simplex virus type 1. The isolation of temperature sensitive mutants, their arrangement into complementation groups and recombination analysis leading to a linkage map. *Journal of General Virology* **18**: 329-346.

Broyles, S.S., (1993). Vaccinia virus encodes a functional dUTPase. *Virology* **195**: 863-865.

Buckley, C.H. (1994). The pathology of cervical intraepithelial neoplasia, carcinoma and human papillomavirus infection. In: *Human Papillomaviruses and Cervical Cancer: Biology and Immunology*. pp1-26. Edited by Stern, P.L. and M.A. Stanley: Oxford University Press, Oxford.

Buckmaster A.E., S.D. Scott, M.J.S. Sanderson, M.E.G. Boursnell, N.L.J. Ross and M.M. Binns (1988). Gene sequence and mapping data from Marek's disease virus and herpesvirus of turkeys: implications for herpesvirus classification. *Journal of General Virology* **69**: 2033-2042.

Calder, J.M., and N.D. Stow (1990). Herpes Simplex Virus helicase-primase- the UL8 protein is not required for DNA dependent ATPase and DNA helicase activities. *Nucleic Acids Research* **18**: 3573-3578.

Camacho, A., R. Arrebola, J. PenaDiaz, L.M. LuisPerez and D. GonzalezPacanowska (1997). Description of a novel eukaryotic deoxyuridine 5'-triphosphate nucleotidohydrolase in *Leishmania major*. *Biochemical Journal* **325**: 441-447.

Camacho, J., and P.G. Spear (1978). Transformation of hamster embryo fibroblasts by a specific fragment of the herpes simplex virus genome. *Cell* **15**: 993-1002.

Cameron, I.R., M. Park, B.M. Dutia, A. Orr and J.C.M. Macnab (1985). Herpes simplex virus sequences involved in the initiation of oncogenic morphological transformation of rat cells are not required for maintenance of the transformed state. *Journal of General Virology* **69**: 517-527.

Campbell, M.E.M., J.W. Palfreyman and C.M. Preston (1984). Identification of the herpes simplex virus DNA sequences which encodes a trans-activating polypeptide responsible for the stimulation of the immediate early transcription. *Journal of Molecular Biology* **180**: 1-19.

Campo, M.S. (1994). Towards vaccines against papillomavirus. In: *Human Papillomaviruses and Cervical Cancer: Biology and Immunology*. pp177-189. Edited by Stern, P.L. and M.A. Stanley: Oxford University Press, Oxford.

Caradonna S. J., and D. M. Adamkiewich (1984). Purification and properties of the deoxyuridine triphosphate nucleotidohydrolase enzyme derived from HeLa S3 cells. Comparison to a distinct dUTP nucleotidohydrolase induced in herpes simplex virus infected HeLa S3 cells. *Journal of Biological Chemistry* **259**: 5459-5464.

Cedergren-Zeppezauer E.S., G. Larsson, P.O. Nyman, Z. Dauter and K. Wilson (1992). Crystal structure of a dUTPase. *Nature* **355**: 740-743.

Chen, J., and B. Roizman (1992). Herpes simplex viruses with mutations in the gene encoding ICP0 are defective in gene expression. *Journal of Virology* **66**: 2916-2927.

Chirgwin, J.M., A.C. Przybyla, R.J. MacDonald and W.J. Rutter (1979). Isolation of biologically active ribonucleic acid from sources enriched in ribonuclease. *Biochemistry* **18**: 5294-5299.

Chomczynski , P., and N. Sacchi (1987). Single step method of RNA isolation by acid guanidinium thiocyanate-phenol-chloroform extraction. *Analytical Biochemistry* **162**: 156-159.

Chou, J., and B. Roizman (1989). Characterisation of DNA sequence-common and sequence-specific proteins binding to cis-acting sites for cleavage of the terminal a-sequence of the herpes simplex virus-1 genome. *Journal of Virology* **63**: 1059-1068.

Chou, J., and B. Roizman (1992). The γ34.5 gene of herpes simplex virus 1 precludes neuroblastoma cells from triggering total shutoff of protein synthesis characteristic of programmed cell death in neuronal cells. *Proceedings of the National Academy of Sciences of the United States of America* **89**: 3266-3270.

Chou, J., and B.Roizman (1994). Herpes simplex virus 1 γ34.5 gene function which blocks the host response to infection maps in the homologous domain of the genes expressed during growth arrest and DNA damage. *Proceedings of the National Academy of Sciences of the United States of America* **91**: 5247-5251.

Chung, C.T., and R.H. Miller (1988). A rapid and convenient method for the preparation and storage of competent bacterial cells. *Nucleic Acids Research.* **16**: 3580.

Church, G.A., and D.W. Wilson (1997). Study of Herpes Simplex Virus Maturation during a Synchronous Wave of Assembly. *Journal of Virology* **71**: 3603-3612.

Ciechanover, A., (1994). The ubiquitin-proteasome proteolytic pathway. *Cell* **79**: 13-21.

Clarke, P., and J.B. Clements (1991). Mutagenesis occuring following infection with herpes simplex virus does not require virus replication. *Virology* **182**: 597-606.

Climie, S., T. Lutz, J. Radul, M. Sumnersmith, E. Vandenberg and E. McIntosh (1994). Expression of trimeric human dUTP pyrophosphatase in *Escherichia coli* and purification of the enzyme. *Protein Expression and Purification* **5**: 252-258.

Cook, M.L., and J.G. Stevens (1973). Pathogenesis of herpetic neuritis and ganglionitis in mice: evidence of intra-axonal transport of infection. *Infection and Immunity* **7**: 272-288.

Corey, L., R.J. Whitley, E.F. Stone and K. Mohan (1988). Difference between herpes simplex virus type 1 and type 2 neonatal encephalitis in neurological outcome. *Lancet* **1:8575**: 1-4.

Costello, L.C., Y. Liu and R.B. Franklin (1995). Prolactin specifically increases pyruvate dehydrogenase E1α in rat lateral prostate epithelial cells. *Prostate* **26**: 189-193.

Courtneidge, S.A., (1985). Activation of the pp60 (c-src) kinase by middle T antigen binding or by dephosphorylation. *Journal of the European Molecular Biology Organisation* **4**: 1471-1477.

Cress, W.D., and S. Triezenberg (1991). Critical structural elements of the VP16 transcriptional activation domain. *Science* **51**: 87-90.

Crook, T., D.Wrede and K.H. Vousden (1992). Clonal p53 mutation in primary cervival cancer: Association with human paillomavirus-negative tumours. *Lancet* **339**: 1070-1073.

Crute, J.J., and I.R. Lehman (1989). Herpes Simplex-1 DNA polymerase- identification of an intrinsic 5'-3' exonuclease with RNaseH activity. *Journal of Biological Chemistry* **264**: 19266-19270.

Crute, J.J., T. Tsurumi, L.A. Zhu, S.K. Keller and P.D. Olivo (1989). Herpes Simplex Virus -1 helicase primase- a complex of 3 Herpes encoded gene products. *Proceedings of the National Academy of Sciences of the United States of America* **86**: 2186-2189.

Curran, T. And P.K. Vogt (1991). Dangerous Liasons: Fos and Jun- oncogenic transcription factors. In: *Transcriptional Regulation.* Edited by McKnight, S.L and K.R. Yamamoto: Cold Spring Harbour Laboratory, New York.

Danovich, R.M., and N. Frenkel (1988). Herpes simplex virus induces the replication of foreign DNA. *Molecular and Cellular Biology* **8**: 3272-3281.

Deb, S., and S.P. Deb (1991). A 269 amino acid segment with a pseudo-leucine zipper and a helix-turn-helix motif codes for the sequence specific DNA binding domain of Herpes Simplex Virus type-1 origin binding protein. *Journal of Virology* **65**: 2829-2838.

DeBritton, R.C., A. Hildesheim, S.L. DeSalo, L.A. Brinton, P. Sathya and W.C. Reeves (1993). Human papillomaviruses and other influences on survival from cervical cancer in Panama. *Obstetrics and Gynecology.* **81**: 19-24.

Deiss, L.P., J. Chou and N. Frenkel (1986). Functional domains within the a-sequence involved in the cleavage-packaging of Herpes Simplex Virus DNA. *Journal of Virology* **59**: 605-618.

Dennett, C., G.M. Cleator and P.E. Klapper (1997). HSV-1 and HSV-2 in Herpes Simplex Encephalitis. *Journal of Medical Virology* **53**: 1-3.

Dennis, D., and J.R. Smiley (1984). Transactivation of a late herpes simplex virus promoter. *Molecular and Cellular Biology* **4**: 544-551.

Desai, D., S.C. Watkins and S. Person (1994). The size and symmetry of B capsids of herpes simplex virus type 1 is determined by the gene products of the UL26 open reading frame. *Journal of Virology* **68**: 5365-5374.

Devi-Rao, G.B., S.A. Goddart, L.M. Hecht, R. Rochford, M.K. Rice and E.K. Wagner (1991). Relationship between polyadenylated and non-polyadenylated herpes simplex virus type 1 latenct associated transcripts. *Journal of Virology* **65**: 2179-2190.

Digard, P., K.P.Williams, P. Hensley, I.S. Brooks, C.E. Dahl and D.M. Coen (1995). Specific inhibition of Herpes Simplex Virus DNA polymerase by helical peptides corresponding to the subunit interface. *Proceedings of the National Academy of Sciences of the United States of America* **92**: 1456-1460.

Dilanni, C.L., C. Mapelli, D.A. Drier, J. Tsao, S. Natarajan, D. Riexinger, S.M. Festin, , M. Bolgar, G. Yamanaka, S.P. Weinheimer, C.A. Meyers and R. J. Colonno (1993). *In vitro* activity of the Herpes Simplex type 1 protease with peptide substrates. *Journal of Biological Chemistry* **268**: 25449-25454.

DiPaolo, J.A., N.C. Popescu, L. Alvarez and C.D. Woodworth (1993). Cellular and molecular alterations in human epithelial cells transformed by recombinant HPV DNA. *Critical Reviews in Oncogenesis* **44**: 337-360.

Docherty, J.J., Subak-Sharpe, J.H. and C.M. Preston (1981). Identification of a virus specific polypeptide associated with a transforming fragment (BglIIN) of herpes simplex virus type 2 DNA. *Journal of Virology* **40**: 126-132.

Doerig, C., L.I. Pizer and C.L. Wilcox (1991). Detection of the latency associated transcript in neuronal cultures during the latent infection with herpes simplex virus type 1. *Virology* **183**: 423-426.

Dubin, G., E. Socolof, I. Frank and H.M. Friedman (1991). Herpes simplex virus type 1 F_c receptor protects infected cells from antibody dependent cellular cytotoxicity. *Journal of Virology* **65**: 7046-7050.

Dutch, R.E., B.V. Zemelmann and I.R. Lehman (1994). Herpes Simplex Virus type-1 recombination- The U_c-DR1 region is required for high level a-sequence mediated recombination. *Journal of Virology* **68**: 3733-3741.

el Dierry, R.N., T. Tokino, V.E. Velculescu, D.B. Levy, R. Parsons, J.M. Trent, D. Lin, W.E. Mercer, K.W. Kinzler and B. Vogelstein (1993). WAF1, a potential mediator of p53 tumour supression. *Cell* **75**: 817-825.

Elias, P., C.M. Gustafsson, O. Hammarsten and N.D. Stow (1992). Structural elements required for the cooperative binding of the Herpes Simplex Virus origin binding protein to ori_S reside in the N-terminal part of the protein. *Journal of Biological Chemistry* **267**: 17424-17429.

Elliot, G.D., and D.M. Meredith. (1992). The herpes simplex virus type 1 tegument protein VP22 is encoded by gene UL49. *Journal of General Virology* **73**: 723-726.

Elliot, G.D., G. Mouzakitis and P. O'Hare. (1995). VP16 interacts via its' activation domain with VP22, a tegument protein of herpes simplex virus, and is relocated to a novel macromolecular assembly in coexpressing cells. *Journal of Virology* **69**: 7932-7941.

Estridge, J.K., L.M. Kemp, N.B. LaThangue, B.S. Mann, A.S. Tyms and D.S. Latchman (1989). The Herpes Simplex Virus Type 1 Immediate Early Protein ICP27 is Obligately Required for the Accumulation of a Cellular Protein during Viral Infection. *Virology* **168**: 67-72.

Everett, R.D., and M.L. Fenwick (1990). Comparative DNA sequence analysis of the host shutoff genes of different strains of herpes simplex virus- Type 2 strain HG52 encodes a truncated UL41 product. *Journal of General Virology* **71**: 1387-1390.

Fahien, L.A., M.J. MacDonald, J.K. Teller, B. Fibich and C.M. Fahien (1989). Kinetic advantages of hetero-enzyme complexes with Glutamate Dehydrogenase and the α-Ketogluturate Dehydrogenase complex. *Journal of Biological Chemistry* **264**: 12303-12312.

Fakharzadeh, S.S., S.P. Trusko and D. L. George (1991). Tumourogenic potential associated with enhanced expression of a gene that is amplified in a mouse tumour cell line. *Journal of the European Molecular Biology Organisation* **10**: 1565-1569.

Farrell, M.J., A.T. Dobson and L.T. Feldman (1991). Herpes simplex virus latency associated transcript is a stable intron. *Proceedings of the National Academy of Sciences of the United States of America* **88**: 790-794.

Fierer, D.S., and M.D. Challberg (1992). Purification and characterisation of UL9, the Herpes Simplex Virus type-1 origin binding protein. *Journal of Virology* **66**: 3986-3895.

Fisher, F. B., and V. G. Preston (1986). Isolation and characterisation of herpes simplex virus type 1 mutants which fail to induce dUTPase activity. *Virology* **148**: 190-197.

Franklin, R.B., and L.C.Costello (1984). Glutamate dehydrogenase and a proposed 'glutamate-aspartate' pathway for citrate synthesis in rat ventral prostate. *Journal of Urology* **132**: 1239-1243.

Franklin, R.B., B.I. Kukoyi, V. Akuffo and L.C. Costello (1987). Testosterone stimulation of mitochondrial aspartate aminotransferase levels and biosynthesis in rat ventral prostate. *Journal of Steroid Biochemistry* **28**: 247-256.

Franklin, R.B., D.B. Ekiko and L.C. Costello (1992). Prolactin stimulates transcription of aspartate aminotransferase in prostate cells. *Molecular and Cellular Endocrinolgy* **90**: 27-32.

Franklin, R.B., J. Zou, E. Gorski, Y.H. Yang and L.C. Costello (1997). Prolactin regulation of mitochondrial aspartate aminotransferase and protein kinase C in human prostate cancer cells. *Molecular and Cellular Endocrinology* **127**: 19-25.

Fraser, N.W., T.M. Block and J.G. Spivack (1992). The latency associated transcripts of herpes simplex virus: RNA in search of a function. *Virology* **191**: 1-8.

Fries, K.H., W.E. Miller and N. Raab-Traub (1996). Epstein-Barr virus latent membrane protein 1 blocks p53 mediated apoptosis through activation of the A20 gene. *Journal of Virology* **70**: 8653-8659.

Fuller, A.O., and P.G. Spear (1985). Specificities of monoclonal and polyclonal antibodies that inhibit adsorption of herpes simplex virus to cells and lack of inhibition by potent neutralising antibodies. *Journal of Virology* **55**: 475-482.

Funk, W.D., D.T. Pak, R.H. Karas, W.E. Wright and J.W. Shay (1992). A transcriptionally active DNA bindiing site for human p53 protein complexes. *Molecular and Cellular Biology* **12**: 2866-2871.

Galloway, D.A., J.A. Nelson and J.K. McDougall (1984). Small fragments of herpesvirus DNA with transforming activity contain insertion sequence-like structures. *Proceedings of the National Academy of Sciences of the United States of America* **81**: 4736-4740.

Ganem, D., (1996). Human herpesvirus 8 and the biology of Kaposi's sarcoma. *Seminars in Virology* **7**: 325-332.

Gao, M., L. Matusick-Kumar, W. Hurlburt, S.F. Ditusa, W.W. Mewcomb, J.C. Brown, P.J. McCann, I. Deckman and R.J. Collono (1994). The protease of herpes simplex virus type 1 is essential for functional capsid formation and viral growth. *Journal of Virology* **68**: 3702-3712.

Garlatti, M., V. Tchesnokov, M. Daheshia, S. Feilleux_Duche, J. Hanoune, M. Aggerbeck and R. Barouki (1993). CCAAT/Enhancer-binding Protein-related Proteins Bind to the Unusual Promotor of the Aspartate Aminotransferase Gene. *Journal of Biological Chemistry* **268**: 6567-6574.

Giannattasio, S., A. Azzariti, E. Marra and E. Quagliariello (1994). The N-terminal region of mature mitochondrial aspartate aminotransferase can direct cytosolic dihydrofolate reductase into mitochondria *in vitro*. *Biochem. Biophys. Res. Comm.* **201**: 1059-1065.

Gius, D., and L.A. Laimins (1993). Activation of HPV18 gene expression by herpes simplex virus type 1 viral transactivators and phorbol ester. *Journal of Virology* **63**: 555-563.

Gottlieb, J., and M.D. Challberg (1994). Interaction of Herpes Simplex Virus type-1 DNA polymerase and the UL42 accessory protein with a model primer template. *Journal of Virology* **68**: 4937-4945.

Gradlione, A., R. Vericillo, M. Napolitano, G. Cardinali, P. Gazzaniga, I. Silvestri, O. Gandini, S. Tomao and A.M. Agliano (1996). Prevalence rates of human papillomavirus, cytomegalovirus and Epstien-Barr virus in the cervix of healthy women. *Journal of Medical Virology* **50**: 1-4.

Grassie, M.A. (1993). U90, a tumour associated polypeptide altered by HSV infection. PhD. Thesis, University of Glasgow.

Grassie, M., D. McNab and J.C.M. Macnab (1993). The characteristic which makes the cell coded HSV-inducible U90 distinctive in transformed cells is its greatly increased half-life. *Journal of Cell Science* **104**: 1083-1090.

Greenhouse, W.V., and A.L. Lehninger (1977). Magnitude of malate-aspartate reduced nicotinamide adenine dinucleotide shuttle activity in intact respiring tumour cells. *Cancer Research* **37**: 4137-4181.

Griffiths, A., S. Renfrey and T. Minson (1998). Glycoprotein C deficient mutants of two strains of herpes simplex virus type 1 exhibit unaltered adsorption characteristics on polarised and non polarised cells. *Journal of General Virology* **79**: 807-812.

Gruenheid, S., L. Gatzke, H. Meadows and F. Tufaro (1993). Herpes simplex virus infection and propagation in a mouse L cell mutant lacking heparan sulphate proteoglycans. *Journal of Virology* **67**: 93-100.

Gu, W., J.W. Schneider, G. Conderelli, S. Kaushall, V. Mahdavi and B. Nadal Ginard (1993). Interaction of myogenic factors and the retinoblastoma protein mediates muscle cell commitment and differentiation. *Cell* **72**: 309-324.

Hagmar, B., J.J.P. Christensen, B. Johansson, M. Kalantari, W. Ryd,B. Skyldberg, L. Walaas, B. Warleby and G.B. Kristensen (1995). Implications of human papillomavirus type for survival in cervical squamous-cell carcinoma. *International. Journal of Gynecological Cancer* **5**: 341-345.

Hall, J.D., K.L. Orth and D. Claus-Walker (1996). Evidence that the nuclease activities associated with the Herpes Simplex type-1 DNA polymerase are due to the 3'-5'-exonuclease. *Journal of Virology* **70**: 4816-4818.

Hara, Y., T. Kimoto, Y. Okuno and Y. Minekawa (1997). Effect of Herpes Simplex Virus on the DNA of Human Papillomavirus 18. *Journal of Medical Virology* **53**: 4-12.

Hardy, W.R., M.A. Hardwicke and R.M. Sandri-Goldin (1992). The HSV-1 regulatory protein ICP27 appears to impair host cell splicing. In: *Abstracts of the 17th International Herpesvirus Workshop, Edinburgh*:105.

Hawley-Nelson, P., K.H. Vousden, N.L. Hubbert, D.R. Lowy and J.T. Schiller (1989). HPV16 E6 and E7 proteins co-operate to immortalise human foreskin keratinocytes. *Journal of the European Molecular Biology Organisation* **8**: 3905-3910.

Hazuda, D.J., H.C. Perry and W.L. McClements (1992). Co-operative interactions between replication origin bound molecules of Herpes Simplex Virus origin binding protein are mediated via the amino terminus of the protein. *Journal of Biological Chemistry* **267**: 14309-14315.

Heilbronn, R., S.K. Weller and H. zurHausen (1990). Herpes simplex virus type 1 mutants for the origin binding protein induce DNA amplification in the absence of viral replication. *Virology* **179**: 478-481.

Heine, J.W., R.W. Honess, E. Cassai and B. Poizman (1974). Proteins specified by herpes simplex virus. XII. The virion polypeptides of type 1 strains. *Journal of Virology* **14**: 640-651.

Hellberg, D., S. Nilsson, N.J. Halet, D. Hoffman and E. Wynder (1988). Smoking and cervical intraepithelial neoplasia; nicotine and cotinine in serum and cervical mucus in smokers and nonsmokers. *American Journal of Obstetrics and Gynecology* **158**: 910-913.

Herold, B.C., R.J. Visalli, N. Susmarski, C.R. Brandt and P.G. Spear (1994). Glycoprotein C independent binding of herpes simplex virus to cells requires cell surface heparan sulphate and glycoprotein B. *Journal of Virology* **75**: 1211-1222.

Herrin, D.L., and G.W. Schmidt (1988). Rapid reversible staining of northern blots prior to hybridisation. *Biotechniques* **6**: 196-0.

Hesketh, R. (1995). In: *The Oncogene FactsBook*: Academic Press, London.

Hewitt, R.E.P., M. Grassie, D. McNab, A. Orr, J-F. Lucasson and J.C.M. Macnab (1991). A transformation specific polypeptide distinct from heat shock proteins is induced by herpes simplex virus type 2 infection. *Journal of General Virology* **72**: 3085-3089.

Hildesheim, A., V. Mann, L.A. Brinton, M. Szklo, W.C. Reeves and W.E Rawls (1991). Herpes simplex virus type 2- A possible interaction with human papillomavirus types 16/18 in the development of cervical cancer. *International Journal of Cancer* **49**: 335-340.

Hildesheim, A., C.L. Han, L.A. Brinton, P.C. Nasca, R.M. Richart, R.B. Jones, R.L. Ashley, R.G. Zeigler and J.T. Schiller (1997a). Sexually transmitted agents and risk of carcinoma of the vagina. *International Journal of Gynecological Cancer* **7**: 251-255.

Hildesheim, A., C.L. Han, L.A. Brinton, R.J. Kurman and J.T. Schiller (1997b). Human papillomavirus type 16 and risk of preinvasive and invasive vulvar cancer: Results from a seroepidemiological case-control study. *Obstetrics and Gynecology* **90**: 748-754.

Hildt, E., P.H. Hofschneider and S. Urban (1996). The role of hepatitis B virus (HBV) in the development of hepatocellular carcinoma. *Seminars in Virology* **7**: 333-347.

Hill, J.M., F. Sederati, R.T. Javier, E.K. Wagner and J.G. Stevens (1990). Herpes simplex virus latent phase transcription facilitates *in vivo* reactivation. *Virology* **174**: 117-125.

Hill, J.M., H.H. Garza, Y-H. Su, M. Rapalie, L.C. Hanna, J.M. Loutsch, H.W. Thompson, E.D. Varnell, D.C. Bloom and T.M. Block (1997). A 437bp deletion at the beginning of the LAT promoter significantly reduces adrenergically induced HSV-1 ocular reactivation in latently infected rabbits. *Journal of Virology* 7**1**: 6555-6559 .

Hill, A., P. Jugovic, I. York, G. Russ, J. Bennink, J. Yewdell, H. Pleogh and D. Johnson (1995). Herpes simplex virus turns off the TAP to evade host immunity. *Nature* **375**: 411-415.

Ho, D.Y., and E.S. Mocarski (1989). Herpes simplex virus latent RNA (LAT) is not required for latent infection in the mouse. *Proceedings of the National Academy of Sciences of the United States of America* **86**: 7596-7600.

Homa, F.L., T.M. Otal, J.C. Glorioso and M. Levine (1986). Transcriptional control signals of a herpes simplex virus type 1 late (γ) gene lie within bases -34 to -124 relative to the 5' terminus of the mRNA. *Molecular and Cellular Biology* **6**: 3652-3666.

Homa, F.L., and J.C. Brown (1997). Capsid assembly and DNA packaging in Herpes Simplex Virus. *Reviews in Medical Virology* **7**: 107-122.

Honess R.W., and B. Roizman (1974). Regulation of herpesvirus macromolecular synthesis I. Cascade regulation of the synthesis of three groups of viral proteins. *Journal of Virology* **14**: 8-19.

Hong, Z., M. Beaudet-Miller, J. Durkin, R. Zhang and A.D. Kwong (1996). Identification of a minimal hydrophobic domain in the herpes simplex virus type 1 scaffolding protein which is required for interaction with the major capsid protein. *Journal of Virology* **70**: 533-540.

Hossain, A., T. Holt, J. Ciacci-Zanella and C. Jones (1997). Analysis of cyclin dependent kinase activity after herpes simplex virus type 2 infection. *Journal of General Virology* **78**: 3341-3348.

Hughes, S., J.J. Greenhouse, C.J. Petropoulos and P. Sutrave (1987). Adapter plasmids simplify the insertion of foreign DNA into helper-independent retroviral vectors. *Journal of Virology* **61**: 3004-3012.

Huibregste, J.M., M. Scheffner and P.M. Howley (1992). A cellular protein mediates association of p53 with the E6 oncoprotein of human papillomavirus types 16 or 18. *Journal of the European Molecular Biology Organisation* **10**: 4129-4135.

Hung, S-L., S. Srinivasan, H.M. Friedman, R.J. Eisenberg and G.H. Cohen (1992). Structural basis of C3b binding by glycoprotein C of herpes simplex virus. *Journal of Virology* **66**: 4013-4027.

Huynh, Q. K., R. Sakakibara, T. Watanabe and W. Hioroshi (1980). Glutamic oxaloacetic transaminase isozymes from rat liver. *Journal of Biochemistry* **88**: 231-239.

Huynh, Q.K., R. Sakakibara, T. Watanabe and H. Wada (1981). The complete amino acid sequence of mitochondrial glutamic oxaloacetic transaminase from rat liver. *Journal of Biochemistry* **90**: 863-875.

Igarashi, K., R. Fawl, R.J. Roller and B. Roizman (1993). Construction and properties of a recombinant Herpes Simplex Virus-1 lacking both S-component origins of DNA synthesis. *Journal of Virology* **67**: 2123-2132.

Isola, L.M., S.L. Zhou, C.L. Kiang, D.D. Stump, M.W. Bradbury and P.D. Berk (1995). 3T3 fibroblasts transfected with a cDNA for mitochondrial aspartate aminotransferase express plasma membrane fatty acid binding protein and saturable fatty acid uptake. *Proceedings of the National Academy of Sciences of the United States of America* **92**: 9866-9870.

Iwasawa, A., P. Nieminen, M. Lehtinen and J. Paavonen (1996). Human papillomavirus DNA in uterine cervix squamous-cell carcinoma and adenocarcinoma detected by polymerase chain reaction. *Cancer* 77: 2275-2279.

Jang, K-L., B. Pulverer, J.R. Woodgett and D.S. Latchman (1991). Activation of the cellular transcription factor AP-1 in herpes simplex virus infected cells is dependent on the viral immediate early protein ICP0. *Nucleic Acids Research* 18: 4879-4883.

Jariwalla, R.J., L. Aurelian and P.O.P. Ts'O (1983). Immortalisation and neoplastic transformation of normal diploid cells by defined cloned fragments of herpes simplex virus type 2. *Proceedings of the National Academy of Sciences of the United States of America* 80: 5902-5906.

Jeon, S., and P.F. Lambert (1995). Integration of human papillomavirus type 16 into the human genome leads to increased stability of E6 and E7 mRNAs; implications for cervical carcinogenesis. *Proceedings of the National Academy of Sciences of the United States of America* 92: 1654-1658.

Johnson, D.C., P.G. Spear (1982). Momensin inhibits the processing of herpes simplex virus glycoproteins, their transport to the cell surface, and the egress of virions from infected cells. *Journal of Virology* 43: 1102-1112.

Johnson, D.C., and M.W. Ligas (1988). Herpes simplex viruses lacking glycoprotein D are unable to inhibit virus penetration: quantitative evidence for virus specific cell surface receptors. *Journal of Virology* 62: 4605-4612.

Johnson, D.C., M.C. Frame, M.W. Ligas, A.M. Cross and N.D. Stow (1988). Herpes simlex virus immunoglobulin G F_c receptor activity depends on a complex of two viral glycoproteins, gE and gI. *Journal of Virology* 62: 1347-1354.

Johnson, D.C., R.L. Burke and T. Gregory (1990). Soluble forms of herpes simplex virus glycoprotein D bind to a limited number of cell surface receptors and inhibit virus entry into cells. *Journal of Virology* 61: 2208-2216.

Johnson, P.A., and R.D. Everett (1986). The control of herpes simplex virus type 1 late gene transcription: A TATA box/cap site region is sufficient for fully efficient regulated activity. *Nucleic Acids Research* 51: 389-394.

Jones, C., (1995). Cervical cancer- Is herpes simplex virus type 2 a co-factor? *Clinical Microbiology Reviews* 8: 549.

Jons, A., and T.C. Mettenleiter (1996). Identification and characterisation of Pseudorabies Virus dUTPase. *Journal of Virology* 70: 1242-1245.

Juang, H.H., L.C. Costello and R.B. Franklin (1995). Androgen modulation of multiple transcriptional start sites of the mitochondrial aspartate aminotransferase gene in rat prostate. *Journal of Biological Chemistry* 270: 12629-12634.

Kaneko, T., and N. Mizuno (1994). Glutamate synthesising enzymes in GABAergic neurons of the neocortex- A double immunofluorescence study in the rat. *Neuroscience* 61: 839-849.

Kaner, R.A., A. Baird, A. Mansukhani, C. Basilico, B. Summers, R. Florkiewicz and D. Hajjar (1990). Fibroblast growth factor receptor is a portal of cellular entry for herpes simplex virus type 1. *Science* **248**: 1410-1413.

Kang, J., J.E. Kuhn, P. Schafer, A. Immelmann and K. Henco (1995). Quantification of DNA and RNA by PCR. In: *PCR 2, A Practical Approach.* pp119-133. Edited by McPherson, M.J., B.D. Hames and G.R. Taylor: IRL Press at Oxford University Press, UK.

Kasper, P., M. Sterk, P. Christen and H. Gehring (1996). Molecular Dynamics simulation of domain movements in aspartate aminotransferase. *European Journal of Biochemistry* **240**: 751-755.

Kawai, S., and H. Hanafusa (1971). The effects of reciprocal changes in the temperature on the transformed state of cells infected with a Rous sarcoma virus mutant. *Virology* **46**: 470-479.

Keler, T., and S. Sorof (1993). Growth promotion of transfected hepatoma cells by liver fatty acid binding protein in human hepatoma (HepG2) cells. *Journal of Cellular Physiology* **157**: 33-40.

Kelleher, R.J., P.M. Flanagan and R.D. Kornberg (1990). A novel mediator between activator proteins and the RNA polymerase II transcription apparatus. *Cell* **61**: 1209-1215.

Kemp, L.M., P.M. Brickell, N.B. LaThangue and D.S. Latchman (1986). Transcriptional induction of cellular gene expression during lytic infection with Herpes Simplex Virus. *Bioscience Reports* **6**: 945-951.

Kemp, L.M., and D.S. Latchman (1988). The Herpes Simplex Virus Type 1 Immediate Early Protein ICP4 Specifically Induces Increased Transcription of the Human Ubiquitin B gene without Affecting the Ubiquitin A and C Genes. *Virology* **166**: 258-261.

Kidd, K.K. and G. Ruano (1995). Optimising PCR. In: *PCR 2, A Practical Approach.* pp1-21. Edited by McPherson, M.J., B.D. Hames and G.R. Taylor: IRL Press at Oxford University Press, UK.

Kieff, E. (1996). Epstein-Barr virus and its' replication. In: *Fields Virology*, Third Edition. pp2346-2396. Edited by Fields, B.N., D.M. Knipe, P.M. Howley *et al.*: Lippincott-Raven Publishers, Philadelphia.

Kim, N.W., M.A. Piatyszek, K.R. Prowse, C.B. Harley, M.D. West, P.L. Ho, G.M. Corvello, W.E. Wright, S.L. Weinrich and J.W. Shay (1994). Specific association of human telomerase activity with immortal cells and cancer. *Science* **266**: 2011-2015.

Kjaer, S.K., E-M. DeVilliers, B.J. Haugaard, R.B. Christensen, C. Teisen, K.A. Moller, P.Poll, H. Jensen, B.F. Vestergaard, E. Lynge and O.M. Jensen (1988). Human papillomavirus, herpes simplex virus and cervical cancer in Greenland and Denmark. A population based cross-sectional study. *International Journal of Cancer* **41**: 518-524.

Kjaer, S.K., A.J.C. VandenBrule, J.E. Bock, P.A. Poll, G. Engholm, M.E. Sherman, J.M.M. Walboomers and C.J.L.M. Meijer (1997). Determinants for genital human papillomavirus infection in 1000 randomly chosen young Danish women with normal Pap smear: Are there different risk profiles for oncogenic and non-oncogenic HPV types. *Cancer Epidemiology, Biomarkers and Prevention* **6**: 799-805.

Klinedinst, D.K., and M.D. Challberg (1994). Helicase-primase complex of Herpes Simplex Virus type-1. A mutation in the UL52 subunit abolishes primase activity. *Journal of Virology* **68**: 3693-3701.

Klingelhutz, A.J., S.A. Foster and J.K. McDougall (1996). Telomerase activation by the E6 gene product of human papillomavirus type 16. *Nature* **380**: 79-82.

Koelle, D.M., J. Genedetti, A. Langenberg and L. Corey (1992). Asymptomatic reactivation of herpes simplex virus in women after the first episode of genital herpes. *Annals of Internal Medicine* **116**: 433-437.

Koppe, B., L. Menendezarias and S. Oroszlan (1994). Expression and purification of the mouse mammary tumour virus gag-pro transframe protein P-30 and characterisation of its dUTPase activity. *Journal of Virology* **68**: 2313-2319.

Kristensson, K., E. Lycke, M. Roytta, B. Svennerholm and A. Vahlne (1986). Neuritic transport of herpes simplex virus in rat sensory neurons *in vitro*. Effects of substances interacting with microtubular function and axonal flow. *Journal of General Virology* **67**: 2023-2028.

Kubbutat, M.H.G., and K.H. Vousden (1996). Role of E6 and E7 oncoproteins in HPV induced anogenital malignancies. *Seminars in Virology* **7**: 295-304.

Kulomaa, P., J. Panoven and M. Letinen (1992). Herpes simplex virus induces unscheduled DNA synthesis in virus infected cervical cancer cell lines. *Research in Virology* **143**: 351-359.

Kushuhara, M., K. Yamaguchi, M. Kuranami, A. Suzaki, S. Ishikawa, H. Moon, I. Adachi, S. Hori and S. Handa (1992). Stimulation of anchorage independent growth by endothelin in NRK-49F cells. *Cancer Research* **52**: 3011-3014.

Kwong, A.D., J.A. Kruper and N. Frenkel (1988). Herpes simplex virus virion host shutoff function. *Journal of Virology* **62**: 912-921.

LaBella, F., H.L. Sive, R.G. Roeder and N. Heintz (1988). Cell-cycle regulation of a human histone H2b gene is mediated by the H2b subtype-specific consensus element. *Genes and Development* **2**: 32-39.

Ladner, R.D., D.E. McNulty, S.A. Carr, G.D. Roberts and S.J. Caradonna (1996). Characterisation of distinct nuclear and mitochondrial forms of human deoxyuridine triphosphate nucleotidohydrolase. *Journal of Biological Chemistry* **271**: 7752-7757.

Laemelli, U.K., (1970). Cleavage of structural proteins during the assembly of the head of bacteriophage T4. *Nature* **227**: 680-685.

Lagunoff, M., and B. Roizman (1994). Expression of a herpes simplex virus 1 open reading frame antisense to the γ34.5 gene and transcribed by an RNA 3' coterminal with the unspliced latency associated transcript. *Journal of Virology* **68**: 6021-6028.

Lain, B., A. Iriate, J.R. Mattingley, J.I. Moreno and M. Martinez-Carrion (1995). Structural features of the precursor to mitochondrial aspartate aminotransferase responsible for binding to hsp70. *Journal of Biological Chemistry* **270**: 24732-24739.

Lane, D.P., and L.V. Crawford (1979). T-antigen is bound to a host protein in SV40 transformed cells. *Nature* **278**: 261-263.

Lane, D.P., (1992). Cancer- p53 guardian of the genome. *Nature* **358**: 15-16.

Larsson, G., L.A. Svensson and P.O. Nyman (1996). Crystal structure of the *Escherichia coli* dUTPase in complex with a substrate analog (dUDP). *Nature Structural Biology* **3**: 532-538.

Latchman, D.S., (1988). Effect of herpes simplex virus infection on mitochondrial gene expression. *Journal of General Virology* **69**: 1405-1410.

LaThangue, N.B., and D.S. Latchman (1988). A cellular heat shock protein related to heat shock protein 90 accumulates during herpes simplex virus infection and is over-expressed in transformed cells. *Experimental Cell Research* **178**: 167-179.

Leader, D.P., I. Gall and H. Lehrach (1985). The structure of a cloned γ-actin processed pseudogene. *Gene* **36**: 369-374.

Lee, C.K., and D.M. Knipe (1985). An immunoassay for the study of DNA binding activities of Herpes Simplex Virus protein ICP8. *Journal of Virology* **54**: 731-738.

Lehrach, H., D. Diamond, J.M. Wozney and H. Boedtker (1977). RNA molecular weight determinations by gel electrophoresis under denaturing conditions; A critical re-examination. *Biochemistry* **16**: 4743-4751.

Leslie, J. (1996). An investigation into factors that influence the incorporation of proteins into the HSV-1 tegument. PhD. Thesis, University of Glasgow.

Liang, X., M. Tang, B. Manns, L.A. Babiuk and T.J. Zamb (1993). Identification and deletion mutagenesis of the bovine herpesvirus 1 dUTPase gene and a gene homologous to Herpes Simplex Virus UL49.5. *Virology* **195**: 42-50.

Lin, Y-S. and M.R. Green (1991). Mechanism of action of an acidic transcriptional activator *in vitro*. *Cell* **64**: 971-981.

Lorincz, A.T., R. Reid, A.B. Jenson, M.D. Greenberg, W. Lancaster and R.J. Kurman (1992). Human papillomavirus infection of the cervix- relative risk associations of 15 common anogenital types. *Obstetrics and Gynecology* **79**: 328-337.

Lucasson, J-F. (1992). Identification of a 40kDa protein increased by HSV-2 infection. PhD. Thesis, University of Glasgow.

Lucasson, J-F., D.McNab, T.C. Collins, J.R. Mattingley, J.N. Keen, A.B. Maclean and J.C.M. Macnab (1994). HSV-2 increases the mitochondrial aspartate amino-transaminase characteristic of tumour cells. *Virology* **205**: 393-405.

Lycke, E., K. Kristensson, B. Svennerholm, A. Vahlne and R. Zeigler (1984). Uptake and transport of herpes simplex virus in neurites of rat dorsal root ganglia cells in culture. *Journal of General Virology* **65**: 55-64.

Mackem, S., and B. Roizman (1982). Structural features of the herpes simplex virus α gene 4, 0 and 27 promotor-regulatory sequences which confer α regulation on chimeric thymidine kinase genes. *Journal of Virology* **44**: 939-949.

Macnab, J.C.M. (1979). Tumour production by HSV-2 transformed lines in rats and the varying response to immunosuppression. *Journal of General Virology* **43**: 39-56.

Macnab, J.C.M. and J.K. McDougall (1980). Transformation by herpesviruses. In: *The Human Herpesviruses*. p634. Edited by Nahmias, W.R. Dowdle and R.F. Schinazi: Elsevier/North-Holland, New York.

Macnab, J.C.M., A. Orr and N.B. LaThangue (1985). Cellular proteins expressed in herpes simplex virus transformed cells also accumulate on herpes simplex virus infection. *Journal of the European Molecular Biology Organisation* **12**: 3223-3228.

Macnab, J.C.M., S.A. Walkinshaw, J.W. Cordiner and J.B. Clements (1986). Human papillomavirus in clinically and histologically normal tissue of patients with genital cancer. *New England Journal of Medicine* **315**: 1052-1058.

Macnab, J.C.M. (1987). Herpes Simplex Virus and Human Cytomegalovirus: Their Role in Morphological Transformation and Genital Cancers. *Journal of General Virology* **68**: 2525-2550.

Macnab, J.C.M., J.S. Nelson, S.Daw, R.E.P. Hewitt, J-F. Lucason and P.V. Shirodaria (1992). Patients with cervical cancer produce an antibody response to an HSV-inducible tumour specific cell polypeptide. *International Journal of Cancer* **50**: 578-584.

Macpherson, I.A., and M.G.P. Stoker (1962). Polyoma transformation of hamster cell clones- an investigation of genetic factors affecting cell competence. *Virology* **16**: 147-151.

Macpherson, I.A., and L. Montagnier (1964). Agar suspension culture for the selective assay of cells transformed by polyoma virus. *Virology* **23**: 291-294.

Maden, B.E.H., C.L. Dent, T.E. Farrell, J. Garde, F.S. McCallum and J.A. Wakeman (1987). Clones of human ribosomal DNA containing the complete 18S-rRNA and 28S-rRNA genes. *Biochemical Journal* **246**: 519-527.

Magder, L.S., A.J. Nahmias, R.E. Johnson, F.K. Lee, C. Brooks and C. Snowden (1989). The prevalence and distribution of herpes simplex virus type 1 and 2 antibodies in the United States population. *New England Journal of Medicine* **321**: 7-12.

Maggioncalda, J., A. Mehta, Y.H. Su, N.W. Fraser and T.M. Block (1996). Correlation between herpes simplex virus type 1 rate of reactivation from latent infection and the number of infected neurons in trigeminal ganglia. *Virology* **225**: 72-81.

Makhov, A.M., P.E. Boehmer, I.R. Lehman and J.D. Griffith (1996). The Herpes Simplex Virus type-1 origin binding protein carries out origin specific DNA unwinding and forms unwound stem-loop structures. *Journal of Molecular Biology* **258**: 789-799.

Malashkevich, V.N., M.D. Toney and J.N. Jansonius (1993). Crystal structures of true enzymatic reaction intermediates- aspartate and glutamate ketimines in aspartate aminotransferase. *Biochemistry* **32**: 13451-134620.

Maniatis, T. (1989). *Molecular Cloning: A Laboratory Manual*, Second Edition. Edited by Sambrook, J., E.F. Fritsch and T. Maniatis: Cold Spring Harbour Laboratory Press, USA.

Markovichousley, Z., T. Schrimer, E. Hohenester, A.R. Khomutov, R.M. Khomutov, M.Y. Karpeisky, E. Sandmeier, P. Christen and J.N. Jansonius (1996). Crystal structures and solution studies of oxime adducts of mitochondrial aspartate aminotransferase. *European Journal of Biochemistry* **236**: 1025-1032.

Martinez, R., R.T. Sarisky, P.C. Weber and S.K. Weller (1996). Herpes Simplex Virus type -1 alkaline nuclease is required for efficient processing of viral DNA replication intermediates. *Journal of Virology* **70**: 2075-2085.

Massimi, P., D. Pim, A. Storey and L. Banks (1996). HPV16 E7 and adenovirus E1A complex formation with TATA box binding protein is enhanced by casein kinase II phosphorylation. *Oncogene* **12**: 2325-2330.

Mattingley, J.R., F.J. Rodriguez-Berrocal, J. Gordon, A. Iriate and M. Martinez-Carrion (1987). Molecular cloning and *in vivo* expression of a precursor to rat mitochondrial aspartate aminotransferase. *Biochem. Biophys. Res. Comm.* **149**: 859-865.

Mattingley, J.R., J. Youssef, A. Iriate and M. Martinez-Carrion (1993). Protein Folding in a Cell-free Translation System. *Journal of Biological Chemistry* **268**: 3925-3937.

McCarthy, A.M., L. McMahan and P.A. Schaffer (1989). Herpes simplex virus type 1 ICP27 deletion mutants exhibit altered patterns of transcription and are DNA deficient. *Journal of Virology* **63**: 18-27.

McGeoch D.J., M.A. Dalrymple, A. J. Davison, A. Dolan, M.C. Frame, D. McNab, L.J. Perry, J. E. Scott and P.Taylor (1988). The complete DNA sequence of the long unique region in the genome of herpes simplex virus type 1 *Journal of General Virology* **69**: 1531-1574.

McGeoch, D.J., (1990). Protein sequence comparisons show that the 'pseudoproteases' encoded by poxviruses and certain retroviruses belong to the deoxuridine triphosphatase family. *Nucleic Acids Research* **18**: 4105-4110.

Mcknight, J.L.C., T.M. Kristie and B. Roizman (1987). Binding of the virion protein mediating α gene induction in herpes simplex virus 1 infected cells to its *cis* site requires cellular factors. *Proceedings of the National Academy of Sciences of the United States of America* **84**: 7061-7065.

McLauchlan, J., S. Simpson and J.B. Clements (1989). Herpes simplex virus induces a processing factor that stimulates poly(A) site usage. *Cell* **59**: 1093-1105.

McNab, A.R., L.L. Roof, D.R. Thomsen et al (1996). The HSV-1 UL25 gene is required for DNA encapsidation, but not for cleavage of viral DNA: isolation and characterisation of a HSV-1 UL25 null mutant. In: *Abstracts of the 22nd International Herpesvirus Workshop* **210**.

McPhalen, C.A., M.G. Vincent and J.A. Jansonius (1992a). X-ray structure refinement and comparison of three forms of mitochondrial aspartate aminotransferase. *Journal of Molecular Biology* **225**: 495-517.

McPhalen, C.A., M.G. Vincent, D. Picot, J.N. Jansonius, A.M. Lesk and C. Chothia (1992b). Domain closure in mitochondrial aspartate aminotransferase. *Journal of Molecular Biology* **227**: 197-213.

Mead, D.J., D.C.J. Gardi and S.G. Oliver (1986). The yeast 2-mu plasmid- strategies for the survival of a selfish DNA. *Molecular and General Genetics* **205**: 417-421.

Mellerick, D.M., and N.W. Fraser (1987). Physical state of the latent herpes simplex virus genome in a mouse model system: evidence suggesting an episomal state. *Virology* **158**: 265-275.

Michael, N., and B. Roizman (1990). Detremination of the number of protein monomers binding to DNA molecules with F_{ab} fragments of monoclonal antibodies to the protein. *Methods in Molecular and Cellular Biology* **1**: 203-211.

Mitchell, W.J., R.P. Lirette and N.W. Fraser (1990). Mapping of low abundance latency associated RNA in the trigeminal ganglia of mice latently infected with herpes simplex virus type 1. *Journal of General Virology* **71**: 125-132.

Miyahara, I., K. Hirotsu, H. Hayashi and H. Kagamiyama (1994). X-ray crystallographic study of pyridoxamine 5'-phosphate type aspartate aminotransferases from *Escherichia coli* in 3 forms. *Journal of Biochemistry* **116**: 1001-1012.

Miyashita, T., and J.C. Reed (1995). Tumour supressor p53 is a direct transcriptional activator of the human bax gene. *Cell* **80**: 293-299.

Miyazawa, T., K. Tomanga, Y. Kawaguchi and T. Mikami (1994). The genome of feline immunodeficiency virus. *Archives of Virology* **134**: 221-234.

Mocarski, E.S. and B. Roizman (1982). Structure and role of the Herpes Simplex Virus DNA termini in inversion, circularisation and generation of virion DNA. *Cell* **31**: 89-97.

Mol C.D., J.M. Haris, E.M. McIntosh and J.A. Tainer (1996). Human dUTP pyrophosphatase- Uracil recognition by a beta hairpin and active sites formed by 3 seperate subunits. *Structure* **4**: 1077-1092.

Montgomery, R.I., M.S. Warner, B.J. Lum and P.G. Spear (1996). Herpes simplex virus-1 entry into cells mediated by a novel member of the TNF/NGF receptor family. *Cell* **87**: 427-436.

Morino, Y., K. Shimada and H. Kagamiyama (1990). Mammalian Aspartate Aminotransferase Isozymes. *Annals of the New York Academy of Sciences* **585**: 32-47.

Munoz, N., F. X. Bosch, S. DeSanjose, L. Tafur, I Izarugaza, M. Gili, P. Viladiu, C. Navarro, C. Martos, N. Ascunce, L.C. Gonzalez, J.M. Kaldor, E. Guerrero, A. Lorincz, M. Sanatmaria, P.A. Deruiz, N. Aristizabal and K. Shah (1992). The causal link between human papillomavirus and invasive cervical cancer; a population based study in Columbia and Spain. *International Journal of Cancer* **52**: 743-749.

Nahmias, A.J., F.K. Lee and S. Bechman-Nahmias (1990). Sero-epidemiological and sociological patterns of herpes simplex virus infection in the world. *Scandinavian Journal of Infectious Disease* **69**: 19-36.

Nevins, J.R. and P.K. Vogt (1996). Cell Transformation by Viruses. In: *Fields Virology*, Third Edition. pp301-335. Edited by Fields, B.N., D.M. Knipe, P.M. Howley *et al.*: Lippincott-Raven Publishers, Philadelphia.

Newcomb, W.W., and J.C. Brown (1991). Structure of the herpes simplex virus capsid: Effects of extraction with guanidine-HCl and partial reconstitution of extracted capsids. *Journal of Virology* **65**: 613-620.

Newcomb, W.W., B.L. Trus, F.P.Booy, A.C. Steven, J.S.Wall and J.C. Brown (1993). Structure of the herpes simplex virus capsid: molecular composition of the pentons and triplexes. *Journal of Molecular Biology* **232**: 499-511.

Newcomb, W.W., F. L. Homa, D.R. Thomsen, F.P. Booy, B.L. Trus, A.C. Steven, J.V. Spencer and J.C. Brown (1996). Assembly of the herpes simplex virus capsid: characterisation of intermediates observed during cell free capsid assembly. *Journal of Molecular Biology* **263**: 432-446.

Offord, E.A., R.E. Leake and J.C.M. Macnab (1989). Stimulation of Estrogen Receptor mRNA Levels in MCF-7 Cells by Herpes SImplex Virus Infection. *Journal of Virology* **63**: 2388-2391.

Oroskar, A.A., and G.S. Read (1989). Control of mRNA stability by the virion host shutoff function of HSV. *Journal of Virology* **63**: 1897-1906.

Ostrander, M., and Y-C. Cheng (1980). Properties of the herpes simplex virus type 1 and type 2 DNA polymerase. *Biochim. Biophys. Acta* **609**: 232-245.

Pan, H., and A.E. Griep (1994). Altered cell cycle regulation in the lens of HPV-16 E6 or E7 transgenic mice: implications for tumour supressor genes in development. *Genes and Development* **8**: 1285-1299.

Paradies, G., F. Capuano, G. Palombini, T. Galeotti and S. Papa (1983). Transport of pyruvate in mitochondria from different tumour cells. *Cancer Research* **43**: 5068-5071.

Patel, A.H., and J.B. MacLean (1995). The product of the UL6 gene of herpes simplex virus type 1 is associated with virus capsids. *Virology* **206**: 465-478.

Patel, R., W.L. Chan, L.M. Kemp, N.B. LaThangue and D.S. Latchman (1986). Isolation of cDNA clones derived from a cellular gene transcriptionally induced by herpes simplex virus. *Nucleic Acids Research* **14**: 5629-5640.

Pave-Preux, M., N. Ferry, J. Bouguet, J. Hanoune and R. Barouki (1988). Nucleotide sequence and glucocorticoid regulation of the mRNAs for the isoenzymes of rat aspartate aminotransferase. *Journal of Biological Chemistry* **263**: 17459-17466.

Perdue, M. L., J.C. Cohen, C.C. Randall and D.J. O'Callaghan (1976). Biochemical studies on the maturation of herpesvirus nucleocapsid species. *Virology* **74**: 194-208.

Perng, G-C., S.M. Slania, H. Ghiasi, A.B. Nesburn and S.L. Wechsler (1996). A 371bp region between the herpes simplex virus type 1 LAT promoter and the 2 kilobase LAT is not essential for efficient spontaneous reactivation of latent HSV-1. *Journal of Virology* **70**: 2014-2018.

Pilon, L., A. Royal and Y. Langelier (1985). Increased mutation frequency after herpes simplex virus type 2 infection in non-permissive XC cells. *Journal of General Virology* **66**: 259-265.

Piva, T.J., and E. McEvoy-Bowe (1998). Oxidation of glutamine in HeLa cells: Role and control of truncated TCA cycles in tumour mitochondria. *Journal of Cellular Biochemistry* **68**: 213-225.

Post, L.E., S. Mackem and B. Roizman (1981). Regulation of α genes of herpes simplex virus: expression of chimeric genes produced by fusion of thymidine kinase with α gene promotors. *Cell* **24**: 555-565.

Prasad, G.S., E.A. Stura, D.E. McRee, G.S. Laco, C. Hasselkuslight, J.H. Elder and C.D. Stout (1996). Crystal structure of dUTP pyrophosphatase from feline immunodeficiency virus. *Protein Science* **5**: 2429-2437.

Preston V. G., and F. B. Fisher (1984). Identification of the herpes simplex virus type 1 gene encoding the dUTPase. *Virology* **138**: 58-68.

Preston, C.M., and E.L. Notarianni (1983). Poly (ADP-ribosyl)ation of a herpes simplex virus immediate early polypeptide. *Virology* **131**: 492-501.

Preston, V.G., (1990). Herpes Simplex Virus activates expression of a cellular gene by specific binding to the cell surface. *Virology* **176**: 474-482.

Prevelige, P.E., and J. King (1993). Assembly of bacteriophage P22: A model for ds-DNA virus assembly. *Progress in Medical Virology* **40**: 206-221.

Qian, K., R.B. Franklin and L.C. Costello (1993). Testosterone regulates mitochondrial aspartate aminotransferase gene expression and messenger RNA stability in prostate. *Journal of Steroid Biochemistry and Molecular Biology* **44**: 13-19.

Qin, X.Q., T. Chittenden, D.M. Livingston and W.G. Kaelin (1992). Identification of a growth suppression domain within the retinoblastoma gene product. *Genes and Development* **6**: 953-964.

Quinn, J.P., and D.J. McGeoch (1985). DNA sequence of the region in the genome of Herpes Simplex Virus type-1 containing the genes for DNA polymerase and the major DNA binding protein. *Nucleic Acids Research* **13**: 8143-8163.

Raab-Traub, N., (1996). Pathogenesis of Epstein-Barr virus and its associated malignancies. *Seminars in Virology* **7**: 315-323.

Reddig, P.J., L.A. Grinstead, S.J. Monahan, P.A. Johnson and D.S. Parris (1994). The essential *in-vivo* function of the Herpes Simplex Virus UL42 protein correlates with its ability to stimulate the viral DNA polymerase *in-vitro*. *Virology* **200**: 447-456.

Rickinson, A.B. and E. Kieff (1996). Epstein-Barr virus. In: *Fields Virology*, Third Edition. pp2343-2396. Edited by Fields, B.N., D.M. Knipe, P.M. Howley *et al.*: Lippincott-Raven Publishers, Philadelphia.

Rigby, P.W.J., M. Dieckman, C. Rhodes and P. Berg (1977). Labelling deoxyribonucleic acid to high specific activity *in vitro* by nick translation with DNA polymerase 1. *Journal of Molecular Biology* **113**: 237-251.

Rixon, F. J., (1993). Structure and assembly of herpes viruses. *Seminars in Virology* **4**: 135-144.

Rixon, F.J., C. Addison, A. McGregor, S.J. Macnab, P. Nicholson, V.G. Preston and J.D. Tatman (1996). Multiple interactions control the intracellular localisation of the herpes simplex virus type 1 capsid proteins. *Journal of General Virology* **77**: 2251-2260.

Rock, D.L., and N.W. Fraser (1985). Latent herpes simplex virus type 1 DNA contains two copies of the virion DNA joint region. *Journal of Virology* **55**: 849-852.

Rodahl, E., and L. Haarr (1997). Analysis of the 2-kilobase latency associated transcript expressed in PC12 cells productively infected with herpes simplex virus type 1: evidence for a stable, non-linear structure. *Journal of Virology* **71**: 1703-1707.

Roizman, B., and A.E. Sears (1987). An inquiry into the mechanism of herpes simplex virus latency. *Annual Review of Microbiolgy* **41**: 543-571.

Roizman, B., R.C. Desrosiers, B. Fleckenstein, C. Lopez, A.C. Minson and M.J. Studdert (1992). The family Herpesviridae: An update. *Archives of Virology* **123**: 425-449.

Roizman, B. (1996). Herpesviridae. In: *Fields Virology*, Third Edition. pp2221-2229. Edited by Fields, B.N., D.M. Knipe, P.M. Howley *et al.*: Lippincott-Raven Publishers, Philadelphia.

Roizman, B. and A. E. Sears (1996). Herpes Simplex Viruses and Their Replication. In: *Fields Virology*, Third Edition. pp2232-2278. Edited by Fields, B.N., D.M. Knipe, P.M. Howley *et al.*: Lippincott-Raven Publishers, Philadelphia.

Rugsti, A.K., N. Dyson and R. Bernards (1991). Amino terminal domains of c-myc and N-myc proteins mediate binding to the retinoblastoma gene product. *Nature* **352**: 541-544.

Sadowski, I., J. Ma, S. Triezenberg and M. Ptashne (1988). GAL4-VP16 is an unusually potent transcriptional activator. *Nature* **335**: 563-564.

Scheffner, M., B.A. Werness, J.M. Huibregste, A.J. Levine and P.M. Howley (1990). The E6 oncoprotein encoded by human papillomavirus types 16 and 18 promotes the degradation of p53. *Cell* **63**: 1129-1136.

Schleofer, J.R., L. Gissman, B. Matz and H. ZurHausen (1983). Herpes simplex virus induced amplification of SV40 sequences in transformed Chinese hamster embryo cells. *International Journal of Cancer* **32**: 99-103.

Schrag, J.D., B.V. Venkatarum Prasad, F.J. Rixon and W. Chiu (1989). Three dimensional structure of the HSV-1 nucleocapsid. *Cell* **46**: 651-660.

Schraub, S., X.S. Sun, P. Maingon, J.C. Horiot, N. Daly, R. Keiling, J. Pigneux, H. Pourquier, R. Rozan and C. Vrousos (1992). Cervical and vaginal cancer associated with pessary use. *Cancer* **69**: 2505-2509.

Schriemer, E.C., L.S. Wyatt, K. Yamanishi, W.J. Rodriguez and N. Frenkel (1991). Differentiation between two distinct classes of viruses now classified as human herpesvirus 6. *Proceedings of the National Academy of Sciences of the United States of America* **88**: 5922-5926.

Schultzcherry, S., and J.E. Murphy-Ullrich (1993). Thrombospondin causes activation of latent transforming growth factor beta secreted by endothelial cells by a novel mechanism. *Journal of Cell Biology* **122**: 923-932.

Seaman, C.H., M.M. Palcie, C.A. McPhalen, M.P. Gore, L.K.P. Lam and J.C. Vederas (1991). Inhibition of Cytoplasmic Aspartate Aminotransferase from Porcine Heart by R and S isomers of Aminooxysuccinate and Hydrazinosuccinate. *Journal of Biological Chemistry* **266**: 5525-5533.

Sears, A.E., and B. Roizman (1990). Amplification by host factors of a sequence contained within the herpes simplex virus 1 genome. *Proceedings of the National Academy of Sciences of the United States of America* **87**: 9441-9445.

Sears, A.E., B.S. McGwire and B, Roizman (1991). Infection of polarised MDCK cells with herpes simplex virus 1: two asymmetrically distributed cell receptors interact with different viral proteins. *Proceedings of the National Academy of Sciences of the United States of America* **88**: 5087-5091.

Seidel-Dugan, C., M. Ponce de Leon, H.M. Friedman, L.F. Fries, M.M. Frank, G.H. Cohen and R.J. Eisenberg (1988). C3b receptor activity on transfected cells expressing glycoprotein C of herpes simplex types 1 and 2. *Journal of Virology* **62**: 4027-4036.

Setoyama, C., S-H. Ding, B.K. Choudhury, T. Joh, H. Takeshima, T. Tsuzuki and K. Shimada (1990). Regulatory Regions of the Mitochondrial and Cytosolic Genes Participating in the Malate-Aspartate Shuttle. *Journal of Biological Chemistry* **265**: 1293-1299.

Severini, A., A.R. Morgan, D.R. Tovell and D.J. Tyrrell (1994). Study of the structure of replicative intermediates of HSV-1 DNA by pulsed field gel electrophoresis. *Virology* **200**: 428-435.

Severini, A., D.G. Scraba and D.J. Tyrrell (1996). Branched structures in the intracellular DNA of Herpes Simplex Virus type-1. *Journal of Virology* **70**: 3169-3175.

Shieh, M.T., D. WuDunn, R.I. Montgomery, J.D. Esko and P.G. Spear (1992). Cell surface receptors for herpes simplex virus are heparan sulphate proteoglycans. *J. Cell Biol.* **116**: 1273-1281.

Shih, T.Y., M.O. Weeks, H.A. Young and E. Scolnick (1979). p21 of Kirsten murine sarcoma virus is thermolabile in a viral mutant temperature sensitive for the maintenance of transformation. *Journal of Virology* **31**: 546-556.

Ship, I.I., M.F. Muller and C. Ram (1977). A retrospective study of recurrent herpes labialis in a professional population, 1958-1971. *Oral Surgery, Oral Medicine and Oral Pathology* **44**: 723.

Skinner, G.B.R., (1976). Transformation of primary hamster embryo fibroblasts by type 2 herpes simplex virus: evidence for a hit and run mechanism. *British Journal of Experimental Pathology* **57**: 361-376.

Slagle, B.L., S.A. Becker and J.S. Butel (1994). Hepatitis Viruses and Liver Cancer. In: *Viruses and Cancer*, pp149-163. Edited by Minson, A., J. Neil and M. McCrae: Cambridge University Press, Cambridge.

Smibert, C.A., B. Popova, P. Xiao, J.P. Capone and J.R Smiley (1994). Herpes simplex virus VP16 forms a complex with the virion host shutoff protein *vhs*. *Journal of Virology* **68**: 2339-2346.

Smith, C.A., P. Bates, R. Rivera-Gonzales, B. Gu and N.A. DeLuca (1993). ICP4, the major transcriptional regulatory protein of herpes simplex virus type 1 forms a tripartite complex with TATA-binding protein and TFIIB. *Journal of Virology* **67**: 4676-4687.

Sommer, P., E. Kremmer, S. Bier, S. Konig, P. Zalud, M. Zeppezauer, J.F. Jones, N. Muellerlantzsch and F.A. Grasser (1996). Cloning and expression of the Epstein Barr Virus encoded dUTPase- Patients with acute, reactivated or chronic virus infection develop antibodies against the enzyme. *Journal of General Virology* **77**: 2795-2805.

Sonderegger, P., R. Jaussi, P. Christen and H. Gehring (1982). Biosynthesis of aspartate aminotransferases- both the higher molecular weight precursor of mitochondrial aspartate aminotransferase and the cytoplasmic isoenzyme are synthesised on free polysomes. *Journal of Biological Chemistry* **257**: 3339-3345.

Southern, P.J. and P. Berg (1982). Transformation of mammalian cells to antibiotic resistance with a bacterial gene under the control of the SV40 early region promoter. *Journal of Molecular Applied Genetics* **1**: 327-341.

Spear, P.G. (1985). Glycoproteins specified by herpes simplex viruses. In: *The herpesviruses*. Vol 3. pp315-356. Edited by Roizman, B.: Plenum Press, New York.

Stackpole, C.W., (1969). Herpes type virus of the frog renal adenocarcinoma I. Virus development in tumour transplants maintained at low temperature. *Journal of Virology* **4**: 75-93.

Stanberry, L.R., E.R. Kern, J.T. Richards, T.H. Abott and J.C. Overall (1982). Genital herpes in guinea pigs: pathogenesis of the primary infection and description of recurrent disease. *Journal of Infectious Diseases* **146**: 397-404.

Steffy, K.R., and Weir, J.P (1991). Mutational analysis of two herpes simplex virus type 1 late promoters. *Journal of Virology* **65**: 6454-6460.

Steinthorsdotir, V., and V. Mautner (1991). Enteric adenovirus type 40: E1B transcription map and identification of novel E1A-E1B co-transcripts in lytically infected cells. *Virology* **181**: 139-149.

Sterk, M., H. Hauser, D. Marsh and H. Gehring (1994). Probing conformational states of spin-labelled aminotransferase by ESR. *European Journal of Biochemistry* **219**: 993-1000.

Stern, S., and W. Herr (1991). The herpes simplex virus trans-activator VP16 recognises the Oct-1 homeo domain: evidence for a homeo domain recognition sub domain. *Genes and Development* **5**: 2555-2566.

Stevens, J.G., and M.L. Cook (1971). Latent herpes simplex virus in spinal ganglia of mice. *Science* **173**: 843-845.

Stevens, J.G., E.K. Wagner, G.B. Devi-Rao, M.L. Cook and L.T. Feldman (1987). RNA complimentary to a herpes virus alpha gene mRNA is prominent in latently infected neurons. *Science* **235**: 1056-1059.

Stevens, J.G., (1994). Overview of herpes virus latency. *Seminars in Virology* **5**: 191-196.

Stow, N.D., and N.M. Wilkie (1976). An improved technique for obtaining enhanced infectivity with herpes simplex virus type 1 DNA. *Journal of General Virology* **66**: 31-42.

Stow, N.D., (1982). Localisation of an origin of DNA replication within the TRs/IRs repeated region of the Herpes Simplex Virus type-1 genome. *Journal of the European Molecular Biology Organisation* **1**: 863-867.

Stow, N.D., O. Hammarsten, M.I. Arbuckle and P. Elias (1993). Inhibition of Herpes Simplex Virus type-1 DNA replication by mutant forms of the origin-binding protein. *Virology* **196**: 413-418.

Stremmel, W., H-E. Diede, E. Rodilla-Sala, K. Vyska, M. Schrader, B. Fitscher and S. Passarella (1990). The membrane fatty acid protein is not identical to mitochondrial glutamic-oxaloacetic transaminase (mGOT). *Molecular and Cellular Biochemistry* **98**: 191-199.

Stringer, K.F., C.J. Ingles and J. Greenblatt (1990). Direct and selective binding of an acidic transcriptional activation domain to the TATA-box factor TFIID. *Nature* **345**: 783-786.

Stryer, L. (1988). *Biochemistry*, Third Edition. W.H. Freeman and Co., New York.

Strzelecki, T., D. Strzelecka, C.D. Koch and K.F. Lanoue (1988). Sites of action of glucagon and other Ca^{2+} mobilising hormones on the malate-aspartate cycle. *Archives of Biochemistry and Biophysics* **264**: 310-320.

Stuart, R.A., D.M. Cyr, E.A. Craig and W. Neupert (1994). Mitochondrial molecular chaperones: their role in protein translocation. *Trends in Biological Sciences* **19**: 87-92.

Stump, D.D., S.L. Zhou and P.D. Berk (1993). Comparison of the plasma membrane FABP and mitochondrial form of aspartate aminotransferase from rat liver. *American Journal of Physiology* **265**: 894-902.

Sturm, R.A., and Herr W (1988). The POU domain is a bipartite DNA binding structure. *Nature* **336**: 601-604.

Sugden, B., (1992). EBV's Open Sesame. *Trends in Genetics* **17**: 239-240.

Tan, T.M., and R.C. Ting (1995). *In vitro* and *in vivo* inhibition of of human papillomavirus type 16 E6 and E7 genes. *Cancer Research* **55**: 45999-4605.

Tatman, J.D., V.G. Preston, P. Nicholson, R.M. Elliott and F.J Rixon (1994). Assembly of herpes simplex virus type 1 capsids using a panel of recombinant baculoviruses. *Journal of General Virology* **75**: 1101-1113.

Tenney, D.J., W.W. Hurlburt, M. Bifano, J.T. Stevens,P.A. Micheletti, R.K. Hamatke and M.G. Cordingley (1993). Mutations in the C-terminus of Herpes Simplex Virus type-1 DNA polymerase can affect binding and stimulation by its accessory protein UL42 without affecting basal polymerase activity. *Journal of Virology* **67**: 1959-1966.

Tenney, D.J., W.W. Hurlburt, P.A. Micheletti, M. Bifano and R.K. Hamatake (1994). The UL8 component of the Herpes Simplex Virus helicase-primase complex stimulates primer synthesis by a subassembly of the UL5 and UL52 components. *Journal of Biological Chemistry* **269**: 5030-5035.

Thomasset, N., L. Goetsch, F. Hamedi-Sangsari, R. Tournaire, S. Malley, C. Navarro, J-F. Dore and J. Vila (1992). Inhibition of malate-aspartate shuttle by the anti-tumour drug L-glutamic acid gamma-monohydroxamate in L1210 leukaemia cells *International Journal of Cancer* **51**: 329-332.

Thomsen, D.R., L.L. Roof and F. L. Homa (1994). Assembly of herpes simplex virus (HSV) intermediate capsids in insect cells infected with recombinant baculoviruses expressing the HSV capsid proteins. *Journal of Virology* **68**: 2442-2457.

Timbury, M.C., (1971). Temperature sensitive mutants of herpes simplex virus type 2. *Journal of General Virology* **13**: 373-376.

Torella, C., J.R. Mattingley, A. Artigues, A. Iriate and M. Martinez-Carrion (1998). Insight into the conformation of protein folding intermediates trapped by GroEL. *Journal of Biological Chemistry* **273**: 3915-3925.

Truant, R., J. Antounovic, J. Greenbolt, C. Prives and J.A. Cromlish (1995). Direct interaction of the hepatitis B virus HBX protein with p53 leads to inactivation by HBX of p53 response element directed transactivation. *Journal of Virology* **69**: 1851-1859.

Trybala, E., T. Bergstrom, B. Svennerholm, S. Jeansson. J.C. Glorioso and S. Olafsson (1994). Localisation of a functional site on herpes simplex virus type 1 glycoprotein C involved in binding to cell surface heparan sulphate. *Journal of General Virology* **75**: 743-752.

Turcotte, L.P., A.K. Srivastava and J.L. Chiasson (1997). Fasting increases plasma membrane fatty acid binding protein (FABP(pm)) in red skeletal muscle. *Molecular and Cellular Biochemistry* **166**: 156-158.

Turner, A., B. Bruun, A. Minson and H. Browne (1998). Glycoproteins gB, gD and gH:gL of herpes simplex virus type 1 are necessary and sufficient to mediate membrane fusion in a Cos cell transfection system. *Journal of Virology* **72**: 873-875.

Valyi-Nagy, T., S. Deshmane, A. Dilliner and N.W. Fraser (1991). Induction of cellular transcriptional factors in trigeminal ganglia of mice by corneal scarification, herpes simplex virus type 1 infection and explantation of trigeminal ganglia. *Journal of Virology* **65**: 4142-4152.

vanGenderen, I.L., R. Bradimarti, M.R. Torrisi, G. Campadelli and G. vanMeer (1994). The phospholipid composition of extracellular herpes simplex virions differs from that of host cell nuclei. *Virology* **200**: 831-832.

Verreault, R., J. Chu, M. Mandelson and K. Shy (1989). A case control study of diet and invasive cervical cancer. *International Journal of Cancer* **43**: 1050-1054.

Vlazny, D.A., A. Kwong and N. Frenkel (1982). Site specific cleavage packaging of herpes simplex virus DNA and the selective maturation of nucleocapsids containing full length viral DNA. *Proceedings of the National Academy of Sciences of the United States of America* **79**: 1423-1427.

Vossbeck, H., B. Strahm, P. Hofler and G. Bauer (1995). Direct transforming ability of TGF-β on rat fibroblasts. *International Journal of Cancer* **61**: 92-97.

Vousden, K.H. (1994a). Cell transformation by human papillomaviruses. In: *Viruses and Cancer*, pp27-40. Edited by Minson, A., J. Neil and M. McCrae: Cambridge University Press, Cambridge.

Vousden, K.H. (1994b). Mechanisms of transformation by HPV. In: *Human Papillomaviruses and Cervical Cancer.* pp92-110. Edited by Stern, P.L. and M.A. Stanley: Oxford University Press, Oxford.

Wagner, E.K. (1994). Herpes simplex viruses: molecular biology. In: *Encyclopedia of Virology*, Volume 2. pp593-603. Edited by Webster, R.G. and A. Granoff: Academic Press, London, UK.

Wagner, E.K., G.B. Devi-Rao, L.T. Feldman, A.T. Dobson, Y.F. Zhang, W.M. Flanagan and J.G. Stevens (1988). Physical characterisation of the herpes simplex virus latency associated transcript in neurons. *Journal of Virology* **62**: 1194-1202.

Welch, J.W., and J.R. Feramisco (1985). Rapid purification of mammalian 70,000 Dalton stress proteins: Affinity of the proteins for nucleotides. *Molecular and Cellular Biology* **5**: 1229-1237.

Wentz, W.B., J.W. Reagan, A.D. Heggie, Y-S. Fu and D.D. Anthony (1981). Induction of uterine cancer with inactivated herpes simplex virus types 1 and 2. *Cancer* **48**: 1783-1790.

Whitbeck, J.C., C. Peng, H. Lou, R. Xu, S. H. Willis, M. Ponce de Leon, T. Peng, A.V. Nicola, R.I. Montgomery, M.S. Warner and others (1997). Glycoprotein D of herpes simplex virus binds directly to HVEM, a member of the TNF/NGF receptor superfamily and a mediator of HSV entry. *Journal of Virology* **71**: 6083-6093.

White, E., and R. Cipriani (1989). Specific disruption of intermediate filaments and the nuclear lamina by the 19kDa product of the adenovirus E1B oncogene. *Proceedings of the National Academy of Sciences of the United States of America* **86**: 9886-9890.

Whitley, R.J. (1996). Herpes Simplex Viruses. In: *Fields Virology*, Third Edition. pp2298-2330. Edited by Fields, B.N., D.M. Knipe, P.M. Howley *et al.*: Lippincott-Raven Publishers, Philadelphia.

Whitley, R.J., E. Kern, S. Chattopadhay, J. Chou and B. Roizman (1993). Replication, establishment of latency, and induced reactivation of herpes simplex virus γ34.5 deletion mutants in rodent models. *Journal of Clinical Investigation* **91**: 2837-2843.

Wilcox, C.L., and E.M. Johnson (1987). Nerve growth factor deprivation results in the reactivation of latent herpes simplex virus *in vitro*. *Journal of Virology* **61**: 2311-2315.

Williams, M. V., and D. S. Parris (1987). Characterisation of a Herpes Simplex Virus Type 2 Deoxyuridine Triphosphate Nucleotidohydrolase and Mapping of a Gene Conferring Type Specificity for the Enzyme. *Virology* **156**: 282-292.

Williams, M.V., (1984). Demonstration of a Herpes Simplex Virus type-2 induced deoxyuridine triphosphate nucleotidohydrolase in infected KB cells and in biochemically transformed HeLa cells. *Journal of General Virology* **65**: 209-213.

Wilson, J., J.L. Bell and A.J. Levine (1996). Expression of Epstein-Barr virus nuclear antigen 1 induces B cell neoplasia in transgenic mice. *Journal of the European Molecular Biology Organisation* **15**: 3117-3126.

Wiman, K.S., (1997). p53: Emergency Brake and target for Cancer Therapy. *Experimental Cell Research* **237**: 14-18.

Wohlrab, F., B. K. Garrett and B. Francke (1982). Control of expression of the herpes simplex virus induced deoxypyrimidine triphosphatase in cells infected with mutants of HSV types 1 and 2 intertypic recombinants. *Journal of Virology* **43**: 935-942.

Woodman, C. (1994). Epidemiology of HPV and cervical cancer. In: *Human Papillomaviruses and Cervical Cancer: Biology and Immunology*. pp72-87. Edited by Stern, P.L. and M.A. Stanley: Oxford University Press, Oxford.

Woodworth, C.D., E.McMullin, M. Iglesias and G.D. Plowman (1995). Interleukin 1α and tumour necrosis factor α stimulate autocrine amphiregulin expression and proliferation of human papillomavirus immortalised and carcinoma derived cervical epithelial cells. *Proceedings of the National Academy of Sciences of the United States of America* **92**: 2840-2844.

Wu, T-T., Y-H. Su, T.M. Block and J.M. Taylor (1996). Evidence that two latency associated transcripts of herpes simplex virus type 1 are non linear. *Journal of Virology* **70**: 5962-5967.

WuDunn, D., and P.G. Spear (1989). Initial interaction of herpes simplex virus with cells is binding to heparan sulphate. *Journal of Virology* **63**: 52-58.

Xi, L.F., L.A. Koutsky, D.A. Galloway, J. Kupyers, J.P.Hughes, C.M. Wheeler, K.K. Holmes and N.B. Kiviat (1997). Genomic variation of human papillomavirus type 16 and risk for high grade cervical intraepithelial neoplasia. *Journal of the National Cancer Institute* **89**: 796-802.

Xiong, Y., G.J. Hannon, H. Zhang, D. Casso, R. Kobayashi and D. Beach (1993). p21 is a universal inhibitor of cyclin kinases. *Nature* **366**: 701-704.

York, I.A., and D.C. Johnson (1993). Direct contact with herpes simplex virus infected cells results in inhibition of lymphokine activated killer cells because of cell-to-cell spread of virus. *Journal of Infectious Disease* **168**: 1127-1132.

York, I.A., C. Roop, D.W. Andrews, S.R. Riddell, F.L. Graham and D.C. Johnson (1994). A cytosolic herpes simplex virus protein inhibits antigen presentation to $CD8^+$ T-lymphocytes. *Cell* **77**: 525-535.

Zhou, S.L., D. Stump, C.L. Kiang, L.M. Isola and P.D. Berk (1995). Mitochondrial aspartate aminotransferase expressed on the surface of 3T3-L1 adipocytes mediates saturable fatty acid uptake. *Proceedings of the Society for Experimental Biology and Medicine* **208**: 263-270.

Zhou, Z. H., J. He, J. Jakana, J.D.Tatman, F.J.Rixon and W. Chiu (1995). Assembly of VP26 in herpes simplex virus type 1 inferred from structures of wild type and recombinant capsids. *Nature Structural Biology* **2**: 1026-1030.

zurHausen, H., (1991a). Human papillomaviruses in the pathogenesis of anogenital cancer. *Virology* **184**: 9-13.

zurHausen, H, (1991b). Viruses in human cancer. *Science* **254**: 1167-1172.

Appendices

Appendix 1: *Homology within the Aspartate Aminotransferase family.*

Appendix 2A: *FASTA comparison of the derived peptide sequences of rat mAspAT and HSV-1 dUTPase.*

Appendix 2B: *Gap alignment of HSV-1 UL50 ORF DNA sequence and rat mAspAT cDNA sequence.*

Appendix 2C: *Common motifs within the HSV-1 UL50 ORF DNA sequence and the cDNA sequence of rat mitochondrial aspartate aminotransferase.*

Appendix 1. Homology within the Aspartate aminotransferase family- FASTA search results.

Em-ro:Mmaspatm
ID MMASPATM standard; RNA; ROD; 2346 BP.
DT 16-JUN-1993 (Rel. 36, Last updated, Version 3)
DE Mouse mitochondrial aspartate aminotransferase isoenzyme mRNA, . . .
SCORES Init1: 6661 Initn: 8528 Opt: 8109 z-score: 7971.2 E(): 0
93.4% identity in 1860 bp overlap

Em_New:Mmu82470
ID MMU82470 standard; RNA; ROD; 1408 BP.
DT 19-DEC-1997 (Rel. 54, Last updated, Version 2)
DE Mus musculus mitochondrial aspartate aminotransferase precursor . . .
SCORES Init1: 6358 Initn: 6358 Opt: 6374 z-score: 6266.2 E(): 0
94.7% identity in 1408 bp overlap

Em_Hum1:Hsaspat
ID HSASPAT standard; RNA; HUM; 2339 BP.
DT 23-NOV-1994 (Rel. 41, Last updated, Version 2)
DE Human mitochondrial aspartate aminotransferase mRNA, complete cds. . . .
SCORES Init1: 5147 Initn: 6243 Opt: 5729 z-score: 5628.0 E(): 0
81.0% identity in 1813 bp overlap

Em_Om:Ssaspat
ID SSASPAT standard; RNA; MAM; 2533 BP.
DT 24-NOV-1994 (Rel. 41, Last updated, Version 2)
DE Pig mitochondrial aspartate aminotransferase mRNA, complete cds. . . .
SCORES Init1: 5156 Initn: 6067 Opt: 5518 z-score: 5419.7 E(): 0
86.2% identity in 1478 bp overlap

Em_Om:Btaspamta
ID BTASPAMTA standard; RNA; MAM; 2347 BP.
DT 08-NOV-1995 (Rel. 45, Last updated, Version 13)
DE B.taurus mitochondrial aspartate aminotransferase mRNA, complete CDS. . . .
SCORES Init1: 5100 Initn: 5557 Opt: 5419 z-score: 5322.7 E(): 0
85.6% identity in 1481 bp overlap

Em_Ov:Ggaspatm
ID GGASPATM standard; RNA; VRT; 1350 BP.
DT 22-NOV-1994 (Rel. 41, Last updated, Version 2)
DE Chicken mitochondrial isoenzyme of aspartate aminotransferase mRNA, . . .
SCORES Init1: 3813 Initn: 3813 Opt: 3860 z-score: 3791.2 E(): 0
79.3% identity in 1231 bp overlap

Em_New:Ac003997
ID AC003997 standard; DNA; ROD; 122176 BP.
DT 17-JAN-1998 (Rel. 54, Last updated, Version 1)
DE Mouse BAC mbac20 from 14D1-D2 (T-Cell Receptor Alpha Locus),
SCORES Init1: 1942 Initn: 3599 Opt: 1954 z-score: 1886.4 E(): 0
88.1% identity in 497 bp overlap

Em_Pl:Pmaat1
ID PMAAT1 standard; RNA; PLN; 1677 BP.
DT 20-MAR-1992 (Rel. 31, Last updated, Version 3)
DE P.miliaceum mRNA for aspartate aminotransferase (pmAAT1) . . .
SCORES Init1: 784 Initn: 951 Opt: 1465 z-score: 1431.8 E(): 0
59.2% identity in 1313 bp overlap

Em_Pl:D67043
ID D67043 standard; RNA; PLN; 1578 BP.
DT 11-DEC-1997 (Rel. 53, Last updated, Version 1)
DE Oryza sativa mRNA for aspartate aminotransferase, complete cds. . . .
SCORES Init1: 315 Initn: 566 Opt: 1397 z-score: 1365.2 E(): 0
59.6% identity in 1216 bp overlap

Em_Pl:Pmaa
ID PMAA standard; RNA; PLN; 1681 BP.
DT 16-AUG-1996 (Rel. 49, Last updated, Version 5)
DE Panicum miliaceum mRNA for plastidic aspartate aminotransferase , . . .
SCORES Init1: 601 Initn: 829 Opt: 1298 z-score: 1267.4 E(): 0
57.4% identity in 1168 bp overlap

Em_Pl:Osd14673
ID OSD14673 standard; RNA; PLN; 1514 BP.
DT 11-DEC-1997 (Rel. 53, Last updated, Version 3)
DE Rice mRNA for aspartate aminotransferase, complete cds. . . .
SCORES Init1: 249 Initn: 604 Opt: 1241 z-score: 1211.9 E(): 0
58.5% identity in 1129 bp overlap

Em_Pl:At15034
ID AT15034 standard; RNA; PLN; 1548 BP.
DT 18-OCT-1995 (Rel. 45, Last updated, Version 2)
DE Arabidopsis thaliana aspartate aminotransferase (Asp3) mRNA, . . .
SCORES Init1: 266 Initn: 532 Opt: 1220 z-score: 1191.1 E(): 0
57.9% identity in 1189 bp overlap

Em_Pl:Laaspat
ID LAASPAT standard; RNA; PLN; 1645 BP.
DT 05-MAY-1995 (Rel. 43, Last updated, Version 11)
DE L.angustifolius mRNA for aspartate aminotransferase . . .
SCORES Init1: 356 Initn: 655 Opt: 1193 z-score: 1164.1 E(): 0
57.2% identity in 1177 bp overlap

Em_Pl:Clu89494
ID CLU89494 standard; RNA; PLN; 1737 BP.
DT 09-SEP-1997 (Rel. 52, Last updated, Version 4)
DE Canavalia lineata aspartate aminotransferase 2 precursor (AAT2) . . .
SCORES Init1: 208 Initn: 360 Opt: 1146 z-score: 1117.5 E(): 0
57.7% identity in 1182 bp overlap

Legend. A nucleotide FASTA search (GCG, Wisconsin Package) for DNA sequences with homology to the rat mitochondrial aspartate aminotransferase (Em-ro:M18467) was performed. The top scoring sequences are shown. Due to space limitations only the summary data is provided.

Appendix 2A. FASTA comparison of the derived peptide sequences of rat mAspAT and HSV-1 dUTPase

```
27.9% identity in 68 aa overlap

                10        20        30        40        50        60
Aspat.Pep       RLGFSGRFPXSPFYHHPLPSYHPPWPSCTPVASSPGWLLPFTQALQPQPLPEPAPGG---
                                                :|: |:   |::    ||  | |  |:
Hsv1ul50        GTVMAVVVAPKRTREFAPGTLRVDVTFLDILATPPALTEPISLRQFPQLAPPPPTGAGIR
                      110       120       130       140       150       160

                       70        80        90       100       110       120
Aspat.Pep       --PMLKWDLQIPSWEXPKPSREIPTARRXTWELVPTGTITESLTCSPVFGRQRPRLLGKI
                  | |:  |  ||  :  |:|:   :   : ||:|: |
Hsv1ul50        EDPWLEGALGAPSVTTALPARRRGRSLVYAGELTPVQTEHGDGVREAIAFLPKREEDAGF
                      170       180       190       200       210       220

                      130       140       150       160       170       180
Aspat.Pep       WTKNTYPSGDWLIFVRLLQNWPWARTAKCXKAAGLXLCRPFPGLEPXGSEPAFCKDFLSS

Hsv1ul50        DIVVRRPVTVPANGTTVVQPSLRMLHADAGPAACYVLGRSSLNARGLLVVPTRWLPGHVC
                      230       240       250       260       270       280
```

Legend. All the manipulations were performed using GCG Wisconsin package version 9. The cDNA sequence of rat mitochondrial aspartate aminotransferase (Em-ro:M18467) was translated, and the derived amino acid sequence compared to the derived amino acid sequence of the HSV-1 UL50 ORF. FASTA comparison shows that there is limited similarity between the derived amino acid sequences.

Appendix 2B. Gap alignment of HSV-1 UL50 ORF DNA sequence and rat mAspAT cDNA sequence.

```
Gap Weight:     50      Average Match: 10.000
Length Weight:   3      Average Mismatch:  0.000

            Quality:   3636            Length:   2330
              Ratio:  3.267              Gaps:     10
 Percent Similarity: 38.628   Percent Identity: 28.430

       Match display thresholds for the alignment(s):
                  | = IDENTITY
                  : =   5
                  . =   1

 Hsv1ul50.Seq x Aspat.Seq
                .         .         .         .         .
      1 .....................................AUGUCCCAGUG..  11
                                            |  :|||||  |
    651 GGCTTTGACTTCTCTGGAGCCTTAGAAGACATATCAAAAATCCCAGAGCA 700
                .         .         .         .         .
     12 ..GGGUUCCGGUGCUAUCCUGGUUCAGCCGGACUCCCUGGGUCGUGGUUA  59
          | |::|   : |:   |   : |   |  |  |||  || ||:||
    701 GAGTGTTCTCCTTCTGCACGCCTGCGCTCACAACCCCACGGGCGTGGACC 750
                .         .         .         .         .
     60 CGACGGUGACUGGCACACCGCUGUUGCUACCCGUGGUGGUGGUGUUGUUC 109
        ||              |    :|    | |:||:|  |     |
    751 CGCGTCCAGAGCAGTGGAAGGAAATGGCGGCGGTGGTGAAGAAAAAGAAT 800
                .         .         .         .         .
    110 AGCUGAACCUGGUUAACCGUCGUGCUGUUGCUUUCAUGCCGAAAGUUUCC 159
          |:   | :  ::   | :   ||         | :  | |  |
    801 CTCTTCGCATTCTTTGACAT..GGCCTACCAAGGCTTTGCCAGCGGCGAT 848
                .         .         .         .         .
    160 GGUGACUCCGGUUGGGCUGUUGGUCGUGUUUCCCUGGACCUGCGUAUGGC 209
        ||:||    |         |  |  ||    : | : || | | | |:
    849 GGTGATAAGGACGCCTGGGCCGTGCGGCACTTCATCGAGCAGGGCATCAA 898
                .         .         .         .         .
    210 UAUGCCGGCUGACUUCUGCGCUAUCAUCCACGCUCCGGCUCUGGCUUCCC 259
        : :          |   : |  :  ||   ||  :  | |: :    :
    899 TGTCTGCCTCTGCCAATCCTATGCCAAGAAC.ATGGGCCTGTACGGTGAG 947
                .         .         .         .         .
    260 CGGGUCACCACGUUAUCCUGGGUCUGAUCGACUCCGGUUACCGUGGUACC 309
        || |:     | ::  |   ||:|:|      : | |      |    |
    948 CGTGTGGGAGCCTTCACTGTGGTCTGCAAAGATGCAGAAGAAGCCAAAAG 997
                .         .         .         .         .
    310 GUUAUGGCUGUUGUUGUUGCUCCGAAACGUACCCGUGAAUUCGCUCCGGG 359
        | :   |     | :|  | :||  | |   ||| :| |::|   || |
    998 GGTGGAGTCACAGCTGAAGATCCTGATCCGCCCCTTGTATTCCAACCCG. 1046
                .         .         .         .         .
    360 UACCCUGCGUGUUGACGUUACCUUCCUGGACAUCCUGGCUACCCCGCCGG 409
          | |:   :|  | |   | |  |     ||:||:| |: | ||
   1047 .CCTCTCAATGGAGCCCGGATCGCCGCAACCATCCTGACTTCTCCAGACT 1095
                .         .         .         .         .
    410 CUCUGACCGAACCGAUCUCCCUG.....CGUCAGUUCCCGCAGCUGGCUC 454
          | ||   ||  | :      |      | ||   |   | ||    :|
   1096 TGCGGAAGCAATGGTTGCAGGAGGTGAAAGGCATGGCTGACCGCATCATC 1145
                .         .         .         .         .
    455 CGCCGCCGCCGACCGGUGCUGGUAUCCGUGAAGACCCGUGGCUGGAAGGU 504
         ||    |    | | :| :      | :|||||     |||: |
   1146 AGCATGAGGACCCAGTTGGTCTCCAACCTGAAGAAAGAGGGCTCGTCCCA 1195
```

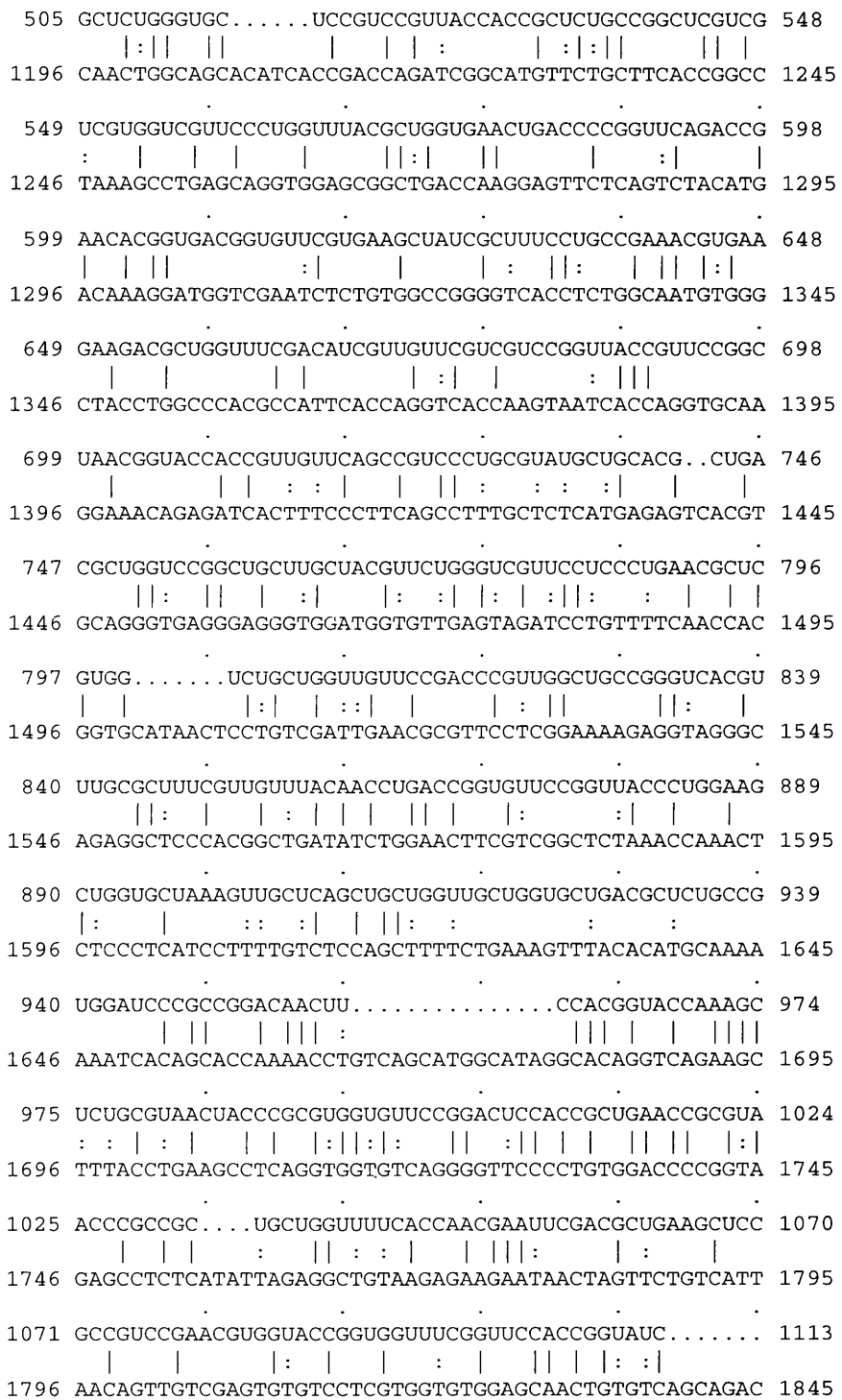
505 GCUCUGGGUGC......UCCGUCCGUUACCACCGCUCUGCCGGCUCGUCG 548
1196 CAACTGGCAGCACATCACCGACCAGATCGGCATGTTCTGCTTCACCGGCC 1245
549 UCGUGGUCGUUCCCUGGUUUACGCUGGUGAACUGACCCCGGUUCAGACCG 598
1246 TAAAGCCTGAGCAGGTGGAGCGGCTGACCAAGGAGTTCTCAGTCTACATG 1295
599 AACACGGUGACGGUGUUCGUGAAGCUAUCGCUUUCCUGCCGAAACGUGAA 648
1296 ACAAAGGATGGTCGAATCTCTGTGGCCGGGGTCACCTCTGGCAATGTGGG 1345
649 GAAGACGCUGGUUUCGACAUCGUUGUUCGUCGUCCGGUUACCGUUCCGGC 698
1346 CTACCTGGCCCACGCCATTCACCAGGTCACCAAGTAATCACCAGGTGCAA 1395
699 UAACGGUACCACCGUUGUUCAGCCGUCCCUGCGUAUGCUGCACG..CUGA 746
1396 GGAAACAGAGATCACTTTCCCTTCAGCCTTTGCTCTCATGAGAGTCACGT 1445
747 CGCUGGUCCGGCUGCUUGCUACGUUCUGGGUCGUUCCUCCCCUGAACGCUC 796
1446 GCAGGGTGAGGGAGGGTGGATGGTGTTGAGTAGATCCTGTTTTCAACCAC 1495
797 GUGG.......UCUGCUGGUUGUUCCGACCCGUUGGCUGCCGGGUCACGU 839
1496 GGTGCATAACTCCTGTCGATTGAACGCGTTCCTCGGAAAAGAGGTAGGGC 1545
840 UUGCGCUUUCGUUGUUUACAACCUGACCGGUGUUCCGGUUACCCUGGAAG 889
1546 AGAGGCTCCCACGGCTGATATCTGGAACTTCGTCGGCTCTAAACCAAACT 1595
890 CUGGUGCUAAAGUUGCUCAGCUGCUGGUUGCUGGUGCUGACGCUCUGCCG 939
1596 CTCCCTCATCCTTTTGTCTCCAGCTTTTCTGAAAGTTTACACATGCAAAA 1645
940 UGGAUCCCGCCGGACAACUU..............CCACGGUACCAAAGC 974
1646 AAATCACAGCACCAAAACCTGTCAGCATGGCATAGGCACAGGTCAGAAGC 1695
975 UCUGCGUAACUACCCGCGUGGUGUUCCGGACUCCACCGCUGAACCGCGUA 1024
1696 TTTACCTGAAGCCTCAGGTGGTGTCAGGGGTTCCCCTGTGGACCCCGGTA 1745
1025 ACCCGCCGC....UGCUGGUUUUCACCAACGAAUUCGACGCUGAAGCUCC 1070
1746 GAGCCTCTCATATTAGAGGCTGTAAGAGAAGAATAACTAGTTCTGTCATT 1795
1071 GCCGUCCGAACGUGGUACCGGUGGUUUCGGUUCCACCGGUAUC....... 1113
1796 AACAGTTGTCGAGTGTGTCCTCGTGGTGTGGAGCAACTGTGTCAGCAGAC 1845

Appendix 2C. Common motifs within the HSV-1 UL50 ORF DNA sequence and the cDNA sequence of rat mitochondrial aspartate aminotransferase.

Motifs within the HSV-1 UL50 ORF DNA sequence.

```
MOTIFS from: hsv1ul50.seq

Hsv1ul50.Seq  Check: 3178  Length: 1,113 !

-------------------------------------------------------------

2fe2s_Ferredoxin      C~(C)~(C)(G,A)~(C)C(G,A,S,T)~(C,P,D,E,K,R,H,F,Y,W)C
                            C~C~C(A)~CC(G)~(C,P,D,E,K,R,H,F,Y,W)C
          283: UGGGU                      CUGAUCGAC                    UCCGG

                            C~C~C(G)~CC(A)~(C,P,D,E,K,R,H,F,Y,W)C
          385: CCUUC                      CUGGACAUC                    CUGGC

************************************************************
* 2Fe-2S ferredoxins, iron-sulfur binding region signature *
************************************************************

Ferredoxins are a group of iron-sulfur proteins which mediate electron
transfer in a wide variety of metabolic reactions. Ferredoxins can be divided
into several subgroups depending upon the physiological nature of the iron
sulfur cluster(s) and according to sequence similarities. One of these
subgroups are the 2Fe-2S ferredoxins, which are proteins or domains of around
one hundred amino acid residues that bind a single 2Fe-2S iron-sulfur cluster.

-------------------------------------------------------------

4fe4s_Ferredoxin      Cx2Cx2Cx3C(P,E,G)
                      Cx{2}Cx{2}Cx{3}C(G)
          454: UGGCU   CCGCCGCCGCCG    ACCGG

                      Cx{2}Cx{2}Cx{3}C(G)
          458: UCCGC   CGCCGCCGACCG    GUGCU

                      Cx{2}Cx{2}Cx{3}C(G)
        1,067: UGAAG   CUCCGCCGUCCG    AACGU
 ************************************************************
* 4Fe-4S ferredoxins, iron-sulfur binding region signature *
************************************************************

Ferredoxins are a group of iron-sulfur proteins which mediate electron
transfer in a wide variety of metabolic reactions. Ferredoxins can be
divided into several subgroups depending upon the physiological nature of the
iron-sulfur cluster(s). One of these subgroups are the 4Fe-4S ferredoxins,
which are found in bacteria and which are thus often referred as
'bacterial-type' ferredoxins. The structure of these proteins consists of
the duplication of a domain of twenty six amino acid residues; each of these
domains contains four cysteine residues that bind to a 4Fe-4S center.
```

```
Egf                     CxCx5Gx2C
                        CxCx{5}Gx{2}C
            165: GGUGA CUCCGGUUGGGC UGUUG

                        CxCx{5}Gx{2}C
            351: GAAUU CGCUCCGGGUAC CCUGC

                        CxCx{5}Gx{2}C
            401: GGCUA CCCCGCCGGCUC UGACC

                        CxCx{5}Gx{2}C
            410: GCCGG CUCUGACCGAAC CGAUC

                        CxCx{5}Gx{2}C
            443: GUUCC CGCAGCUGGCUC CGCCG

                        CxCx{5}Gx{2}C
            506: AGGUG CUCUGGGUGCUC CGUCC

                        CxCx{5}Gx{2}C
            533: CACCG CUCUGCCGGCUC GUCGU

                        CxCx{5}Gx{2}C
            785: UUCCU CCCUGAACGCUC GUGGU

                        CxCx{5}Gx{2}C
            989: CUACC CGCGUGGUGUUC CGGAC

                        CxCx{5}Gx{2}C
          1,070: AGCUC CGCCGUCCGAAC GUGGU

*********************************************
* EGF-like domain cysteine pattern signature *
 *********************************************
```

A sequence of about thirty to forty amino-acid residues long found in the sequence of epidermal growth factor (EGF) has been shown to be present, in a more or less conserved form, in a large number of other proteins.

```
Prokar_Lipoprotein    ~(D,E,R,K)6(L,I,V,M,F,W,S,T,A,G)2(L,I,V,M,F,Y,S,T,A,G,C,Q)
(A,G,S)C
                                                ~(D,E,R,K){6}(G){2}(C)(A)C
             65: CGACG                                  GUGACUGGCAC
          ACCGC

                                               ~(D,E,R,K){6}(A,G){2}(A)(A)C
            327: GUUGU                                  UGCUCCGAAAC
          GUACC

                                                ~(D,E,R,K){6}(A){2}(G)(A)C
            479: UGGUA                                  UCCGUGAAGAC
          CCGUG

                                                ~(D,E,R,K){6}(A){2}(C)(A)C
            593: GGUUC                                  AGACCGAACAC
          GGUGA
```

```
                                                ~(D,E,R,K){6}(A,G){2}(A)(G)C
  613: ACGGU                                            GUUCGUGAAGC
UAUCG

                                                ~(D,E,R,K){6}(A,G){2}(A)(A)C
  633: GCUUU                                            CCUGCCGAAAC
GUGAA

                                                 ~(D,E,R,K){6}(A){2}(G)(A)C
  644: GAAAC                                            GUGAAGAAGAC
GCUGG

                                                ~(D,E,R,K){6}(A,G){2}(C)(G)C
  646: AACGU                                            GAAGAAGACGC

  739: UGCUG                                            CACGCUGACGC
UGGUC

                                                 ~(D,E,R,K){6}(A){2}(C)(G)C
  784: GUUCC                                            UCCCUGAACGC
UCGUG

                                                ~(D,E,R,K){6}(A,G){2}(A)(G)C
  880: CGGUU                                            ACCCUGGAAGC
UGGUG

                                                ~(D,E,R,K){6}(A,G){2}(C)(G)C
  922: UUGCU                                            GGUGCUGACGC
UCUGC

                                                 ~(D,E,R,K){6}(A){2}(A)(G)C
  964: UCCAC                                            GGUACCAAAGC
UCUGC

                                                ~(D,E,R,K){6}(A,G){2}(C)(G)C
1,051: CCAAC                                            GAAUUCGACGC
UGAAG
UGGUU


                                                ~(D,E,R,K){6}(A,G){2}(A)(G)C
1,057: AAUUC                                            GACGCUGAAGC
UCCGC
```

****
* Prokaryotic membrane lipoprotein lipid attachment site *
****

In prokaryotes, membrane lipoproteins are synthesized with a precursor signal peptide, which is cleaved by a specific lipoprotein signal peptidase (signal peptidase II). The peptidase recognizes a conserved sequence and cuts upstream of a cysteine residue to which a glyceride-fatty acid lipid is attached.

Motifs within the mAspAT cDNA sequence.

MOTIFS from: em_ro:rsaspata

Rsaspata Check: 7270 Length: 2,325 ! M18467 Rattus norvegicus mitochondrial aspartate aminotransferase mRNA.

```
2fe2s_Ferredoxin      C~(C)~(C)(G,A)~(C)C(G,A,S,T)~(C,P,D,E,K,R,H,F,Y,W)C
                            C~C~C(G)~CC(A)~(C,P,D,E,K,R,H,F,Y,W)C
          888: TCGAG                        CAGGGCATC                       AATGT

                            C~C~C(A)~CC(G)~(C,P,D,E,K,R,H,F,Y,W)C
        1,218: CCGAC                        CAGATCGGC                       ATGTT

                            C~C~C(G)~CC(G)~(C,P,D,E,K,R,H,F,Y,W)C
        2,127: CCCAG                        CTGGACGTC                       CTCAT
```

****
* 2Fe-2S ferredoxins, iron-sulfur binding region signature *
****

Ferredoxins are a group of iron-sulfur proteins which mediate electron transfer in a wide variety of metabolic reactions. Ferredoxins can be divided into several subgroups depending upon the physiological nature of the iron sulfur cluster(s) and according to sequence similarities. One of these subgroups are the 2Fe-2S ferredoxins, which are proteins or domains of around one hundred amino acid residues that bind a single 2Fe-2S iron-sulfur cluster.

```
4fe4s_Ferredoxin      Cx2Cx2Cx3C(P,E,G)
                      Cx{2}Cx{2}Cx{3}C(G)
           64: ACCAC   CATCCACTGCCG    TCTTA
```

****
* 4Fe-4S ferredoxins, iron-sulfur binding region signature *
****

Ferredoxins are a group of iron-sulfur proteins which mediate electron transfer in a wide variety of metabolic reactions. Ferredoxins can be divided into several subgroups depending upon the physiological nature of the iron-sulfur cluster(s). One of these subgroups are the 4Fe-4S ferredoxins, which are found in bacteria and which are thus often referred as 'bacterial-type' ferredoxins. The structure of these proteins consists of the duplication of a domain of twenty six amino acid residues; each of these domains contains four cysteine residues that bind to a 4Fe-4S center.

A number of proteins have been found that include one or more 4Fe-4S binding domains similar to those of bacterial-type ferredoxins.

```
Egf                    CxCx5Gx2C
                       CxCx{5}Gx{2}C
              84: TACCA CCCACCATGGCC CTCCT

                       CxCx{5}Gx{2}C
             164: GCAGC CTCTGCCAGAGC CAGCT

                       CxCx{5}Gx{2}C
             179: GCCAG CTCCTGGTGGAC CCATG

                       CxCx{5}Gx{2}C
             708: GTGTT CTCCTTCTGCAC GCCTG

                       CxCx{5}Gx{2}C
             751: GGACC CGCGTCCAGAGC AGTGG

                       CxCx{5}Gx{2}C
           1,728: GGGTT CCCCTGTGGACC CCGGT

                       CxCx{5}Gx{2}C
           1,738: GTGGA CCCCGGTAGAGC CTCTC

                       CxCx{5}Gx{2}C
           2,260: ATAAC CACCATCTGCTC TAACC

**********************************************
* EGF-like domain cysteine pattern signature *
**********************************************
```

A sequence of about thirty to forty amino-acid residues long found in the sequence of epidermal growth factor (EGF) has been shown to be present, in a more or less conserved form, in a large number of other proteins.

```
Prokar_Lipoprotein    ~(D,E,R,K)6(L,I,V,M,F,W,S,T,A,G)2(L,I,V,M,F,Y,S,T,A,G,C,Q)
(A,G,S)C
                                                ~(D,E,R,K){6}(G){2}(A)(G)C
              5:  TTTT                                 TTTTTAGGAGC
          CCGCG

                                                ~(D,E,R,K){6}(A,G){2}(C)(G)C
             29: CGGTT                                 TCAGCGGACGC
          TTCCC

                                                ~(D,E,R,K){6}(T,A){2}(G)(G)C
             84: TACCA                                 CCCACCATGGC
          CCTCC

                                                ~(D,E,R,K){6}(T,G){2}(C)(A)C
             94: CATGG                                 CCCTCCTGCAC
          TCCGG

                                                ~(D,E,R,K){6}(T,G){2}(C)(G)C
            103: CCTGC                                 ACTCCGGTCGC
          GTCCT

                                                ~(D,E,R,K){6}(T,A){2}(G)(G)C
            120: TCCTC                                 TCCGGGATGGC
          TGCTG

                                                 ~(D,E,R,K){6}(T){2}(C)(A)C
            133: GGCTG                                 CTGCCTTTCAC
          CCAGG
```

```
2,210: TCTGG                              GGTTTGTATGC
TACCA

                                    ~(D,E,R,K){6}(T,A){2}(A)(A)C
2,249: CCTTG                              GGAAAGATAAC
CACCA

                                    ~(D,E,R,K){6}(T,A){2}(G)(A)C
2,274: CTCTA                              ACCGTGTAGAC
GTACC

                                    ~(D,E,R,K){6}(T,G){2}(T)(A)C
2,295: TGGTT                              TTCTCTGTTAC
AATAA

                                    ~(D,E,R,K){6}(T,A){2}(T)(A)C
2,306: GTTAC                              AATAAAATTAC
TACAG

**********************************************************
* Prokaryotic membrane lipoprotein lipid attachment site *
**********************************************************

In prokaryotes, membrane lipoproteins are synthesized  with a precursor signal
peptide, which is cleaved  by  a specific lipoprotein signal peptidase (signal
peptidase II). The peptidase recognizes a conserved sequence and cuts upstream
of a cysteine residue  to which a  glyceride-fatty acid lipid is attached.
```

Note that many more examples of the 'prokaryotic membrane lipoprotein attachment site' motif were present within the mAspAT cDNA sequence, but that only those at either end are shown here due to space limitations.